

HORMONAL VOICES IN SEED/POD COMMUNICATION: A STUDY OF PARTHENOCARPY

by

Sara Fuentes

Thesis submitted for the degree of Doctor of Philosophy

University of East Anglia

School of Biological Sciences

Norwich, United Kingdom

September 2010

© This copy of the thesis has been supplied on condition that anyone who consults it is understood to recognise that its copyright rests with the author and that no quotation from the thesis, nor any information derived therefrom, may be published without the author's prior, written consent.

ACKNOWLEDGEMENTS

Firstly I would like to thank my supervisor Dr. Lars Østergaard. Thank you for all your time, patience, support, encouragement and optimism throughout my PhD. It has been a huge privilege to be part of the Østergaard's lab. I would also like to thank past and present members of the Østergaard's lab; I will miss working with you. A special thanks goes to Tom Woods and Dr. Thomas Girin. Tom had to put up with me during my MSc and PhD; I don't know how I will manage without our little chats and without your understanding. Thomas has been a great source of support and advice throughout my PhD. I have learnt so much from you that I don't think I could ever thank you enough for all your help, patience and friendship. I wish you all the best in your new adventure in France and, I hope to keep our friendship alive.

I would also like to thank Pauline, the best Research Assistant ever, for being great to work with and for solving my constant string of problems. Thanks to the ever changing supervisory committee, to those who started this journey with me (Prof. Liam Dolan and Dr. Karim Sorefan) and to those who finished it with me (Dr. Phil Wigge and Dr. Thomas Girin).

My deepest thank you goes to my partner, Phil, for his continued support and love. Sin ti jamás hubiera comenzado esta locura y, menos aún, ¡acabado! My most sincere gratitude also goes to my parents for their constant love, friendship and encouragement to pursue my goals. Aún no comprendo como podéis creer tanto en mí, espero jamás defraudaros. I would also like to thank the rest of my family and friends, particularly my brother, who has always been there for me and I love to bits. ¡Gracias a todos!

Finally, I am grateful to the Marie Curie programme and to the JIC for funding the work presented here.

ABSTRACT

Fruit initiation and development are key processes in the life cycle of most angiosperms and, consequently, they are subjected to tight developmental control. This complex regulatory network involves genetic and hormonal activities and ensures the coordinated development of seed and ovary structures. The overall aim of this thesis is to contribute towards a better understanding of the mechanisms involved in the control of fruit development upon fertilisation by focusing particularly on the study of parthenocarpy, that is, on the growth of the ovary into a seedless fruit in the absence of fertilisation. In order to achieve this objective, three major strategies were undertaken.

Firstly, an in-depth analysis into the role of DELLA proteins in fruit-set and growth was carried out. This revealed that the *Arabidopsis* DELLA proteins function redundantly to repress fruit growth in the absence of fertilisation such that combinations of mutations in *DELLA* genes result in parthenocarpy. Although the majority of growth repression in the absence of fertilisation can be attributed to the effect of DELLA proteins, a DELLA-independent GA-pathway was discovered and characterised. Secondly, a forward genetic approach was adopted for the discovery of novel mutations conferring fertilisation-independent fruit development. This screen resulted in the isolation of several mutant lines with parthenocarpic fruit growth of which one was chosen for a more detailed analysis. Finally, the investigation of seed-pod communication was pursued to improve the understanding of the coordinated development of seed and fruit structures.

Taken together, the results presented in this thesis demonstrate that control of fruit initiation and fruit development relies on a complex interplay between genetic and hormonal activities. In addition to describing these activities in more detail, the work presented here uncovers further levels of regulatory complexity as shown by the existence of a DELLA-independent GA response.

TABLE OF CONTENTS	page
Abstract	ii
Acknowledgements	iii
Table of contents	iv
CHAPTER 1: General introduction	
1.1 Introduction	2
1.2 Pollination	4
1.2.1 Pollen-stigma interaction	4
1.2.2 Pollen germination and pollen-tube growth	5
1.2.3 Pollination in the context of fruit initiation	5
1.3 Fertilisation	6
1.3.1 Pollen-tube guidance	6
1.3.2 Double fertilisation	9
1.4 Fertilisation-independent fruit development	9
1.4.1 Apomixis	10
1.4.1.1 The role of the egg cell and central cell in fruit initiation	10
1.4.1.2 The role of integuments in fruit initiation	12
1.4.2 Parthenocarpy	12
1.4.2.1. The role of auxin in parthenocarpic fruit growth	13

	page
1.4.2.2. The role of gibberellins in parthenocarpic fruit growth	14
1.4.2.3 The role of cytokinins in parthenocarpic fruit growth	15
1.5 Hormonal cues during fruit initiation and development	16
1.5.1 Auxin	16
1.5.1.1 Auxin biosynthesis in the context of fruit initiation and fruit	16
1.5.1.2 Auxin signalling in the context of fruit initiation and fruit development	18
1.5.2 Gibberellins	20
1.5.2.1 Gibberellin biosynthesis in the context of fruit initiation and fruit development	20
1.5.2.2 Gibberellin signalling in the context of fruit initiation and fruit development	20
1.5.3 Cytokinin	22
1.5.4 Ethylene	22
1.5.5 Hormonal cross-talk	23
1.6 Aim of this thesis	26

	page
CHAPTER 2: General materials and methods	
2.1 Introduction	28
2.2 Materials and methods	28
2.2.1 Edwards' quick DNA extraction	28
2.2.2 General PCR and colony PCR conditions	29
2.2.3 Sequencing reactions	29
2.2.4 <i>E. coli</i> heatshock transformation	29
2.2.5 <i>Agrobacterium tumefaciens</i> electroporation transformation	30
2.2.6 <i>Arabidopsis thaliana</i> floral dip transformation	30
2.2.7 GUS staining	31
2.2.8 Tissue fixation	31
2.2.9 Tissue staining	31
2.2.10 Light microscopy	32
2.2.11 Cell measurements and cell count	32
CHAPTER 3: Fruit development and DELLAs	
3.1 Introduction	34
3.1.1 GA metabolism during fruit development	34
3.1.2 GA signalling during fruit development	37

	page
3.2 Materials and methods	39
3.2.1 Plant materials and growth conditions	39
3.2.2 Quantitative real-time PCR (qRT-PCR) analysis	39
3.2.3 Hormone treatments	40
3.2.4 Endogenous IAA quantification	40
3.2.5 Protein extraction	40
3.2.6 Protein quantification: Bradford assay	41
3.2.7 Western blotting	41
3.2.8 Yeast two-hybrid assays	42
3.2.9 Promoter <i>GUS</i> transgenic line construction	43
3.3 Results	47
3.3.1 Lack of DELLA proteins causes facultative parthenocarpy in <i>Arabidopsis</i>	47
3.3.2 Other flower and fruit phenotypes caused by lack of DELLA proteins	47
3.3.3 In-depth characterisation of DELLA-related facultative parthenocarpy	52
3.3.4 The facultative parthenocarpy observed in <i>global-DELLA</i> mutants is not due to an auxin imbalance	55

	page
3.3.5 Auxin application does not promote pistil elongation in <i>global-DELLA</i> mutants	58
3.3.6 DELLA-independent GA-response in pistils	61
3.3.7 Molecular basis underlying DELLA-independent GA-response	64
3.3.7.1 DELLA-independent response is GID dependent	64
3.3.7.2 DELLA-independent response is 26S proteasome dependent	64
3.3.7.3 SPT is part of the DELLA-independent GA-response pathway	67
3.3.8 Histological analysis of <i>Ler</i> , <i>global-DELLA</i> and <i>ga1-3 global-DELLA</i> pistils	73
3.3.9 Analysis of the GA-response at the tissue level	74
3.4 Discussion	79
3.4.1 Role of DELLA-dependent GA signalling in the control of gynoecium and fruit growth	79
3.4.1.1 Lack of DELLA proteins promotes style and stigma growth	79
3.4.1.2 Lack of DELLA proteins causes facultative parthenocarpy	80

	page
3.4.2 DELLA-independent GA-response during fruit development	82
3.4.3 GA signalling during fruit development	86
3.4.4 Future work	88
 CHAPTER 4: Protein-protein interactions and DELLAS	
4.1 Introduction	91
4.1.1 DELLA proteins' mode of action	91
4.2 Materials and methods	94
4.2.1 Plasmid construction for yeast assays	94
4.2.2 LiAc yeast transformation	95
4.2.3 Integration of plasmids into the yeast genome (for yeast two-one hybrid assays)	96
4.2.4 Yeast mating	96
4.2.5 Yeast two hybrid: protein-protein interaction	97
4.2.6 Yeast two-one hybrid interactions: Colony-lift filter assay	97
4.2.7 Quantification of protein-protein interaction: β -galactosidase ONPG assay	98

	page
4.3 Results	100
4.3.1 DELLA proteins interact with several bHLH transcription factors involved in fruit development and/or fruit patterning	100
4.3.2 In-depth characterisation of IND-SPT protein interaction	105
4.3.3 IND and SPT bind to a putative E-box variant in <i>SPT</i> promoter	109
4.4 Discussion	110
4.4.1 Interaction of DELLA proteins with key bHLH regulators of fruit development and/or fruit patterning	110
4.4.2 Interaction of DELLA proteins with non-bHLH transcription factors involved in fruit development and/or fruit patterning	111
4.4.3 IND-SPT protein interaction and downstream targets	112

CHAPTER 5: EMS mutagenesis: Screening for parthenocarpy

5.1 Introduction	116
5.2 Materials and methods	117

	page
5.2.1 EMS treatment	117
5.2.2 Plant materials and growth conditions	118
5.2.3 Map-based cloning	118
5.3 Results	119
5.3.1 EMS mutagenesis	119
5.3.2 Forward screening and putative mutant isolation	126
5.3.3 Putative mutant confirmation	130
5.3.3.1 Mutant 35.1	135
5.3.3.2 Mutant 117.1	135
5.3.4 Characterisation of mutant 117.1	135
5.3.4.1 117.1 is a parthenocarpic mutant	135
5.3.4.2 117.1 <i>pi-1</i> show longer mesocarp cells than <i>pi-1</i> mutants	138
5.3.5 Mapping of 117.1 mutant	138
5.4 Discussion	142
5.4.1 EMS mutagenesis as a discovery tool in parthenocarpy studies	142
5.4.2 117.1 is a parthenocarpy conferring mutation and acts at the mesocarp tissue level	143
5.4.3 Future work	145

	page
CHAPTER 6: Unexpected consequences of investigating seed-pod communication	
6.1 Introduction	149
6.1.1 Seed-pod communication during fruit development	149
6.1.2 <i>GAL4-GFP</i> enhancer-trap system	152
6.1.3 Targeting seed-pod communication	152
6.2 Materials and methods	153
6.2.1 TAIL-PCR	153
6.2.2 <i>PAP10::GUS</i> transgenic line construction	154
6.2.3 PCR genotyping of T-DNA insertion mutants	155
6.2.4 Analysis of <i>PAP10::GUS</i> expression in response to various stimuli	155
6.2.5 Pollen grain analysis	155
6.3 Results	157
6.3.1 Funiculus-specific gene expression of <i>GAL4-GFP</i> enhancer-trap lines	157
6.3.2 Isolation of GFP-expression drivers: <i>PAP10</i>	157
6.3.3 Expression analysis of <i>PAP10</i>	163

	page
6.3.4 GUS expression in <i>PAP10::GUS</i> lines varies in response to different stimuli	167
6.3.5 <i>pap10</i> , <i>pap12</i> and <i>pap10pap12</i> mutant isolation	173
6.3.6 <i>pap10-2</i> mutation results in tetrad pollen formation	174
6.4 Discussion	174
6.4.1 Interruption of seed-pod communication by funiculus-specific gene expression	174
6.4.2 Purple acid phosphatases and <i>PAP10</i>	176
6.4.3 Phenotypes related to reproductive development in <i>pap10-2</i> mutants	178
6.4.4 Future work	179
 CHAPTER 7: General discussion	
7.1 Aim and approaches	181
7.2 Conclusions	181
7.2.1 DELLA-independent GA-signalling during fruit development	182
7.2.2 DELLA protein interaction with transcription factors involved in fruit development	184

	page
7.2.3 Forward genetic screens as discovery tools in parthenocarpy studies	185
7.3 Questions and future work	185
7.3.1 DELLA independent GA signalling	185
7.3.2 Tissue-specific GA signal attenuation	186
7.3.3 Forward genetic screens and parthenocarpic mutant characterisation	187
7.3.4 Seed-pod communication	187
7.3.5 <i>PAP10</i>	188
7.4 Concluding remarks: Parthenocarpy in the context of crop improvement	189

List of illustrations

Figure 1.1 Chronological representation of fruit development	3
Figure 1.2 Double fertilisation	7
Figure 1.3 Model of ARF-Aux/IAA auxin signal transduction	17
Figure 3.1 Schematic representation of GA metabolism pathway in higher plants	35
Figure 3.2 Lack of DELLA proteins causes parthenocarpic fruit development in <i>Arabidopsis</i>	44

	page
Figure 3.3 Fruit development in <i>Ler</i> , <i>global-DELLA</i> and <i>ga1-3 global-DELLA</i> mutant plants	45
Figure 3.4 Seed count in selfed, hand pollinated and cross pollinated <i>Ler</i> , <i>global-DELLA</i> and <i>ga1-3 global-DELLA</i> mutants	46
Figure 3.5 Style and stigma development in <i>global-DELLA</i> and <i>ga1-3 global-DELLA</i> mutants compared to wild type	48
Figure 3.6 Style elongation is mediated by gibberellins	49
Figure 3.7 Transcript levels of <i>DELLA</i> genes through stages 11-12, 15, 17a and 17b of <i>Arabidopsis</i> flower and fruit development	51
Figure 3.8 Analysis of the parthenocarpy conferring capacity of the different <i>della</i> mutant combinations	53
Figure 3.9 Facultative parthenocarpic <i>della</i> -mutants	54
Figure 3.10 IAA concentration measurements in emasculated and hand-pollinated <i>Ler</i> , <i>global-DELLA</i> mutant and <i>ga1-3 global-DELLA</i> mutant gynoecia 7 DPA	56
Figure 3.11 IAA promotes wild-type pistil elongation	57
Figure 3.12 GA ₃ promotes pistil elongation in wild-type, <i>global-DELLA</i> mutant and <i>ga1-3 global-DELLA</i> mutant plants	59
Figure 3.13 GA ₄ promotes pistil elongation in <i>global-DELLA</i> mutant and <i>ga1-3 global-DELLA</i> mutant plants	60

page

Figure 3.14 IAA and GA ₃ promote pistil elongation in gai-1 mutants	62
Figure 3.15 GA ₃ treatment of <i>gid1a/1b/1c</i> triple mutants	63
Figure 3.16 DELLA-independent GA response is 26S proteasome dependent	65
Figure 3.17 SPATULA's role in the DELLA-independent GA response	66
Figure 3.18 STP-HA is stable upon GA ₃ treatment	68
Figure 3.19 SPT does not interact with GID1A receptor in yeast-two-hybrid	69
Figure 3.20 Tissue analysis of Ler, <i>global-DELLA</i> mutant and <i>ga1-3 global-DELLA</i> mutant pistils	71
Figure 3.21 Comparison of cell length and cell number in Ler, <i>global-DELLA</i> and <i>ga1-3 global-DELLA</i> pistil sections	72
Figure 3.22 <i>ML1::GUS</i> expression pattern at flowers stages 7-13	75
Figure 3.23 <i>ML1::GUS</i> expression pattern at fruits stages 14-17a	76
Figure 3.24 <i>ACI1::GUS</i> expression pattern at fruits stages 6-17a	77

	page
Figure 3.25 GA signalling during fruit development	85
Figure 4.1 DELLA proteins' mode of action	92
Figure 4.2 Schematic representation of the yeast two-hybrid system	93
Figure 4.3 Complete yeast matrix	99
Figure 4.4 ALC-DELLA interaction	101
Figure 4.5 Quantification of ALC-DELLA interaction	102
Figure 4.6 Characterisation of IND-SPT protein interaction	104
Figure 4.7 Quantification of IND-SPT interaction	106
Figure 4.8 Schematic representation of the yeast two-one hybrid system	107
Figure 4.9 Binding of IND and/or SPT to a putative E-box variant in <i>SPT</i> promoter	108
Figure 5.1 Sequence analysis of heterozygous <i>pistillata-1</i> mutants	120
Figure 5.2 Diagram of the forward-genetic approach	121
Figure 5.3 Growth of the 10,200 individuals of the M1 population	122
Figure 5.4 Somatic mutations commonly observed in M1 population	124
Figure 5.5 Effectiveness of EMS treatment	125
Figure 5.6 Putative parthenocarpic mutants	127

	page
Figure 5.7 Mutant 35.1	129
Figure 5.8 Mutant 117.1	131
Figure 5.9 Pistil close-ups of mutant 117.1 showing consistent fertilisation-independent pistil elongation	132
Figure 5.10 117.1 <i>pi-1</i> pistils are significantly longer than <i>pi-1</i> pistils	133
Figure 5.11 117.1 carries a parthenocarpy-conferring mutation and results in enlarged mesocarp cells	134
Figure 5.12 Tissue analysis of longitudinal sections of fully elongated 117.1 <i>pi-1</i> mutant pistils	136
Figure 5.13 Recombination frequency of markers used in 117.1 Mapping	139
Figure 5.14 Three-point cross-analysis to determine the correct order of the three loci	140
Figure 6.1 Representation of stage 13 <i>Arabidopsis</i> pistil	150
Figure 6.2 <i>GAL4-GFP</i> enhancer-trap system	151
Figure 6.3 GFP expression in the <i>GAL4-GFP</i> enhancer-trap lines used in this study	156
Figure 6.4 Characterisation of <i>GAL4-VP16</i> insertion site in M0064 and M0070 by TAIL-PCR	158

	page
Figure 6.5 Confirmation of the <i>GAL4-VP16</i> insertion site in M0064 and M0070 by PCR	159
Figure 6.6 GUS staining of <i>PAP10::GUS</i> in three weeks old seedlings of transgenic line 4	160
Figure 6.7 GUS staining of <i>PAP10::GUS</i> in three weeks old seedlings of transgenic line 6	161
Figure 6.8 GUS staining of <i>PAP10::GUS</i> in three weeks old seedlings of transgenic line 10	162
Figure 6.9 GUS staining of <i>PAP10::GUS</i> in floral and fruit tissue of transgenic line 4	164
Figure 6.10 GUS staining of <i>PAP10::GUS</i> in floral and fruit tissue of transgenic line 6	165
Figure 6.11 GUS staining of <i>PAP10::GUS</i> in floral and fruit tissue of transgenic line 10	166
Figure 6.12 GUS expression pattern in root tips in two independent transgenic lines in response to a variety of stimuli	168
Figure 6.13 Cluster analysis of amino acid sequences of PAPs in Arabidopsis	170
Figure 6.14 Representation of the mutant T-DNA insertion lines of <i>pap10</i> and <i>pap12</i> used in this study	171

	page
Figure 6.15 List of <i>pap10</i> and <i>pap12</i> mutant lines used in this study	172
Figure 6.16 General diagram of a novel three-component gene expression system	175

Appendices

Appendix 1 Tables and statistics	191
Appendix 2 PhD Rotations	237
Appendix 3 Publications	272

References 274

List of abbreviations xxi

LIST OF ABBREVIATIONS

ABA	Abscisic acid
ACC	1-aminocyclopropane-1-carboxylic acid
<i>ACI1</i>	<i>ALCATRAZ-INTERACTING PROTEIN 1</i>
-AD	GAL 4 activation domain
AD primer	Arbitrary degenerate primer
ALC	ALCATRAZ
ARF	AUXIN RESPONSE FACTOR
<i>ats</i>	<i>aberrant testa shape</i>
-BD	GAL4 DNA-binding domain
bHLH	basic helix-loop-helix
BSA	Bovine serum albumin
<i>CER6</i>	<i>ECERIFERUM 6</i>
CI	Confidence interval
Col-0	Columbia-0
CPS	<i>ENT-COPALYL DIPHOSPHATASE SYNTHASE</i>
<i>ctr1</i>	<i>constitutive triple response 1</i>
DEX	Dexamethasone
DMSO	Dimethyl sulfoxide
DNA	Deoxyribonucleic acid
dNTP	Deoxyribonucleotide triphosphate
DPA	Days post-anthesis
E	Emasculated
EMS	Ethanyl methanesulfonate
ETT	ETTIN
<i>fer/srn</i>	<i>feronia/sirene</i>

FIE	FERTILISATION INDEPENDENT ENDOSPERM
FIS1	FERTILISATION INDEPENDENT SEED 1
FIS2	FERTILISATION INDEPENDENT SEED 2
FUL	FRUITFULL
GA	Gibberellin
GA1	GIBBERELLIN REQUIRING 1
GA13ox	GIBBERELLIN 13-OXIDASE
GA20ox	GIBBERELLIN 20-OXIDASE
GA2ox	GIBBERELLIN 2-OXIDASE
GA3ox	GIBBERELLIN 3-OXIDASE
GABA	γ -amino butyric acid
GAI	GIBBERELLIN INSENSITIVE
GFP	Green fluorescent protein
GID1	GIBBERELLIN INSENSITIVE DWARF 1
GSI	Gametophytic self-incompatibility
GUS	Beta-glucuronidase
HAP2	HAPLESS 2
HP	Hand pollinated
IAA	Indole-3-acetic acid
IND	INDEHISCENT
IPT	ISOPENTENYL-TRANSFERASE
KAO	<i>ENT</i> -KAURENOIC ACID OXIDASE
KO	<i>ENT</i> -KAURENE OXIDASE
KS	<i>ENT</i> -KAURENE SYNTHASE
LB	Lysogeny broth

Ler	<i>Landsberg erecta</i>
Leu	Leucine
LiAc	Lithium acetate
Man	Mannitol
MEA	MEDEA
MeJa	Methyl jasmonate
MET1	METHYLTRANSFERASE 1
ML1	<i>MERISTEM LAYER 1</i>
MS medium	Murashige and Skoog medium
MSI1	MULTICOPY SUPPRESSOR OF IRA 1
NAA	α -naphthalene acetic acid
OD	Optical density
O-GlcNAc	O-linked n-Acetylglucosamine
ONPG	o-nitrophenyl β -D-galactopyranoside
P	Probability
PAP	PURPLE ACID PHOSPHATASE
PAT	Polar auxin transport
pat2	<i>parthenocarpic fruit 2</i>
PCR	Polymerase chain reaction
PEG	Polyethylene glycol
pi-1	<i>pistillata-1</i>
PIF	PHYTOCHROME INTERACTING FACTOR
PIL	PHYTOCHROME INTERACTING FACTOR LIKE
pop-1	<i>pollen-pistil incompatibility 1</i>
Q-PCR	Quantitative PCR

RBR1	RETINOBLASTOMA-RELATED PROTEIN 1
RGA	REPRESSOR OF GA
RGL	RGA-LIKE
RNA	Ribonucleic acid
RNAi	RNA interference
RPL	REPLUMLESS
RPM	Revolutions per minute
RT	Room temperature
S	Selfed
SD	Standard deviation
SI	Self-incompatibility
SLY1	SLEEPY 1
SPT	SPATULA
SPY	SPINDLY
SRK	S-receptor kinase
SSI	Sporophytic self-incompatibility
syl	<i>scylla</i>
T-DNA	Transfer DNA
TE buffer	Tris EDTA buffer
TIR1	TRANSPORT INHIBITOR RESPONSE 1
Trp	Tryptophan
<i>tt1</i>	<i>transparent testa 1</i>
UAS	Upstream activator sequences
Ura	Uracil
VM	Valve margin

YPD

Yeast extract-peptone-dextrose

CHAPTER 1

General introduction

CHAPTER 1

General introduction

1.1 Introduction

Fruit initiation and fruit development are key steps in the dispersal and survival strategies of many flowering plants. The fruit can be generally defined as the mature ovary that forms a specialised structure to protect the seeds and disperse them at maturity (Roeder and Yanofski, 2006). Not surprisingly, due to its biological importance, fruit development is a tightly regulated process which relies on the coordinated development of seed and ovary structures. This coordination is achieved through active seed-pod communication and three hormones (auxin, gibberellins and cytokinins) are believed to play a central role in the control of fruit growth (King, 1947; Ozga et al, 2002; Ozga et al, 2003; Srinivasan and Morgan, 1996; Vivian-Smith and Koltunow, 1999). In the last decade, particular interest has been paid to the study of the molecular and genetic basis underlying hormonal control of fruit initiation and growth (Vivian-Smith et al, 2001; Wang et al, 2005; Goetz et al, 2006; Goetz et al, 2007; Marti et al, 2008; Ross et al, 2008; de Jong et al, 2009b; Dorcey et al, 2009; Molesini et al, 2009). However, relatively few molecular players have been isolated and little is known about the spatio-temporal coordination of the different signalling cascades. The aim of the present study is to contribute towards a better understanding of the hormonal and genetic mechanisms involved in the control of fruit initiation and growth by focusing particularly on the discovery of novel components of this regulatory network and by further elucidating GA-signalling during fruit initiation and growth in the model plant *Arabidopsis thaliana* (named Arabidopsis hereafter).

Arabidopsis fruit develops from a gynoecium formed by two fused carpels (Smyth et al, 1990). Flower and fruit development in this species has been comprehensively summarised and divided into 20 stages (Smyth et al, 1990) and two events mark the beginning of fruit initiation: pollination which occurs at

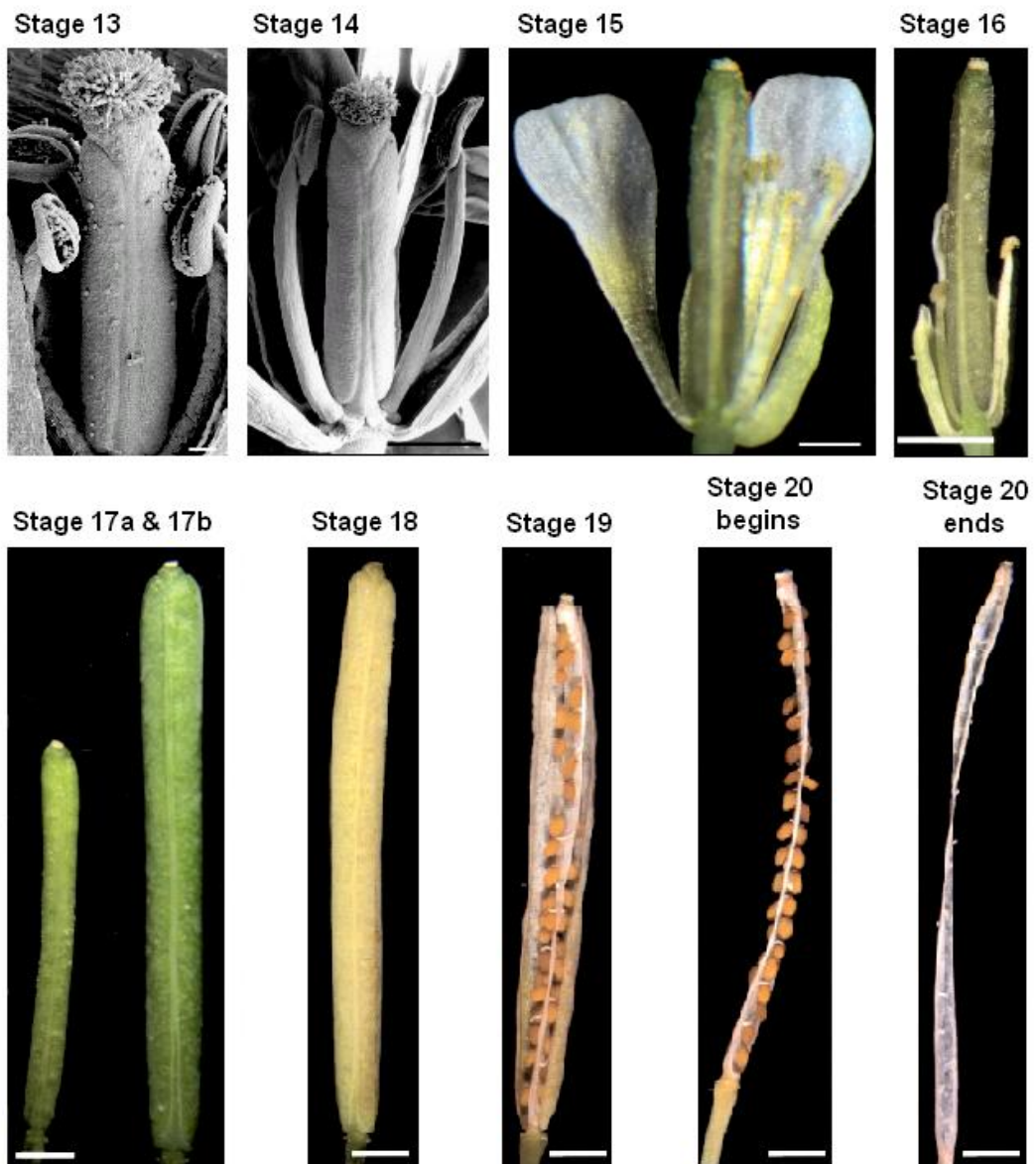


Figure 1.1 Chronological representation of fruit development. Stage 13 or anthesis, the flower opens and self pollinates. Bar = 100 µm. Stage 14, the stamens extend above the stigma and fertilisation occurs. Bar = 500 µm. Stage 15, the gynoecium extends above the stamens. Bar = 500 µm. Stage 16, the sepals, petals and stamens wither and fall. Bars= 1 mm. Stage 17a, all the organs fall from the green siliques. Stage 17b, the siliques elongates completely. Bar = 1 mm. Stage 18, the siliques turns yellow. Bar = 1 mm. Stage 19, the siliques turns brown and dehiscence occurs. Bar = 1 mm. Stage 20, seed abscission occurs. Bar = 1 mm. (Adapted from Smyth et al, 1990; Roeder and Yanofski, 2006).

anthesis or stage 13 of *Arabidopsis* flower development once anthers dehisce, and fertilisation, which occurs at stage 14 of *Arabidopsis* flower development when the flower is fully opened (Smyth et al, 1990; Roeder and Yanofski, 2006) (see Figure 1.1).

1.2 Pollination

1.2.1 Pollen-stigma interaction

Sexual reproduction in flowering plants relies on complex communication events which will ensure the coordinated development of seed and ovary structure, and pollen-stigma recognition can be considered the first event of this communication network. Upon landing of the pollen grain on the stigma, a signalling cascade commences which determines whether the pollination event would lead to fertilisation.

Three types of mating systems can be found in flowering plants: self-fertilisation, cross-fertilisation and mixed mating systems where both self- and cross-fertilisation can occur (Goodwillie et al, 2005). The main mechanism to impair self-fertilisation is the self-incompatibility (SI) system which can be of a gametophytic nature (GSI) or sporophytic nature (SSI) (Suzuki, 2009). In SSI systems, as a result of intercellular communication self pollen is rejected on the stigma papilla cells while in GSI systems, self pollen tube growth is arrested before reaching the female gametophytes (Suzuki, 2009). The best understood SI systems are: S-receptor kinase (SRK)-based SSI systems in Brassicaceae; S-RNase-based GSI systems in Solanaceae, Rosaceae and Plantaginaceae; and S-glycoprotein-based GSI systems in Papaveraceae (Suzuki, 2009; Tarutani et al, 2010; for a detailed review on this subject see Franklin-Tong, 2008).

1.2.2 Pollen germination and pollen-tube growth

In viable crosses, re-hydration of the pollen grains in the stigma surface leads to pollen germination and pollen tube emergence. The pollen tube is a fast tip-growing cytoplasmic extension, the role of which is to deliver the two sperm cells in to the embryo sac to allow double fertilisation (Boavida et al, 2005).

The first evidence for the hormonal control of fruit initiation and development can be found during pollen germination and pollen-tube growth. In rice, *de novo* GA synthesis in the pollen grains is required for pollen germination (Chhun et al, 2007). Gibberellins have also been shown to be necessary for pollen-tube growth across different species (Singh et al, 2002; Cox and Swain, 2006; Chhun et al, 2007). In addition to gibberellins, female-origin auxin has also been suggested to play a role in pollen germination and pollen-tube growth (Chen et al, 2008; Wu et al, 2008a, Wu et al, 2008b).

1.2.3 Pollination in the context of fruit initiation

In most cases, pollination followed by successful fertilisation marks the beginning of fruit initiation. However, fertilisation independent fruit development is also commonly observed in species such as tomato (Goetz et al, 2007) and citrus plants (Talon et al, 1992) among other species. Orchid flowers have provided one of the best model systems for the study of pollination regulated ovary and fruit development due to the time elapsed between pollination and fertilisation, which can vary from 7 to up to 130 days depending on the orchid species (Duncan and Curtis, 1942). Unlike most flowers, at anthesis the ovary in orchids is still immature and pollination alone is able to induce certain developmental programmes such as ovule differentiation and maturation (Zhang and O'Neill, 1993). Nevertheless, there is no evidence suggesting that pollen-stigma recognition alone may induce fruit initiation (Zhang and O'Neill, 1993).

In contrast, early studies of the role played by the pollen tube in fruit initiation suggested that pollen-tube growth in self-incompatible pollinations in orchids is

enough to stimulate fruit development (Hildebrand, 1865). Later measurements of pollen-tube growth suggested that the base of the style had to be reached to induce fruit initiation (Yasuda, 1936). It was initially hypothesised that pollen-tube growth facilitated the transfer of growth promoting substances from the pollen to the ovary (Gustafson, 1939). This hypothesis was soon ruled out due to the low quantities of hormones present in pollen tubes and it was followed by the proposal that pollen tubes may secrete an enzyme responsible for the activation of auxin synthesis in the ovary (van Overbeek et al, 1941; Muir, 1942). Although relatively high concentrations of free IAA have been shown in germinating pollen grains and in growing pollen tubes (Aloni et al, 2006), how pollen-tube growth may stimulate fruit initiation remains to be clarified. Furthermore, it is likely that the role of pollen tubes in fruit initiation may vary between different species. In tomato RNAi-mediated silencing of Chalcone synthase, an enzyme involved in flavonoid synthesis, results in fertilisation-independent fruit development and impaired pollen-tube growth (Schijlen et al, 2007). The fertilisation-independent fruit development in this case has also been associated with observed pollen-tube growth (Schijlen et al, 2007). However, it is interesting to note that in many species with late-acting self-incompatibility where self pollen tubes can successfully grow through the ovary, no fruit initiation has been reported (Bittencourt et al, 2003; Gibbs et al, 2004; Bittencourt and Semir, 2005). Thus, it is possible that the fruit initiating capacity of pollen tubes may not only vary between different species but also in relation to their self-incompatibility systems.

1.3 Fertilisation

1.3.1 Pollen-tube guidance

Successful fertilisation relies on the delivery of the two sperm cells by the pollen tube to the female gametophyte and, thus, pollen-tube guidance towards a receptive ovule is vital for successful fertilisation. Pollen-tube growth through the transmitting tract and guidance towards a receptive ovule is controlled firstly by sporophytic signals followed by gametophytic signals (Fan et al, 2008). Female sporophytic tissue provides in first instance long-range signals to guide the pollen

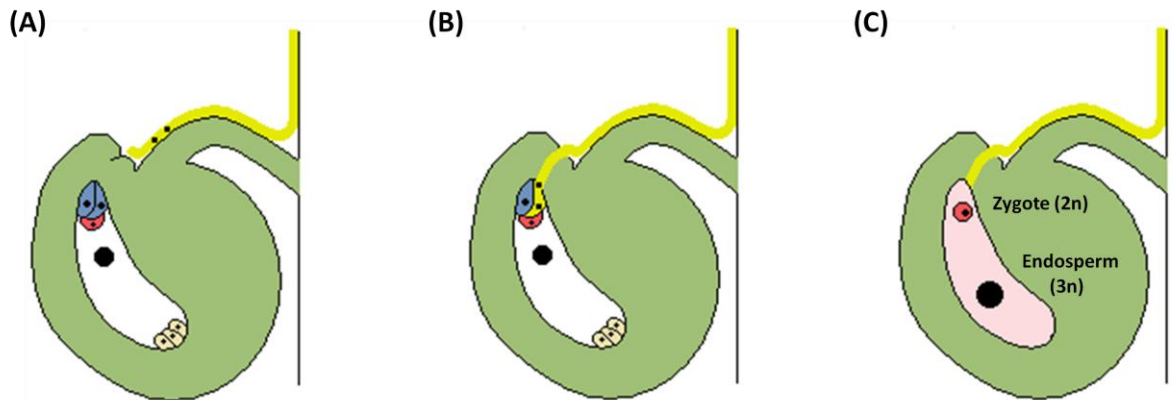


Figure 1.2 Double fertilisation. (A) Representation of receptive *Arabidopsis* ovule upon pollination. Pollination occurs at stage 13 of *Arabidopsis* flower development. The pollen tubes grow through the transmitting tract of the pistil to encounter the receptive ovules. Mature ovules contain the synergid cells (in blue), the egg cell (in red), the central cell (in the centre) and three antipodal cells. (B) Degeneration of synergid cell and discharge of sperm cells. (C) Formation of diploid zygote (by fusion of egg cell and a sperm cell) and triploid endosperm (by fusion of the two polar nuclei of the central cell and a sperm cell).

tube. For example, a γ -amino butyric acid (GABA) gradient throughout the pollen-tube pathway has been found to guide pollen-tube growth in the ovary (Palanivelu et al, 2003). Similarly, disruption of the plantacyanin gradient in *Arabidopsis* pistils by overexpression of this extracellular matrix protein also results in disrupted pollen-tube guidance (Dong et al, 2005). Several studies have shown that the female gametophyte is not required for pollen-tube growth through the stigma and style (Hülskamp et al, 1995; Higashiyama et al, 1998). However, receptive ovule targeting requires short-range signals which are provided by both female and male gametophytes.

The female gametophyte is a relatively complex structure containing seven specialised cells: two synergid cells and an egg cell located at the micropylar end, a central cell and three antipodal cells located in the chalazal end (opposite to the micropylar end) (see Figure 1.2A). Three types of female gametophytic cells (synergid cells, central cell and egg cells) have been shown to play a role in micropylar pollen-tube guidance (Higashiyama et al, 2001; Kashara et al, 2005; Chen et al, 2007; Alandete-Saez et al, 2008; Rotman et al, 2008). For example in *Arabidopsis*, mutation of *MYB98* transcription factor leads to defects in the development of synergid cells which, in turn, are unable to attract pollen tubes (Kashara et al, 2005). This short range guidance of pollen tubes is believed to rely on chemo-attractant production and secretion by the female gametophyte. Consistent with this hypothesis, two cysteine-rich polypeptides belonging to the subgroup of defensin like proteins (LUREs) and secreted by the synergid cells were recently found to act as chemo-attractants (Okuda et al, 2009). Interestingly, fertilised ovules repel supernumerary pollen tubes suggesting that either the release of ovule attractants such as LUREs terminates after fertilisation or, alternatively but not mutually exclusively, a new signal repels additional pollen tubes (Palanivelu and Preuss, 2006).

The role played by the male gametophyte in pollen-tube guidance has been studied to a lesser degree and, to date, only *HAP2*, a sperm-specific gene has been shown to be required for optimal ovule targeting (von Besser et al, 2006).

1.3.2 Double fertilisation

In flowering plants, double fertilisation refers to the two fertilisation events that take place in a coordinated manner to give rise to the endosperm and embryo. In *Arabidopsis*, upon arrival of the pollen tube to the micropylar end of the ovule, death of one of the synergid cells occurs (Sandaklie-Nikolova et al, 2007). Pollen-tube entrance through the degenerated synergid cell is followed by the cessation of pollen-tube growth and discharge of the sperm cells (see Figure 1.2B). Although initially synergid degeneration was considered to be sufficient for pollen-tube rupture and sperm cell release, more recent studies have shown that in *Arabidopsis* the FERONIA/SIRENE receptor-like kinase expressed in the synergid cells is necessary for pollen-tube growth arrest and sperm cell release (Huck et al, 2003; Rotman et al, 2003; Escobar-Restrepo et al, 2007). Non motile sperm cells are transported along microfilaments to the egg and central cell (Ye et al, 2002; Weterings and Russell, 2004) where they fuse to form a diploid zygote and a triploid endosperm respectively (Faure et al, 2002; see Figure 1.2C). Following double fertilisation, ovule integuments in *Arabidopsis* differentiate into the seed coat which encloses the developing endosperm and embryo (Ingouff et al, 2006).

A complex signalling cascade ensures the optimal coordination of double fertilisation events (for a detailed review on this topic see Dresselhaus, 2005). However, miscommunication during pollination/fertilisation or female gametophytic development can result in fertilisation-independent fruit development.

1.4 Fertilisation independent fruit development

In general terms, two types of fertilisation-independent fruit development can be distinguished: apomictic fruit development (fertilisation-independent fruit development containing asexually formed seeds) and parthenocarpic fruit development (fertilisation-independent fruit development lacking seeds). Miscommunication events during pollination/fertilisation or female gametophytic development can lead to apomictic fruit development emphasizing the role of ovule and seed development in the control of fruit initiation. On the other hand,

parthenocarpic fruit development is often related to a hormonal imbalance in the ovary structures leading to the release of fruit growth repression.

1.4.1 Apomixis

The word apomixis is derived from the latin prefix *apo-* (from, off, separate) and the greek *mixis* (mingling) (Oxford dictionary). In flowering plants, apomixis is defined as the asexual formation of a seed from the maternal tissues of ovules, avoiding the processes of meiosis and fertilisation (Bicknell and Koltunow, 2004) and, although often considered a rare event, it is relatively common, occurring in approximately 60% of the British flora (Richards, 2003). Independently of the mechanism giving rise to apomictic seeds, apomixis has traditionally been divided into three developmental steps: the generation of a cell capable of forming an embryo without meiosis (apomeiosis); the fertilisation-independent development of the embryo (parthenogenesis) and the ability to produce an autonomous endosperm or to use an endosperm resulting from fertilisation (Koltunow, 1993; Bicknell and Koltunow, 2004). Thus, as with sexual reproduction, apomixis has traditionally been considered to result in viable seed production. To the author's knowledge, no apomictic food crops have been described to date; however, the discovery of *dyad/swi1* mutants in *Arabidopsis* may contribute towards the engineering of apomictic plants. Mutation of a regulator of meiotic chromosome organisation in *dyad/swi1* mutants leads to triploid seeds as the result of female diploid (apomeiosis) and male haploid gamete fusion (Ravi et al, 2008). This represents the first step towards viable apomictic seed development in *Brassicaceae*. However, in the context of apomictic fruit development and for the purpose of this study, all spontaneous initiation of seed development resulting in fertilisation independent fruit growth has been considered, even when the developmental programme does not result in viable seed production.

1.4.1.1 The role of the egg cell and central cell in fruit initiation

Fertilisation-independent endosperm development can often result in fertilisation-independent fruit initiation (Ohad et al, 1996; Grossniklaus et al, 1998; Luo et al,

1999; Kohlen et al, 2003; Jullien et al, 2008). Several genes which result in endosperm development in the absence of fertilisation have been characterised including: *FERTILISATION INDEPENDENT ENDOSPERM (FIE)* (Luo et al, 1999; Ohad et al, 1999), *MULTICOPY SUPPRESSOR OF IRA1 (MSI1)* (Kohler et al, 2003), *FERTILISATION INDEPENDENT SEED2 (FIS2)* (Chaudhury et al, 1997; Luo et al, 1999), *MEDEA (MEA*, also known as *FIS1*) (Chaudhury et al, 1997; Grossniklaus et al, 1998; Luo et al, 1999) and *RETINOBLASTOMA-RELATED PROTEIN1 (RBR1)* (Ebel et al, 2004). *MEA*, *FIE* and *FIS2* are collectively known as the *FIS* class genes and are primarily involved in the restriction of central cell proliferation in the absence of fertilisation (Grossniklaus et al, 2001). The *FIS* class-proteins are likely to interact together to form a multiprotein Polycomb group (PcG) complex and together with *MSI1* and *RBR1* are predicted to act as transcriptional repressors through chromatin remodelling (Kohler et al, 2003; Makaverich et al, 2006; Pien and Grossniklaus, 2007). In *msi* and *fis* mutants in addition to autonomous endosperm development, embryo-like structures are also occasionally observed in their asexual seeds (Chaudhury et al, 1997; Guitton and Berger, 2005), suggesting that the central cell may also play a role in the control of fruit initiation.

More recently characterisation of *scylla (sy1)* mutants lead to the discovery of a link between autonomous endosperm development and short-range pollen-tube guidance by the FERONIA/SIRENE receptor-like kinase. As in *fer/srn* mutant ovules, in *sy1* ovules pollen tubes fail to stop and burst once the synergid cell is reached and, consequently, continue to grow inside the female gametophyte (Huck et al, 2003; Rotman et al, 2003; Escobar-Restrepo et al, 2007; Rotman et al, 2008). In addition, a low percentage of *srn* ovules also show a fertilisation independent endosperm development reminiscent of the *fis* class mutants (Rotman et al, 2008). Following this discovery, detailed characterisation of *fer/srn* mutants showed that a low proportion of ovules also showed autonomous endosperm development while, conversely, a small percentage of *msi1* ovules showed abnormal pollen-tube reception phenotype (Rotman et al, 2008). Taken together, these findings suggest a link between the *FIS* pathway controlling endosperm development and the pollen-tube guidance imposed by the FERONIA/SIRENE receptor-like kinase. However while in *fis* class mutants and

msi and *rbr1* mutants, autonomous endosperm development triggers fertilisation-independent pistil elongation (Ohad et al, 1996; Grossniklaus et al, 1998; Luo et al, 1999; Kohlen et al, 2003; Jullien et al, 2008), no fertilisation-independent fruit initiation has been described to date in *syl* or *srn* mutants (Rotman et al, 2008).

1.4.1.2 The role of integuments in fruit initiation

Several observations suggest that integument development also play a role in the control of fruit initiation. In *msi* and *fis* mutants, which show autonomous endosperm development, a marked integument growth has also been reported (Chaudhury et al, 1997; Ingouff et al, 2006). Although detailed analysis concluded that the autonomous endosperm development in these mutants was responsible for the integument growth (Ingouff et al, 2006), it is possible that the fertilisation-independent pistil elongation observed may be triggered by both endosperm and integument development. In support of this hypothesis, loss-of-function of the DNA methyltransferase *MET1*, promotes cell proliferation in the integuments which in turn results in fertilisation-independent fruit initiation (FitzGerald et al, 2008). Furthermore, the facultative parthenocarpy observed in *arf8* mutants is also significantly enhanced as a result of integument defects in the *ats arf8* double mutants (Vivian-Smith et al, 2001). Mutation of *ATS* (*ABERRANT TESTA SHAPE*) results in misshapen seeds due to the formation of a three cell layer integument in place of the normal inner and outer integuments composed of five cell layers (Leon-Kloosterziel et al, 1994; Schneitz et al, 1995). However, mutation of *ats* alone does not result in fruit growth promotion (Vivian-Smith et al, 2001).

1.4.2 Parthenocarpy

The word parthenocarpy is derived from the greek *parthenos* (virgin) and *karpos* (fruit) (Oxford dictionary). In botany, parthenocarpy is defined as the growth of the ovary into a seedless fruit in the absence of pollination and/or fertilisation (Lukyanenko, 1991). As is the case with apomixis, parthenocarpy fruit production is not uncommon and parthenocarpic crop plants have long been cultivated by humankind. For example, parthenocarpic figs have been known and actively

cultivated for approximately 11,000 years (Kislev et al, 2006). The prevalence of certain capacity for parthenocarpy in many common crops is evident when considering commercial tomato cultivars as examination of 23 cultivars concluded that all of them exhibited certain degree of ovary growth after emasculation (Goetz et al, 2007).

In broad terms, two types of parthenocarpic fruit production can be distinguished: obligate parthenocarpy (when only seedless fruits are produced) and facultative parthenocarpy (when seedless fruits are only produced if fertilisation is impaired) (Varoquaux et al, 2000). Parthenocarpy has traditionally been associated with high levels of growth promoting substances (phytohormones) in the ovary (Varoquaux et al, 2000) and three hormones (auxin, gibberellins and cytokinins) have been shown to promote parthenocarpic fruit development in a variety of species (King, 1947; Ozga et al, 2002; Ozga et al, 2003; Srinivasan et al, 1996; Vivian-Smith and Koltunow, 1999).

14.2.1 The role of auxin in parthenocarpic fruit growth

Auxin has long been known to be involved in the control of fruit initiation and growth (Gustafson, 1936). Application of NAA (α -naphthalene acetic acid, a synthetic auxin-like growth regulator) to unpollinated ovaries promotes parthenocarpic fruit development in many species such as pea (Eeuwens and Schwabe, 1975), tomato (King, 1947; Chareonboonsit et al, 1985) and *Arabidopsis* (Vivian-Smith and Koltunow, 1999) amongst others. Similarly to auxin application, *DefH9-iaaM* gene construct also results in parthenocarpic fruit development in several solanaceous and rosaceae crops (Rotino et al, 1997; Mezzetti et al, 2004). The *iaaM* gene product from *Pseudomonas syringae* pv *savastanoi* converts tryptophane to indole-3-acetamide which is then hydrolysed to the auxin indole acetic acid (IAA) and, thus, results in increased levels of IAA in young flower buds when expressed under control of the *DefH9* promoter (placenta/ovule-specific *Antirrhinum majus* gene) (Rotino et al, 1997; Mezzetti et al, 2004).

Although application of auxin to unpollinated ovaries causes parthenocarpic fruit growth across several species, its effects at tissue level vary from species to species. In *Arabidopsis*, auxin treatment of emasculated pistils results mainly in exocarp and mesocarp cell expansion perpendicular to the plane of elongation with only a small increase normal to the plane of elongation (Vivian-Smith and Koltunow, 1999). A slight increase in cell numbers has also been reported normal to the plane of elongation in the mesocarp and exocarp layers, although the increase was not comparable to that observed upon pollination or GA₃ treatment (Vivian-Smith and Koltunow, 1999). In spring rape (*Brassica napus*), cell expansion of the mesocarp layer was also recorded (Srinivasan and Morgan, 1996) while in tomato auxin application has been reported to cause both cell number and cell size increase particularly in the placental tissue (King, 1947). The differences observed between the different species at the tissue level upon auxin treatment may underlie the wider developmental differences between dry and fleshy fruits. However, further histological analysis of auxin mediated parthenocarpic fruits would be required to confirm this hypothesis.

In addition to auxin application, molecular misregulation of the auxin signalling pathway can also lead to parthenocarpic fruit development. In particular, mutation of several members of the AUXIN/INDOLE-3-ACETIC ACID (Aux/IAA) and AUXIN RESPONSE FACTOR (ARF) family of transcription factors have been shown to cause parthenocarpic fruit development in *Arabidopsis* and/or tomato (Wang et al, 2005; Goetz et al, 2006; Goetz et al, 2007; de Jong et al, 2009b; for further information see Section 1.5.1.2).

1.4.2.2 The role of gibberellins in parthenocarpic fruit growth

Application of GA₃ (a synthetic gibberellin) at anthesis to emasculated *Arabidopsis* wild type pistils stimulates pistil elongation but to a lesser degree than pollination and fertilisation (Vivian-Smith and Koltunow, 1999). Although application of GA₃ to unpollinated ovaries causes parthenocarpic fruit development across several species, as for auxin, the effects of GA at the tissue level also vary from species to species. In *Arabidopsis*, GA₃ application influences mesocarp cell division in a

similar way to that observed upon pollination while cell elongation was mainly observed in the exocarp layer (Vivian-Smith and Koltunow, 1999). This is in contrast with spring rape and tomato where GA₃ application resulted primarily in mesocarp cell expansion (Bunger-Kibler and Bangerth, 1982; Srinivasan and Morgan, 1996; Marti et al, 2008),

Irrespective of the complexity of the GA biosynthetic pathway, attempts to increase bioactive gibberellins levels by overexpression of GA biosynthetic enzymes have been relatively successful (Huang et al, 1998; Israelsson et al, 2004; Radi et al, 2006; Fagoaga et al, 2007). However none of these studies focused on the potential parthenocarpy conferring capacity of increased endogenous gibberellins levels. In contrast, mutation of *DELLA* genes, which are major components of the GA signalling pathway, have regularly been shown to cause parthenocarpic fruit development across different species (Marti et al, 2008; Ross et al, 2008; Dorcey et al, 2009; for further information see Section 1.5.2.2).

1.4.2.3 The role of cytokinins in parthenocarpic fruit growth

Application of cytokinins results in parthenocarpic fruit development across different plant species including pea (Garcia-Martinez, 1980), soybean (Crosby et al, 1981), mango (Chen, 1983), spring rape (Srinivasan and Morgan, 1996) and *Arabidopsis* (Vivian-Smith and Koltunow, 1999). Furthermore, cytokinin related parthenocarpic fruit development can also be achieved in tomato by ovary-specific expression of *ISOPENTENYL-TRANSFERASE (IPT)* from *Agrobacterium tumefaciens*, which results in increased cytokinin levels in the ovary (Zichao et al, 2002).

Cytokinins have traditionally been considered to promote growth by inducing plant cell division (Miller et al, 1955). In accordance with this, cytokinin mediated parthenocarpic spring rape is characterised by increase cell numbers across all tissue layers (Srinivasan and Morgan, 1996). Unfortunately, few studies have focused on the parthenocarpy conferring capacity of cytokinins and, consequently,

little is known about the genetic and molecular mechanisms underlying the role of cytokinins in fruit growth promotion (see Section 1.5.3).

1.5 Hormonal cues during fruit initiation and growth

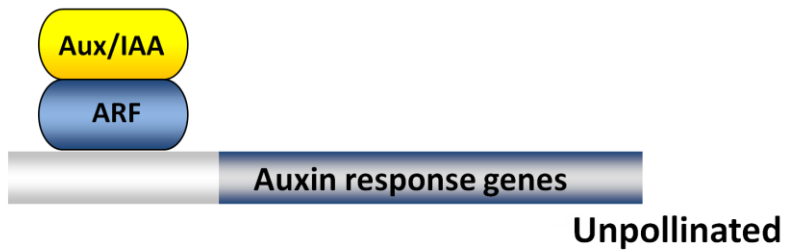
Fruit-growth stimulation by auxin application (Gustafson, 1936) opened the doors to the study of the role played by different hormones in fruit initiation and development. At present three phytohormones, gibberellins, auxins and cytokinins are believed to play a major role in the control of fruit growth upon ovule fertilisation. Application of these hormones alone or in combination has been shown to induce parthenocarpy across different plant species (King, 1947; Ozga et al, 2002; Ozga et al, 2003; Srinivasan et al, 1996; Vivian-Smith and Koltunow, 1999; see Section 1.4.2) which has led to the conclusion that the hormonal control imposed by pollination and fertilisation is required for fruit set and growth. Application of a single hormone to unpollinated ovaries does not promote fruit growth to the same extent as pollination in pea (Ozga et al, 2002), *Brassica napus* (Srinivasan et al, 1996) or *Arabidopsis* (Vivian-Smith and Koltunow, 1999) suggesting that a hormonal interplay is required for normal fruit development (Ozga et al, 2003).

1.5.1 Auxin

1.5.1.1 Auxin biosynthesis in the context of fruit initiation and growth

De novo auxin biosynthesis in ovules upon pollination/fertilisation has long been hypothesised to be required to induce fruit initiation. As previously mentioned, placental and ovule-specific expression of the *iaaM* gene (which results in increased levels of IAA) induces parthenocarpic fruit development in several species (Rotino et al, 1997; Ficcadenti et al, 1999; Mezzetti et al, 2004; Yin et al, 2006) suggesting that seed-originated auxin production is necessary for fruit initiation and growth. The observation that a positive correlation exists between final fruit size and the number of seeds in the fruit supports the existence of a

(A)



(B)

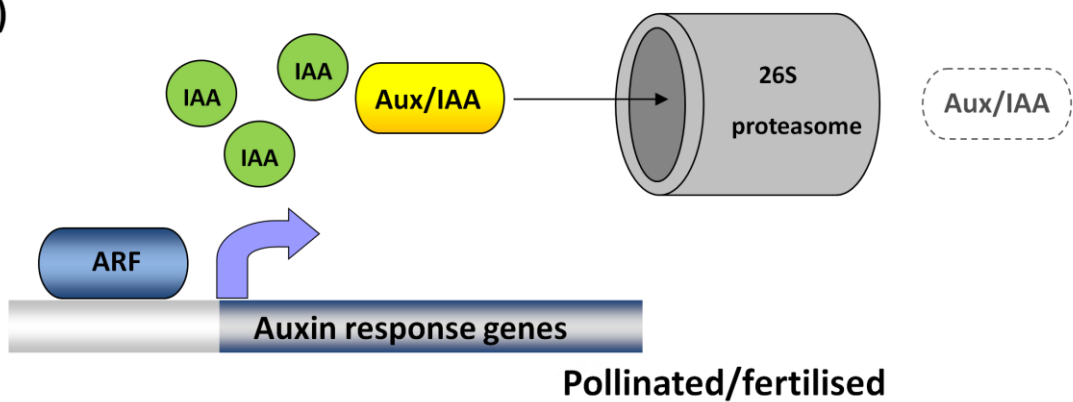


Figure 1.3 Model of ARF-Aux/IAA auxin signal transduction. (A) Before pollination, the activity of ARF transcription factors is inhibited by Aux/IAA protein complexes. (B) Upon pollination/fertilisation, the levels of free auxin increases and Aux/IAA are rapidly ubiquitinated and degraded through the 26S proteasome allowing auxin response gene transcription.

seed-origin growth promoting substance (Varga and Bruinsma, 1976; Vivian-Smith and Koltunow, 1999; Cox and Swain, 2006). A strong indication of increased auxin biosynthesis in ovules upon pollination/fertilisation was finally achieved by visualisation of the synthetic auxin-regulated promoter *DR5* fused to GFP during fruit initiation which showed a high GFP signal in ovules, detected in *Arabidopsis* soon after fertilisation (Dorcey et al, 2009).

1.5.1.2 Auxin signalling in the context of fruit initiation and fruit growth

Several components of auxin signalling have been shown to play a role in the control of fruit initiation and growth, many of which are members of the ARF-Aux/IAA signal transduction pathway (see Figure 1.3). Auxin-dependent transcriptional regulation is believed to rely on the capacity of ARF-Aux/IAA to form heterodimers and repress the transcription of the early auxin response genes (Ulmasov et al, 1997; Tiwari et al, 2001) and auxin mediated binding of the Aux/IAA proteins to the receptor TIR1 (F-box protein part of the E3 ubiquitin ligase complex) is predicted to be required for Aux/IAA degradation via the 26S proteasome (Dharmasari et al, 2005; Kepinski and Leyser, 2005; Maraschin et al, 2009) (see Figure 1.3). Degradation of Aux/IAA leads to the activation of auxin response genes (Dharmasari et al, 2005; Kepinski and Leyser, 2005; Maraschin et al, 2009) (see Figure 1.3). The role of Aux/IAA as negative auxin response regulators during fruit initiation is clear in the case of *IAA9* since downregulation of *IAA9* results in parthenocarpic fruit development in tomato (Wang et al, 2005). Furthermore, transcriptome analysis in tomato has shown that Aux/IAAs and ARFs are strongly regulated during fruit initiation, suggesting that the coordinated regulation of these genes is vital for successful fruit initiation and growth (Wang et al, 2009). However, it is likely that Aux/IAA may play a far more complex role than simple fruit growth repression as upregulation of several tomato Aux/IAA genes has also been reported in response to auxin treatment (*IAA1*, *IAA2*, *IAA3*, *IAA9* and *IAA14*) (Serrani et al, 2008) or pollination (*IAA1*, *IAA3*, *IAA11*, *IAA13*, *IAA14* and *IAA30*) (Want et al, 2009). Although a rapid turnover of the newly synthesised Aux/IAA proteins may occur after pollination (de Jong et al, 2009a) a minimum Aux/IAA level may also be necessary to create a negative feedback loop in the

auxin signal pathway and allow the fine-tuning of the response (Gray et al, 2001; de Jong et al, 2009a). Further characterisation of the role played by individual Aux/IAA transcription factors during fruit initiation particularly with regards to their protein levels would undoubtedly be required in order to fully understand their role as fruit growth repressors.

The role of several *ARFs* in the context of fruit initiation has also been described. In *Arabidopsis* and tomato, expression of aberrant forms of *ARF8* results in parthenocarpic fruit development (Goetz et al, 2006; Goetz et al, 2007). Based on the proposed mode for auxin signal transduction (see Figure 1.3), it has been suggested that *ARF8* and Aux/IAA9 may form a transcription repressing complex (Goetz et al, 2007). Aberrant forms of *ARF8* could act to destabilise this complex allowing the transcription of auxin response genes (Goetz et al, 2007). Silencing of *IAA9* does indeed result in parthenocarpic fruit development (Wang et al, 2005), supporting the *ARF8*-Aux/IAA9 model. Nevertheless, no experimental confirmation of the *ARF8*-Aux/IAA9 interaction exists and it is possible that *ARF8* may similarly interact with other Aux/IAA members. In addition to *ARF8*, *ARF7* has also been shown to play a role in fruit initiation and silencing of *ARF7* results in parthenocarpic fruit development in tomato (de Jong et al, 2009b). The transcript downregulation of *ARF7* upon pollination together with the parthenocarpic fruit phenotype observed, suggests that *ARF7* is a fruit growth repressor (de Jong et al, 2009b) which is in contrast with the predicted role of *ARF8* during fruit initiation (Goetz et al, 2007) and the proposed ARF-Aux/IAA mode of action (see Figure 1.3). Thus, and in agreement with the up regulation of Aux/IAA observed upon pollination, it is likely that auxin signal transduction during fruit initiation may be far more complex than originally anticipated and careful characterisation of the role of the different ARF and Aux/IAA involved in fruit initiation would be required.

In addition to the components of the ARF-Aux/IAA signal transduction pathway, other auxin signal transduction components with unknown functions have also been shown to play a role in fruit initiation and growth. This is the case of the *AUCS1A* gene in tomato, silencing of which results in parthenocarpic fruit development suggesting that a fruit growth repressor function (Molesini et al, 2009). The pleiotropic phenotype observed upon silencing of *AUCS1A* genes was

attributed to increased auxin levels; however, the mechanism for the observed increase in auxin remains to be clarified (Molesini et al, 2009).

1.5.2 Gibberellins

1.5.2.1 Gibberellin biosynthesis in the context of fruit initiation and growth

Several studies have focused on the effect that pollination/fertilisation has on gibberellin biosynthesis. In tomato, pollination/fertilisation results in increased expression levels of GA 20-OXIDASES in the ovary (Serrani et al, 2008). GA 20-OXIDASES together with GA 3-OXIDASES catalyse the final steps of GA biosynthesis (for more detailed review on GA biosynthesis see Olszewski et al, 2002 and Chapter 3). Similarly, in other species such as Arabidopsis and pea, pollination/fertilisation also results in the upregulation of the final steps of GA biosynthesis (Garcia-Martinez et al, 1997; Hu et al, 2008; Ozga et al, 2009; Dorcey et al, 2009). In Arabidopsis, *de novo* GA biosynthesis upon pollination/fertilisation has mainly been located in the fertilised ovules (Dorcey et al, 2009). Although previous studies suggested that GA biosynthesis in maternal tissues also plays a role during fruit development (BenCheikh et al, 1997; Hu et al, 2008; Rieu et al, 2008a).

The upregulation of GA biosynthesis observed upon pollination/fertilisation is in agreement with the studies carried out in *pat* tomato mutants where the parthenocarpic phenotype can at least partially be explained by the higher concentration of gibberellins in *pat* ovaries due to different alterations in the GA biosynthesis pathway (Fos et al, 2000; Fos et al, 2001; Olimpieri et al, 2007).

1.5.2.2 Gibberellin signalling in the context of fruit initiation and growth

The study of the gibberellin signalling pathway has further contributed to the understanding of fruit growth regulation by GA. SPINDLY (SPY) was one of the first molecular players of the GA signalling pathway shown to be involved in the control of fruit initiation and fruit growth in Arabidopsis (Jacobsen et al, 1993). SPY

shows significant homology to animal tetratricopeptide repeat (TRP)-containing serine and threonine O-linked *N*-acetylglucosamine (O-GLcNAc) transferases (Jacobsen et al, 1996) which are involved in post-translational modifications by GlcNAc transfer (Wells et al, 2001). Although doubts still persist about the precise role played by SPY in the control of GA-mediated responses particularly in relation to other components of the signalling pathway (Silverstone et al, 1998; Maymon et al, 2009), it is generally considered to be a negative regulator of the GA response pathway (Jacobsen et al, 1993). Jacobsen et al (1993) showed that several *spy* mutant alleles show facultative parthenocarpy in *Arabidopsis*. This and other phenotypes of the *spy* mutants were suggested to be the consequence of the constitutive activation of the GA perception and/or GA signal transduction (Jacobsen et al, 1993). However, attempts by Vivian-Smith and Koltunow (1999) to repeat the parthenocarpic pistil elongation observed in *spy* mutants failed and, thus, the role of SPY in the control of fruit initiation and/or fruit growth remains to be clarified (Vivian-Smith and Koltunow, 1999).

Other molecular players of the GA signalling pathway known to be involved in fruit development are DELLA proteins. DELLA proteins are members of the GRAS family of regulatory proteins (Bolle, 2004) characterised by a DELLA-motif in their N-terminal domain and SCARECROW-like motif in the C-terminal (Peng et al, 1997; Silverstone et al, 1998). DELLA proteins act as growth repressors by impairing the activity of bHLH transcription factors by interacting with their DNA-binding domain (de Lucas et al, 2008; Feng et al, 2008). GA-mediated degradation of DELLA proteins through the 26S proteosome pathway is required in order to allow transcription factor accumulation and promote growth (for a more detailed review on this subject see Harberd et al, 2009 and Chapters 3 and 4). In accordance with DELLA proteins' role as growth repressors, lack of DELLA proteins results in parthenocarpic fruit development across different species (Martí et al, 2008; Ross et al, 2008; Dorcey et al, 2009). The study of the spatio-temporal expression of *GFP-RGA* in *Arabidopsis* has shown that before fertilisation *RGA* expression is mainly localised in the ovules with a weaker signal in the valves (Dorcey et al, 2009). Fertilisation results in increased GA levels which promote the decrease of *GFP-RGA* signal both in the ovules and valves (Dorcey et al, 2009)

and, thus, allow the release of the repression imposed by DELLA proteins on downstream growth factors.

1.5.3 Cytokinin

Relatively little is known about the genetic and molecular mechanisms underlying the role of cytokinins in fruit initiation and growth. However, several lines of evidence suggest that cytokinins may be involved in the control of endosperm development. High levels of cytokinins have been reported in developing seeds particularly in the endosperm in various species (Burrows and Carr, 1970; Blumenfeld and Gazit, 1970; Emery et al, 1998; Tarkowski et al, 2006). Furthermore, a positive correlation was found between cell division in the endosperm and the level of cytokinins (Emery et al, 1998; Yang et al, 2002; Tarkowski et al, 2006). The role of cytokinins in endosperm development is further supported by transcriptome analysis which showed that cytokinin-responsive and cytokinin biosynthetic gene expression is significantly enriched in the developing endosperm (Day et al, 2008). It is therefore possible that the effect of cytokinins in fruit initiation and growth may occur via endosperm development, as shown by the role played by the central cell/endosperm in the control of fruit initiation (see Section 1.4.1.1). However, due to the lack of genetic evidence linking cytokinin induced endosperm development and fruit initiation and/or growth, it is impossible to conclude whether this is indeed the case.

1.5.4 Ethylene

Although ethylene has traditionally been associated with flower and fruit abscission and fruit ripening (Lin et al, 2009), some data suggest that it may also play a role in the control of fruit initiation. In many species a rapid increase in ethylene is observed upon pollination (Zhang and O'Neill, 1993; Llop-Tous et al, 2000) and, although no fruit initiation and/or growth has been reported, in orchids the elevated ethylene levels contribute to the differentiation and maturation of the ovules and ovaries (Zhang and O'Neill, 1993). A more direct proof of the role of ethylene in fruit initiation and growth was provided by Fang (2003) who showed

that application of 1-aminocyclopropane-1-carboxylic acid (ACC, an ethylene precursor) results in fruit growth promotion in *Arabidopsis*. Furthermore, although the ethylene perception mutant *ctr1-1* does not show parthenocarpic fruit development (Vivian-Smith and Koltunow, 1999), combination of *ctr1-1* mutation with ovule integument defective mutations resulted in facultative parthenocarpic fruit development (Vivian-Smith, 2001), suggesting that the effect of ethylene in fruit growth promotion may require the removal of additional growth repressing factors.

1.5.5 Hormonal cross-talk

Several studies have concluded that a complex hormonal interplay is necessary for normal fruit development. For example in *Arabidopsis*, application of gibberellin together with either cytokinin or auxin is required to restore pistil length to that of pollinated siliques (Vivian-Smith et al, 2001).

Gibberellin and auxin interaction has been the most widely studied hormonal interaction in the context of fruit initiation and fruit growth. Several lines of evidence have shown that upon fertilisation, a seed-origin auxin signal is generated which results in the stimulation of fruit growth by upregulation of gibberellin synthesis. Application of auxin can mimic the stimulation by seeds of fruit growth by promoting gibberellin biosynthesis (Van Huizen et al, 1995; Ngo et al, 2002; Serrani et al, 2007; Serrani et al, 2008; Dorcey et al, 2009; Ozga et al, 2009). Although auxin-mediated GA upregulation is a common feature in all the species investigated, different steps of the GA metabolism have been found to be affected in the different species. In pea and tomato, *GIBBERELLIN 20-OXIDASE* (*GA20ox*) gene expression has been reported to be upregulated in response to auxin or fertilisation, suggesting that *GA20ox* activity is the limiting factor prior to pollination/fertilisation (Van Huizen et al, 1995; Ngo et al, 2002; Serrani et al, 2007; Serrani et al, 2008; Ozga et al, 2009). On the other hand in *Arabidopsis*, an increase in both *GA3ox* and *GA20ox* gene expression is observed upon auxin treatment or fertilisation (Dorcey et al, 2009). It is also interesting to notice that whilst in tomato a downregulation of the GA catabolism (*GA2ox*) was also reported

(Serrani et al, 2007; Serrani et al, 2008; Ozga et al, 2009), in *Arabidopsis* upregulation of the transcription of GA inactivation genes was recorded in response to auxin or fertilisation (Dorcey et al, 2009) and, thus, the regulation of GA catabolism upon auxin and/or fertilisation remains to be further clarified.

In addition to the transcript analysis mentioned previously and, in agreement with the observation that the effect of auxin in fruit initiation and development is at least partially mediated by GA, auxin induced fruit set and development can be significantly reduced by simultaneous application of GA biosynthesis inhibitors (Serrani et al, 2008). In recent years a more detailed reconstruction of the auxin and GA responses triggered upon fertilisation has also been made possible by visualisation of auxin and gibberellin reporter constructs. The synthetic auxin reporter *DR5::GFP* showed that an increase in auxin response is observed in the ovules upon fertilisation (Dorcey et al, 2009). As previously mentioned auxin or fertilisation induced the upregulation of GA biosynthesis (Van Huizen et al, 1995; Ngo et al, 2002; Serrani et al, 2007; Serrani et al, 2008; Dorcey et al, 2009; Ozga et al, 2009) which in turn resulted in the activation of GA signalling in the ovules and valves shown by the downregulation of the fusion protein RGA-GFP in both ovules and valves (Dorcey et al, 2009).

Interestingly, although the results presented above suggest that auxin stimulation of fruit initiation and development is at least partially mediated by GA, no effects in auxin response gene transcription (Vriezen et al, 2007) or *DR5::GFP* expression (Dorcey et al, 2009) was observed upon GA treatment. Thus, it is likely that fertilisation may involve auxin-mediated GA upregulation while the evidence to date would suggest that the opposite is highly improbable. However, additional levels of auxin and GA interaction may also be in place during fruit initiation and growth. Application of auxin or upregulation of the auxin response by introduction of the *arf8-4* mutation does not promote parthenocarpic fruit development in *ga1-3* mutants (Vivian-Smith and Koltunow, 1999; Vivian-Smith et al, 2001). *ga1-3* mutants are impaired in an early step of GA biosynthesis (Sun et al, 1994) and, consequently, produce very low levels of active gibberellins. *ga4-1* and *ga5-1* catalyse later steps of GA biosynthesis and are part of highly redundant enzymatic families (Talon et al, 1990; Chiang et al, 1995; Phillips et al, 1995; Sponsel et al,

1997) and, consequently, produce higher levels of bioactive gibberellins than *ga1-3* mutants. In these weaker GA biosynthesis mutants, in contrast to *ga1-3* mutants, auxin application promotes parthenocarpic fruit development (Vivian-Smith and Koltunow, 1999). Taken together these results suggest that a threshold of endogenous gibberellins is required for auxin-induced fruit development (Vivian-Smith and Koltunow, 1999).

The study of the hormonal regulation of fruit set and development has mainly focused on the role played by gibberellins and auxin and, thus, relatively little is known about the cross-talk between other hormones during fruit initiation. Recent studies have shown that application of cytokinins to unpollinated *Arabidopsis* pistils increased seed-originated auxin, suggesting that cytokinin stimulation of fruit initiation may be at least partially mediated by auxins (Vivian-Smith and Offringa, personal communication). Transcriptome analysis of tomato ovaries during pollination also suggested a possible role of ethylene and abscisic acid (ABA) during fruit initiation and growth (Vriezen et al, 2007; Pascual et al, 2009); although the precise role played by these hormones in the context of fruit initiation and growth remains to be clarified. Initial experiments reported a downregulation of ethylene and ABA biosynthesis is observed upon fruit initiation and, thus, it was proposed that ABA and ethylene may play an antagonistic role to that of GA and auxin by preventing fertilisation-independent fruit initiation (Vriezen et al, 2007). However, more recent transcriptome analysis of parthenocarpic tomatoes revealed an upregulation of ethylene biosynthesis during fruit development (Pascual et al, 2009). It is possible that ethylene might play a role in both fruit growth promotion and repression, and additional levels of regulation such as the spatio-temporal regulation of ethylene synthesis or dosage-dependent regulation may specify its role in fruit initiation and growth. This hypothesis may explain the reported dual role of ethylene in abscission and fruit initiation (Zhang and O'Neill, 1993; Llop-Tous et al, 2000; Lin et al, 2009). Nevertheless further experiments would be required to understand the complex role of ethylene in the context of fruit initiation and growth. In contrast, the role of ABA in the repression of fertilisation-independent fruit initiation is better understood and both auxin and GA treatment reduced ABA biosynthesis in tomato ovaries (Nitsch et al, 2009). However, inhibition of ABA alone does not promote fruit development, suggesting that the

coordination of the different hormonal pathways may also be required (Nitsch et al, 2009).

1.6 Aim of this thesis

Many studies have contributed to a better understanding of fruit initiation and growth. Nevertheless, due to the complex nature of the regulatory pathways governing these processes, many key questions remain to be answered particularly regarding the integration of the components of the different signalling cascades and the spatio-temporal regulation of these. The overall aim of this thesis is to contribute towards a better understanding of the hormonal and genetic mechanisms involved in the control of fruit development upon fertilisation by focusing particularly on the study of parthenocarpy. Three main approaches have been adopted to achieve this aim:

- In-depth characterisation of GA-signalling during fruit initiation and/or growth with particular emphasis on the role played by DELLA proteins
- A forward genetic screen for the discovery of novel mutations resulting in fertilisation-independent fruit development
- Understanding of seed-pod communication to further characterise the coordinated development of seed and fruit structures

CHAPTER 2

General materials and methods

CHAPTER 2

General materials and methods

2.1 Introduction

In this chapter a compilation of the materials and methods repetitively used throughout this thesis is presented. The materials and methods specifically used in the particular projects will be later specified at the beginning of each individual chapter.

2.2 Materials and methods

2.2.1 Edwards' quick DNA extraction

Two young leaves of the plants to be genotyped were collected in Eppendorf tubes containing a stainless steel ball bearing and stored at -80°C. For DNA extraction, the tissue was ground using a 2000 Geno/Grinder (from Spex/Sampleprep) by shaking it at 500rpm for 30 seconds. 400 µl of DNA extraction buffer (200mM Tris HCl pH7.5, 250mM NaCl, 25mM EDTA, 0.5% SDS) was added to the ground tissue and vortexed for 5 seconds. This mixture was subsequently centrifuged at 13,000rpm for 1 minute and 300µl of the supernatant was transferred to a fresh Eppendorf tube. The supernatant was mixed with 300µl isopropanol and left at room temperature for 2 minutes. Following centrifugation at 13,000rpm for 5 minutes, the supernatant was discarded and the pellet was resuspended in 70% ethanol. After a second round of centrifugation at 13,000rpm for 5 minutes, the pellet was air dried and dissolved in 80µl H₂O. The extracted DNA samples were stored at -20°C (modified from Edwards et al, 1991).

2.2.2 General PCR and colony PCR conditions

Generally, PCR reactions (20 μ l) contained 1xPCR buffer, 0.5mM of total dNTPs, 1 μ M of each of the specific primers, 1 μ l taq DNA polymerase and 1 μ l of gDNA or 2 μ l of a 10 μ l miniculture in the case of colony PCRs. PCR reactions were carried out in a Mjresearch-ptc-200PCR Thermal cycler and amplified products from the reactions were analysed by agarose gel electrophoresis.

2.2.3 Sequencing reactions

Sequencing reactions (10 μ l) contained 1 μ l Big Dye v3.1, 1.5 μ l 5xSequencing reaction buffer, 0.32 μ M of the specific primer and 1 μ l DNA (approx. 100-200 ng/ μ l) or PCR products (2-5ng/ μ l per 100bp). Sequencing reactions were carried out in a Mjresearch-ptc-200PCR Thermal cycler with the following cycle:

96°C (1min)	x1
96°C (10sec), 50°C (5sec), 60°C (4min)	x25
10°C (for ever)	

2.2.4 *E. coli* heatshock transformation

DH5 α or Top10 *E. coli* competent cells were used for transformation. Competent cells were thawed and kept on ice for 5-10min. 1-10 μ l of the DNA ligation or plasmid to be transformed was gently mixed with 100 μ l of competent cells and left on ice for another 20min. Following this, competent cells were heatshocked for 90sec at 42°C and chilled on ice for 1-2min. Finally, 500 μ l of LB was added to the cells and incubated at 37°C shaking at 200rpm for 1hr. Transformed cells were plated on selective media and incubated at 37°C overnight until colonies appeared.

2.2.5 *Agrobacterium tumefaciens* electroporation transformation

AGL1 electro-competent cells (25 μ g/ml carbenicillin, 25 μ g/ml rifampicin) were used for transformation. 50-200ng of the DNA to be transformed was added to 40 μ l of electro-competent cells and mixed gently. This mix was placed in a pre-chilled electroporation cuvette and subjected to a pulse length of 8-12 ms in Biorad GenePulser (settings: 2.50kV, 25 μ FD and 400 Ohms). 1ml of LB was immediately added to the cuvette following the pulse and, subsequently, cells were incubated at 28°C with shaking at 250rpm for 2-3hrs. Transformed cells were plated on the appropriate selective media (which included the AGL1 specific antiabiotics and the plasmid specific antibiotics) and incubated at 28°C for 2-3 days until colonies appeared.

2.2.6 Arabidopsis floral dip transformation

A single *A. tumefaciens* colony carrying the plasmid to be transformed was grown in 5 ml of LB medium with the appropriate antibiotics (which included 25 μ g/ml rifampicin and the plasmid specific antibiotics) at 28°C with shaking at 250rpm for 24hrs. This preculture was used to inoculate 500ml of LB with the vector specific antibiotic(s) and the new culture was incubated at 28°C with shaking at 250rpm overnight until a saturated OD₆₀₀ was reached (OD₆₀₀>1.5). The next morning the OD₆₀₀ of the overnight culture was recorded and the culture was centrifuged at 5000rpm for 20 mins at room temperature. The pellet was resuspended in 5% sucrose to an OD₆₀₀ approximately of 0.8 taking the saturation OD₆₀₀ as refence. Just before the floral dipping, Silwet L77 was added to 0.05%. Ten pots containing five Arabidopsis plants each were dipped per plasmid to be transformed. Plants were dipped for approximately 2 mins with the occasional shaking. After the dipping, plants were bagged overnight to maintain the humidity and the next day were transferred to containment.

2.2.7 GUS staining

Sample tissues were prefixed in 90% acetone (4°C) for 20 min at room temperature. After prefixation, samples were rinsed with the reaction buffer (50 mM Na₂PO₄ [pH 7.2], 0.2% triton X-100, 5 mM ferrocyanide, 5 mM ferricyanide) and incubated overnight (if not otherwise specified) in the reaction buffer with 2 mM X-gluc at 37°C. To eliminate endogenous pigments, a series of 30-minute ethanol washes were performed (20%, 30%, 50%, 60% and 70%) after incubation.

2.2.8 Tissue fixation

Tissue fixation was carried out by vacuum-infiltration with FAA solution (3.7% formaldehyde, 5% acetic acid and 50% ethanol) followed by a series of 30-minute ethanol washes (50%, 60%, 70%, 80% and 90%). Tissue was stored overnight in 95% ethanol at 4°C. A second round of 30-minute washes was carried out the following day (3x100% ethanol, 75% ethanol/25% histoclear, 50% ethanol/50% histoclear, 25% ethanol/75% histoclear and 3x100% histoclear). Tissue was stored overnight in 50% histoclear/50% paraplast at 60°C and, to conclude the tissue fixation, six washes of paraplast were performed during a two-day period. Pistils were finally embedded in paraffin and stored at 4°C. A RM 2255 rotary microtome (Leica) was used to make 8 µm thin longitudinal carpel sections.

2.2.9 Tissue staining

In order to visualise the different tissue layers in the tissue sections, tissue staining with Alcian blue 8Gx (which dyes un lignified tissue blue) and Safranin-O (which dyes lignified tissue red) was carried out. After deparaffinisation, sections were treated with Alcian Blue 8Gx/Safranin-O solution (0.05% Alcian Blue 8Gx and 0.01% Safranin-O in 0.1 M acetate buffer [pH 5.0]) for 20 min.

2.2.10 Light microscopy

GUS stained samples or tissue sections were examined under light microscopy using a MZ 16 stereomicroscope (Leica) and the images were captured with a DFC 280 digital camera (Leica).

2.2.11 Cell measurements and cell count

For cell length measurements, cell length normal to the plane of siliques elongation was measured on captured images using ImageJ software (freely available at <http://rsbweb.nih.gov/ij/>). Cell counts were carried out manually.

CHAPTER 3

Fruit development and DELLAs

CHAPTER 3

Fruit development and DELLAs

3.1 Introduction

Fruit initiation has traditionally been attributed to the action of three hormones namely auxin, gibberellins and cytokinins (Gillaspy et al., 1993). Accordingly, application of these hormones either alone or in combination can induce fruit growth even in the absence of fertilisation across a wide variety of plant species (Gustafson, 1936; King, 1947; Srinivasan and Morgan, 1996; Vivian-Smith et al, 1999; Ozga et al, 2002; Ozga et al, 2003). In recent years, many of the molecular and genetic mechanisms underlying the action of phytohormones during fruit initiation and fruit development have been identified, uncovering as a result, the complexity of this regulatory network.

3.1.1 GA metabolism during fruit development

GA metabolism highlights the complexity of the hormonal regulation of fruit development. The first step of GA biosynthesis is controlled through the action of a single enzyme, *ENT-COPALYL DIPHOSPHATE SYNTHASE* (*CPS*) (Olszewski et al, 2002). Strong mutant alleles of *CPS* such as *ga1-3* result on a lack of gibberellins and have been widely used in the study of GA signalling (Cheng et al, 2004; Tyler et al, 2004; Archard et al, 2009; Ubeda-Tomas et al, 2009). *ga1-3* seeds required GA application to germinate and, similarly, GA treatment is also needed to induce flowering (Silverstone et al, 1998). Despite the importance of *CPS*, GA biosynthesis is mainly regulated through the action of two multigenic families encoding GA 20-oxidases (*GA20ox*) and GA 3-oxidases (*GA3ox*) (Chiang et al., 1995; Xu et al., 1995; Phillips et al., 1995). These enzymes catalyse consecutive steps of GA biosynthesis leading to bioactive gibberellin production (see Figure 3.1). *Arabidopsis* contains five *GA20ox* genes

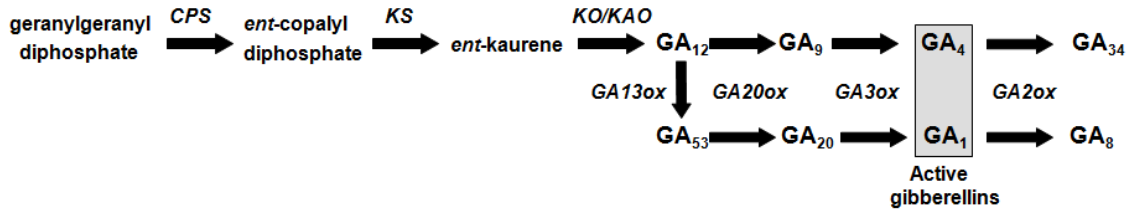


Figure 3.1 Schematic representation of GA metabolism pathway in higher plants. The pathway is shown from the common precursor geranylgeranyl diphosphate to the active gibberellins GA₁ and GA₄. The names of the enzymes catalysing each step are shown in italics.

and four *GA3ox* genes with distinct developmental expression profiles (Mitchum et al., 2006; Rieu et al., 2008a). Functional characterisation through mutant analysis has revealed the relative importance of individual family members during fruit development (Hu et al., 2008; Rieu et al., 2008a). *GA20ox2* and *GA3ox1* play a major role in GA biosynthesis in maternal tissues during fruit development (Hu et al., 2008; Rieu et al., 2008a) whereas *GA3ox4* action appears to be limited to the endosperm of the seed (Hu et al., 2008). In addition to mutant studies, extensive transcript analysis of the genes involved in GA metabolism have also been carried out during fruit initiation and/or development. In *Arabidopsis*, fertilisation-dependent fruit development results in the upregulation of GA biosynthesis genes in the fertilised ovules (Dorcey et al, 2009). Transcriptional induction of the different GA biosynthesis genes follow different time frames with *GA20ox1* and *GA3ox1* being upregulated early on while other genes including *GA20ox3*, *GA20ox5*, *GA3ox3* and *GA3ox4* are induced later (Dorcey et al, 2009). Overall, these data are in agreement with previous mutant analysis (Mitchum et al., 2006; Hu et al., 2008; Rieu et al., 2008a) and it is consistent with the upregulation of GA biosynthesis recorded upon fertilisation in other species such as pea (Garcia-Martinez et al, 1997; Ozga et al, 2009) and tomato (Rebers et al, 1999; Olimpieri et al, 2007; Serrani et al, 2007).

GA metabolism also comprises GA inactivating pathways. The major GA inactivating pathway, 2β -hydroxylation pathway, is catalysed by GA 2-oxidases (*GA2ox*) (see Figure 3.1). Five functional *GA2ox* genes have been identified in *Arabidopsis* (Thomas et al., 1999) which are expressed throughout the different stages of plant development (Rieu et al., 2008b). Mutant analysis suggested that *GA2ox2* is the major *GA2ox* gene controlling fruit initiation although a certain degree of functional redundancy has also been described (Rieu et al., 2008b). Transcriptional analysis in *Arabidopsis* has shown that upregulation of GA inactivation genes is also recorded in valves and ovules upon fertilisation (Dorcey et al, 2009). This is in marked contrast not only to mutant analysis in *Arabidopsis* which have shown that lack of *GA2ox* increases the parthenocarpic potential of pistils (Rieu et al, 2008b) but also with transcript analysis in other species which have shown that *GA2ox* expression decreased after fertilisation (Serrani et al,

2007; Ozga et al, 2009). Thus, the spatio-temporal regulation of GA inactivation upon fertilisation remains to be further clarified.

Another level of complexity of GA metabolism to be considered during fruit initiation and/or development is the feedback regulation of GA biosynthesis and catabolism. The expression of most *GA20ox* and *GA3ox* genes is downregulated in response to elevated bioactive GA levels or increased GA signalling whereas the opposite is true for *GA2ox* gene expression (Hedden et al., 2000; Silverstone et al., 2001; Olszewski et al., 2002; Dill et al., 2001; Zentella et al., 2007; Achard and Genschik, 2008; Rieu et al., 2008b). However, whether the feedback regulation of GA biosynthesis and catabolism holds true during fruit initiation and/or development remains to be confirmed.

3.1.2 GA signalling during fruit development

In addition to GA metabolism, GA signalling also controls fruit initiation and/or growth. Central to GA signalling are DELLA proteins, nuclear proteins characterised by a conserved DELLA-motif in their N-terminal domain (Peng et al., 1997; Silverstone et al., 1998). DELLA proteins form part of the wider GRAS family of regulatory proteins (Bolle, 2004) and five *DELLA* genes have been identified in *Arabidopsis* (*GA-INSENSITIVE [GAI]*, *REPRESSOR OF GA1-3 [RGA]*, *RGA-LIKE1 [RGL1]*, *RGL2* and *RGL3*) (Peng et al., 1997; Silverstone et al., 1998; Sanchez-Fernandez et al., 1998; Dill et al., 2001; King et al., 2001; Lee et al., 2002; Wen et al., 2002). According to the “relief of restraint” model (Harberd, 2003), which summarises the main GA-signalling pathway, DELLA proteins act as growth repressors and GA-mediated DELLA degradation is required in order to overcome this restraint. The binding of GA to the GA-receptor GID1 promotes the interaction between the DELLA-domain of DELLA proteins and GID1-GA complex (Griffiths et al., 2006; Ueguchi-Tanaka et al., 2007; Willige et al., 2007; Murase et al., 2008) which in turn results in the interaction of DELLA proteins with the SCF^{SLY1/GID2} E3 ubiquitin-ligase complex (McGinnis et al., 2003; Sasaki et al., 2003; Dill et al., 2004; Fu et al., 2004). Subsequently, ubiquitinylation of DELLA proteins by the SCF^{SLY1/GID2} E3 complex promotes DELLA protein degradation by the 26S proteasome (McGinnis

et al., 2003; Sasaki et al., 2003; Dill et al., 2004; Fu et al., 2004; Feng et al., 2008). Hence, according to this model, GA-dependent developmental responses rely on GA-mediated DELLA protein degradation. Nevertheless in more recent years, a proteolysis-independent mechanism of DELLA inactivation has also been discovered (Ariizumi et al, 2008). Overexpression of *GID1* can rescue some of the severe phenotypes observed in *sly-1* mutants without affecting DELLA protein levels (Ariizumi et al, 2008). Thus, although proteasome-dependent DELLA-degradation is likely to be the main GA-signalling pathway, GA-mediated GID1-DELLA protein interaction is sufficient to stimulate some GA responses (Ariizumi et al, 2008).

DELLA proteins have also been shown to play a crucial role in GA signalling in the context of fruit initiation and/or development. For example during the course of this study, several reports showed that lack of DELLA proteins results in facultative parthenocarpic fruit development (Marti et al, 2007; Ross et al, 2008; Dorcey et al, 2009). The study of the spatio-temporal expression of *GFP-RGA* before and after fertilisation has further contributed towards the understanding of the role of DELLA proteins in fruit growth repression. At anthesis, prior to fertilisation, *GFP-RGA* expression is mainly localised in the ovules with a weaker GFP signal also visible in the valves (Dorcey et al, 2009). Fertilisation results in the decrease of *GFP-RGA* signal in both ovules and valves, suggesting that the upregulation of GA synthesis in ovules leads to DELLA protein degradation both in fertilised ovules and valves (Dorcey et al, 2009).

In addition to DELLA proteins, SPINDLY (SPY) a negative regulator of the GA response pathway has also been suggested to be involved in fruit growth repression (Jacobsen and Olszewski, 1993). SPY encodes a protein with similarity to O-linked N-acetylglucosamine transferases (Jacobsen et al, 1996; Kreppel et al, 1997; Lubas et al, 1997) and it is believed to play a role in DELLA protein modification and activation (Silverstone et al, 2007). According to Jacobsen and Olszewsky (1993), *spy-1* mutants show facultative parthenocarpic pistil development; however, these results could not be repeated in later studies (Vivian-Smith et al, 1999). Thus, the role of SPY in the context of fruit initiation and/or growth remains to be further clarified.

In this study an in-depth insight into GA signalling in the context of gynoecium and fruit development was initiated by the systematic analysis of the role of DELLA proteins during fruit initiation and growth in *Arabidopsis*.

3.2 Materials and methods

3.2.1 Plant material and growth conditions

The *global-DELLA* mutant (lacking all five *DELLA* genes) was obtained as described by Koini et al (2009) and knockout identity was confirmed by RT-PCR (data not shown). The *ga1-3 global-DELLA* mutant was isolated from a cross between a *ga1-3 quadruple* mutant (Cheng et al., 2004) and a *gai rga rgl1^{+/-}rgl2 rgl3^{+/-}* mutant plant. PCR-genotyping was used to isolate both *global-DELLA* and *ga1-3 global-DELLA* mutant plants (data not shown). Seeds from both mutants were kindly provided by Dr. Liz Alvey. Seeds from *quadruple-DELLA spt-2* mutant and 35S::SPT-HA were kindly provided by Dr. Steve Penfield.

Plants were grown in a Controlled Environment Room at 20°C under 16 h light/ 8 h dark photoperiod prior to which seeds were stratified at 4°C in darkness for 4 days. All experiments and measurements were carried out in mid stage flowers in order to avoid the increased sterility observed in young and terminal flowers.

3.2.2 Quantitative real-time PCR (qRT-PCR) analysis

Total RNA was extracted from homogenised samples of stage 11-12, 15, 17a and 17b flowers and fruits using RNeasy® Plant Mini Kit (Qiagen) according to manufacturer's protocol. Three micrograms of total RNA were used to synthesise first-strand cDNA, using M-MLV reverse transcriptase (Invitrogen) and oligo dT (18) primers. Gene expression was determined by quantitative real-time PCR (Chromo4 real-time PCR detector, Biorad) using the SYBR® Green JumpStart Taq ReadyMix™ PCR Master Mix (Sigma). Expression levels of *DELLA* genes were calculated relative to the average expression level of *TUBULIN8* (AT5G23860),

UBIQUITIN-CONJUGATING ENZYME9 (AT4G27960) and *UBIQUITIN-CONJUGATING ENZYME10* (AT5G5330) genes. The gene-specific primer sequences used in this study are shown in Table 3.1.

3.2.3 Hormone treatments

Hormone treatments were performed as described by Vivian-Smith et al., 1999 and dose-response experiments were carried out to further determine the optimal hormone concentration. A 1- μ l droplet containing 0.1 mM, 1 mM or 10 mM of GA₃ or IAA with 0.01% (v/v) Triton X-100 buffered to pH 7.0 was used to uniformly coat emasculated pistils at stage 13. 0.01% (v/v) Triton X-100 buffer solution was used as the control solution. During 26S proteasome inhibition experiments, a 1- μ l droplet containing 0.01% DMSO or 100 μ M MG132 was applied and let to dry prior to control or GA treatment.

Final pistil length following pollination, hormone or control treatment was measured 7 days post anthesis (DPA) once pistils had fully elongated. Pistils were examined under light microscopy using an MZ 16 stereomicroscope (Leica) and the images were captured with a DFC 280 digital camera (Leica). Measurements were performed on captured images using ImageJ software.

3.2.4 Endogenous IAA quantification

IAA quantification was carried out by Dr. Karin Ljung (Univ. Umeå, Sweden) as described by Sorefan et al. 2009. For each measurement, three independent pooled samples (10-20 mg fresh weight) of emasculated and self-pollinated Ler, *global-DELLA* and *ga1-3 global-DELLA* mutant gynoecia 7 DPA were collected.

3.2.5 Protein extraction

Approximately 300mg of plant tissue was collected in Eppendorf tubes containing stainless steel ball bearings and stored at -80°C. The tissue was ground using a

2000 Geno/Grinder (from Spex/Sampleprep) by shaking it at 500rpm for 30 seconds. 1ml of protein extraction buffer (50mM Tris HCl pH7.5, 400mM NaCl, 1mM EDTA) with 10 μ l sigma complete protease inhibitor cocktail and 0.5 μ l of 200 μ M MG132 which was added on the day of use was mixed with the ground tissue and mix thoroughly. The debris was removed by centrifugation at 14,000rpm at 4°C for 10 minutes. The supernatant was transferred to a fresh Eppendorf tube and stored at -80°C.

3.2.6 Protein quantification: Bradford assay

A series of BSA solutions at different concentrations (100 μ g/ml, 200 μ g/ml, 400 μ g/ml, 600 μ g/ml, 1000 μ g/ml) were prepared in the protein extraction buffer previously described. The Bradford solution was diluted 1/5 and 10 μ l of the different BSA solutions was added to 190 μ l of the Bradford working solution. After 2 min, the absorbance at 595nm was measured and a standard curve/equation was calculated by plotting 595nm absorbance (y) against BSA protein concentration (x). This standard curve/equation was used to calculate the protein concentration of our samples based on the 595nm absorbance of 1/50 dilutions.

3.2.7 Western blotting

10 days old seedlings and stage 12-15 flowers were used as plant materials. After protein extraction and quantification (see Sections 3.2.5, 3.2.6), sample running buffer and reducing agent were added to samples according to the RunBlue protocol

(<http://www.expedeon.com/TECHNICALRESOURCES/PRODUCTMANUALS/tabid/125/Default.aspx>) and this mixture was heated for 10 min at 70 °C. Protein extracts were separated by SDS-PAGE (12%) and transferred to a nitrocellulose membrane. A rabbit anti-HA polyclonal Chip-grade antibody (Abcam) was applied in 1:1000 dilution. A goat anti-rabbit IgG antibody (InmunoPure Antibody, Thermo) was used in a 1:20000 dilution as a secondary antibody to enable immunoreactive polypeptides visualization after film development with Supersignal West Pico Chemiluminescent substrate (Thermo).

3.2.8 Yeast two-hybrid assays

For the yeast two hybrid assays, GID1A-BD vector used as bait in this study was kindly provided by Prof. Claus Schwechheimer. For the activation-domain vectors, the GAI, RGA and SPT coding regions were amplified by PCR with primers containing *Sma*I and *Pst*I restriction sites (see Table 3.1). The amplicons were cloned in frame between *Sma*I and *Pst*I sites of pGAD424 to form the prey vectors. After confirming the plasmid quality by sequencing, prey plasmids were transformed into yeast Y187 (-Leu) and bait plasmids into AH109 (-Trp). Prey transformants were selected in SD-L media whilst bait transformants were selected in SD-T media.

Yeast transformation was carried out as described in the Clontech Laboratories Yeast Protocols Handbook (www.clontech.com). 1ml of YPD liquid media was inoculated with several colonies of 2-3mm in diameter (Y187 for prey plasmids and/or AH109 for bait plasmids) and vortexed vigorously for 5 minutes to disperse any clumps. These minicultures were transferred into a flask containing 50ml of YPD and incubated at 30°C shaking at 250rpm overnight or until the stationary phase was reached ($OD_{600}>1.5$). Approximately 30ml of the overnight culture was transferred to a flask containing 300ml of YPD ($OD_{600}= 0.2\text{-}0.3$). The diluted culture was incubated at 30°C shaking at 250rpm for around 3hr until an OD_{600} of 0.4-0.6 was reached. 100ml of these cultures were centrifuged at 1,000xg for 5 minutes at RT. The supernatants were discarded and the cell pellets were resuspended in freshly-made sterile TE and centrifuged again at 1,000xg for 5 minutes at RT. The supernatant was discarded and the cell pellet resuspended in 1.5ml freshly prepared sterile 1xTE/1xLiAc. Simultaneously, 0.1µg of the plasmid DNA to be transformed was mixed with 0.1mg of herring testes carrier DNA in a new eppendorf tube. 0.1ml of the yeast competent cells was added to each eppendorf tube and mixed by vortexing. Following this, 0.6ml of sterile PEG/LiAc solution was added to each tube and vortexed for 10sec. The cells were incubated at 30°C for 30min with shaking at 250rpm after which 70µl of DMSO was added and gently mixed by inversion. The yeast cells were heatshocked for 15min in a water bath at 42°C and, then, chilled on ice for 1-2min. Finally, cells were

centrifuged for 10sec at 14,000rpm at RT and resuspended in 0.5ml of freshly-made sterile TE. In order to select the desired transformants, 150 μ l of the resuspended cells were plated on SD-L (prey transformants), SD-T (bait transformants), SD-LT (prey and bait transformants for yeast two-one hybrid) or SD-U (for transformants carrying the DNA target sequence for yeast two-one hybrid) media and incubated up-side-down at 30°C until colonies appear (approximately 3 days).

For each plasmid of interest to be tested, a single yeast transformant colony was resuspended in 500 μ l of YPD. The tubes were vigorously vortexed to disperse the cells. For each mating combination, a 20 μ l aliquot of each of the plasmids was mixed into 160 μ l of YPD medium and incubated overnight at 30°C shaking at 200rpm. In order to confirm mating efficiency and protein-protein interactions, 10 μ l of each mating culture was plated on SD-LT (growth confirms mating) and SD-LTHA plates (growth confirms interaction) and incubated up-side-down at 30°C until colonies grew (3-5 days).

3.2.9 Promoter *GUS* transgenic line construction

To generate the *ML1::GUS* fusion construct, 4955bp of the *ML1* promoter was amplified by using SF00156 as forward primer containing the *HindIII* restriction site and SF00157 as reverse primer containing the *BamHI* restriction site (see Table 3.1). The amplified fragment was digested with *HindIII* and *BamHI* and cloned into pBI101 which contains the reporter gene *GUS*. After *Arabidopsis* floral-dip transformation (see Chapter 2), transgenic plants were selected in MS medium supplemented with 50 μ g/ml Kanamycin. The presence of the *ML1::GUS* in the transgenic seedlings was checked by genomic PCR with primers SF00189 (promoter-specific primer) and SF0171 (GUS-specific primer). An identical strategy was adopted to generate the *ACI1::GUS* fusion construct but in this case 4100bp of the *ACI1* promoter was amplified by using SF00164 and SF00165 primers (see Table 3.1). After selection of Kanamycin resistant transgenic plants, presence of *ACI1::GUS* was checked by genomic PCR with primers SF00191 (promoter-specific primer) and SF0171 (GUS-specific primer).



E P E P E P
Ler global ga1-3 global

Figure 3.2 Lack of DELLA proteins causes parthenocarpic fruit development in *Arabidopsis*. Representative emasculated (E) and hand-pollinated (P) *Ler*, *global-DELLA* and *ga1-3 global-DELLA* gynoecia 7 days post anthesis (DPA). E= Emasculated, P= Pollinated. Scale bar, 5 mm.

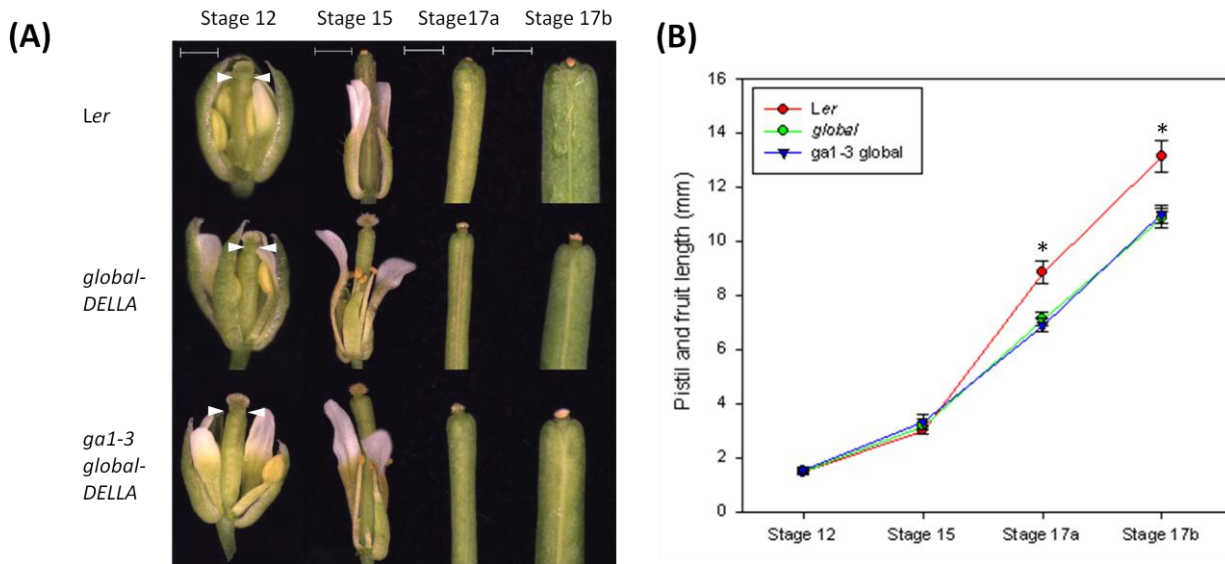
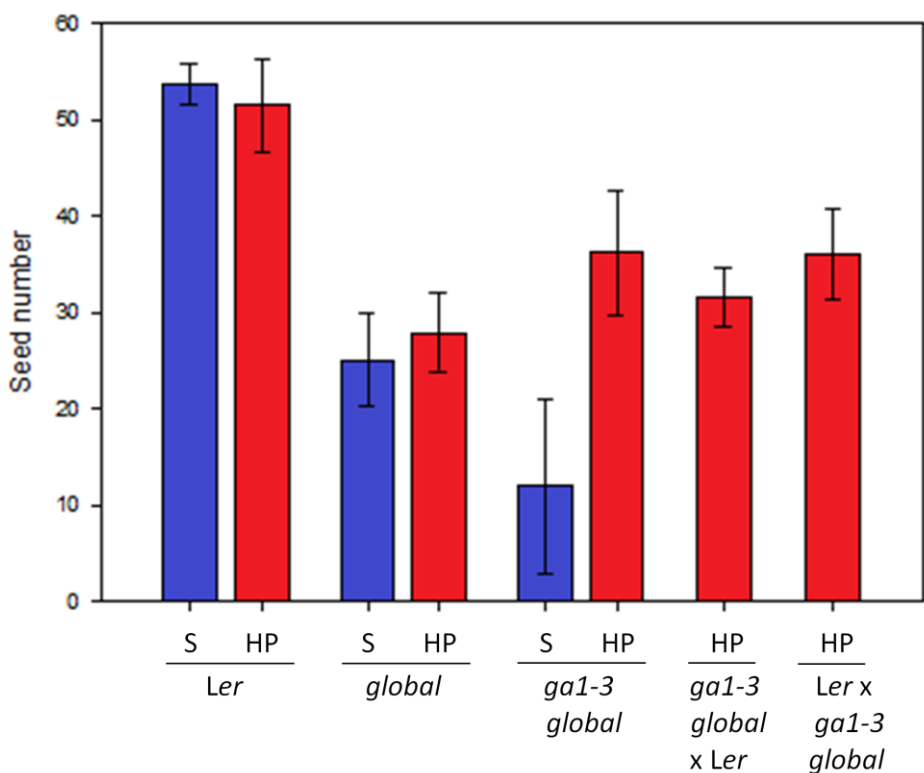


Figure 3.3 Fruit development in *Ler*, *global-DELLA* and *ga1-3 global-DELLA* mutant plants. (A) Representative pistil development in *Ler*, *global-DELLA* mutant and *ga1-3 global-DELLA* mutant plants through stages 11-12, 15, 17a and 17b of *Arabidopsis* flower and fruit development. White arrows indicate basal style boundary at stage 12. Scale bars, stage 12 = 0.5 mm, stage 15, 17a and 17b = 1 mm. (B) Pistil length in *Ler*, *global-DELLA* mutant and *ga1-3 global-DELLA* mutant plants. Asterisks indicate values significantly different from *global-DELLA* and *ga1-3 global-DELLA* mutants (* for P<0.05). Error bars: 95% CI, n≥22

(A)



(B)

	Ler S	Ler HP	global S	global HP	ga1-3 global S	ga1-3 global HP	ga1-3 global x Ler	Ler x ga1-3 global
Ler S								
Ler HP	0.288							
global S	<0.001 (***)	<0.001 (***)						
global HP	<0.001 (***)	<0.001 (***)	0.393					
ga1-3 global S	<0.001 (***)	<0.001 (***)	0.005 (**)	0.001 (**)				
ga1-3 global HP	<0.001 (***)	0.001 (**)	0.013 (*)	0.021 (*)	<0.001 (***)			
ga1-3 global x Ler	<0.001 (***)	<0.001 (***)	0.032 (*)	0.140	<0.001 (***)	0.127		
Ler x ga1-3 global	<0.001 (***)	<0.001 (***)	0.002 (**)	0.023 (*)	<0.001 (***)	0.976	0.138	

Figure 3.4 Seed count in selfed, hand pollinated and cross pollinated Ler, global-DELLA and ga1-3 global-DELLA mutants. (A) Graph showing seed number in selfed, hand pollinated and cross pollinated Ler, global-DELLA and ga1-3 global-DELLA mutants. Error bars: 95% CI, n≥10 (B) Statistical analysis of seed count graph. Probability values are indicated and values significantly different are represented by asterisks (* for P<0.05, ** for P<0.01 and *** for P < 0.001). S= Selfed, HP= Hand pollinated.

3.3 Results

3.3.1 Lack of DELLA proteins causes facultative parthenocarpy in *Arabidopsis*

Silencing of a single *DELLA* gene in tomato (*SIDELLA*) results in facultative parthenocarpic fruit development (Marti et al., 2007). In order to establish whether this was also the case in *Arabidopsis*, *global-DELLA* (which lacks all five DELLA proteins) and *ga1-3 global-DELLA* (which lacks all five DELLA proteins and the first enzyme in GA biosynthesis) pistils were emasculated two days before anthesis. Whilst emasculated wild-type pistils did not elongate significantly, emasculated *global-DELLA* and *ga1-3 global-DELLA* pistils developed into parthenocarpic fruits more than twice as long as wild-type emasculated pistils (see Figure 3.2). DELLA proteins are involved in the positive regulation of GA biosynthesis and, thus, *global-DELLA* mutants lacking DELLA proteins are likely to have low levels of biologically active gibberellins (Hedden et al., 2000; Silverstone et al., 2001; Olszewski et al., 2002; Dill et al., 2001; Zentella et al., 2007; Achard and Genschik, 2008). Nevertheless, to further ensure that the phenotypes observed in *global-DELLA* mutants are due to the upregulation of the GA-signalling pathway and not due to a GA imbalance, *ga1-3 global-DELLA* mutants were also used throughout this study.

3.3.2 Other flower and fruit phenotypes caused by lack of DELLA proteins

To further characterise the role of DELLA proteins in pistil development, gynoecium, stigma and style development in wild type, *global-DELLA* and *ga1-3 global-DELLA* mutant flowers were compared at different stages of flower development (see Figure 3.3). As previously described in *quadruple-DELLA* mutants lacking GAI, RGA, RGL1 and RGL2 (Cheng et al., 2004), it was noticed that *global-DELLA* and *ga1-3 global-DELLA* mutants exhibit slightly longer floral organs than wild-type flowers (see Figure 3.3A). This was particularly obvious at

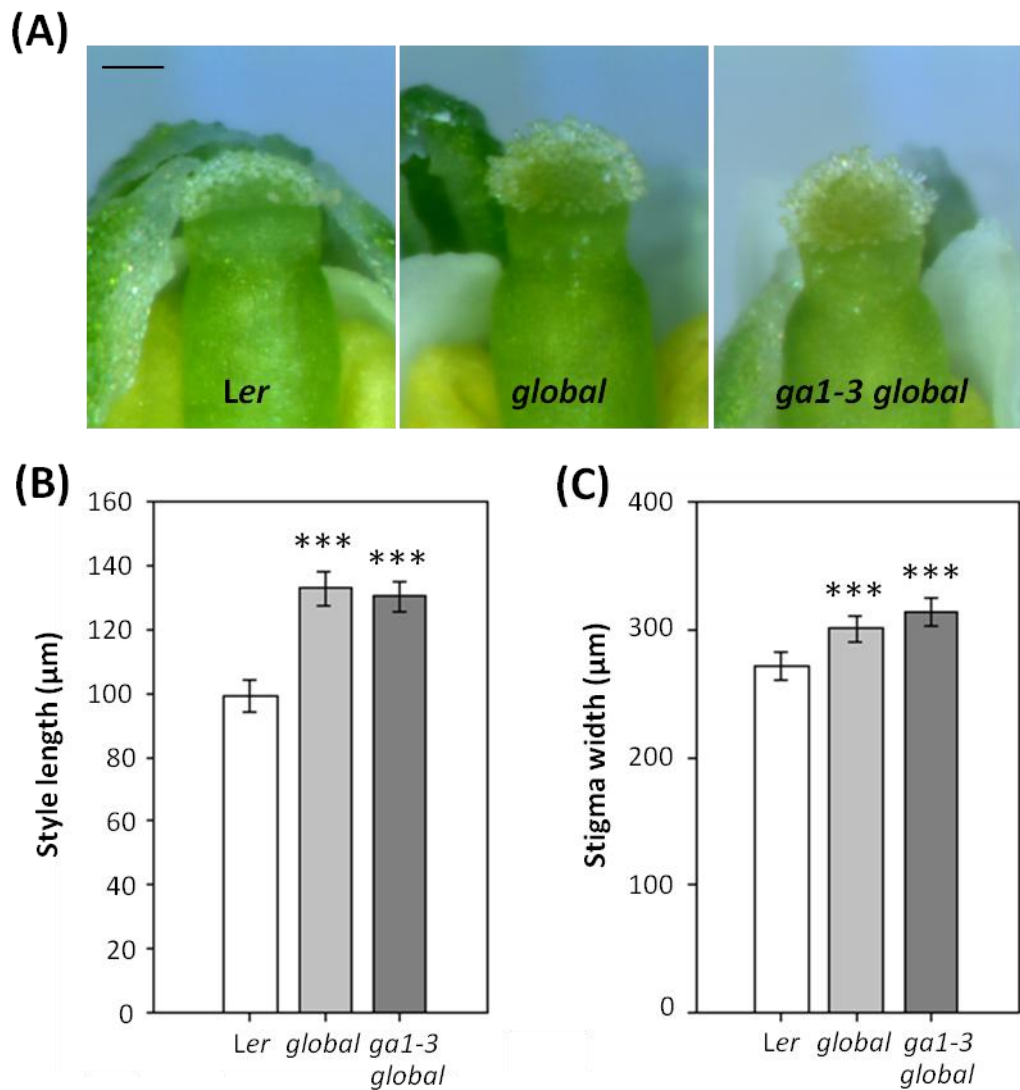


Figure 3.5 Style and stigma development in *global-DELLA* and *ga1-3 global-DELLA* mutants compared to wild type. (A) Representative style and stigma development in *Ler*, *global-DELLA* mutant and *ga1-3 global-DELLA* mutant plants at stage 12 of *Arabidopsis* flower development. Scale bar, 0.12 mm. (B) Style length in *Ler*, *global-DELLA* mutant and *ga1-3 global-DELLA* mutant plants at stage 12. Values significantly different from *Ler* control are indicated by asterisks (** for $P < 0.001$). Error bars: 95% CI, $n \geq 37$ (C) Stigma width in *Ler*, *global-DELLA* mutant and *ga1-3 global-DELLA* mutant plants at stage 12. Values significantly different from *Ler* control are indicated by asterisks (** for $P < 0.001$). Error bars: 95% CI, $n \geq 37$

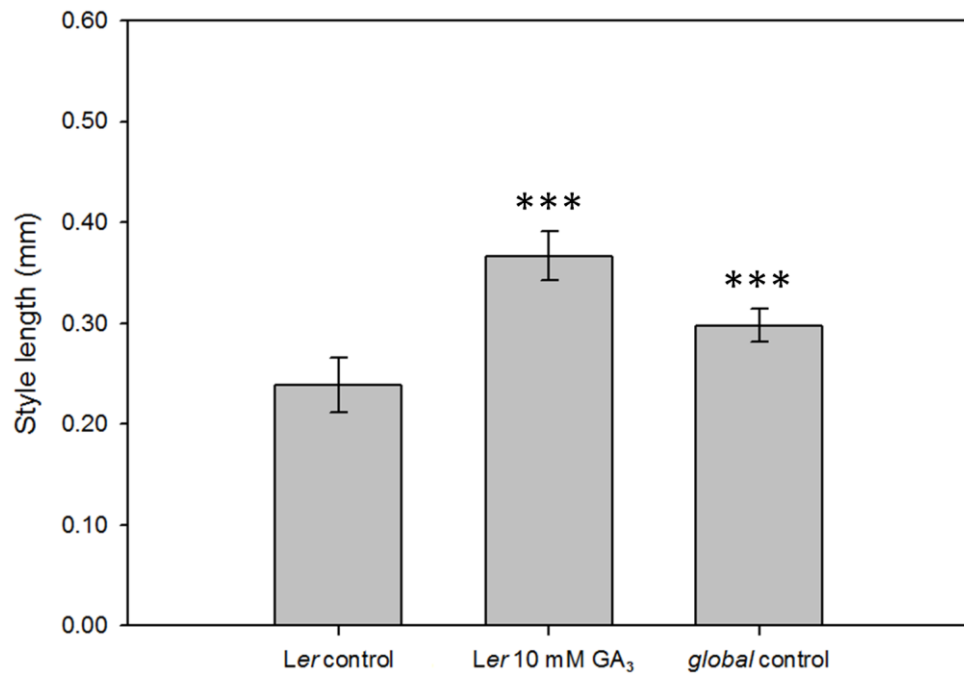


Figure 3.6 Style elongation is mediated by gibberellins. Style length in parthenocarpic Ler pistil induced by GA₃ application (10 mM GA₃) and parthenocarpic *global-DELLA* pistil measured 7DPA. Buffer solution was used as the control solution. Values significantly different from Ler control pistils are indicated by asterisks (*** for P < 0.001). Error bars: 95% CI, n ≥ 12

stage 15 when comparing the size of petals and anther filaments relative to pistil length (see Figure 3.3A). Early gynoecium development in *global-DELLA* and in *ga1-3 global-DELLA* mutants was comparable to that of wild-type plants (see Figure 3.3B). However, from stage 15 onwards reduced size of *global-DELLA* and *ga1-3 global-DELLA* pistils was recorded (see Figure 3.3B) which is likely to be directly related to their reduced fertility (see Figure 3.4). *global-DELLA* and *ga1-3 global-DELLA* mutants often show an altered phyllotactic arrangement of floral organs, particularly of petals and stamens (data not shown), which results in decreased self-pollination partially recovered by hand-pollination (see Figure 3.4). Nevertheless, careful hand-pollinations of *global-DELLA* and *ga1-3 global-DELLA* mutants did not restore wild-type seed set (see Figure 3.4), indicating that the reduced fertility is not only due to an altered phyllotactic arrangement. In order to further investigate whether the reduced fertility observed could be attributed to a paternal or maternal defect, a series of cross pollinations between Ler and *ga1-3 global-DELLA* pistils were carried out. Pollination of *ga1-3 global-DELLA* pistils with *Ler* pollen or vice versa, pollination of *Ler* pistils with *ga1-3 global-DELLA* pollen did not restore normal seed set (see Figure 3.4), indicating that the reduced fertility observed in *ga1-3 global-DELLA* pistils can also be partially attributed both to maternal and paternal origin defects. These results are in contrast to previous studies which suggested that absence of RGL1, RGL2 and RGA is sufficient to restore normal seed set in *ga1-3* mutants (Cheng et al, 2004; Tyler et al, 2004).

Lack of DELLA proteins also results in style and stigma growth promotion (see Figure 3.3A and 3.5). Throughout the different stages of pistil development, *global-DELLA* and *ga1-3 global-DELLA* form longer styles than wild type (see Figure 3.3A). In addition, while in wild-type pistil the stigmatic papillae has already degenerated by stage 15, in *global-DELLA* and *ga1-3 global-DELLA* mutants this degeneration process is delayed (see Figure 3.3A). Quantification of style length and stigma width at stage 12 of flower development showed that *global-DELLA* and *ga1-3 global-DELLA* form significantly longer styles and wider stigmas than wild-type pistils (see Figure 3.5). Furthermore, application of GA₃ to emasculated wild-type pistils mimics the style length promotion observed in *global-DELLA* plants and significantly longer styles where observed in GA₃-treated emasculated wild-type pistils 7 DPA (see Figure 3.6).

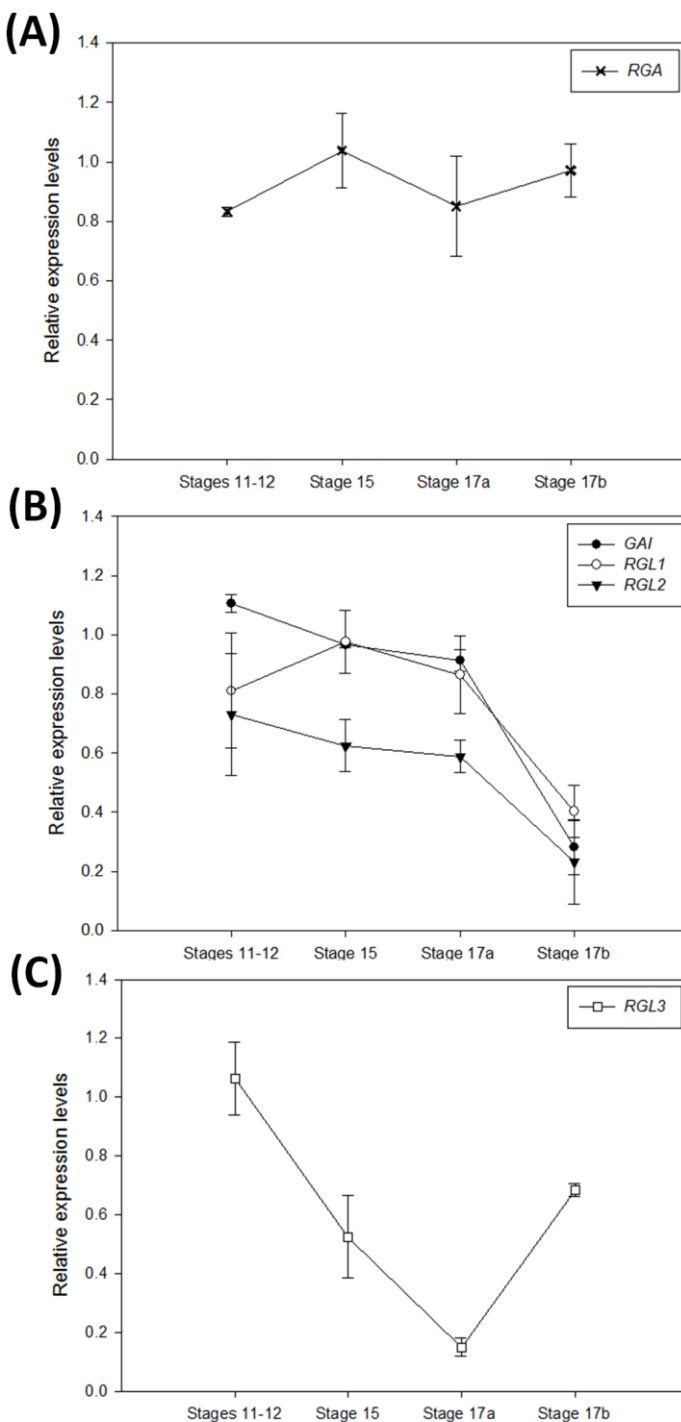


Figure 3.7 Transcript levels of *DELLA* genes through stages 11-12, 15, 17a and 17b of *Arabidopsis* flower and fruit development. (A) *RGA* expression profile. (B) *GAI*, *RGL1* and *RGL2* expression profiles. (C) *RGL3* expression profile. Relative gene expression levels were calculated by qRT-PCR as described in “Materials and Methods”. Error bars: SD, n= 3

3.3.3 In-depth characterisation of DELLA-related facultative parthenocarpy

It has previously been shown that individual *DELLA* genes follow distinct developmental expression profiles in *Arabidopsis* (Tyler et al., 2004). However, the transcriptional profile of *DELLA* genes during the different stages of flower and fruit development remains to be clarified. Thus, in order to determine the role played by individual *DELLA* proteins in fruit development and their possible contribution towards *DELLA*-related facultative parthenocarpy, the expression profiles of the five *Arabidopsis* *DELLA* genes by quantitative real-time PCR throughout different stages of pistil development was analysed. Among the several housekeeping genes examined, *TUBULIN8*, *UBIQUITIN-CONJUGATING ENZYME9* and *UBIQUITIN-CONJUGATING ENZYME10* showed relatively constant expression levels across the different developmental stages and, thus, the average expression level of these genes was used to normalise the samples. The expression profiles of the *DELLA* genes followed three different general trends during pistil development (see Figure 3.7). Consistent with previous data (Tyler et al., 2004), *RGA* expression was high and practically constant throughout the different stages of pistil development (see Figure 3.7A). The transcript levels of *GAI*, *RGL1* and *RGL2* were relatively high prior to fertilisation (stage 11-12) and during pistil elongation (stages 15 and 17a) but decreased when the final pistil length was achieved (stage 17b) (see Figure 3.7B) (developmental stages defined in Smyth et al. (1990)). *RGL3* expression was high before fertilisation (stages 11-12) but decreased soon after until it increased again at the final stage of fruit growth (stage 17b) (see Figure 3.7C). Transcriptional regulation is only one of the many possible mechanisms that control *DELLA* protein activity (Achard and Genschik, 2008). Nevertheless, the fact that all *DELLA* genes do not follow the same expression profile throughout *Arabidopsis* fruit development suggests that different *DELLA* genes might be important at different stages of fruit growth.

Based on the expression profiles of the different *DELLA* genes, it is difficult to determine the relative importance of individual *DELLA* proteins in fruit initiation. Therefore, a detailed analysis of the parthenocarpy conferring capacity of different

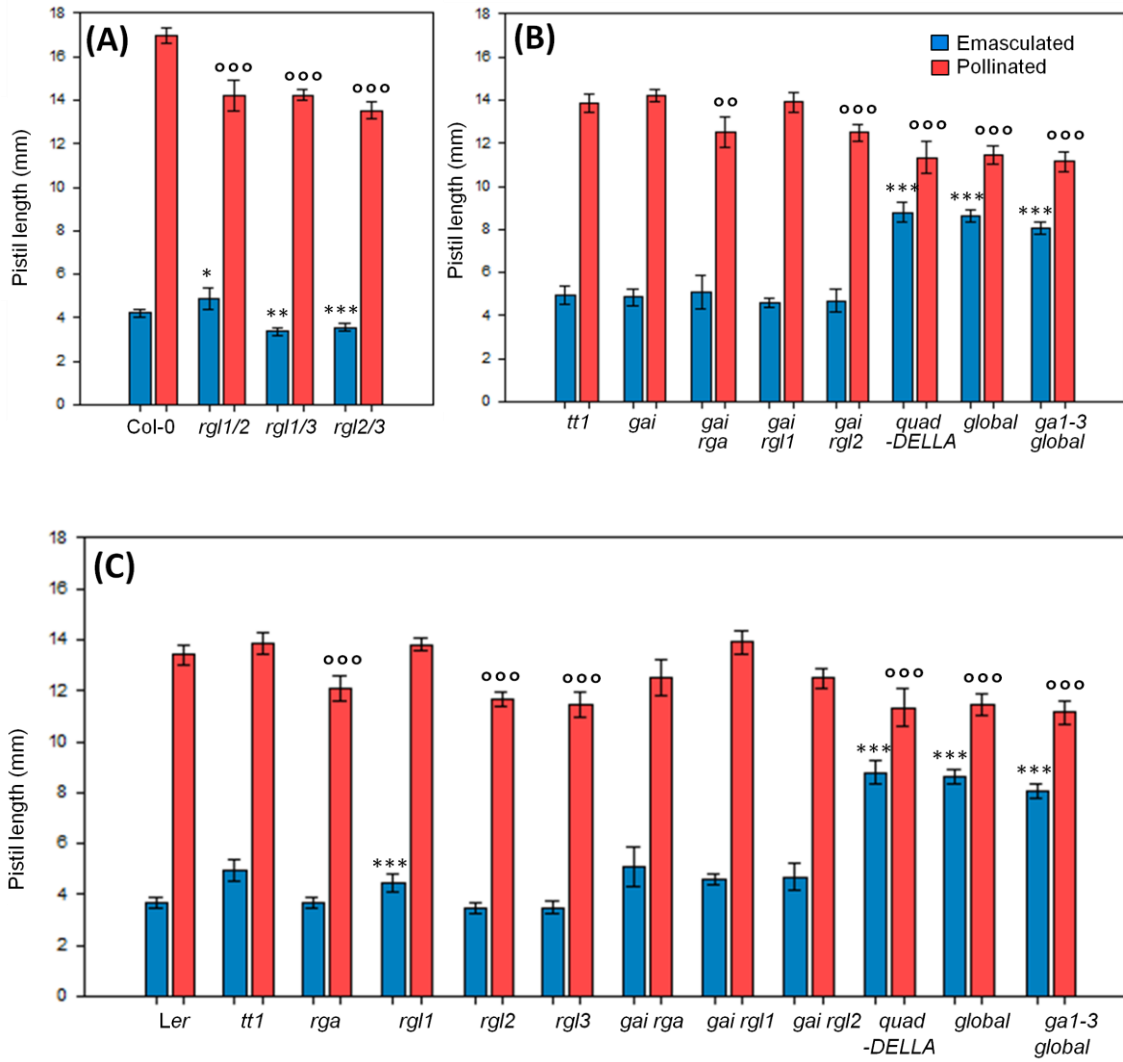


Figure 3.8 Analysis of the parthenocarpy conferring capacity of the different *della* mutant combinations. (A) *della* mutants in Col-0 background. Asterisks indicate values significantly different from control Col-0 emasculated pistils (* for P<0.05, ** for P<0.01 and *** for P<0.001) and control Col-0 hand-pollinated pistils (°°° for P<0.001). (B) *della* mutants in *tt1* mutant background. Asterisks indicate values significantly different from control *tt1* emasculated pistils (*** for P<0.001) and control *tt1* hand-pollinated pistils (°° for P<0.01 and °°° for P<0.001). (C) *della* mutants in Ler background. Note that *gai* mutation is in the *tt1* mutant background, consequently for those mutants with the *gai* mutation *tt1* and Ler are required as controls. Asterisks indicate values significantly different from control emasculated pistils (*** for P<0.001) and control hand-pollinated pistils (°°° for P<0.001). Emasculated (blue) and hand pollinated (red) pistils were measured 7 DPA. Error bars: 95% CI, n(A)≥22, n(B)≥19, n(C)≥19

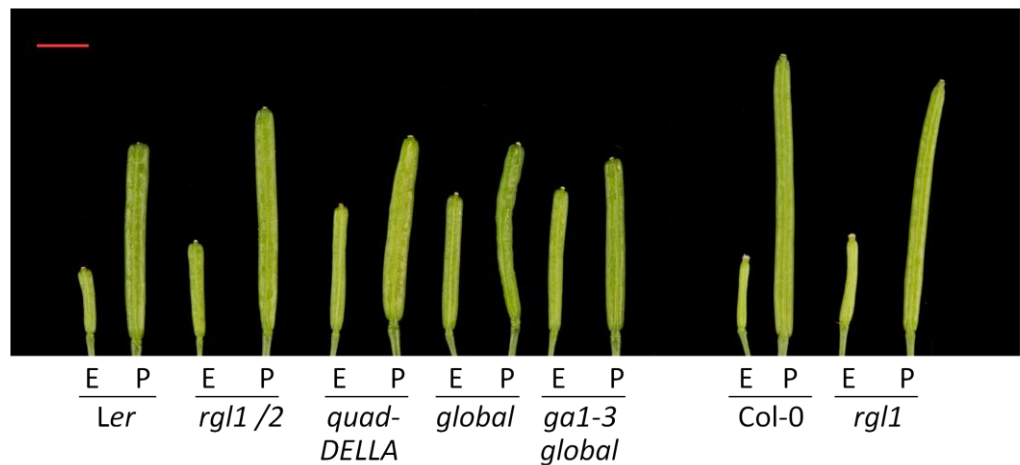


Figure 3.9 Facultative parthenocarpic *della*-mutants. Representative emasculated (E) and hand-pollinated (P) *Ler*, *rgl1/2*, *quadruple-DELLA*, *global-DELLA*, *ga1-3 global-DELLA*, Col-0 and *rgl1* gynoecia 7 days post anthesis (DPA). E= Emasculated, P= Pollinated. Scale bar, 3mm

della mutant combinations was carried out. *ga1-3* plants do not flower or set seeds in the absence of repeated GA treatment (Silverstone et al, 1998). Previous studies have shown that GA treatment results in parthenocarpic fruit development in various species, including *Arabidopsis* (Vivian-Smith and Koltunow, 1999). Consequently, it was impossible to assess the potential parthenocarpy conferring capacity of the *ga1-3* mutation. Emasculation of single *Arabidopsis della* mutants showed that only emasculation of *rgl1* resulted in slight but significant pistil elongation (see Figure 3.8 and Appendix figures 3.1, 3.2). In double *Arabidopsis della* mutants, only emasculation of *rgl1/2* resulted in a small but significant pistil elongation (see Figure 3.8 and Appendix figures 3.1, 3.2). However, an additive effect in pistil elongation was observed upon emasculation of multiple *della* mutants and emasculation of *quadruple-DELLA*, *global-DELLA* and *ga1-3 global-DELLA* pistils resulted in substantial parthenocarpic fruit growth (see Figures 3.8, 3.9 and Appendix figures 3.1, 3.2). Thus, lack of at least four DELLA proteins is required for a sizeable parthenocarpic fruit growth promotion, suggesting a certain degree of functional redundancy.

It is also worth noting that, in general, *della* mutants show significantly shorter hand-pollinated pistils than wild-type plants (see Figures 3.8, 3.9 and Appendix figures 3.1, 3.2). It has previously been shown in this study that the reduced size of pollinated *global-DELLA* and *ga1-3 global-DELLA* pistils can directly be attributed to their reduced fertility (see Figures 3.3, 3.4). Lack of *rga*, *rgl2* and *rgl3* alone was sufficient to cause significantly reduced size in hand-pollinated pistils (see Figure 3.8 and Appendix figures 3.1, 3.2), suggesting that lack of *rga*, *rgl2* and *rgl3* alone may also be sufficient to cause reduced fertility.

3.3.4 The facultative parthenocarpy observed in *global-DELLA* mutants is not due to an auxin imbalance

Facultative parthenocarpy has commonly been associated with increased hormone levels (Vivian-Smith et al., 1999), thus, whether this could explain the facultative parthenocarpic phenotype observed in *global-DELLA* mutants was investigated. Previous studies have already shown that DELLA proteins are

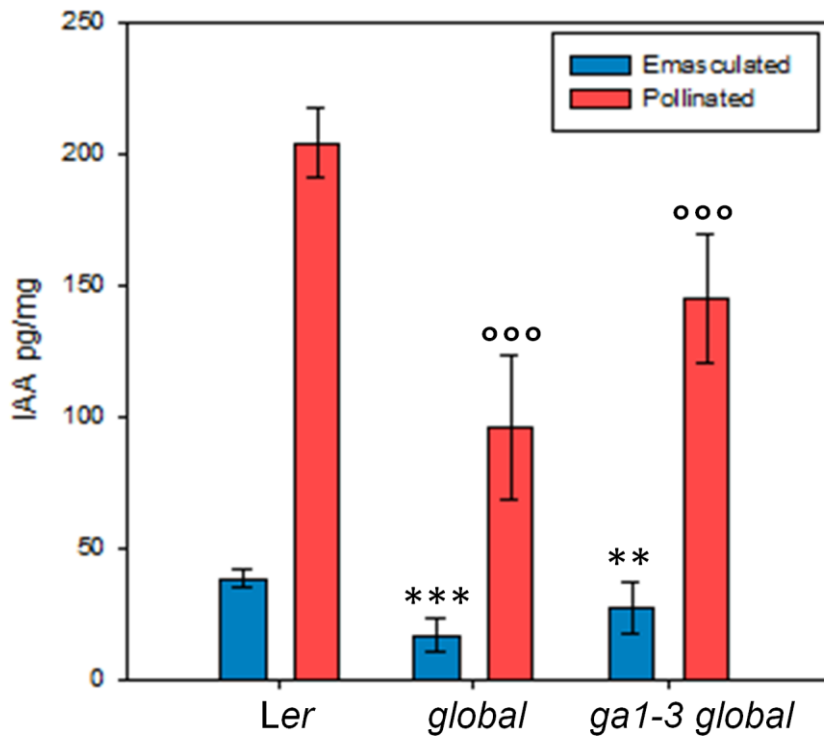


Figure 3.10 IAA concentration measurements in emasculated and hand-pollinated *Ler*, *global-DELLA* mutant and *ga1-3 global-DELLA* mutant gynoecia 7 DPA. Asterisks indicate values significantly different from *Ler* emasculated pistils (** for $P < 0.01$ and *** for $P < 0.001$) and white circles indicate values significantly different from pollinated *Ler* pistils (ooo for $P < 0.001$). Error bars: 95% CI, n= 3

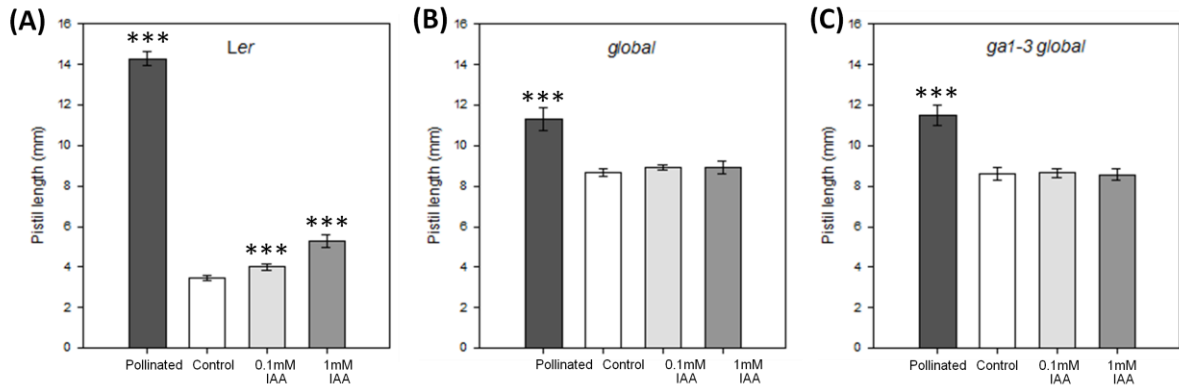


Figure 3.11 IAA promotes wild-type pistil elongation. Pistil length of (A) Ler, (B) *global-DELLA* mutant and (C) *ga1-3 global-DELLA* mutant plants in response to increasing concentrations of IAA. Pistils were measured 7 DPA. Buffer solution was used as the control solution. Values significantly different from control pistils in each of the panels are indicated by asterisks (** for P < 0.001). Error bars: 95% CI, n ≥ 20

involved in positive regulation of GA biosynthesis, suggesting that mutants lacking DELLA proteins have low levels of biologically active gibberellins (Hedden et al., 2000; Silverstone et al., 2001; Olszewski et al., 2002; Dill et al., 2001; Zentella et al., 2007; Achard and Genschik, 2008). Traditionally both gibberellins and auxin have been associated with parthenocarpic fruit growth promotion (Gillaspy et al., 1993) and, in order to discard the possibility that the parthenocarpy observed in emasculated *global-DELLA* and *ga1-3 global-DELLA* pistils is due to high auxin levels, the concentration of endogenous indole-3-acetic-acid (IAA) was measured (see Figure 3.12). Hand-pollinated *global-DELLA* and *ga1-3 global-DELLA* pistils have lower IAA levels than hand-pollinated wild-type pistils (see Figure 3.10) which can be attributed to reduced seed numbers (see Figure 3.4). Interestingly, parthenocarpic *global-DELLA* and *ga1-3 global-DELLA* pistils also show significantly lower IAA levels than emasculated wild-type pistils (see Figure 3.10). These data support the idea that the facultative parthenocarpy observed in *della* mutants is the direct consequence of DELLA protein absence and not the result of elevated gibberellin or auxin levels.

3.3.5 Auxin application does not promote pistil elongation in *global-DELLA* mutants

Although emasculation of *global-DELLA* and *ga1-3 global-DELLA* pistils resulted in significant parthenocarpic fruit development, these parthenocarpic fruits were shorter than pollinated mutant and wild-type pistils (see Figures 3.2, 3.8, 3.9). To investigate whether elongation could be further promoted in emasculated *global-DELLA* and *ga1-3 global-DELLA* pistils, a series of hormonal treatments were carried out. In comparison to tissues such as roots and leaves, relatively high hormone concentrations are required to obtain effects in pistils (Srinivasan and Morgan, 1996; Vivian-Smith et al., 1999; Dorcey et al., 2009). This is most likely due to a reduced absorption capacity through the waxy surface of the pistils. In order to determine the effect of added hormone solutions under our plant-growth conditions, dose-response experiments were carried out based on previous studies (Vivian-Smith et al., 1999). In contrast to what has been reported in other studies (Vivian-Smith et al., 1999), under our growing conditions application of

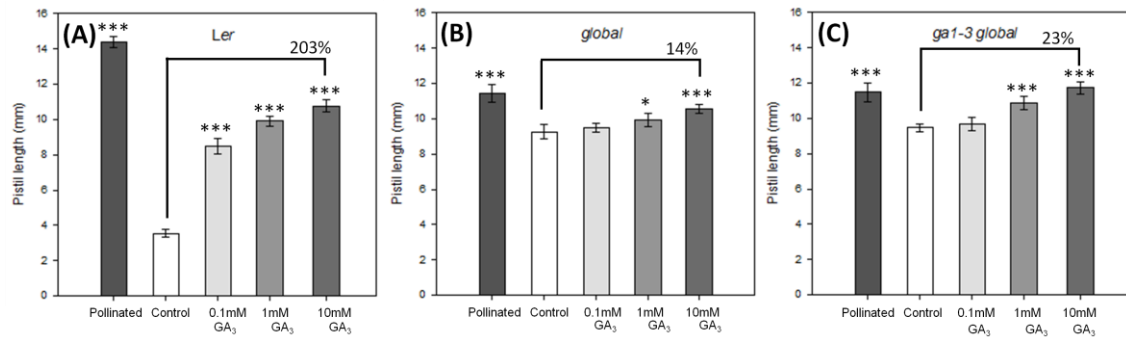


Figure 3.12 GA₃ promotes pistil elongation in wild-type, *global-DELLA* mutant and *ga1-3 global-DELLA* mutant plants. Pistil length of (A) Ler, (B) *global-DELLA* mutant and (C) *ga1-3 global-DELLA* mutant plants in response to increasing concentrations of GA₃. Pistils were measured 7 DPA. Buffer solution was used as the control solution. Values significantly different from control pistils in each of the panels are indicated by asterisks (* for P<0.05 and *** for P < 0.001). Error bars: 95% CI, n ≥ 20

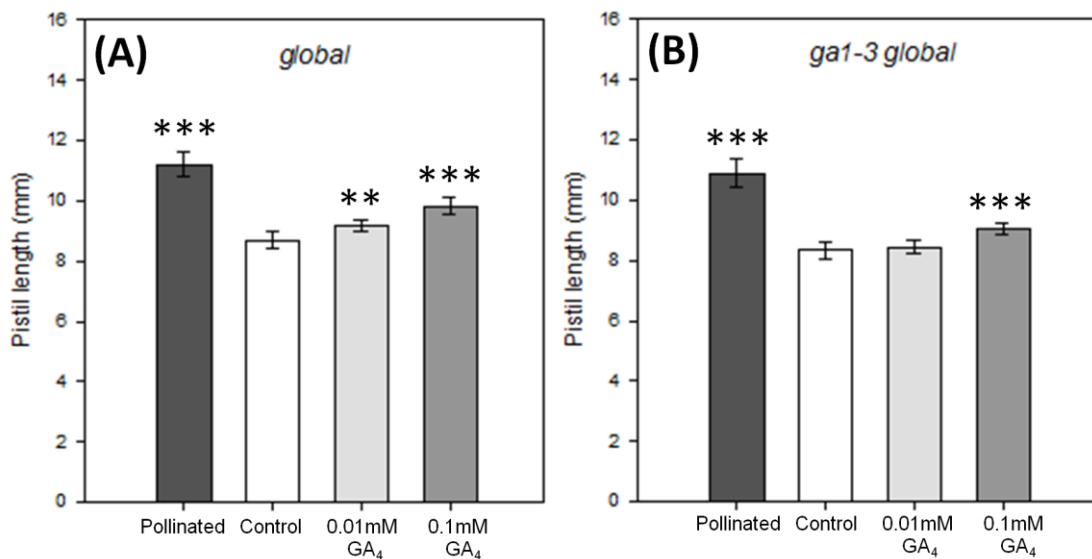


Figure 3.13 GA₄ promotes pistil elongation in *global-DELLA* mutant and *ga1-3 global-DELLA* mutant plants. Pistil length of (A) *global-DELLA* mutant and (B) *ga1-3 global-DELLA* mutant plants in response to increasing concentrations of GA₄. Pistils were measured 7 DPA. Buffer solution was used as the control solution. Values significantly different from control pistils in each of the panels are indicated by asterisks (** for P<0.01 and *** for P < 0.001). Error bars: 95% CI, n ≥ 16

10mM IAA resulted in severe pistil damage (data not shown). As previously reported, application of 0.1mM and 1mM IAA significantly promoted elongation in emasculated wild-type pistils (Vivian-Smith et al., 1999; see Figure 3.11A). However, *global-DELLA* and *ga1-3 global-DELLA* pistils did not respond to IAA treatment (see Figure 3.11B, C).

3.3.6 DELLA-independent GA-response in pistils

Application of GA₃ also promotes parthenocarpic fruit development in wild-type plants (Vivian-Smith et al., 1999; see Figure 3.12A). Surprisingly, significant pistil elongation was also observed in *global-DELLA* and *ga1-3 global-DELLA* upon GA₃ treatment in a dose-dependent manner (see Figure 3.12B, C), revealing for the first time the existence of a DELLA-independent GA response. Application of GA₃ had a greater effect in *ga1-3 global-DELLA* emasculated pistils than in *global-DELLA* pistils and application of 10mM GA₃ to *ga1-3 global-DELLA* emasculated pistils restored pistil length to that of pollinated *ga1-3 global-DELLA* pistils (see Figure 3.12C). An explanation for this could be that endogenous gibberellin levels are lower in *ga1-3 global-DELLA* pistils than in *global-DELLA* pistils and, consequently, *ga1-3 global-DELLA* pistils may have a greater response capacity than *global-DELLA* pistils before reaching saturation point.

GA₃ is not a naturally occurring gibberellin in plants and, in order to rule out that the growth promotion observed in *global-DELLA* and *ga1-3 global-DELLA* pistils could be due to the artificial nature of this compound, pistil growth-promotion experiments were repeated with GA₄ (see Figure 3.13). GA₁ and GA₄ are the two bioactive gibberellins in *Arabidopsis* (Ross et al, 1997), and application of GA₄ to emasculated *global-DELLA* and *ga1-3 global-DELLA* pistils also promoted elongation (see Figure 3.13), confirming the existence of a DELLA-independent GA response in pistils. However in contrast to the GA₃ treatments, application of GA₄ resulted in greater growth promotion in *global-DELLA* emasculated pistils than in *ga1-3 global-DELLA* pistils (see Figure 3.13). No higher concentrations than 1mM GA₄ could be applied as these caused pistil damage (data not shown).

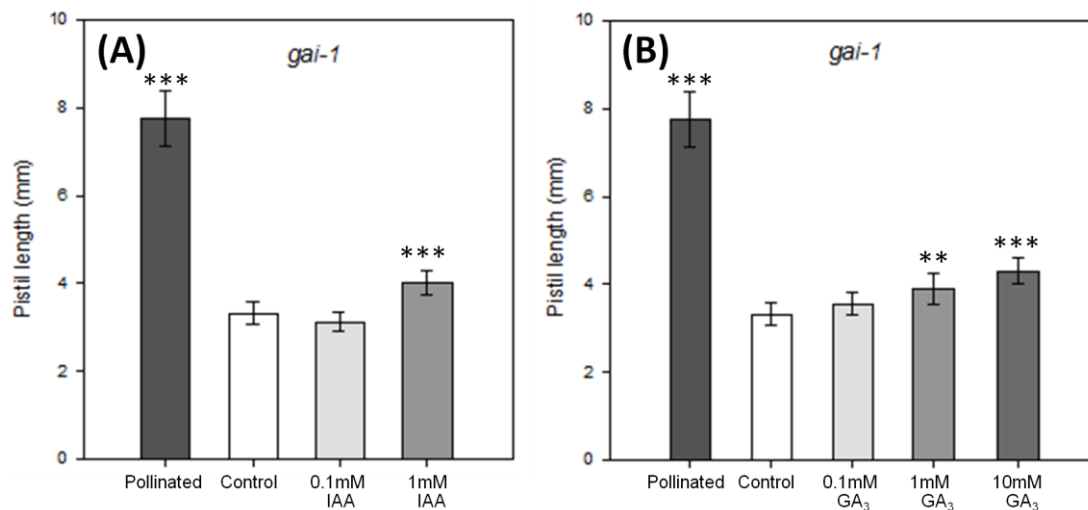


Figure 3.14 IAA and GA₃ promote pistil elongation in *gai-1* mutants. Pistil length of *gai-1* upon (A) IAA and (B) GA₃ treatment. Pistils were measured 7 DPA. Buffer solution was used as the control solution. Values significantly different from control pistils in each of the panels are indicated by asterisks (** for P<0.01 and *** for P < 0.001). Error bars: 95% CI, n ≥ 18

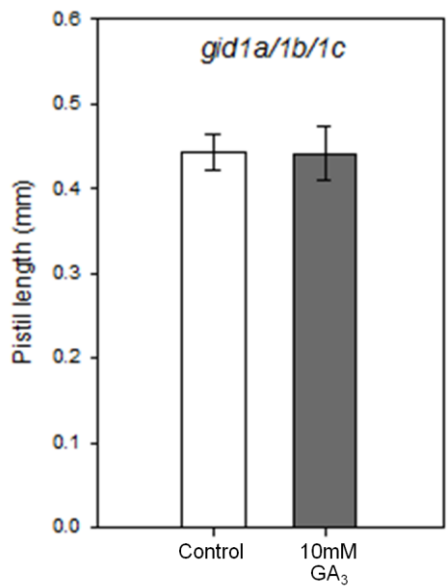


Figure 3.15 GA₃ treatment of *gid1a/1b/1c* triple mutants. Pistil length of triple *gid1a/1b/1c* triple mutants in response to 10mM GA₃. Pistils were measured 7 DPA. Buffer solution was used as the control solution. Error bars: 95% CI, n≥12

pistil elongation (Vivian-Smith et al., 1999; see Figure 3.14A). In contrast to a previous report (Vivian-Smith et al., 1999), application of GA₃ to *gai-1* pistils also resulted in significant growth promotion under our experimental conditions (see Figure 3.14B). Together with the pistil elongation observed in *global-DELLA* and *ga1-3 global-DELLA* mutants upon GA₃ treatment, these results support the existence of a DELLA-independent GA response in fruit development.

3.3.7 Molecular basis underlying DELLA-independent GA-response

3.3.7.1 DELLA-independent response is GID dependent

Three GIBBERELLIN-INSENSITIVE DWARF (GID1) gibberellin receptors have been identified in *Arabidopsis* (Griffiths et al, 2006; Nakajima et al, 2006). Genetic studies have shown that the *gid1a-1 gid1b-1 gid1c-1* (*gid1a/1b/1c*) triple mutant exhibits severe GA-related developmental defects (Griffiths et al, 2006). Furthermore, none of the phenotypic defects observed could be rescued by GA application (Griffiths et al, 2006). In order to determine whether the newly discovered DELLA-independent GA response relies on GID1-mediated GA reception, GA-treatment of *gid1a/1b/1c* triple mutant pistils was carried out (see Figure 3.15). The severe developmental defects observed in *gid1a/1b/1c* triple mutant include delayed flowering time (Griffiths et al, 2006) and under our growing conditions, *gid1a/1b/1c* triple mutant only flowered after two months of vegetative development (data not shown). Due to the reduced number of flowers produced, only the highest GA₃ concentration was used. Application of 10mM GA₃ to *gid1a/1b/1c* triple mutant pistils did not promote pistil elongation (see Figure 3.15), suggesting that the DELLA-independent GA response requires GID1-mediated GA reception.

3.3.7.2 DELLA-independent response is 26S proteasome dependent

Previous studies have shown that 26S proteasome mediated DELLA degradation is necessary for most GA responses (Fu et al, 2002; Feng et al, 2008). Furthermore, the 26S proteasome is a key component of many other hormonal

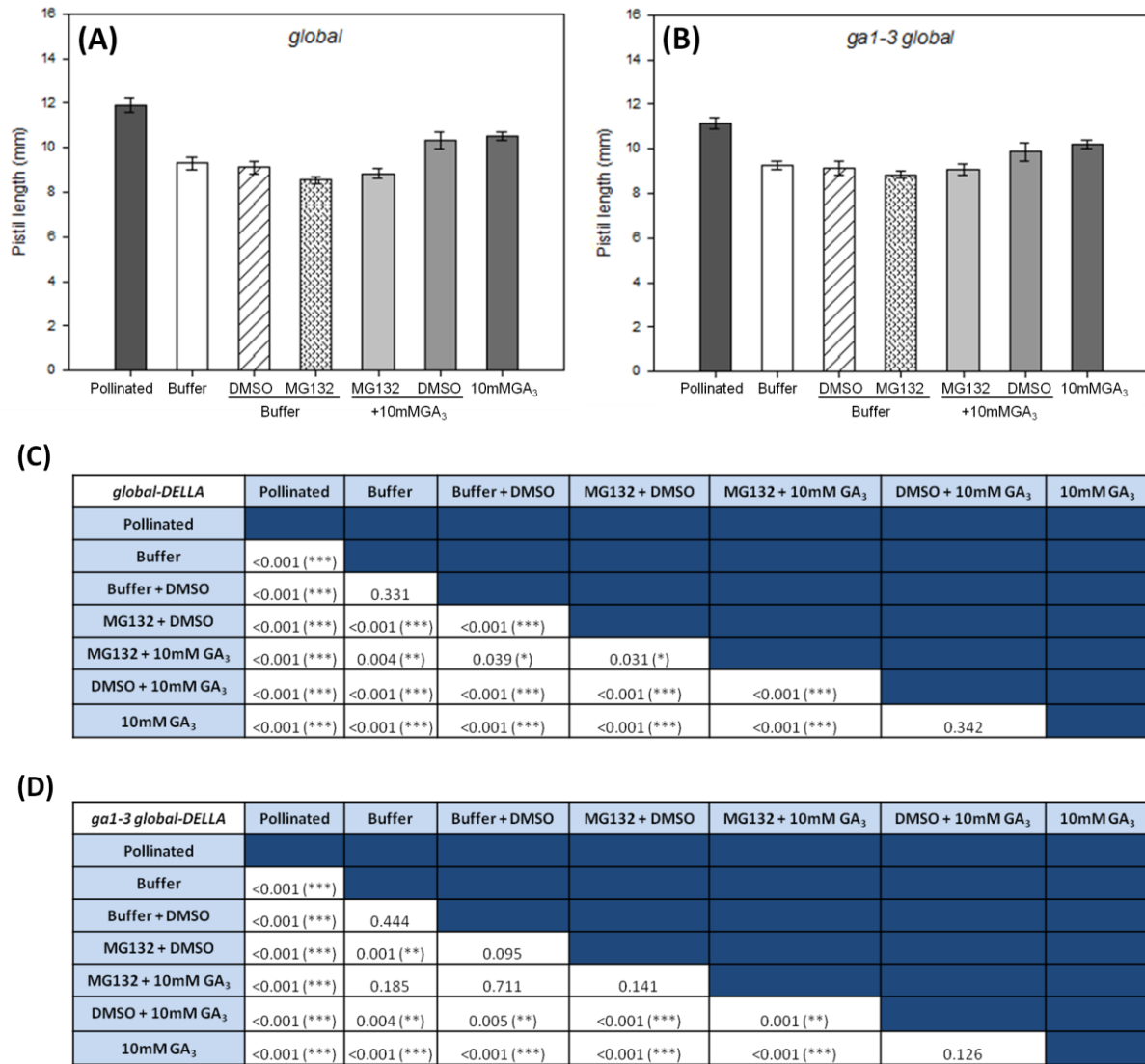


Figure 3.16 DELLA-independent GA response is 26s proteasome dependent.

Pistil length of (A) *global-DELLA* mutant and (B) *ga1-3 global-DELLA* mutant plants in response to MG132 (26s proteasome inhibitor drug) and GA₃ treatment. Pistils were measured 7 DPA. Buffer solution was used as the control solution. Error bars: 95% CI, n(A)≥19, n(B)≥32. Statistical analysis of graphs A and B are shown in (C) and (D) respectively. Probability values are indicated and values significantly different are represented by asterisks (* for P<0.05, ** for P<0.01 and *** for P < 0.001).

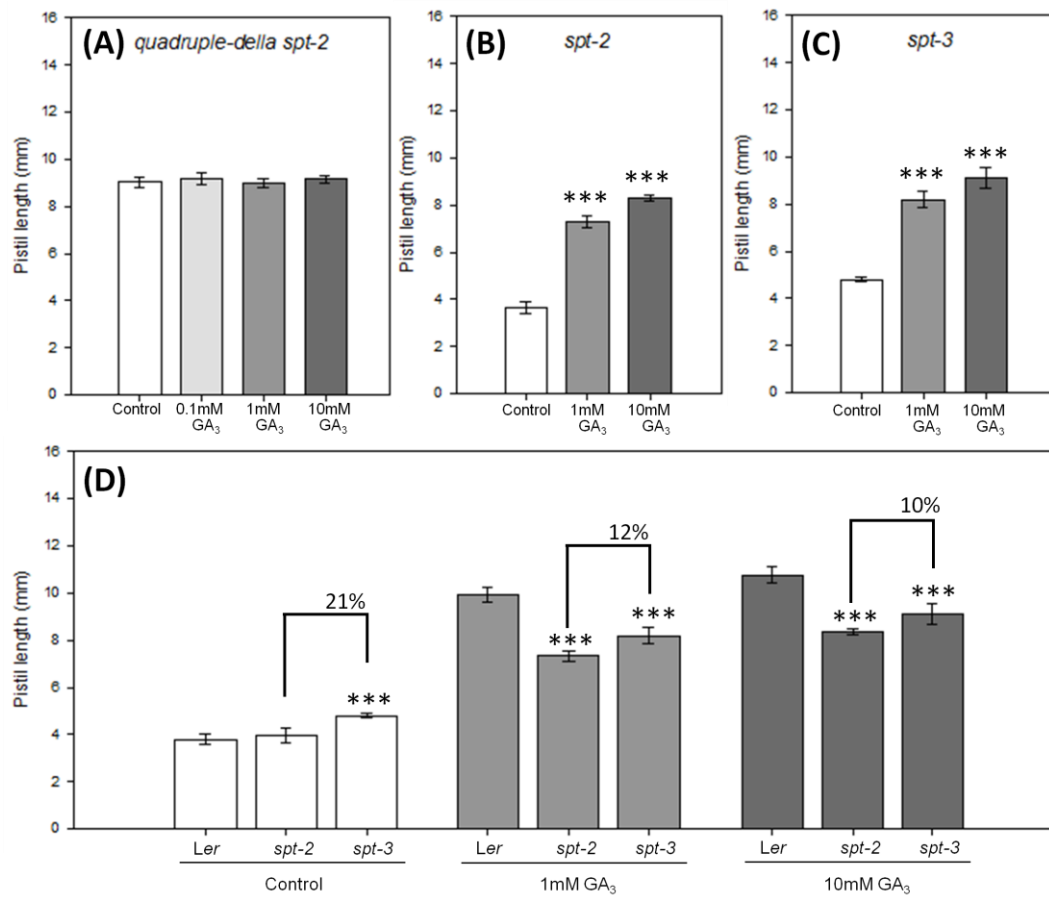


Figure 3.17 SPATULA's role in the DELLA-independent GA response. (A) *quadruple-della spt-2* mutant pistils do not respond to increasing concentrations of GA₃. (B) Pistil length of *spt-2* mutants in respond to increasing concentrations of GA₃. Values significantly different from control pistils are indicated by asterisks (*** for P < 0.001). (C) Pistil length of *spt-3* mutants in respond to increasing concentrations of GA₃. Values significantly different from control pistils are indicated by asterisks (*** for P < 0.001). (D) Pistil length of Ler, *spt-2* and *spt-3* mutants in response to increasing concentrations of GA₃. Values significantly different from Ler pistils are indicated by asterisks (*** for P < 0.001). Error bars: 95% CI, n ≥ 20

signalling cascades (Dreher and Callis, 2007). Thus, in order to determine whether the 26S proteasome is also involved in the DELLA-independent GA response, MG132 treatment (a 26S proteasome specific inhibitor) and GA₃ treatment were combined (see Figure 3.16). As previously recorded, application of 10mM GA₃ promoted elongation of emasculated *global-DELLA* and *ga1-3 global-DELLA* pistils (see Figures 3.12, 3.16). MG132 was diluted in 0.01% DMSO but application of 0.01% DMSO in combination with the control buffer or 10mM GA₃ had no significant effect compared to application of control buffer of 10mM GA₃ alone (see Figure 3.16). However, the growth promotion response observed upon 10mM GA₃ application was completely blocked by pre-treatment with 100µM MG132 (see Figure 3.16), suggesting that the 26S proteasome is part of the newly discovered DELLA-independent GA-response pathway.

3.3.7.3 SPT is part of the DELLA-independent GA-response pathway

SPT is a member of the bHLH family of transcription factors (Heisler et al, 2001) which has been shown to repress GA biosynthesis in dormant seeds (Penfield et al, 2005). The link between SPT and GA-responses is further strengthened by the discovery that SPT can interact with DELLA proteins in yeast two-hybrid assays (Gallego-Bartolome et al, 2010; see Chapter 4). These preliminary results suggest that SPT may play a more active role than previously thought in the GA-response pathway and, therefore, the possible role of SPT in the newly discovered DELLA-independent GA-response pathway was investigated. Whereas combinations of *della* mutants respond to GA application as shown in Figures 3.12-13, application of increasing concentrations of GA₃ to emasculated *quadruple-DELLA spt-2* mutants did not promote pistil elongation (see Figure 3.17A). These data suggest that SPT is part of the newly discovered DELLA-independent GA-response pathway. The *spt-2* mutation has previously been predicted to result in an amino acid substitution in the putative DNA binding domain of SPT and it is suggested to have a dominant-negative effect on fruit development (Heisler et al, 2001; Penfield et al, 2005). Application of GA₃ to emasculated *spt-2* pistils resulted in similar pistil growth promotion to that observed in *spt-3* loss-of-function mutant (see Figure 3.17B, C). Nevertheless, close examination of control-treated emasculated pistils

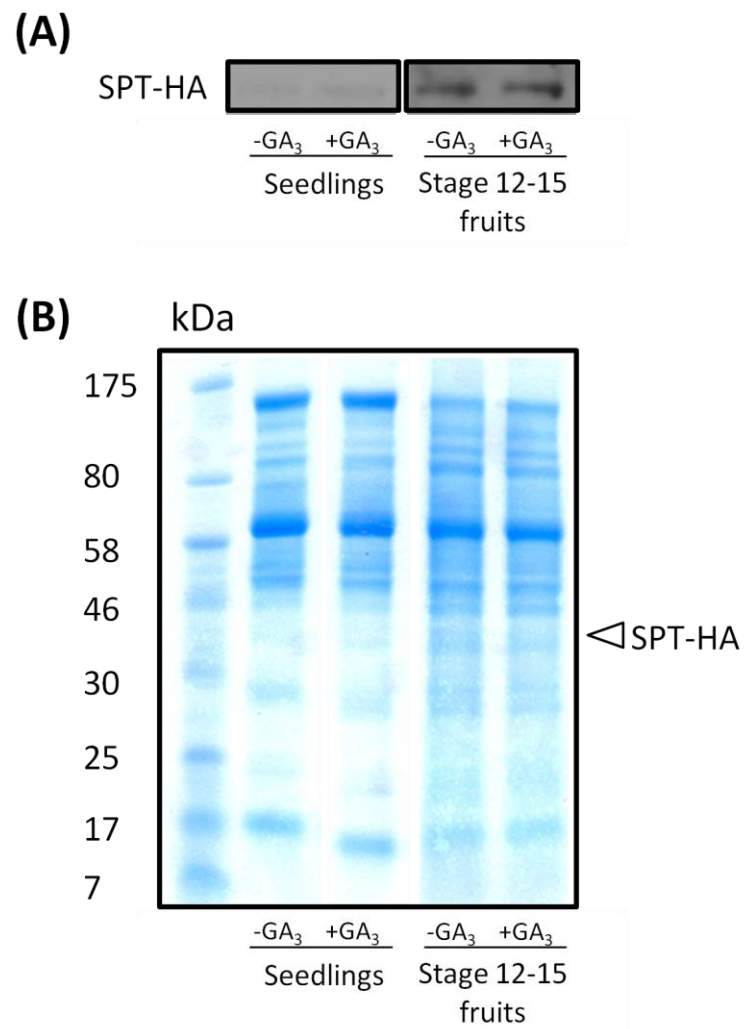


Figure 3.18 SPT-HA is stable upon GA₃ treatment. (A) Western blots showing the stability of SPT-HA upon GA₃ treatment in seedlings and stage 12-15 fruits. (B) Coomassie blue staining of protein gel. SPT-HA size 42 KDa.

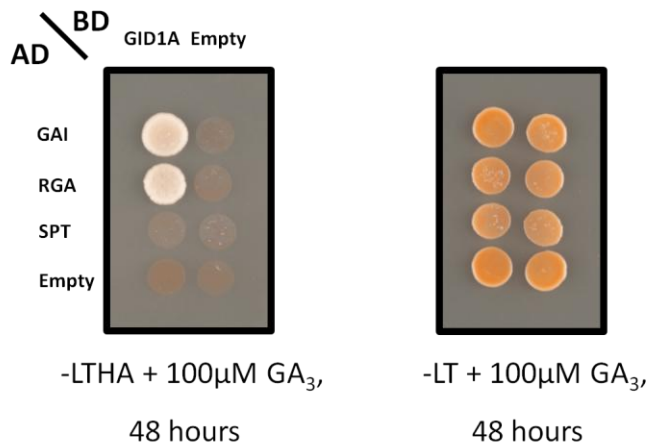


Figure 3.19 SPT does not interact with GID1A receptor in yeast-two-hybrid.

Protein-protein interactions 48 hours after plating in media supplemented with 100μM GA₃.

To gain further insight into how the newly discovered DELLA-independent GA response might be regulated, the *gai Dominant* (*gai-1*) mutant, in which the mutated DELLA protein GAI is resistant to GA-mediated protein degradation, was used (Fleck and Harberd, 2002). These plants were subjected to a series of hormonal treatments. Application of IAA to emasculated *gai-1* pistils promoted showed that *spt-3* pistils were significantly longer than *spt-2* or Ler pistils (see Figure 3.17D), suggesting that SPT is a growth repressor in the context of fruit development.

Taking into consideration the similarities between the DELLA-dependent and DELLA-independent GA pathways, such as the central role that GID1 receptors and the 26S proteasome play in both pathways, it was hypothesised that these similarities may extend even further with SPT fulfilling the growth-repressing role of DELLA proteins in the DELLA-independent GA pathway. DELLA-dependent GA responses rely on GA-mediated DELLA degradation (Silverstone et al, 2001) and, thus, the possible GA-mediated SPT degradation was investigated by western blot analysis (see Figure 3.18). The stability of SPT-HA upon GA₃ treatment was assayed both in seedlings and fruits (see Figure 3.18). GA₃ treatment did not result in SPT-HA protein degradation in seedling or fruits (see Figure 3.18A). It is worth noticing that although Bradford assays were performed to ensure equal total protein loading (data not shown) and coomassie blue staining of protein gels suggested that equal total protein had indeed been loaded (see Figure 3.18B), a considerably lower HA-tag signal was repetitively recorded in seedlings (see Figure 3.18A; data not shown).

Although no GA-mediated SPT protein degradation was observed (see Figure 3.21), the possible similarities between SPT and DELLA proteins were further investigated. Various studies have previously shown that DELLA-domain is essential not only for GA-induced degradation of DELLAs (Dill et al, 2001) but also for GID1 mediated interaction (Willige et al, 2007). Although SPT protein lacks a DELLA-like domain, the possible interaction between SPT and GID1A receptor was assayed (see Figure 3.19). GAI and RGA proteins were used as positive controls and, as previously reported, no interaction between GAI or RGA and GID1A was observed in the absence of gibberellin (Willige et al, 2007; data not

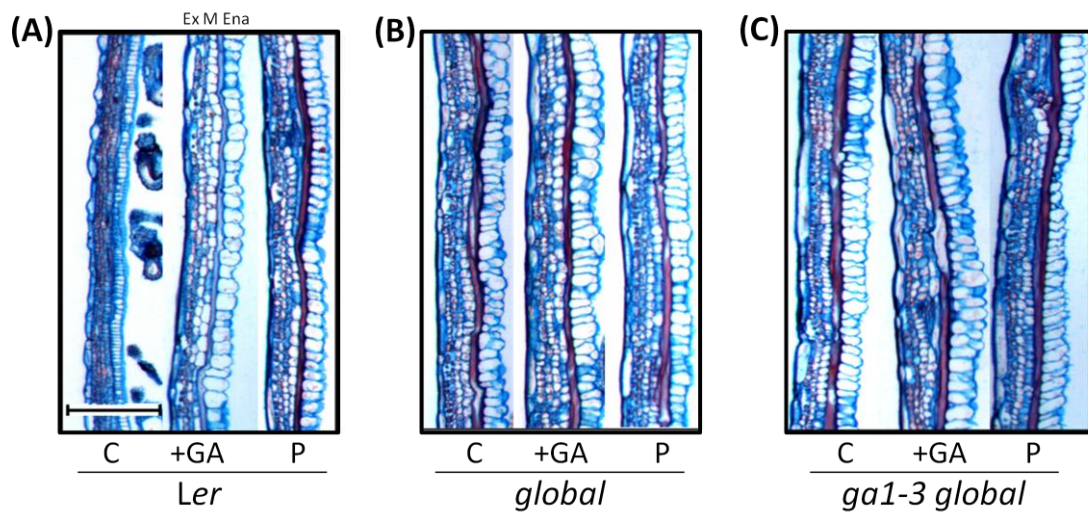


Figure 3.20 Tissue analysis of *Ler*, *global-DELLA* mutant and *ga1-3 global-DELLA* mutant pistils. Longitudinal sections of (A) *Ler*, (B) *global-DELLA* mutant and (C) *ga1-3 global-DELLA* mutant pistils 7 DPA. C= emasculated and control-treated, +GA= emasculated and 10 mM GA₃ treated, P= self-pollinated. Scale bar, 0.2 mm.

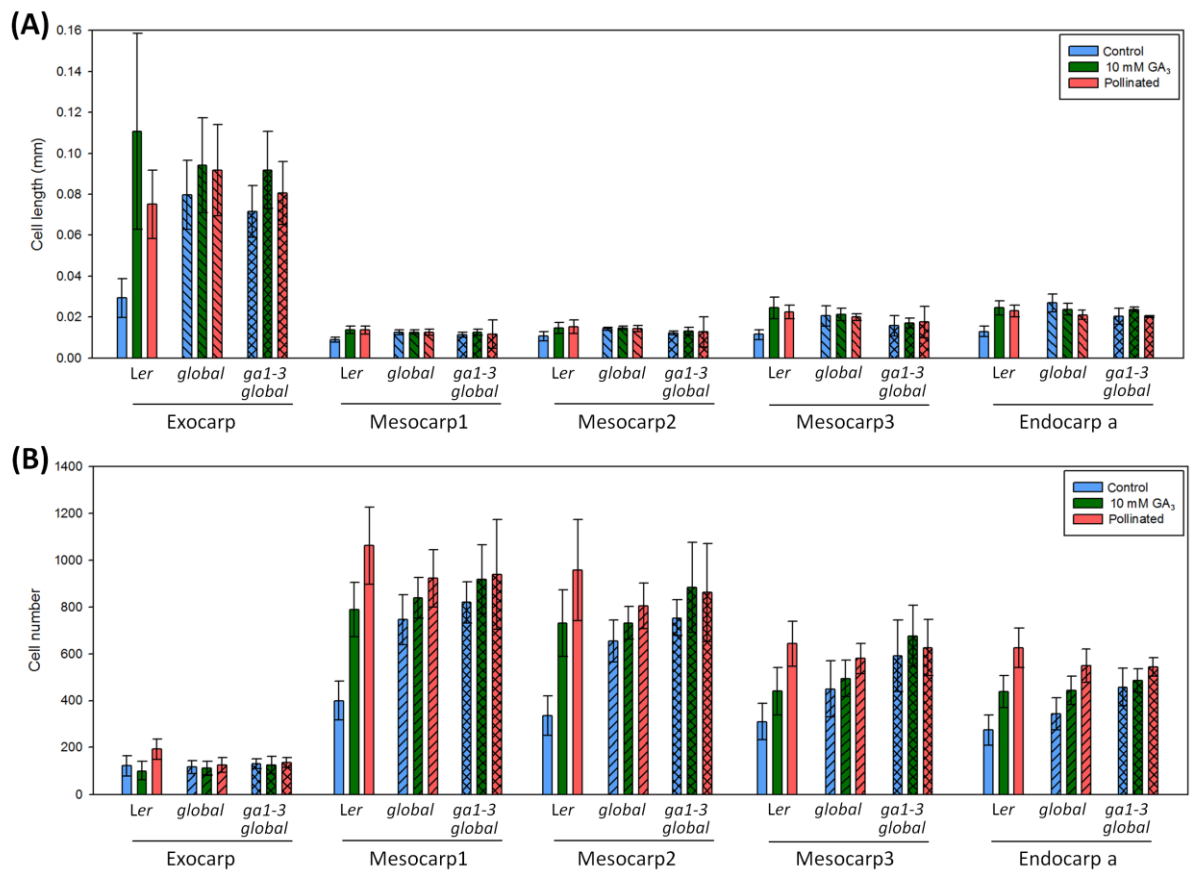


Figure 3.21 Comparison of cell length and cell number in Ler, global-DELLA and ga1-3 global-DELLA pistil sections. (A) Comparison of cell length normal to the pistil elongation axis in Ler, global-DELLA and ga1-3 global-DELLA exocarp, mesocarp (1, 2, 3) and endocarp a tissue layers. (B) Comparison of cell number normal to the pistil elongation axis in Ler, global-DELLA and ga1-3 global-DELLA exocarp, mesocarp (1, 2, 3) and endocarp a (En a) tissue layers.

shown). In the presence of GA₃, a strong interaction between GAI or RGA and GID1A was observed (Willige et al, 2007; see Figure 3.19). However, no interaction was recorded between SPT and GID1A neither in the absence or presence of GA₃ (see Figure 3.19). Taken together, the lack of SPT-GID1A interaction and the lack of GA-mediated SPT degradation suggest that SPATULA's role in the DELLA-independent GA pathway is not equivalent to that of the DELLA proteins' in the DELLA-dependent pathway. Thus, the DELLA-independent pathway is likely to rely on additional molecular players.

3.3.8 Histological analysis of *Ler*, *global-DELLA* and *ga1-3 global-DELLA* pistils

To analyse the cellular basis for the growth observed in parthenocarpic *global-DELLA* and *ga1-3 global-DELLA* pistils, longitudinal carpel wall sections of wild-type and mutant pistils were compared. Three different tissue layers can be differentiated in *Arabidopsis* carpel walls or valves: an outer epidermal layer formed by a single cell-layer (exocarp), a medial tissue-layer formed by three or four cell layers containing chloroplasts (mesocarp) and an inner tissue layer formed by two cell layers (endocarp a, inner cell layer and endocarp b, lignified cell layer formed by narrow elongated cells in between endocarp a and mesocarp layer) (see Figure 3.20). In contrast to emasculated wild-type pistils where the different tissue layers were not clearly differentiated, in *global-DELLA* and *ga1-3 global-DELLA* emasculated pistils all tissue layers were easily distinguishable (see Figure 3.20). Furthermore, lack of DELLA proteins also resulted in significant cell elongation across all tissue layers in parthenocarpic *global-DELLA* and *ga1-3 global-DELLA* pistils, with the greatest effect observed in the exocarp layer (see Figure 3.20, 3.21). Hence, the structure of longitudinal carpel wall sections in *global-DELLA* and *ga1-3 global-DELLA* emasculated pistils resembled more that of GA₃-treated or pollinated wild-type pistils (see Figure 3.20). However, no obvious differences were observed between GA₃-treated and emasculated *global-DELLA* and *ga1-3 global-DELLA* sections (see Figure 3.20).

In order to quantify the effect of GA₃ treatment across the different tissue layers in *global-DELLA* and *ga1-3 global-DELLA* pistils, a detailed histological analysis was carried out. Application of GA₃ to emasculated wild-type pistils promotes cell elongation to a similar extent to pollination across all tissue layers (see Figure 3.21A). However, a greater effect in exocarp cell elongation was recorded upon GA₃ treatment when compared to pollinated wild-type pistils although this difference did not prove to be statistically significant (see Figure 3.21A and Appendix figure 3.3). As previously mentioned, parthenocarpic *global-DELLA* and *ga1-3 global-DELLA* pistils showed significantly longer cells across all tissue layers when compared to emasculated wild-type pistils (see Figure 3.21A and Appendix figure 3.3). However only in m1, m2 and ena tissue layers of parthenocarpic *global-DELLA* and *ga1-3 global-DELLA* pistils showed a greater cell number when compared to emasculated wild-type pistils (see Figure 3.21B and Appendix figure 3.4), suggesting that lack of DELLA proteins may have a greater effect in cell elongation than in cell division. Analysis of GA₃-treated *global-DELLA* and *ga1-3 global-DELLA* pistil sections did not show any significant differences at tissue level when compared to emasculated or pollinated *global-DELLA* and *ga1-3 global-DELLA* pistil sections (see Figure 3.21 and Appendix figures 3.3 and 3.4). Nevertheless, it is interesting to notice that a slight although not significant exocarp cell length promotion was recorded in both *global-DELLA* and *ga1-3 global-DELLA* pistils upon GA₃ treatment (see Figure 3.21A and Appendix figure 3.3). In contrast, a slight although not significant increase in cell number was recorded in the rest of the tissue layers in both *global-DELLA* and *ga1-3 global-DELLA* pistils upon GA₃ treatment (see Figure 3.21B and Appendix figure 3.4).

3.3.9 Analysis of the GA-response at tissue level

The importance of particular tissue layers in the regulation of GA-mediated growth has previously been highlighted by Ubeda-Tomas et al (2008) who showed that DELLA-dependent GA signalling in root endodermis is the rate-limiting factor during root elongation. Furthermore, upregulation of brassinosteroid synthesis in the epidermis has also been shown to promote plant shoot growth (Savaldi-

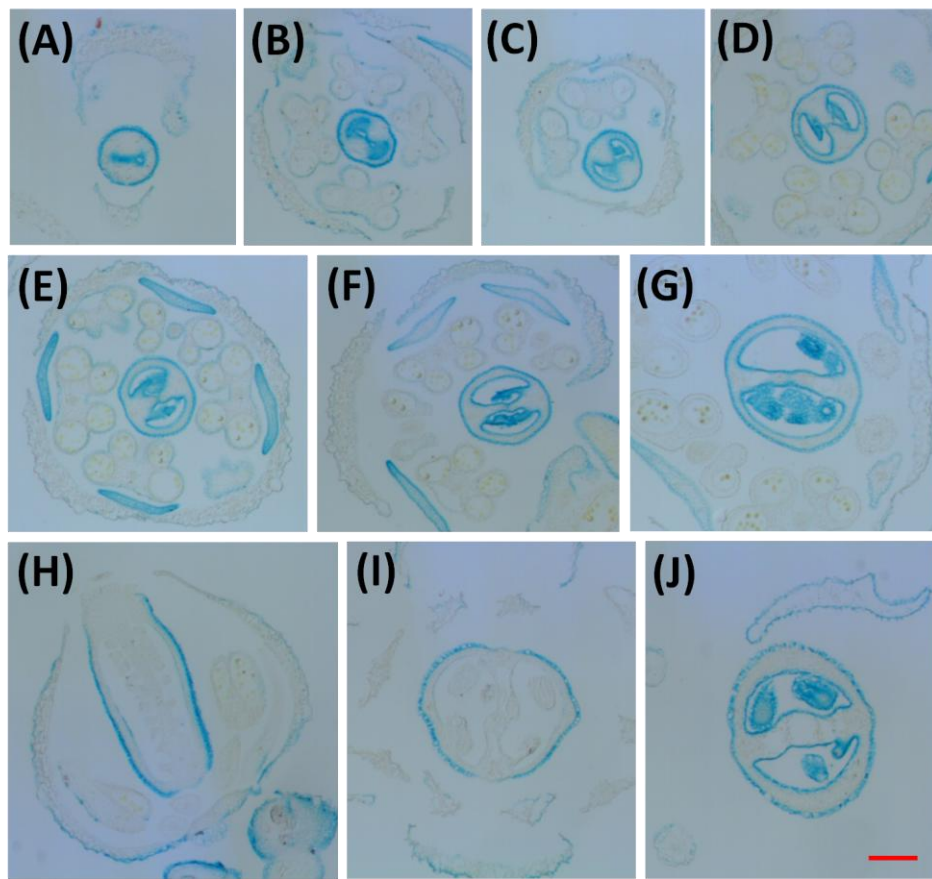


Figure 3.22 *ML1::GUS* expression pattern at flowers stages 7-13. (A) GUS expression at stage 7 of flower development in *ML1::GUS* line 1. (B) GUS expression at stage 9 of flower development in *ML1::GUS* line 1. (C) GUS expression at stage 10 of flower development in *ML1::GUS* line 2. (D) GUS expression at stage 10 of flower development in *ML1::GUS* line 1. (E) GUS expression at stage 11 of flower development in *ML1::GUS* line 2. (F) GUS expression at stage 11 of flower development in *ML1::GUS* line 3. (G) GUS expression at stage 12-13 of flower development in *ML1::GUS* line 2. (H) GUS expression at stage 12-13 of flower development in *ML1::GUS* line 4. (I) GUS expression at stage 12-13 of flower development in *ML1::GUS* line 5. (J) GUS expression at stage 12-13 of flower development in *ML1::GUS* line 6. Scale bar, 0.165mm

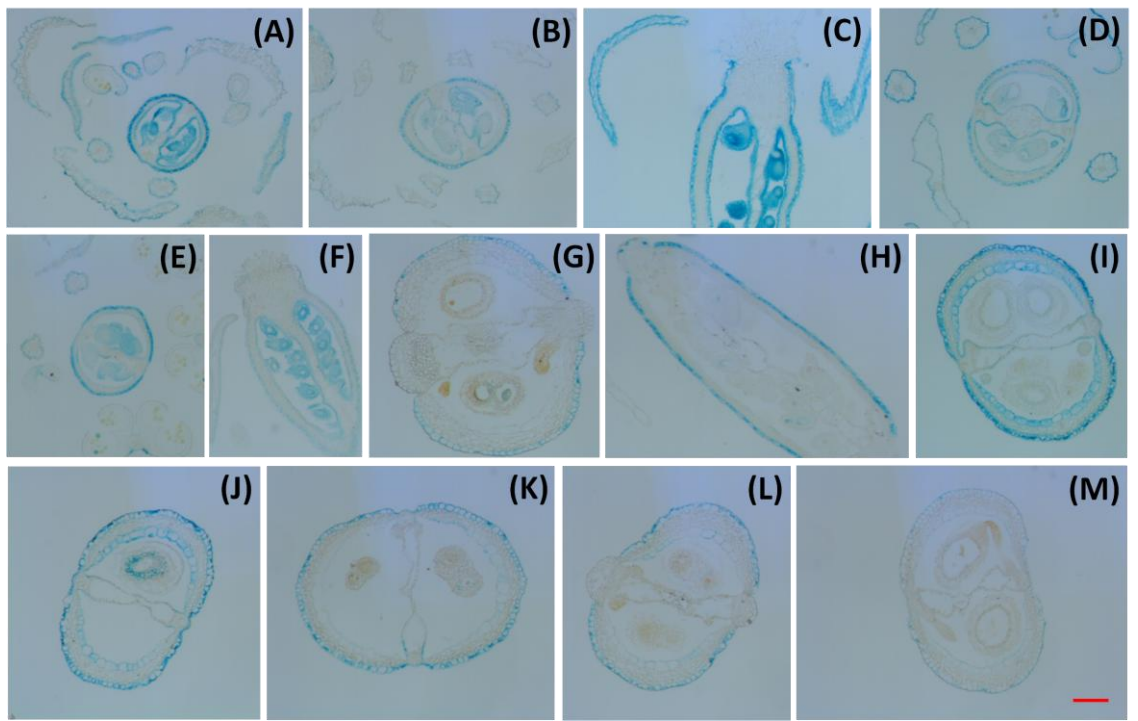


Figure 3.23 *ML1::GUS* expression pattern at fruits stages 14-17a. (A) GUS expression at stage 14 of flower development in *ML1::GUS* line 7. (B) GUS expression at stage 14 of flower development in *ML1::GUS* line 7. (C) GUS expression at stage 14 of flower development in *ML1::GUS* line 6. (D) GUS expression at stage 15 of flower development in *ML1::GUS* line 2. (E) GUS expression at stage 15 of flower development in *ML1::GUS* line 8. (F) GUS expression at stage 15 of flower development in *ML1::GUS* line 3. (G) GUS expression at stage 17a of flower development in *ML1::GUS* line 9. (H) GUS expression at stage 17a of flower development in *ML1::GUS* line 9. (I) GUS expression at stage 17a of flower development in *ML1::GUS* line 2. (J) GUS expression at stage 17a of flower development in *ML1::GUS* line 7. (K) GUS expression at stage 17a of flower development in *ML1::GUS* line 10. (L) GUS expression at stage 17a of flower development in *ML1::GUS* line 4. (M) GUS expression at stage 17a of flower development in *ML1::GUS* line 6. Scale bar, 0.165mm

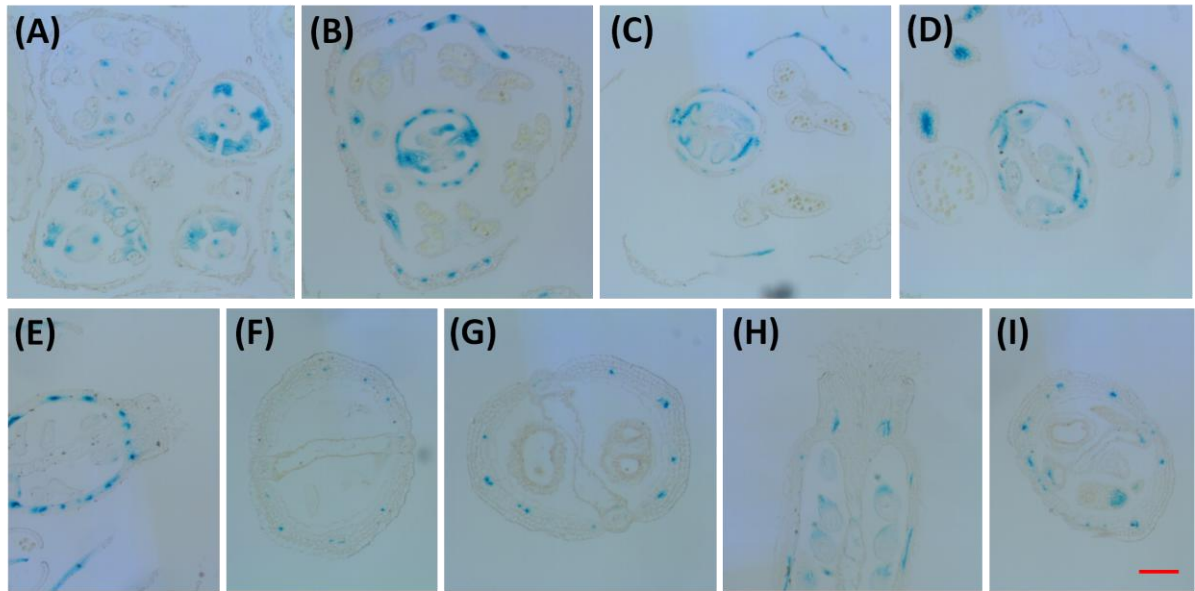


Figure 3.24 *ACI1::GUS* expression pattern at fruits stages 6-17a. (A) GUS expression at stages 6-9 of flower development in *ACI1::GUS* line 1. (B) GUS expression at stage 10 of flower development in *ACI1::GUS* line 2. (C) GUS expression at stage 12 of flower development in *ACI1::GUS* line 1. (D) GUS expression at stage 15 of flower development in *ACI1::GUS* line 1. (E) GUS expression at stage 15 of flower development in *ACI1::GUS* line 3. (F) GUS expression at stage 17a of flower development in *ACI1::GUS* line 4. (G) GUS expression at stage 17a of flower development in *ACI1::GUS* line 2. (H) GUS expression at stage 17a of flower development in *ACI1::GUS* line 2. (I) GUS expression at stage 17a of flower development in *ACI1::GUS* line 1. Scale bar, 0.165mm

Goldstein et al, 2007) suggesting that tissue layer specific regulation of growth is not limited to roots. In order to determine whether a particular tissue layer could also be responsible for DELLA-dependent and/or DELLA-independent GA signalling during fruit development, tissue layer specific disruption of GA signalling would be required. To this end, the expression pattern of different tissue layer specific promoters was studied as a first step for the cloning of tissue layer specific constructs. Full length promoters were cloned to ensure that most of the tissue-specific transcriptional regulatory elements were included.

The *Meristem Layer (ML1)* promoter is specifically expressed in the epidermal layer (L1) of shoots (Sessions et al, 1999) and it has previously been used in tissue-layer specific growth analysis (Savaldi-Goldstein et al, 2007). In order to determine whether the expression pattern of *ML1* promoter is limited to the epidermis at different stages of flower and fruit development, transgenic Arabidopsis plants expressing GUS fusion protein under the control of 4955bp of *ML1* promoter were produced (see Section 3.2.9). Due to time constrains, only analysis of T1 lines was carried out. Nevertheless, in order to ensure that a representative expression pattern was recorded, a number of different transgenic lines were analysed (see Figure 3.22). At stages 7-13 of flower development, strong GUS expression was observed in the epidermal layer of pistils (see Figure 3.22). A strong GUS signal was also observed in the endocarp layer and developing ovules at stages 7-13 (see Figure 3.22). In the two of the weakest GUS expressing lines (line 4 and 5), only the exocarp GUS signal was recorded (see Figures 3.22H, I). In general, after fertilisation (stage 14) *ML1::GUS* expression became weaker in ovules and endocarp layer whilst exocarp GUS signal was still observed in all of the transgenic lines examined (see Figure 3.23). By stage 17a, none of the transgenic lines examined showed an ovule-specific signal (see Figure 3.23H-M). No GUS expression was recorded at the final stages of fruit development (data not shown).

Initial characterisation of the expression pattern of *ALC-INTERACTING PROTEIN1 (ACI1)* in developing fruits showed that *ACI1* expression is restricted to the vascular bundle and mesocarp layer (Fang et al, 2008). Thus, in order to confirm this reported expression pattern, transgenic Arabidopsis plants expressing

GUS fusion protein under the control of 4100bp of *ACI1* promoter were produced (see Section 3.2.9). Although due to time constrains only analysis of T1 lines was feasible, a number of transgenic lines were analysed in order to ensure the most representative expression pattern possible. At stages 6-9 of flower development, *ACI1::GUS* expression in the pistils is restricted to the vascular bundles associated to what would later form the replum (see Figure 3.24A). By stage 10-15, strong GUS expression was still observed in the replum vasculature although a patchy signal was also present in the mesocarp layer (see Figure 3.24B, C, D, E). It is likely that this GUS signal may be associated to vascular bundles as a strong GUS expression was also recorded in the funiculus (see Figure 3.24B, C, D). At stage 17a only mesocarp vascular bundles showed *ACI1::GUS* expression (see Figure 3.24F, G, H, I). No GUS signal was observed at later stages of fruit development (data not shown).

3.4 Discussion

3.4.1 Role of DELLA-dependent GA signalling in the control of gynoecium and fruit growth

DELLA proteins play an important role in the regulation of GA-dependent floral development (Cheng et al, 2004; Tyler et al, 2004). It has previously been shown that *quadruple-DELLA* mutants have longer petals and stamens than wild-type plants, supporting a role for DELLA proteins as key growth repressors during floral growth (Cheng et al, 2004). In order to investigate whether this was also the case during gynoecium and fruit development in *Arabidopsis*, *global-DELLA* and *ga1-3 global-DELLA* pistils were analysed throughout the different stages of pistil development.

3.4.1.1 Lack of DELLA proteins promotes style and stigma growth

As previously described in *quadruple-DELLA* mutants, *global-DELLA* and *ga1-3 global-DELLA* mutants also exhibit elongated floral organs (Cheng et al, 2004; see

Figure 3.3). In addition, detailed characterisation of stage 12 flowers concluded that lack of DELLA proteins also results in style and stigma growth promotion (see Figure 3.5). Although previous studies had already shown that silencing of a single DELLA protein in tomato promoted style growth (Marti et al, 2007), the discovery that lack of DELLA proteins also promoted style elongation in *Arabidopsis* suggests that the role of DELLAs in style development is not limited to fleshy fruit development. Furthermore, style elongation could be phenocopied in wild-type *Arabidopsis* pistils upon GA treatment (see Figure 3.6), supporting the hypothesis that style development is under the control of DELLA-dependent GA signalling.

In addition to gibberellins, auxin has also been shown to play a role in style and stigma development. Polar auxin transport (PAT) disruption in wild-type pistils via NPA-treatment results in auxin accumulation in the apical region and, consequently, in style and stigma growth promotion (Nemhauser et al, 2000). Style and stigma growth promotion via auxin was shown to be tightly linked to a reduction in the overall ovary and valve length (Nemhauser et al, 2000). However, no such reduction was observed in *global-DELLA*, *ga1-3 global-DELLA* or GA-treated wild-type pistils (data not shown). Thus, it is likely that whilst the role of auxin in style and stigma development may be related to boundary establishment and tissue patterning, gibberellins' role may just be limited to growth promotion.

To date to the author's knowledge, all the molecular players known to be involved in style development have been shown to play a tissue patterning role (Roe et al, 1997; Kuusk et al, 2002; Alvarez et al, 2009; Trigueros et al, 2009; Colombo et al, 2010). Thus, DELLA proteins are the first molecular players shown to be involved exclusively in style growth. However, how these tissue patterning and growth factors interact during style development remains to be clarified.

3.4.1.2 Lack of DELLA proteins causes facultative parthenocarpy

The importance of DELLA-dependent GA signalling in gynoecium and fruit development is further supported by the observation that emasculation of *global-DELLA* and *ga1-3 global-DELLA* pistils promotes parthenocarpic fruit development

(see Figures 3.2, 3.8, 3.9). It has previously been reported that emasculation of *quadruple-DELLA* Arabidopsis mutant also results in fertilisation-independent fruit growth (Dorcey et al., 2009). However, the role that individual *DELLA* genes may play during fruit development remains poorly understood.

The Arabidopsis genome encodes five *DELLA* genes (Peng et al., 1997; Silverstone et al., 1998; Sanchez-Fernandez et al., 1998; Lee et al., 2002; Wen et al., 2002) and transcript level analysis showed that their expression profiles follow three different patterns during pistil development (see Figure 3.7). This suggests that different *DELLA* genes may be important at different stages of fruit growth. For example, *RGL3* expression decreases after fertilisation but increases when the maximum fruit length is achieved at stage 17b (see Figure 3.7C) suggesting a possible role of *RGL3* in determining final fruit length. Although *DELLA* protein activity is subjected to many other levels of regulation (Achard and Genschik, 2009), these results are in accordance with previous studies which emphasize the relevance of the transcriptional regulation of *DELLA* genes (Tyler et al., 2004; Oh et al., 2007). A detailed analysis of the parthenocarpic capacity of different *della* mutant combinations was also carried out in order to understand the relative importance of individual *DELLA* proteins in the control of fruit initiation (see Figures 3.8, 3.9). Emasculation of single *della* mutants showed that only emasculation of *rgl1* mutants resulted in slight pistil growth promotion and additional lack of *DELLA* proteins is required to promote substantial fruit elongation (see Figure 3.8, 3.9). However, no difference was observed between parthenocarpic *quadruple-DELLA* and *global-DELLA* mutants (see Figures 3.8, 3.9 and Appendix figures 3.1, 3.2), suggesting at most a very minor contribution from *RGL3* in fruit-growth repression despite its expression profile. Thus, *GAI*, *RGA*, *RGL2* and particularly *RGL1* are likely to play the main role in the control of fruit development.

The facultative parthenocarpy observed in *della* mutants could be due to alterations in hormonal levels. However, *DELLA* proteins are involved in positive regulation of GA biosynthesis (Hedden et al., 2000; Silverstone et al., 2001; Olszewski et al., 2002; Dill et al., 2001; Zentella et al., 2007; Achard and Genschik, 2009) and, consequently, *della* mutants are likely to have low levels of

biologically active gibberellins. In addition to gibberellins, auxin is also known to play a key role in the promotion of fruit growth (Gillaspy et al., 1993). Measurement of endogenous IAA concentration in *global-DELLA* and *ga1-3 global-DELLA* pistils showed that parthenocarpic mutant pistils had significantly lower IAA levels than emasculated wild-type pistils (see Figure 3.10). Together, these data shows that high levels of gibberellins or auxin are not responsible for the observed parthenocarpic fruit growth. Thus, these results confirm that the facultative parthenocarpy observed in *della* mutants is directly attributable to the constitutive activation of DELLA-dependent GA signalling. In the last few years, our understanding of DELLA proteins' growth-repressing action has improved significantly with the discovery that DELLA proteins are capable of blocking the activity of certain bHLH transcription factors by binding to their DNA-binding domain (de Lucas et al, 2008; Feng et al, 2008). It is likely that DELLA-dependent fruit growth repression may also rely on the inactivation of other transcription factors and yeast two-hybrid screening of *Arabidopsis* flower and fruit cDNA library with DELLA proteins could undoubtedly contribute to the uncovering of these transcription factors.

3.4.2 DELLA-independent GA-response during fruit development

Although emasculation of *global-DELLA* and *ga1-3 global-DELLA* pistils results in fruit growth promotion, the parthenocarpic fruits are shorter than seed-bearing siliques (see Figures 3.2, 3.8, 3.9) suggesting that pathways other than DELLA-dependent GA signalling may be involved in the control of fruit development. It has previously been proposed that the inability of auxin to induce fruit-set in *ga1-3* mutants may indicate that a threshold of endogenous GA biosynthesis is required for auxin-induced fruit development (Vivian-Smith et al., 1999). In agreement with this, application of IAA to emasculated *global-DELLA* and *ga1-3 global-DELLA* pistils does not promote pistil elongation (see Figure 3.11). Alternatively, DELLA-dependent GA signalling may be an absolute requirement for auxin-induced fruit development (Dorcey et al., 2009).

The generation of a complete *della* knockout mutant such as *global-DELLA* and *ga1-3 global-DELLA* allows the identification of DELLA-independent GA responses. Such a response was indeed obtained when GA₃ was applied to emasculated *global-DELLA* and *ga1-3 global-DELLA* pistils which resulted in significant growth promotion (see Figure 3.12) revealing the existence of a DELLA-independent GA response. Counter intuitively, this DELLA-independent GA response was not observed when comparing emasculated *global-DELLA* and *ga1-3 global-DELLA* pistils. It has previously been suggested that GA levels may be lower in *ga1-3 global-DELLA* mutants than in *global-DELLA* mutants due to the *ga1-3* mutation (Prof. Nick Harberd, personal communication). If this is indeed the case, longer emasculated *global-DELLA* pistils than emasculated *ga1-3 global-DELLA* pistils would have been expected as a result of the DELLA-independent GA response. However, no significant difference in length was observed between emasculated *global-DELLA* and *ga1-3 global-DELLA* pistils (see Figures 3.11, 3.12, 3.13 and 3.16). An explanation for this may be found in the fact that no quantification of GA has been carried out in *global-DELLA* or *ga1-3 global-DELLA* plants and, thus, it is impossible to conclude whether the levels of bioactive GA are indeed different in these two mutant backgrounds. Alternatively, if a difference in bioactive GA levels is recorded between *global-DELLA* and *ga1-3 global-DELLA* pistils, this difference may not prove to be biologically relevant.

Application of GA₃ to the dominant *gai-1* mutant pistils also promotes elongation (see Figure 3.14) supporting the DELLA-independence of the newly discovered response. However at present, we cannot discard the possibility that the growth promotion observed in *gai-1* pistils could also be partially mediated by degradation of the remaining functional DELLA proteins in the *gai-1* mutant.

In order to further characterise the DELLA-independent GA-pathway, the possible role played by *GID1* receptors and the 26S proteasome was investigated. No growth promotion was recorded in *gid1a/1b/1c* triple mutant pistils upon GA₃ treatment (see Figure 3.15), suggesting that GID1-mediated GA reception is necessary for DELLA-independent GA responses. These results also support the

hypothesis that *GID1A*, *GID1B* and *GID1C* are likely to be the only GA receptors in Arabidopsis.

26S proteasome-mediated degradation has been shown to play a central role in most hormone-signalling pathways (Dreher and Callis, 2007). Pre-treatment of emasculated and GA₃-treated *global-DELLA* and *ga1-3 global-DELLA* pistils with 100μM MG132 (26S proteasome inhibiting drug) blocked the DELLA-independent GA-response (see Figure 3.16), suggesting that 26S proteasome-mediated degradation is also required during DELLA-independent GA- response pathway. It is interesting to notice that application of MG132 alone to emasculated *global-DELLA* and *ga1-3 global-DELLA* pistils also resulted in growth reduction when compared to buffer- or DMSO- and buffer-treated pistils (see Figure 3.16). As previously mentioned, the 26S proteasome is a key component of many hormone signalling pathways (Dreher and Callis, 2007) and, consequently, blocking of the 26S proteasome is likely to affect simultaneously several hormone signalling pathways.

Several lines of evidence, such as SPT repression of GA biosynthesis (Penfield et al, 2005) and SPT-DELLA interactions (Gallego-Bartolome et al, 2010; see Chapter 4), suggest that SPT may be involved in the GA-response pathway. Application of GA₃ to emasculated *quadruple-DELLA spt-2* pistils did not result in growth promotion (see Figure 3.17A), confirming that SPT is part of the the DELLA-independent GA-pathway. By comparison of emasculated *spt-3* (loss-of-function mutant) and *spt-2* (dominant-negative mutant) pistils with emasculated wild-type pistils it was concluded that SPT acts as growth repressor during fruit development (see Figure 3.17). These results are in accordance with a recent report showing that SPT functions as a repressor of leaf growth (Ichihashi et al, 2010). Based on its growth repressing capacity, it was hypothesised that the role of SPT in the DELLA-independent GA pathway may be comparable to that of DELLA proteins, no GA-mediated SPT degradation was observed (see Figure 3.18). Furthermore, GA₃ did not promote GID-SPT interaction in yeast (see Figure 3.19), suggesting that the DELLA-independent signalling pathway is likely to rely on additional molecular players.

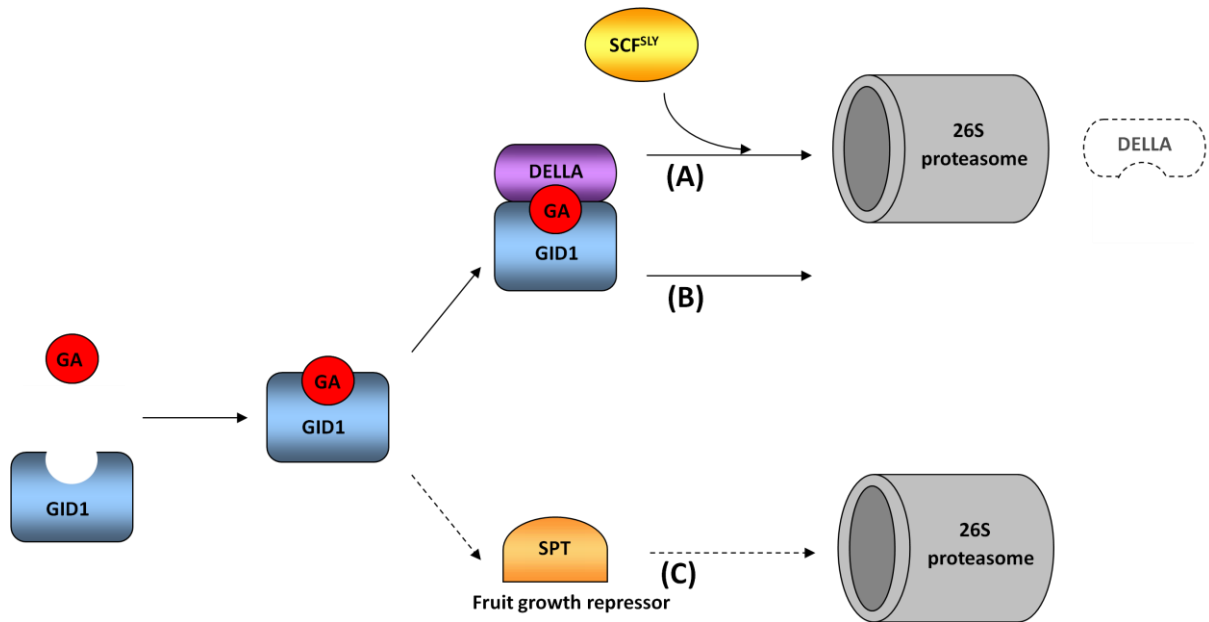


Figure 3.25 GA signalling during fruit development. Gibberellin binding to the GID1 receptors enables the formation of DELLA-GA-GID1 complex resulting in (A) 26s proteasome-dependent DELLA degradation and (B) proteolysis-independent DELLA inactivation. (C) Upon GA reception a DELLA-independent pathway is also activated which relies on SPT action and 26s proteasome mediated degradation.

3.4.3 GA signalling during fruit development

The data presented here show that DELLA proteins play important regulatory roles during gynoecium and fruit development. According to the “relief of restraint” model (Harberd, 2003), GA-mediated DELLA protein degradation by the 26S proteasome is required to activate GA responses. Although this is likely to be the dominant pathway regulating DELLA activity, a recently reported proteolysis-independent mechanism of DELLA inactivation (Ariizumi et al., 2008; Ueguchi-Tanaka et al., 2008) suggests that GA signalling may be a far more complex process than previously described. In accordance with this idea, a DELLA-independent GA response during *Arabidopsis* fruit development was uncovered in this study. Nevertheless, the disparity observed in the range and severity of responses when comparing the effects of DELLA-dependent and DELLA-independent promotion of fruit growth suggests that the core of GA responses is regulated through DELLA protein degradation. A summary of GA signalling during pistil development is shown in Figure 3.25.

At the tissue level, the importance of particular tissue layers in the regulation of GA-mediated pistil growth remains to be clarified. Lack of DELLA proteins in parthenocarpic *global-DELLA* and *ga1-3 global-DELLA* pistils resulted in significant cell elongation across all tissue layers when compared to wild-type pistils (see Figures 3.20, 3.21). However, preliminary evidence suggests that the exocarp may be the primary GA-responsive tissue during fruit development. This hypothesis is based on the following observations: first, GA₃ treatment had a greater effect in exocarp cell elongation than pollination in wild-type pistils (see Figure 3.21 and Appendix figure 3.3). Second, although cell elongation was indeed observed across all tissue layers in parthenocarpic *global-DELLA* and *ga1-3 global-DELLA* pistils and, no statistically significant differences were recorded, the effect was greatest in the exocarp layer although this difference did not prove to be significant (see Figure 3.21 and Appendix figure 3.3). Third, exocarp cell elongation was also very slightly promoted in both *global-DELLA* and *ga1-3 global-DELLA* pistils upon GA₃ application although this promotion did not prove to be statistically significant (see Figure 3.21 and Appendix figure 3.3). Based on these

observations alone, it is not possible to conclude whether the exocarp is indeed the primary GA-responsive tissue during fruit development particularly considering the lack of statistical significance. It is possible that the growth rate dictated by exocarp cells might explain the increased cell numbers recorded in the inner tissue layers upon GA₃ application (see Figure 3.21). But similarly, the inner tissue cell division may be the primary GA response which could in turn drive exocarp cell elongation. Although gibberellin action has traditionally been associated to cell length promotion (Srivastava et al, 1975; Davidonis, 1990; Inada et al, 2000; Cheng et al, 2004; Ubeda-Tomas et al, 2008), it has recently been shown that DELLA growth repressing action involves the reduction of both cell proliferation and expansion rates (Archard et al, 2009a). Thus, further experiments are required to determine the relative importance of particular tissue layers in the regulation of GA-mediated growth.

The use of cell layer-specific attenuation of the GA response will undoubtedly provide the means to answer this conundrum. A similar approach was already used to show that DELLA-dependent GA signalling in root endodermis is the rate-limiting factor during root elongation (Ubeda-Tomas et al, 2008). To this end, characterisation of tissue layer-specific promoters was started in this study. Analysis of *ML1::GUS* expression pattern throughout the different stages of pistil development showed that *ML1* expression is limited to the epidermis and endodermis layers (see Figures 3.22, 3.23). However, in many of the transgenic GUS lines analysed, endodermis GUS signal was weaker than the epidermis signal (see Figures 3.22, 3.23). It is likely that *ML1* promoter could be used to target *GAI-1* expression (resistant to GA-mediated degradation) to cause epidermis-specific attenuation of the GA response in pistils. By construction of a DEX-inducible system and monitoring DEX penetration in pistils it might be possible to achieve epidermis-specific expression.

ACI1::GUS expression pattern was also investigated at different stages of pistil development, in order to determine whether *ACI1* promoter could be used to drive mesocarp-specific expression. However, analysis of several *ACI1::GUS* transgenic lines showed that GUS expression is mainly limited to the vascular bundles of the

mesocarp (see Figure 3.24). Thus, a different mesocarp-specific promoter would be required to drive mesocarp-specific attenuation of the GA response in pistils.

3.4.4 Future work

The in-depth characterisation of GA signalling during fruit development carried out in this study has lead to the discovery of new complexity levels of GA signalling. In addition to the study of the role played by GA in style, stigma and parthenocarpic fruit development, a new DELLA-independent GA-signalling pathway has been uncovered. Although initial characterisation of this pathway allowed the identification of several molecular players involved in DELLA-independent GA-signalling, the role of DELLA-independent GA responses remains to be further clarified. Mutant screenings based on a complete *della* deficient background would undoubtedly provide an excellent opportunity to study DELLA-independent GA signalling. Nevertheless, due to the difficulties associated to working in a quintuple or/and sextuple mutant background, a yeast two-hybrid screen with GID1A receptor as bait could be used as a first step to uncover molecular players involved in the DELLA-independent GA-signalling pathway. As shown in this study, application of GA₃ did not promote SPT-GID interaction; however, based on our understanding of GA perception in the DELLA-dependent pathway, GID1 receptor binding proteins are also likely to exist in the DELLA-independent GA pathway. A yeast-two hybrid screen with GID1a receptor as bait in the presence and absence of GA has already been carried out using a 3 day-old etiolated Col-0 seedlings yeast-two hybrid library. However, in this screen only DELLA proteins were identified as GID1a interactors (Prof. Claus Schwechheimer personal communication). Based on these results, it is likely that a flower and fruit specific yeast-two hybrid library might be required to uncover the potential GID1 receptor binding proteins that could form part of the DELLA-independent GA pathway. Furthermore, if such interactors were identified in a flower and fruit specific yeast-two hybrid library and not in a seedling library, this would suggest that the DELLA-independent GA pathway may be flower and fruit specific.

In addition to the further characterisation of the newly discovered DELLA-independent GA-signalling pathway, the importance of particular tissue layers in the regulation of GA-mediated pistil growth also remains to be clarified. Preliminary steps were adopted during this study for the characterisation of tissue layer specific promoters and, based on the *ML1::GUS* expression pattern, it was concluded that *ML1* could potentially be used to cause epidermis-specific attenuation of the GA response in pistils. However, further promoter GUS studies are required for the identification of other tissue layer specific promoters and later cloning of tissue-specific *GAI-1* inducible constructs.

CHAPTER 4

**Protein-protein interactions and
DELLAs**

CHAPTER 4

Protein-protein interactions and DELLAS

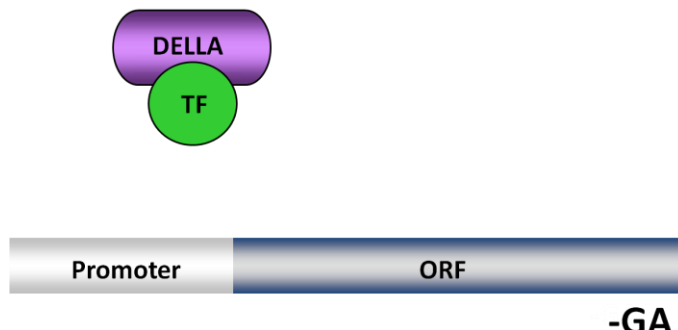
4.1 Introduction

4.1.1 DELLA proteins' mode of action

DELLA proteins are members of the GRAS-domain transcription-factor family (Pysh et al, 1999) and, although they lack a DNA binding domain, their role as transcriptional regulators is clear (Ogawa et al, 2003; Zentella et al, 2007; Hou et al, 2008). Our understanding of the mechanism by which DELLA proteins function improved significantly in 2008 with the discovery that DELLA proteins are capable of blocking the activity of certain members of the bHLH transcription-factor family by interacting with their DNA binding domain (de Lucas et al, 2008; Feng et al, 2008). Thus, the DNA-binding capacity of bHLH transcription factors is compromised and GA-mediated destabilisation of this inactive complex is required to allow bHLH transcription factor accumulation and function (see Figure 4.1; de Lucas et al, 2008; Feng et al, 2008). To date, five members of the bHLH transcription factor family have been found to bind to DELLA proteins, namely PIF3, PIF4, SPT, PIL2 and PIL5 (de Lucas et al, 2008; Feng et al, 2008; Gallego-Bartolome, 2010). Nonetheless, only the biological relevance of DELLA-PIF3 and DELLA-PIF4 protein interactions have been confirmed by further genetic and mutant studies (de Lucas et al, 2008; Feng et al, 2008).

In this chapter the wider role of the newly discovered DELLA proteins' mode of action has been explored, particularly in the area of fruit development, using a yeast two-hybrid approach (see Figure 4.2; Section 4.2). The possible interaction between DELLA proteins and those bHLH transcription factors known to be involved in fruit development and/or patterning (IND, SPT and ALC) has been tested. Additionally, in order to establish whether DELLA- binding capacity is

(A)



(B)

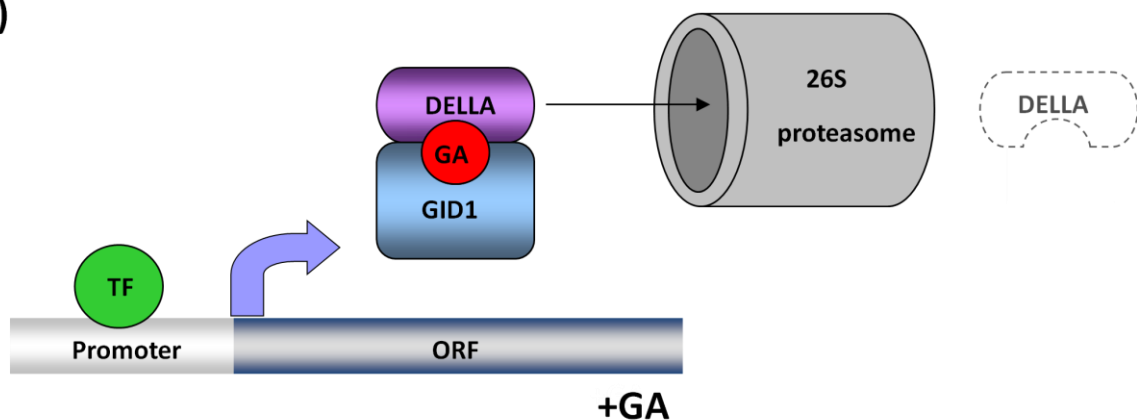


Figure 4.1 DELLA proteins' mode of action. (A) In the absence of GA, DELLA proteins bind to members of the bHLH transcription-factor family (TF), forming an inactive protein complex. (B) In the presence of GA, DELLA proteins are sequestered by the GA-GID complex allowing TF accumulation and function.

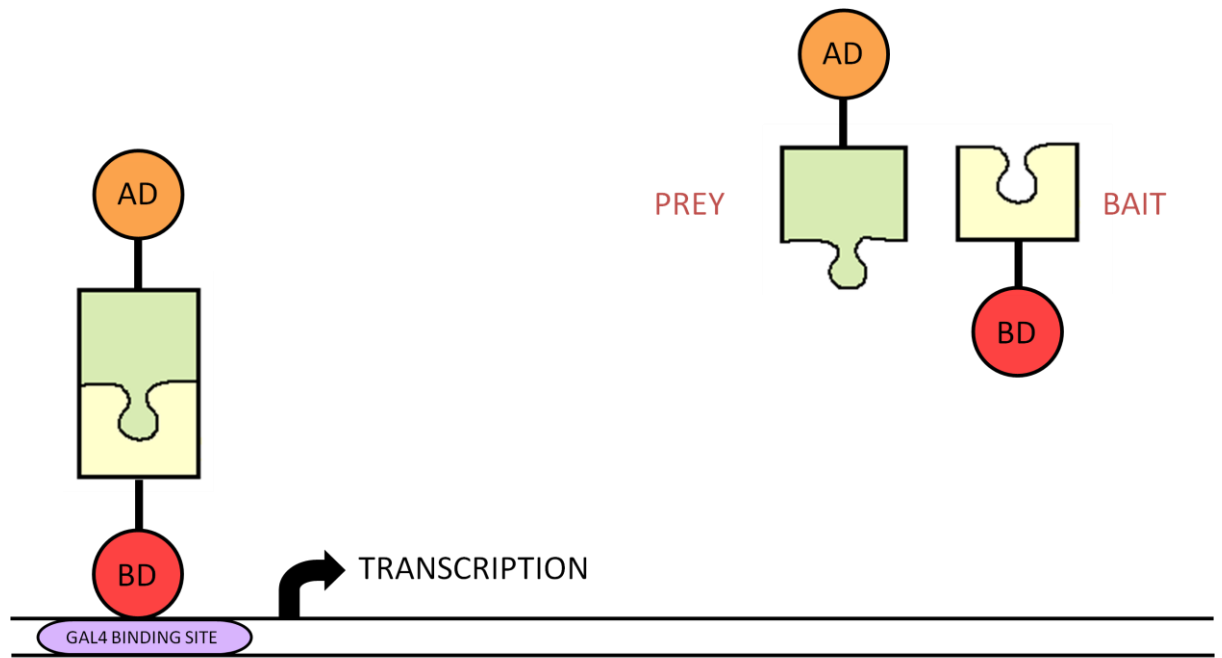


Figure 4.2 Schematic representation of the yeast two-hybrid system. In the yeast two-hybrid assay a prey protein is expressed fused to the GAL4 activation domain (AD) while a bait protein is expressed fused to the GAL4 DNA-binding domain (BD). Interaction of prey and bait fusion proteins activates transcription by binding to the GAL4 binding site which is confirmed by growth in interaction-selective medium.

limited to the bHLH transcription-factor family, other transcription factors known to play a role in fruit development and/or patterning have also been studied, i.e., RPL (a homeodomain transcription factor), FUL (a MADS-domain factor) and ETT (an auxin response transcription factor).

4.2 Materials and methods

4.2.1 Plasmid construction for yeast assays

For the yeast two hybrid assays, the pGAD424 and pGBT9 vectors from Clontech Laboratories Inc. were used as the activation-domain vector and binding-domain vector respectively. The GAI, RGA, RGL2, ALC, SPT, ETT, RPL, FUL and IND coding regions and the truncated versions IND*, IND*1, IND*2 and GAI* were amplified by PCR with primers containing SmaI and PstI restriction sites (see Table 4.1). The amplicons were cloned in frame between SmaI and PstI sites of pGAD424 and pGBT9 to form both preys and baits respectively. After confirming the plasmid quality by sequencing, prey plasmids were transformed into yeast Y187 (-Leu) and bait plasmids into AH109 (-Trp). Prey transformants were selected in SD-L medium (SD broth supplemented with 2% glucose (Formedium), Complete supplement mixture –Leu (Formedium), [pH 5.8] 10% Agar) whilst bait transformants were selected in SD-T medium (SD broth supplemented with 2% glucose (Formedium), Complete supplement mixture –Trp (Formedium), [pH 5.8] 10% Agar).

For the yeast two-one hybrid assays, the pGBT9 vector from Clontech Laboratories Inc. was modified in order to remove the DNA-binding domain. pGBT9 was first linearised with EcoRI followed by a partial digestion with HindIII. After Klenow blunting and purification with PCR-purification kit (Qiagen) the product was ligated overnight. The resulting vector, pG9, was confirmed by sequencing and used to clone the bait proteins in the yeast two-one hybrid assay. In addition to the newly created pG9 vector, the pGAD424 vector from Clontech Laboratories Inc. was also used as the activation-domain vector. The SPT and IND coding regions were amplified by PCR with primers containing SmaI and PstI

restriction sites (see Table 4.1). The amplicons were cloned in frame between SmaI and PstI sites of pGAD424 and pG9 to form both preys and baits respectively. After confirming the plasmid quality by sequencing, prey and bait plasmids were transformed into yeast Y187 (-Leu). Transformants were selected in SD-LT medium (SD broth supplemented with 2% glucose (Formedium), Complete supplement mixture -Leu -Trp (Formedium), [pH 5.8] 10% Agar). Simultaneously, the target DNA sequence (5'-CGCGTG-3') was cloned in tandem into the pLacZi vector. After confirming the plasmid quality by sequencing, the plasmid was transformed into yeast YM4271 and transformants were selected in SD-U medium (SD broth supplemented with 2% glucose (Formedium), Complete supplement mixture -Ura (Formedium), [pH 5.8] 10% Agar).

4.2.2 LiAc yeast transformation

Yeast transformation was carried out as described in the Clontech Laboratories Yeast Protocols Handbook (www.clontech.com). 1ml of YPD liquid medium (20g/l difco peptone, 10g/l yeast extract, 2% glucose [pH 6.4]) was inoculated with several colonies of 2-3mm in diameter (Y187 for prey plasmids and/or AH109 for bait plasmids) and vortexed vigorously for 5 minutes to disperse any clumps. These minicultures were transferred into a flask containing 50ml of YPD and incubated at 30°C shaking at 250rpm overnight or until the stationary phase was reached ($OD_{600}>1.5$). Approximately 30ml of the overnight culture was transferred to a flask containing 300ml of YPD ($OD_{600}= 0.2-0.3$). The diluted culture was incubated at 30°C shaking at 250rpm for around 3hr until an OD_{600} of 0.4-0.6 was reached. 100ml of these cultures were centrifuged at 1,000xg for 5 minutes at RT. The supernatants were discarded and the cell pellets were resuspended in freshly-made sterile TE and centrifuged again at 1,000xg for 5 minutes at RT. The supernatant was discarded and the cell pellet resuspended in 1.5ml freshly prepared sterile 1xTE/1xLiAc. Simultaneously, 0.1 μ g of the plasmid DNA to be transformed was mixed with 0.1mg of herring testes carrier DNA in a new eppendorf tube. 0.1ml of the yeast competent cells was added to each eppendorf tube and mixed by vortexing. Following this, 0.6ml of sterile PEG/LiAc solution was added to each tube and vortexed for 10sec. The cells were incubated at 30°C for

30min with shaking at 250rpm after which 70 μ l of DMSO was added and gently mixed by inversion. The yeast cells were heatshocked for 15min in a water bath at 42°C and, then, chilled on ice for 1-2min. Finally, cells were centrifuged for 10sec at 14,000rpm at RT and resuspended in 0.5ml of freshly- made sterile TE. In order to select the desired transformants, 150 μ l of the resuspended cells were plated on SD-L (prey transformants), SD-T (bait transformants), SD-LT (prey and bait transformants for yeast two-one hybrid) or SD-U (for transformants carrying the DNA target sequence for yeast two-one hybrid) medium and incubated up-side-down at 30°C until colonies appear (approximately 3 days).

4.2.3 Integration of plasmids into the yeast genome (for yeast two-one hybrid assays)

Yeast transformation was carried out as described in the Clontech Laboratories Yeast Protocols Handbook (www.clontech.com). The LiAc transformation procedure (see Section 4.2.2) was followed with the following exceptions:

- Before transformation, the vector was linearised with EcoRI.
- A greater amount of DNA was used for transformation and 1-4 μ l of the plasmid DNA to be transformed was mixed with 0.1mg of herring testes carrier DNA.
- Finally before plating, centrifuged cells were resuspended in a smaller amount of TE (150 μ l of TE buffer).

4.2.4 Yeast mating

For each plasmid of interest to be tested, a single yeast transformant colony was resuspended in 500 μ l of YPD. The tubes were vigorously vortexed to disperse the cells. For each mating combination, a 20 μ l aliquot of each of the plasmids was mixed into 160 μ l of YPD medium and incubated overnight at 30°C shaking at 200rpm.

4.2.5 Yeast two hybrid: protein-protein interaction

In order to confirm mating efficiency and protein-protein interactions, 10 μ l of each mating culture was plated on SD-LT (growth confirms mating) and SD-LTHA (SD broth supplemented with 2% glucose (Formedium), Complete supplement mixture -Ade -His -Leu -Trp (Formedium), [pH 5.8] 10% Agar) plates (growth confirms interaction) and incubated up-side-down at 30°C until colonies grew (3-5 days).

4.2.6 Yeast two-one hybrid interactions: Colony-lift filter Assay

For each of the yeast two-one hybrid interactions to be assessed a single colony from the SD-LTU (SD broth supplemented with 2% glucose (Formedium), Complete supplement mixture -Leu -Trp -Ura (Formedium), [pH 5.8] 10% Agar) plates was resuspended in 5ml of liquid SD-LTU medium (SD broth supplemented with 2% glucose (Formedium), Complete supplement mixture -Leu -Trp -Ura (Formedium) [pH 5.8]) and grown overnight at 30°C shaking at 200rpm. The next day, the overnight cultures were vortexed and 10 μ l of each culture was freshly plated in SD-LTU medium. Once the colonies grew after 2-3 days of incubation at 28-30°C, a filter paper (cut to the size of the plate) was pre-soaked in 2.5-5ml of Z buffer/X-gal solution in a clean Petri dish. Simultaneously, a clean dry filter paper was placed over the surface of the plate of the colonies to be assayed. The filter paper was gently rubbed with clean forceps to help the colonies cling to the filter. Once the filter paper was evenly wetted, it was carefully lifted off from the agar plates with the forceps and submerged in liquid nitrogen with the colonies facing up. After the filter paper was frozen completely, it was allowed to thaw at RT. The thawed filter paper was placed with the colony side up on the previously pre-soaked filter. The filter papers were incubated in the dark at 28°C and checked periodically for the appearance of blue colonies which confirmed yeast two-one hybrid interaction.

4.2.7 Quantification of protein-protein interaction: β -galactosidase ONPG assay

For each of the protein-protein interactions to be quantified, a single colony from the SD-LT or SD-LTU plates was resuspended in 5ml of liquid SD-LT or SD-LTU media and grown overnight at 30°C shaking at 200rpm. Next day, the overnight cultures were vortexed and 2ml of each culture was resuspended in 8ml of YPD. The fresh cultures were incubated at 30°C for 3-5hr with shaking (230-250rpm) until the cells reached mid-log phase ($OD_{600}=0.5-0.8$). At this point, the OD_{600} s were recorded. 1.5ml of each culture was placed in five eppendorf tubes and centrifuged at 14,000rpm for 30sec. Supernatants were carefully removed and cell pellets were resuspended in 1.5ml of Z buffer ($Na_2HPO_4 \cdot 7H_2O$ 16.1 g/L, $NaH_2PO_4 \cdot H_2O$ 5.50 g/L, KCl 0.75 g/L, $MgSO_4 \cdot 7H_2O$ 0.246 g/L, [pH 7.]). Tubes were centrifuged once more and the supernatants removed. Cell pellets were resuspended again in 300 μ l of Z buffer (concentration factor= 5). 0.1ml of each cell suspension was transferred to a new eppendorf tube. The tubes were subsequently frozen in liquid nitrogen for 1min and, then, thawed in a water bath at 37°C. The freeze/thaw cycle was repeated once more to ensure that the cells had broken open. At the same time, a blank tube was set up with 100 μ l of Z buffer. 0.7ml of Z buffer + 0.2 μ l β -mercaptoethanol was added to each of the tubes including the blank tube. Immediately, 160 μ l of ONPG solution was added and the tubes were incubated at 30°C until yellow colour developed. The time of incubation was carefully recorded in minutes. After the yellow colour developed, 0.4ml of 1M Na_2CO_3 was added to stop the reaction and the tubes were centrifuged for 10min at 14,000rpm to pellet cell debris. The OD_{420} of the samples relative to the blank was measured by calibrating the spectrophotometer against the blank and used to calculate the β -galactosidase units:

$$\beta\text{-galactosidase units} = 1000 \times OD_{420} / (t \times V \times OD_{600})$$

t=minutes of incubation for colour to develop

V= 0.1ml x concentration factor

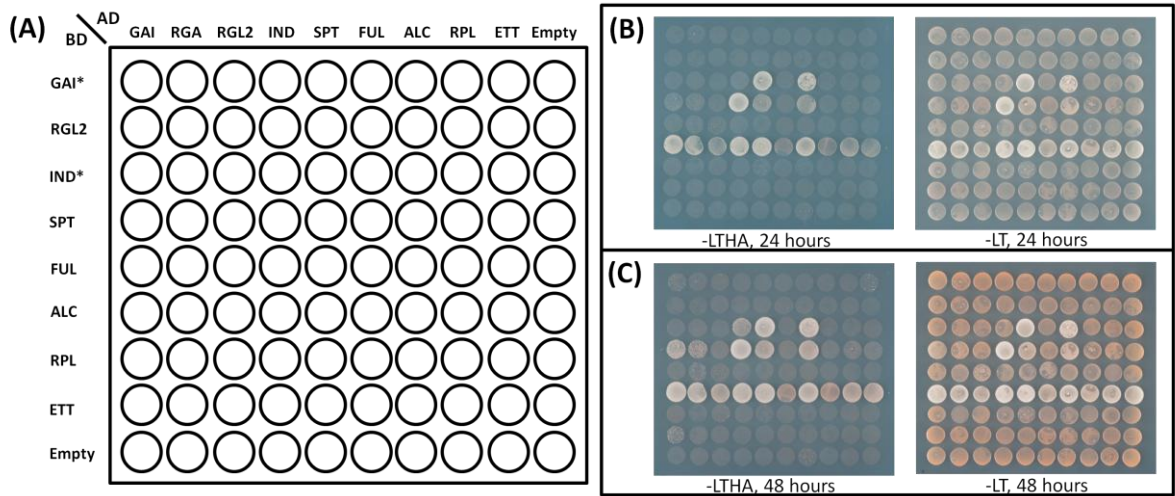


Figure 4.3 Complete yeast matrix. (A) Schematic representation of the protein-protein interactions assayed. (B) Protein-protein interactions 24 hours after plating. (C) Protein-protein interactions 48 hours after plating.

4.3 Results

4.3.1 DELLA proteins interact with several bHLH transcription factors involved in fruit development and/or fruit patterning

A yeast two-hybrid strategy was adopted in order to uncover the possible protein-protein interactions of GAI, RGA and RGL2 with IND, SPT, FUL, ALC, RPL and ETT proteins, which are known to play a role in fruit development and/or fruit patterning. After the cloning of the coding sequences of GAI, RGA, RGL2, IND, SPT, FUL, ALC, RPL and ETT into both pGAD424 and pGBT9 vectors and transformation into yeast (see Sections 4.2.1; 4.2.2), preliminary tests (data not shown) revealed that IND-BD, GAI-BD and RGA-BD showed autoactivation capacity in the interaction-selective medium (SD-LTHA). Thus, truncated versions of IND (IND*) missing the first 56 amino acid (see Figure 4.6A) and of GAI (GAI*) missing the first 156 amino acids were cloned and used as baits in the yeast two-hybrid assay (Figure 4.3A).

For each of the interactions to be tested (see Figure 4.3A), 10 μ l of mating culture (see Sections 4.2.4; 4.2.5) was plated in both SD-LT and SD-LTHA media in order to confirm the mating efficiency and interaction respectively. 24 hours after plating, it was observed that GAI-AD and RGA-AD interact with ALC-BD, that ALC interact with SPT and that both ALC and SPT are capable of forming homodimers (see Figure 4.3B). Previously known interactions were also confirmed namely the IND-ALC interaction (Liljegren et al, 2004) and the IND-SPT interaction (Gremski et al, 2007) (see Figure 4.3B).

During the first 24 hours after plating it was also observed that the ALC-BD/Empty-AD mating culture had started to grow slowly, suggesting a certain degree of autoactivation capacity of the ALC-BD construct. This autoactivation capacity was confirmed 48 hours after plating (see Figure 4.3C). The assessment of the yeast two hybrid matrix after 48 hours also allowed the confirmation of the SPT-DELLA interaction (Figure 4.3C; Gallego-Bartolome, 2010) and the discovery of IND

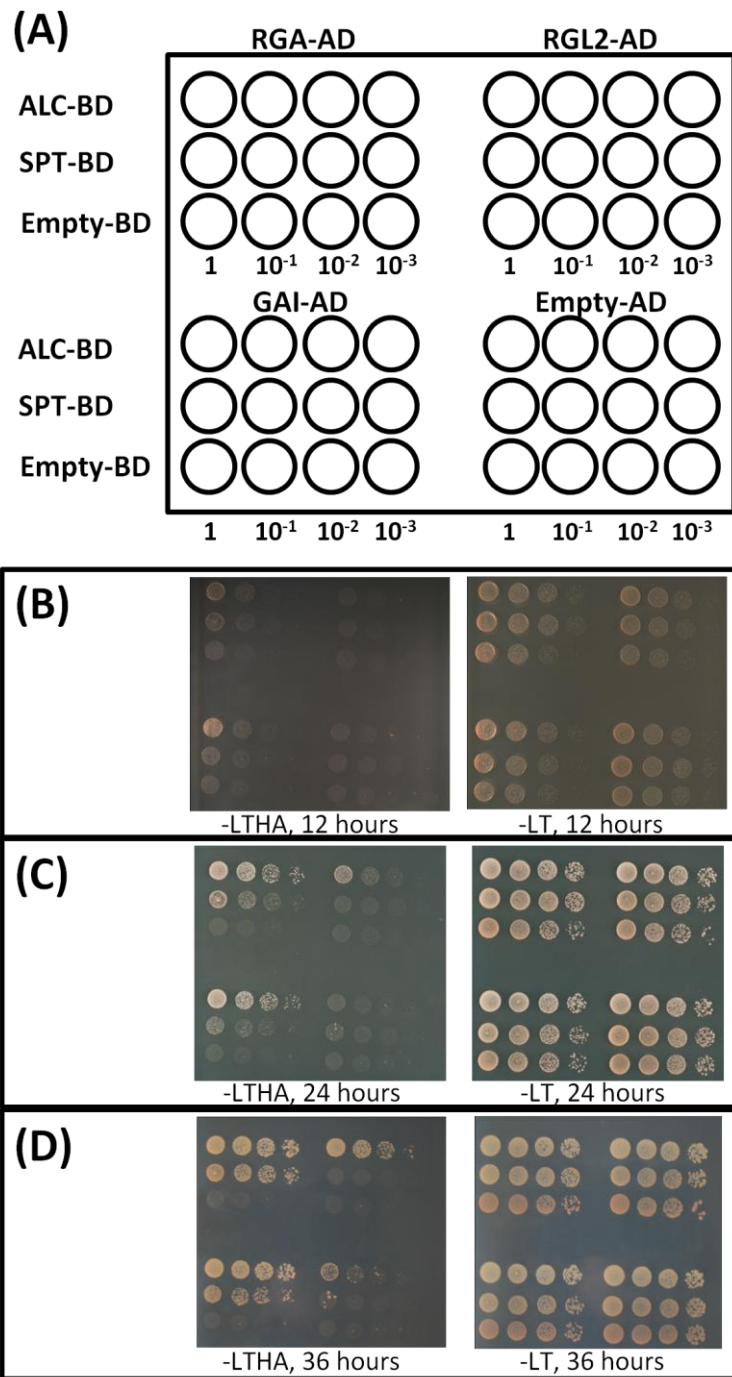


Figure 4.4 ALC-DELLA interaction. (A) Schematic representation of the protein-protein interactions assayed. (B) Protein-protein interactions 12 hours after plating. (C) Protein-protein interaction 24 hours after plating. (D) Protein-protein interaction 36 hours after plating.

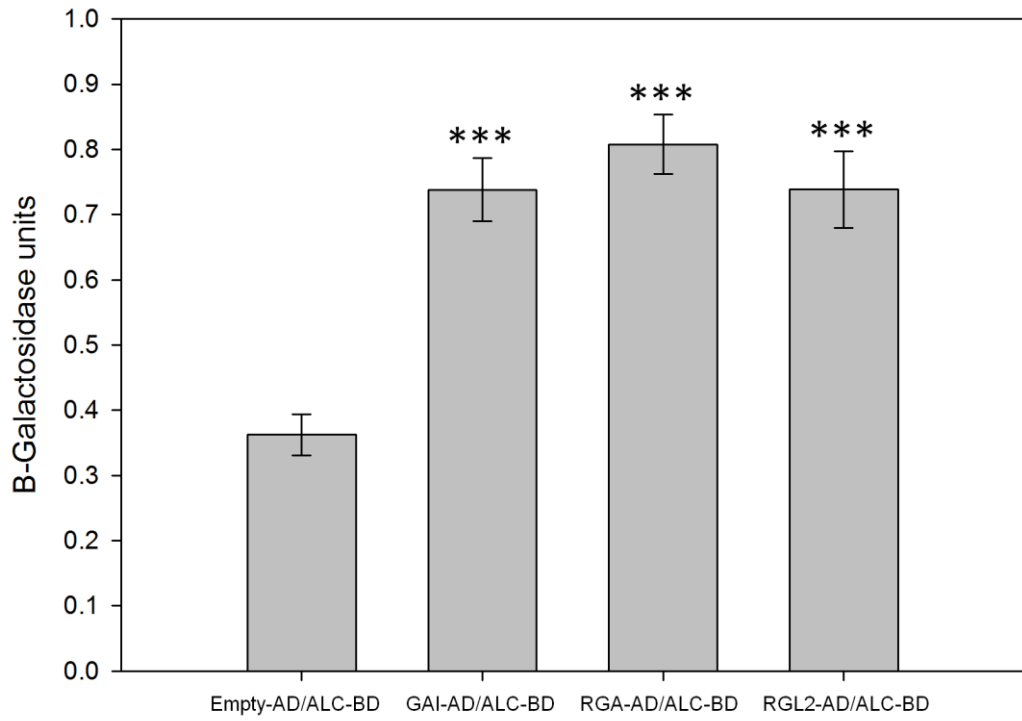


Figure 4.5 Quantification of ALC-DELLA interaction. Asterisks indicate statistically significant differences compared to the Empty-AD/ALC-BD mating *** for P < 0.001). Error bars: 95% CI, n>3

homodimerisation (Figure 4.3C). A weak interaction between GAI-AD and ETT-BD was also observed (Figure 4.3C).

Due to the autoactivation capacity of ALC-BD, it was decided to re-assay the ALC-DELLA interaction and record the growth of a series of mating dilutions at different time points (see Figure 4.4). The growth of non-diluted, 1/10, 1/100 and 1/1000 dilutions of the following matings: GAI-AD/ALC-BD, GAI-AD/SPT-BD, GAI-AD/Empty-BD, RGA-AD/ALC-BD, RGA-AD/SPT-BD, RGA-AD/Empty-BD, RGL2-AD/ALC-BD, RGL2-AD/SPT-BD, RGL2-AD/Empty-BD, Empty-AD/ALC-BD, Empty-AD/SPT-BD and Empty-AD/Empty-BD was recorded 12, 24 and 36 hours after plating. SPT-BD was used as a positive control of the mating whilst Empty-AD was used in order to assess the degree of autoactivation of the different bait constructs. 12 hours after plating, the interaction between the non-diluted matings of GAI-AD/ALC-BD, RGA-AD/ALC-BD and RGA-AD/SPT-BD and the 1/10 diluted matings of GAI-AD/ALC-BD and RGA-AD/ALC-BD was apparent (see Figure 4.4B). 24 hours after plating, the interaction between GAI-AD/ALC-BD, RGA-AD/ALC-BD, GAI-AD/SPT-BD and RGA-AD/SPT-BD was evident in all the mating dilutions whilst the interaction between RGL2-AD/ALC-BD was only observable in the non-diluted and 1/10 diluted matings (see Figure 4.4C). At this point, no autoactivation of any of the bait constructs could be detected, as shown by the lack of growth in the matings with the Empty-AD prey in the SD-LTHA plates (see Figure 4.4C). 36 hours after plating, the autoactivation capacity of ALC-BD became evident as shown from the growth of the non-diluted and 1/10 diluted matings of Empty-AD/ALC-BD plated in SD-LTHA medium (see Figure 4.4D). To further characterise the ALC-DELLA interaction, the β -galactosidase ONPG assay was used to quantify this interaction (see Section 4.2.7). As shown by the dilution series, although a background autoactivation could be detected in the Empty-AD/ALC-BD, the strength of the ALC-DELLA interaction was significantly above the background level (see Figure 4.5).

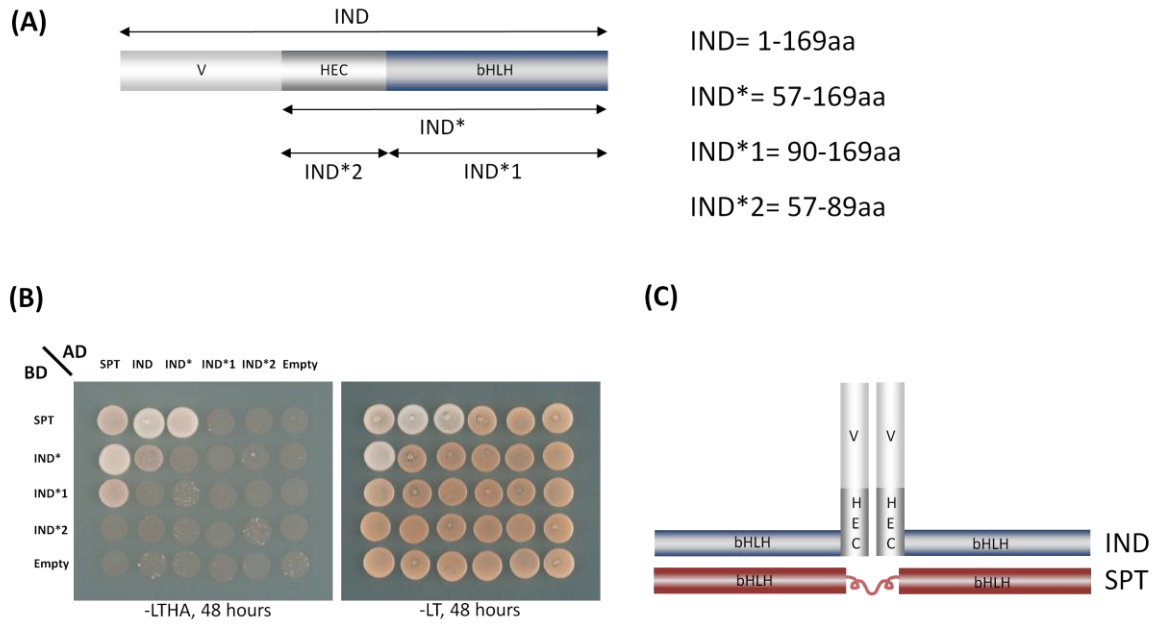


Figure 4.6 Characterisation of IND-SPT protein interaction. (A) Schematic representation of the different truncated IND used in this study. V, variable domain; HEC, hecate-like domain; bHLHL, bHLHL domain. (B) Protein-protein interactions 48 hours after plating. (C) Predicted model of IND-SPT interaction.

4.3.2 In-depth characterisation of IND-SPT protein interaction

Due to the autoactivation capacity of full-length IND coding sequence, a truncated version of IND (IND*) missing the first 56 amino acids (a domain named hereafter as the variable domain) was used as bait to test its possible interaction with DELLA proteins (see Figure 4.3). IND protein is composed by three distinct domains: a variable domain (1-56 amino acids, so called due to its lack of similarity with any other protein domains), the HEC-like domain (57-89 amino acids, so called due to its sequence similarity with the HECATE proteins) (Gremski et al, 2007) and the bHLH domain (90-169 amino acids, conserved DNA-binding domain in the bHLH transcription factors) (Toledo-Ortiz et al, 2003) (see Figure 4.6A). In order to further utilise the truncated IND*, two more truncated versions of IND were cloned: IND*1, missing the first 89 amino acids and, thus, coding only for the bHLH domain (Liljegren et al, 2004) and, IND*2, coding for the region between the 57-89 amino acids, that is, the HEC-like domain (Gremski et al, 2007) (see Figure 4.6A). These three truncated versions of IND together with the full-length IND were used to further characterise the IND-SPT interaction by uncovering the domains involved in IND homodimerisation as well as the domains responsible for the IND-SPT interactions (see Figure 4.6B). 48 hours after plating, it was observed that the full-length IND prey interacts both with SPT and with the truncated IND* missing the variable domain, although this last interaction appeared to be weaker (see Figure 4.6B). The truncated IND* missing the variable domain also interacts with SPT both as prey and as bait whilst the truncated IND*1, which coded for the bHLH domain, only interacts with SPT as bait (see Figure 4.6B). No interactions were detected with the truncated IND*2 coding for the hecate-like domain (see Figure 4.6B). Based on the observed interactions, it was concluded that the IND-SPT interaction relies on their respective bHLH domains (see Figure 4.6C). Regarding IND homodimerisation, it is likely that both the variable and the HEC-like domain are required (see Figure 4.6C). Thus, together these results suggest a polymeric complex, being a tetrameric protein complex formed by two IND protein units and two SPT protein units the simplest scenario (see Figure 4.6C).

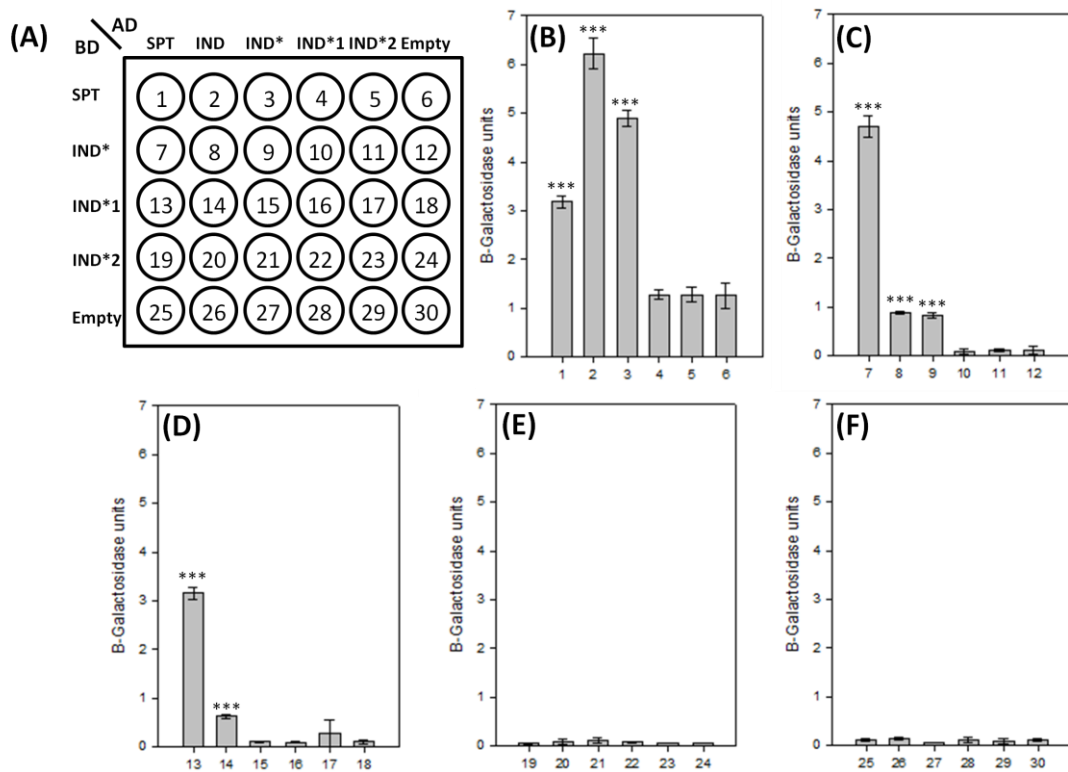


Figure 4.7 Quantification of IND-SPT interaction. (A) Schematic representation of the protein-protein interactions assayed. (B) Asterisks indicate statistically significant differences compared to the Empty-AD/SPT-BD mating. (C) Asterisks indicate statistically significant differences compared to the Empty-AD/IND*-BD mating. (D) Asterisks indicate statistically significant differences compared to the Empty-AD/IND*1-BD mating. (E) Asterisks indicate statistically significant differences compared to the Empty-AD/IND*2-BD mating. (F) Asterisks indicate statistically significant differences compared to the Empty-AD/Empty-BD mating. (*** for $P < 0.001$). Error bars: SD, n=3

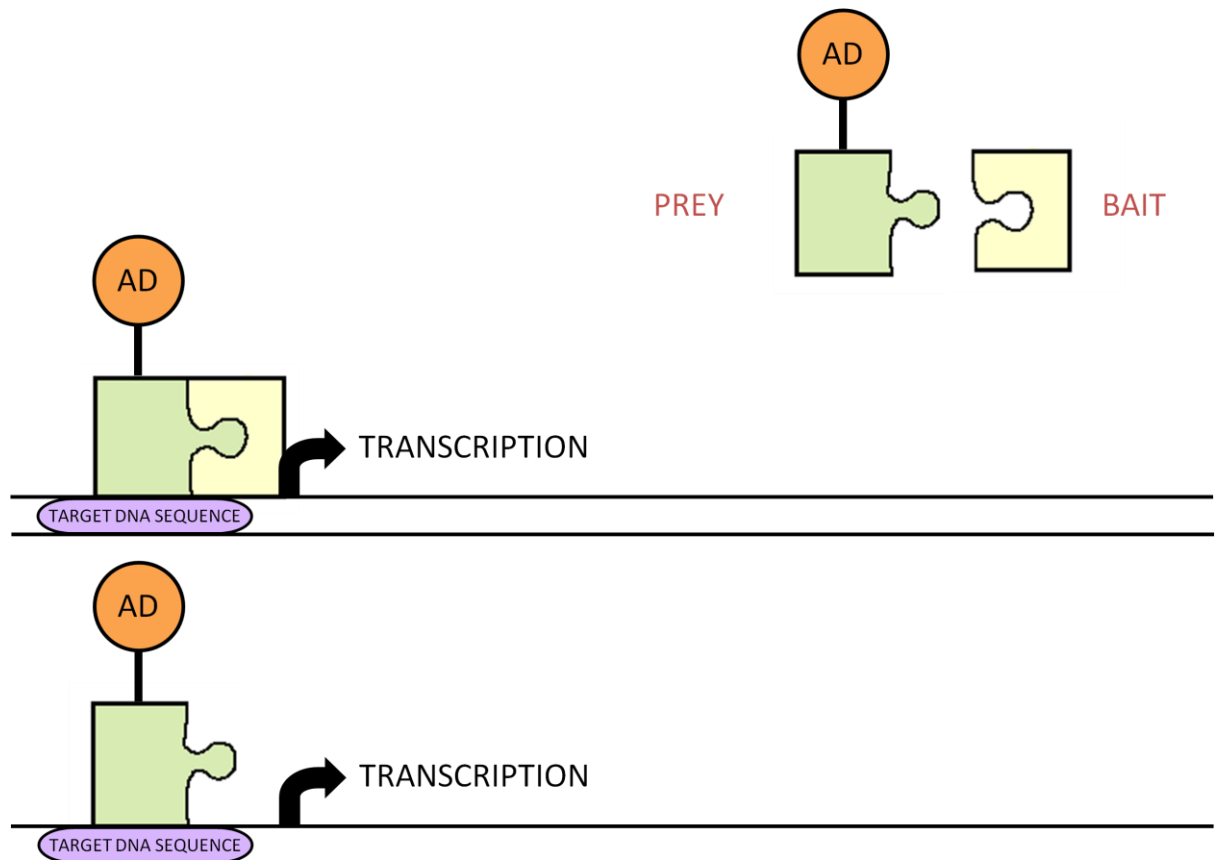


Figure 4.8 Schematic representation of the yeast two-one hybrid system. In the yeast two-one hybrid assay a target DNA sequence is cloned into the pLacZi vector. The potential DNA-binding protein (prey) is fused to the GAL4 activation domain (AD) and expressed alone or together with a bait protein. Binding of the prey protein alone or as a complex together with the bait protein activates transcription by binding to the target DNA sequence.

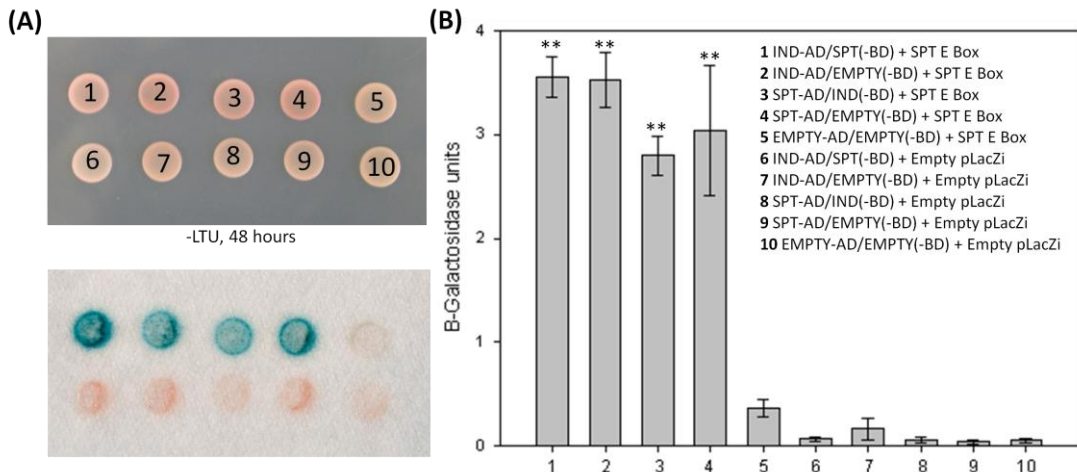


Figure 4.9 Binding of IND and/or SPT to a putative E-box variant in *SPT* promoter. (A) Yeast two-one hybrid assay of IND and/or SPT binding to a putative E-box variant in *SPT* promoter. (B) Quantification of IND and/or SPT binding to a putative E-box variant in *SPT* promoter. Asterisks indicate statistically significant differences compared to the Empty-AD/Empty(-BD) SPT E Box mating. (** for P < 0.01). Error bars: SD, n=3

The β -galactosidase ONPG assay was used to further verify the observed interactions (see Figure 4.7). Quantification of these interactions showed that SPT dimerisation (see Figure 4.7B) is a weaker interaction than any of the IND-SPT interactions (see Figures 4.7B,C,D). It was also confirmed that the interaction between the truncated IND* missing the variable domain with the full-length IND is a relatively weak interaction as observed in the growth assay (see Figures 4.6B, 4.7C). Surprisingly, the interactions between IND*-AD/IND*-BD and IND-AD/IND*1-BD also appeared to be above the background levels (see Figures 4.7C,D). Nevertheless, these interactions were not observed in the growth assay (see Figure 4.6B) and, thus, they remain to be further analysed.

4.3.3 IND and SPT bind to a putative E-box variant in *SPT* promoter

It has recently been shown that *SPT* and *IND* expression overlap in the valve margins (VM) (Liljegren et al, 2004; Groszmann et al, 2010). Furthermore, the targeted-disruption of a putative E-box variant (namely 5'-CGCGTG-3' in the sense strand) in the *SPT* promoter results in a loss of VM expression in wild-type plants whilst *SPT* expression is also specifically abolished in the VM in *ind* mutant plants (Groszmann et al, 2010). Taken together, these results suggest that 5'-CGCGTG-3' may be a potential IND binding site in the *SPT* promoter (Groszmann et al, 2010). In order to investigate whether this is the case, a yeast two-one hybrid approach was adopted (see Figures 4.8, 4.9). The pGBT9 vector from Clontech Laboratories Inc. was modified and a new pG9, which lacked the binding domain, was constructed (see Section 4.2). This vector was used to create the yeast transformants containing both SPT and IND and the yeast transformants containing only SPT or IND (see Section 4.2.1). After mating the resulting yeast transformants with the yeast one-hybrid specific transformants containing the pLacZi empty vector or the putative *SPT* E-box variant, 10 μ l of each of the mating cultures was plated in SD-LTU medium (see Sections 4.2.4; 4.2.6). 48 hours after plating, the possible interactions were assayed (see Section 4.2.6) and it was concluded that both SPT and IND alone or as part of the IND-SPT protein complex are capable of binding to the putative *SPT* E-box variant (see Figure 4.9A).

The β -galactosidase ONPG assay was once again used to further study the observed interactions (see Figure 4.9B) and to determine whether the binding of IND or SPT alone to the putative *SPT* E-box variant was comparable to the binding of the IND-SPT complex (see Figure 4.9B). Quantification of these interactions revealed that IND or SPT alone or as part of the IND-SPT complex bind with similar strength to the putative *SPT* E-box variant (see Figure 4.9B).

4.4 Discussion

4.4.1 Interaction of DELLA proteins with key bHLH regulators of fruit development and/or fruit patterning

DELLA proteins' role as transcriptional regulators relies on their capacity to bind to other transcription factors, and, thus, prevent their DNA-binding capacity (de Lucas et al, 2008; Feng et al, 2008) (see Figure 4.1). In this chapter the wider protein-protein interaction capacity of DELLA proteins has been studied, particularly regarding transcription factors known to be involved in fruit development and/or fruit patterning.

This study has shown that GAI, RGA and RGL2 DELLA proteins interact with ALC (Arnaud et al, *in press*; see Figures 4.3; 4.4; 4.5), a bHLH transcription factor required for the formation of a non-lignified cell layer necessary for fruit dehiscence (Rajani and Sundaresan, 2001). The ALC-DELLA interaction was only observed when ALC was used as a bait protein and DELLAs as preys (see Figure 4.3). It has previously been suggested that directionality in yeast assays may be due to a more favourable protein folding or exposure of binding sites in one direction (Guo et al, 2008). Nevertheless, additional evidence of the ALC-DELLA interaction, particularly *in-vivo*, is desirable and, to this end, biomolecular fluorescence complementation (BiFC) assays *in-planta* have been carried out by other members of the lab.

ALC is closely related to SPT (Toledo-Ortiz et al, 2003) a bHLH transcription factor involved not only in carpel development (Groszmann et al, 2008) but also in seed

germination (Penfield et al, 2005) and leaf growth (Ichihashi et al, 2010). SPT, together with other members of the bHLH transcription family (de Lucas et al, 2008; Feng et al, 2008; Gallego-Bartolome, 2010), was previously shown to bind to DELLA proteins through their bHLH domain which could suggest that DELLA proteins may interact with all the members of the bHLH transcription-factor family. However, the lack of interaction between DELLA proteins and IND (see Figure 4.3), another member of the bHLH family, suggests that DELLA-bHLH interaction is probably limited to only a subset of this large transcription-factor family. This hypothesis is in agreement with the phylogenetic analysis of bHLH transcription factors which shows that PIFs, SPT and ALC belong to the same phylogenetic clade while IND is part of a different clade (Toledo-Ortiz et al, 2003). Thus, it is possible that DELLA proteins may only interact with specific subsets of the bHLH transcription factors.

The discovery of ALC-DELLA interaction has widened the biological role of DELLA-bHLH interaction from the control of hypocotyls cell elongation (de Lucas et al, 2008; Feng et al, 2008) to further aspects of plant development, such as fruit development and/or patterning (Arnaud et al, *in press*). The biological relevance of ALC-DELLA interaction has been proved by the discovery that the DELLA GA-signalling pathway together with ALC is involved in the control of seed dispersal through patterning of the dehiscence zone (Arnaud et al, *in press*).

4.4.2 Interaction of DELLA proteins with non-bHLH transcription factors involved in fruit development and/or fruit patterning

In order to uncover whether DELLA-binding capacity is limited to the bHLH transcription factor family, the interaction between DELLAs and non-bHLH transcription factors involved in fruit development and/or fruit patterning was also tested (see Figure 4.3). Surprisingly 48 hours after plating, a weak interaction between GAI-AD and ETT-BD was recorded (Figure 4.3) 72 hours after plating, the GAI-ETT interaction became stronger and a weak interaction between RGA-AD and ETT-BD was also observed (data not shown). To the author's knowledge,

the ETT-DELLA interaction represents the first DELLA-non bHLH transcription factor interaction described.

ETTIN (or AFR3) is a member of the auxin response factor family of transcription factors (Sessions et al, 1997) and is involved in the patterning of floral meristems and reproductive organs (Sessions and Zambryski, 1995; Sessions et al, 1997). It is thought that ETTIN plays a role in the apical and basal boundaries delimitation during gynoecium development by regulating the expression of auxin responsive genes (Sessions et al, 1997; Nemhauser et al, 2000). Thus, if the biological relevance of ETT-DELLA interaction was to be confirmed by further genetic and mutant studies, the ETT-DELLA protein-protein interaction could represent a joining point of the auxin and gibberellin pathways during gynoecium development. Irrespectively of the ETT-DELLA interaction, it is clear that in order to coordinate and regulate the great variety of gibberellins responses, DELLA proteins are likely to interact with a number of different transcription factors. Consequently, a yeast two-hybrid screening to identify the DELLA proteins' interactome would undoubtedly be a useful basis for any future work in this area.

4.4.3 IND-SPT protein interaction and downstream targets

During the yeast two-hybrid strategy adopted to uncover the possible interactions between DELLA proteins and transcription factors involved in fruit development and/or fruit patterning, a number of already described protein-protein interactions were confirmed including the IND-SPT interaction amongst others (Gremski et al, 2007) (see Figure 4.3). In order to further utilise the resources created, an in-depth characterisation of this interaction was carried out (see Figures 4.6; 4.7).

By specific domain-deletions of IND, it was concluded that the IND-SPT interaction relies on their respective bHLH domains (see Figure 4.6). This is in agreement with previous studies showing that the helix-loop-helix domain promotes dimerisation (Murre et al, 1989b). On the other hand, the variable and the hecate-like domains are likely to be required for IND homodimerisation (see Figure 4.6).

IND shows extensive protein sequence similarity to three other bHLH proteins, HEC1, HEC2 and HEC3, which have been shown to play a role in stigma and transmitting tract development (Gremski et al, 2007). HEC proteins also interact with SPT, but in contrast to IND, cannot homodimerise with each other (Gremski et al, 2007). Based on the wide expression pattern of *SPT* (Heisler et al, 2001; Grozsmann et al, 2010), it has been proposed that SPT is likely to rely on the interaction with different bHLH proteins to carry out distinct developmental programmes (Gremski et al, 2007). In agreement with this hypothesis, SPT is involved in a variety of developmental programmes including carpel development (Grozsmann et al, 2008) seed germination (Penfield et al, 2005) and leaf growth (Ichihashi et al, 2010). It is therefore likely that the IND-SPT interaction may underlie a combined developmental role of IND and SPT. This possibility is currently being addressed by characterisation of *ind spt* double mutants.

The SPT-IND interaction may not be limited only to the protein level as it was recently shown that *SPT* expression is abolished in the valve margin (VM) in *ind* mutant plants and, furthermore, an E-box variant (5'-CGCGTG-3' in the sense strand) responsible for *SPT* expression in the VM has also been identified (Grozsmann et al, 2010). Thus, it has been proposed that the E-box element 5'-CGCGTG-3' is the IND binding site in the *SPT* promoter (Grozsmann et al, 2010). bHLH transcription factors bind to DNA as dimers (Murre et al, 1989b) and, therefore, a yeast two-one hybrid approach was taken to test this possibility. It was concluded that both SPT and IND alone or as part of an IND-SPT complex are able to bind to the *SPT* E-box variant (see Figure 4.9). Previous studies have suggested that *SPT* expression is not likely to be autoregulated as no changes in *SPT* expression were detected in *spt-2* mutants compared to wild type (Heisler et al, 2001). Nevertheless, the nature of the *spt-2* mutations remains unclear (Penfield et al, 2005). In addition, based on the quantification assay carried out in the present chapter, it is not possible to ascertain whether binding of the IND-SPT complex is more likely than binding of SPT or IND alone (see Figure 4.9). Furthermore, it is not possible to rule out whether other members of the bHLH transcription-factor family or of other transcription-factor families may also be part of the IND-SPT complex. Undoubtedly, further characterisation of this complex for example by studying its crystal structure and mutagenising the residues predicted

to be important for DNA binding and/or protein interaction would contribute greatly towards the understanding of its mode of action.

The integration of the hormonal cues and the molecular players known to play a role in fruit development and/or fruit patterning is a key step in the study of this complex molecular network. Since the formulation of the canalisation hypothesis which predicts that an auxin maximum in distinct cellular files is required for vein differentiation (Sachs, 1991), numerous studies have focused on the role of auxin flows and gradients in organ initiation and organ patterning (Friml et al, 2002; Benkova et al, 2003; Friml et al, 2003; Aloni et al, 2006; Scarpella et al, 2006; Grieneisen et al, 2007; Dubrovsky et al, 2008). Auxin gradients have also been shown to be involved in fruit development and fruit patterning. For example, it has been proposed that an apical-basal gradient of auxin is established to pattern the longitudinal development of the gynoecium (Nemhauser et al, 2000). This apical-basal patterning is likely to rely on the action of ETTIN amongst other (Nemhauser et al, 2000). More recently, the role of auxin in radial gynoecium patterning has also been addressed with the discovery that IND regulates the development of the separation layer required for fruit dehiscence by coordinating the formation and maintenance of an auxin minimum (Sorefan et al, 2009). In addition to auxin, gibberellins have also been described to play a role in fruit development (Vivian-Smith and Koltunow, 1999; Hu et al, 2008; Dorcey et al, 2009). However, to the author's knowledge to date, there is no evidence suggesting a possible role of gibberellins in fruit patterning. SPT has previously been shown to repress gibberellin biosynthesis in dormant seeds (Penfield el al, 2005) and it is also involved in the gibberellin-response pathway during fruit development (see Chapter 3). Thus, the study of the possible biological relevance of the IND-SPT interaction by genetic and mutant analysis could uncover an unknown nexus point between the auxin and gibberellin pathways during gynoecium development.

CHAPTER 5

EMS mutagenesis:
Screening for parthenocarpy

CHAPTER 5

EMS mutagenesis: Screening for parthenocarpy

5.1 Introduction

Forward-genetic screens have widely been used in the identification of genes involved in molecular networks, including hormonal-signalling networks. In contrast to reverse-genetic screens where the biological function of particular genes is investigated by targeted mutagenesis, in forward-genetic screens the genetic basis underlying the phenotype of interest is studied. This approach is especially useful when few genetic players controlling the biological function being investigated are known. Classical mutagens employed in genetic screens include both physical and chemical mutagens (Koornneeff, 2002). One of the most commonly used chemical mutagens is ethyl methanesulfonate (EMS) which in >99% of the cases causes G/C to A/T transition mutations (Greene et al, 2003). EMS acts as an alkylating agent mainly by alkylating guanine residues and producing O⁶-ethylguanine which is unable to pair to C and pairs instead to T (Jansen et al, 1995). In most cases, this type of base pair changes leads to amino acid changes which may alter the function of the protein but do not abolish its function (Koornneeff, 2002; Henikoff and Comai, 2003). Thus, EMS mutagenesis is highly desirable when a wide allelic series is sought.

The suitability of EMS mutagenesis for the discovery of new molecular players involved in the control of fertilisation-independent fruit development has previously been shown (Chaudhury et al, 1997; Vivian-Smith et al, 2001). Both parthenocarpic (*arf8*) and apomictic (*fis*) mutants have been isolated through EMS mutagenesis of a heterozygous *pistillata* population (Chaudhury et al, 1997). However to date, relatively few parthenocarpy-conferring mutations have been isolated in *Arabidopsis* and the individual action of only a few components from the auxin signalling pathway, members of the AUXIN RESPONSE FACTOR family (Vivian-Smith et al, 2001; Okushima et al, 2005; Goetz et al, 2006; Schruff et al,

2006; Wu et al, 2006) and the combined action of components from the GA signalling pathway, members of the DELLA family (Dorcey et al, 2009) are only known to result in parthenocarpic fruit development in Arabidopsis. Although other hormones, such as cytokinins are also believed to play a role in the control of Arabidopsis fruit growth (Vivian-Smith and Koltunow, 1999), very little is known about the genetic and molecular mechanisms underlying the role of cytokinins in fruit initiation and growth. In this study, a modified approach of the heterozygous *pistillata* EMS mutagenesis used by Chaudhury et al (1997) was adopted as the base for the identification of parthenocarpy conferring mutations. *PISTILLATA* is a class B homeotic gene involved in the specification of the second (petals) and third (stamens) floral whorls (Goto and Meyerowitz, 1994). Thus, mutation of *PI* results in male sterile plants lacking both petals and stamens which are converted into sepals (Goto and Meyerowitz, 1994). Initial mutagenesis of heterozygous *pistillata-1* mutant seeds ensures the selfing of the M1 population as *pi-1* is a recessive mutation (Goto and Meyerowitz, 1994). In the M2 population, only those plants homozygous for *pistillata-1*, and therefore male sterile, were screened (see Figure 5.2) avoiding the necessity for emasculation during the phenotypic characterisation. In addition to the forward screen, preliminary characterisation and rough mapping of one of the isolated mutants were also carried out.

5.2 Materials and methods

5.2.1 EMS treatment

The EMS mutagenesis of $+/pi-1$ seeds described by Chaudhury et al (1997) was modified as follows. 250 mg of heterozygous $+/pi-1$ seeds ($\geq 15,000$ seeds) were mutagenised with 0.2 % EMS diluted in 0.02% Tween solution. After 18h of continuous agitation, a series of 15-minute washes were performed (0.02% Tween solution). Finally seeds were resuspended in 0.01% bactoagar and sown in 10,200 individual compartments. Each pot of seed- producing M1 plants was harvested and threshed separately in order to identify the wild-type lines. 600 lines were screened in the M2 population from which a third of the lines were expected to be

wild type. In the remaining 400 lines, *+/pi-1* and wild-type plants were identified by the presence of petals and stamens and were subsequently removed.

5.2.2 Plant material and growth conditions

pop-1 ats-1 seeds were kindly provided by Dr. Adam Vivian-Smith (Leiden University). The selfed *+/pi-1* (*Ler*) line used as the starting point for the second EMS treatment was obtained from The Nottingham Arabidopsis Stock Centre (NASC) (NASC ID: NW77). All the plants used in this study were grown under greenhouse conditions at an average temperature of 22°C and 16h photoperiod.

5.2.3 Map-based cloning

The *117.1 pi-1* mutant (ecotype *Ler*) was crossed to *Col-0* plants and the F2 of this cross was used as the mapping population. In order to avoid emasculation in the F2 population, only those plants homozygous for the *pistillata-1* mutation were screened for parthenocarpic fruit development. A segregation rate of 1:15 was expected for homozygous *117.1 pi-1*; however during the confirmation of the *117.1 pi-1* parthenocarpic phenotype in the *Ler* backcross it was observed that *pi-1* mutation in the *117.1 pi-1* x wild type backcross did not follow a 1:3 segregation rate. 120 F2 seeds from the *117.1 pi-1* x *Ler* backcross were sown but only 3 plants showed a *pi-1* phenotype (approximately 1:39 segregation ratio) and, out of these 3 plants, 2 plants a *117.1 pi-1* phenotype (approximately 1:59 segregation ratio). This skewed segregation ratio may be due to many factors including not complete penetrance of the mutations, the influence of environmental factors, or alternatively it might indicate that *pi-1* and *117.1* mutations are linked. In order to ensure at least 50 plants with the *117.1 pi-1* phenotype in the mapping population, which has been estimated to be sufficient to narrow a mutation to about 20cM resolution (Jander, 2006), 3600 F2 seeds from the *117.1 pi-1* x *Col-0* backcross were sown. 65 plants showed consistent parthenocarpic fruit development and leaf material from these was collected for quick DNA extraction (see Section 2.2.1).

The PCR markers used during the map-based cloning were kindly provided by Dr. Freddy Boutrot (Sainsbury Laboratory) and are listed in Table 5.1. PCR markers were initially tested in Ler, Col-0 and F1 leaf material to ensure that the different alleles could be differentiated in agarose gels (data not shown). The PCR conditions used for each primer pair and the expected band sizes are also shown in Table 5.1. The recombination frequency for any marker was calculated as:

$$F = (\text{no.heterozygotes} + 2 \times \text{no.homozygous Col-0}) \times 100 / (2 \times \text{no.plants})$$

For markers not linked to the mutation, a recombination frequency of approximately 50% is expected whilst markers that show linkage to the mutation would have a significantly reduced recombination frequency (overabundance of the Ler allele).

5.3 Results

5.3.1 EMS mutagenesis

A forward-genetic screening approach was adopted in order to uncover novel genetic players involved in fertilisation-independent fruit development. Initially the *pop-1 ats-1* double mutant background was chosen for the genetic screen. *pop-1* (also known as *cer6-2*) is a conditional pollen-fertility mutant which pollen is only able to germinate at humidity levels higher than 90% (Preuss et al, 1993). This mutation was used as an alternative to emasculation to significantly reduce the time and effort required for mutant isolation. The *ats-1* mutation results in aberrant ovule integument formation (McAbee et al, 2006) and it was found to enhance parthenocarpy (Vivian-Smith et al, 2001). Thus, the *ats-1* mutation was introduced in a *pop-1* background in order to enhance the mutant phenotype and facilitate mutant isolation.

Approximately 15,000 *pop-1 ats-1* seeds (250mg) were subjected to 0.2% ethymethane sulfonate (EMS) treatment (see Section 5.2.1). These plants were allowed to selfpollinate at high-humidity conditions at which *pop-1* pollen is able to

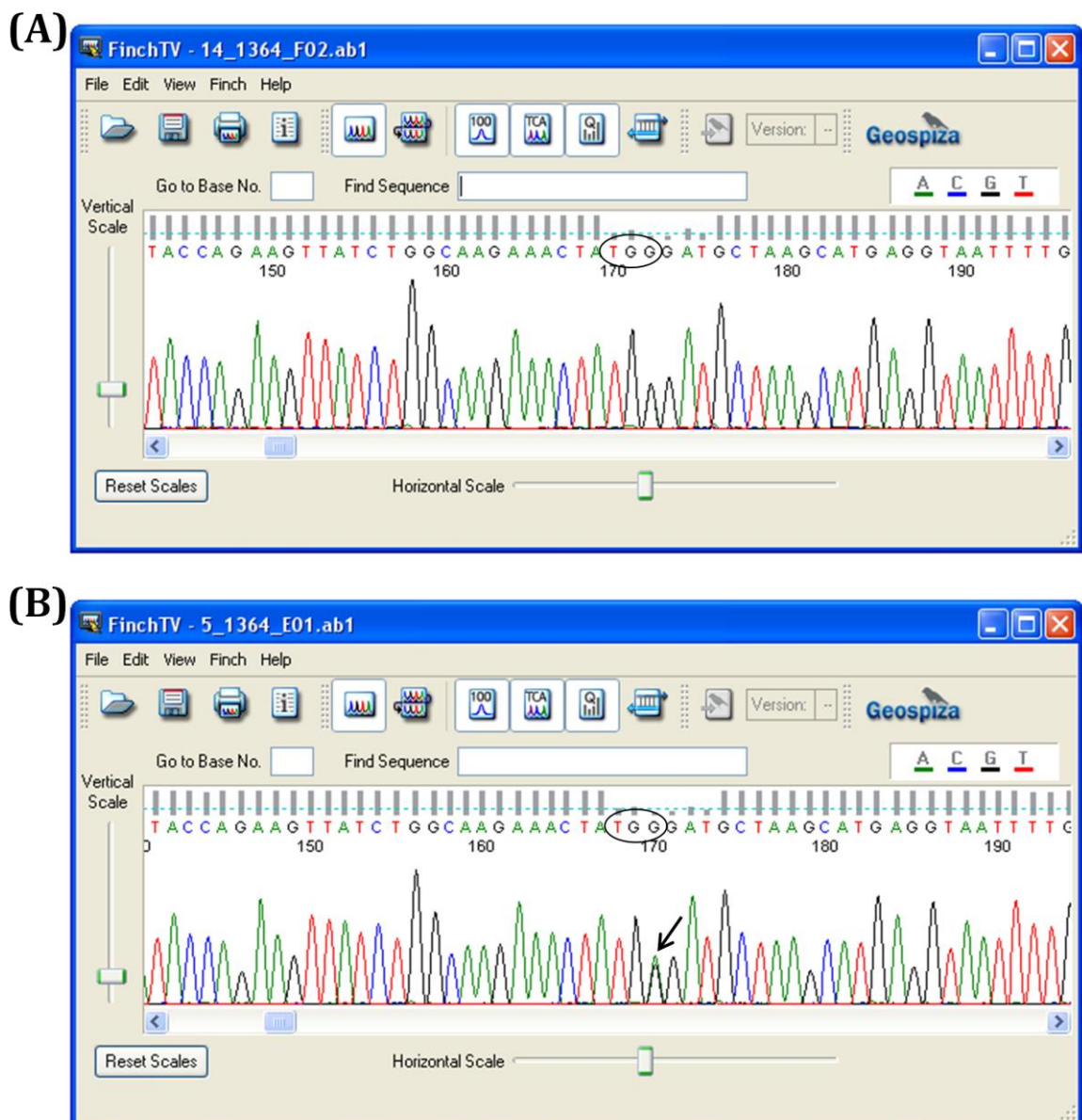


Figure 5.1 Sequence analysis of heterozygous *pistillata-1* mutants. (A) Sequence of wild-type plant. (B) Sequence of $+/pi-1$ plant. The 80Trp is shown enclosed within a circle and the double-peak at the third position of the TGG codon in the heterozygote is indicated by an arrow in (B).

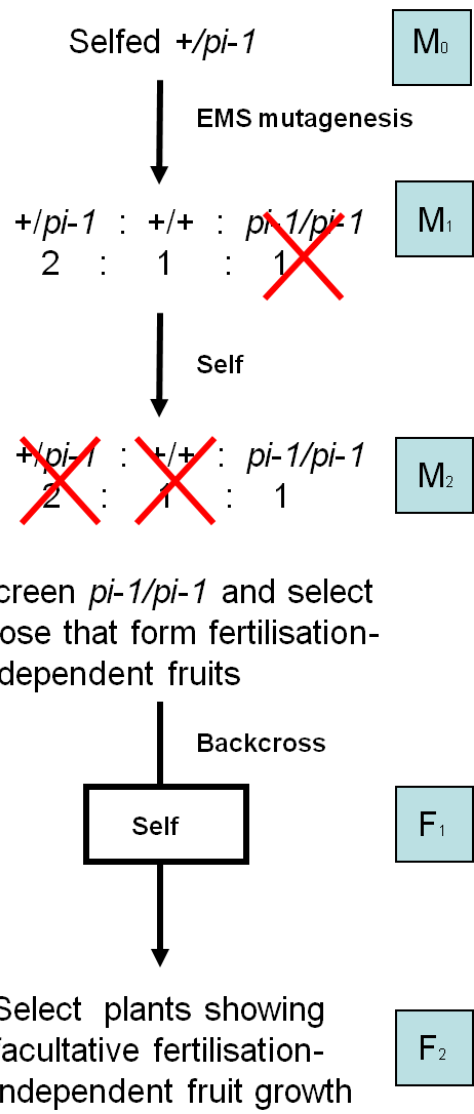
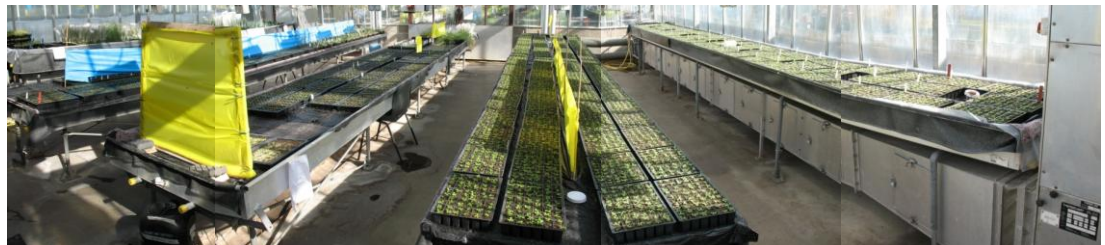


Figure 5.2 Diagram of the forward-genetic approach. Homozygous *pi-1* mutation results in male sterile plants lacking both petals and stamens (Goto and Meyerowitz, 1994). Initially, seeds from selfed *+/pi-1* (Ler) plants were subjected to EMS mutagenesis to ensure the selfing of the *M₁* population. *pi-1* is a recessive mutation (Goto and Meyerowitz, 1994) and, thus, only wt plants and *+/pi-1* plants would set seed in the *M₁* population.. In the next generation (*M₂*), only those homozygous for *pi-1* mutation and, therefore, lacking stamens were screened for pistil elongation avoiding the necessity for emasculation during the phenotypic characterisation. Two types of mutants are expected to show pistil elongation in the absence of pollination/fertilisation: parthenocarpic and apomictic mutants. Mutants were backcrossed to segregate *pi-1* and the fertilisation-independent fruit growth conferring mutation. (Based on Chaudhury et al, 1997).

(A)



(B)



Figure 5.3 Growth of the 10,200 individuals of the M1 population. (A) 10 days after sowing. (B) 6 weeks old M1 plants, individually bagged.

germinate. In the next generation, low-humidity conditions (at which pollen germination is impaired) were going to be used to screen plants and isolate putative mutants. Finally, to recover seeds from the putative mutants, plants would have to be transferred to high-humidity conditions. Unfortunately, no seeds were recovered from the M₁ population probably due to difficulties in keeping the humidity levels above 90% in the growth chamber.

After the failure of the first forward screening attempt, heterozygous *pistillata* (+/*pi*-1) mutant background was adopted as the base for the forward-genetic screening. This approach had already proven to be successful in the isolation of both apomictic (for which ovary will grow into a seeded fruit in the absence of fertilisation) and parthenocarpic (which ovary will grow into a seedless fruit in the absence of fertilisation) mutants (Chaudhury et al, 1997; Vivian-Smith et al, 2001). The B class homeotic gene *PISTILLATA* (*Pl*) is involved in floral whorl specification and *pi* mutants develop sepals instead of petals in the second whorl and carpels instead of stamens in the third whorl (Bowman et al, 1989). Thus, homozygous *pi* mutants are sterile and hand-pollination is required to recover seeds. Other commonly observed defects in the *pi* mutants include fusion of the third whorl carpels with the fourth-whorl organs to form an abnormal gynoecium (Bowman et al, 1989).

For the bulking up of +/*pi*-1 seeds, an *Arabidopsis* line from a selfed +/*pi*-1 (*Ler*) was obtained from The Nottingham *Arabidopsis* Stock Centre (NASC) (NASC ID: NW77). *pi*-1 mutant allele is characterised by a single-base pair substitution which results in the introduction of a premature stop codon (80Trp (TGG)→ STOP (TGA)) (Goto and Meyerowitz, 1994). In order to isolate heterozygous *pi*-1 plants, several plants were sequenced and those plants with a double peak in the third base of the 80Trp were identified (see Figure 5.1). Seeds from eleven +/*pi*-1 plants were collected for the forward screening.

250 mg of seeds (approx. 15000 seeds) from selfed +/*pi*-1 (*Ler*) plants were mutagenised with 0.2% of EMS (see Section 5.2.1) from which *pi*-1/*pi*-1 M₂ male-sterile plants were screened for mutants that produce fertilisation-independent fruits. A schematic representation of the genetic-screen process is shown in Figure

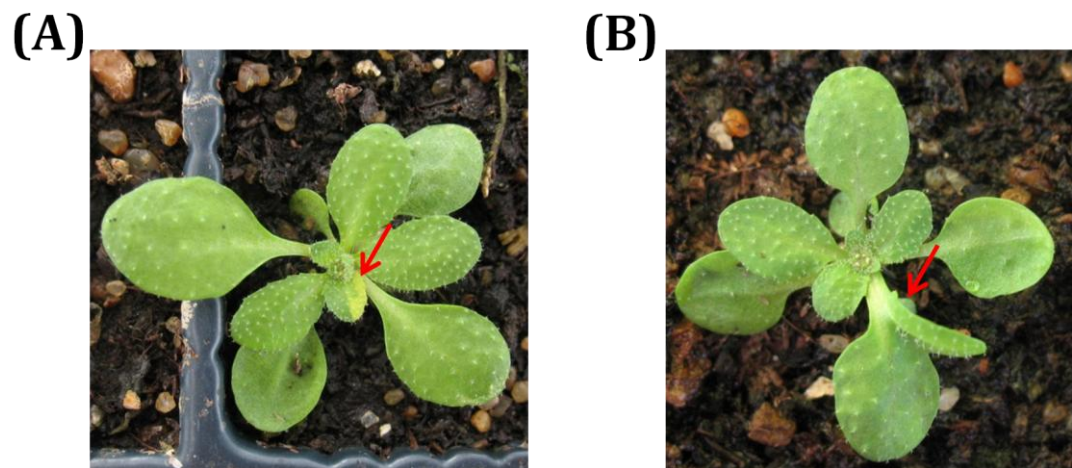
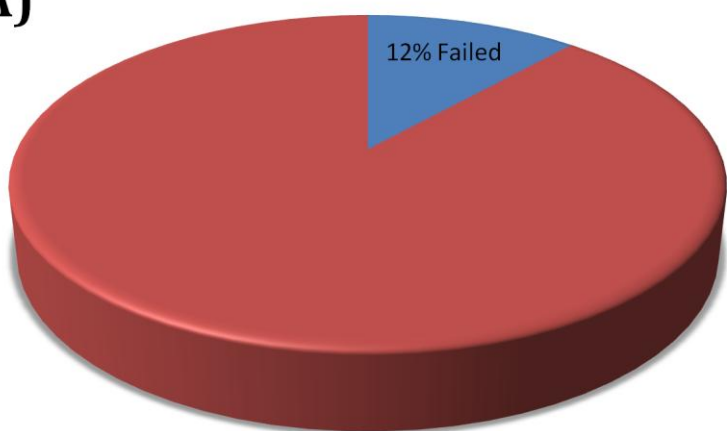


Figure 5.4 Somatic mutations commonly observed in M1 population. (A) Pigment sector mutant with chlorotic leaf phenotype. Chlorotic lesion is indicated by an arrow. (B) Mutant showing fused leaves. Position of the fused leaves is indicated by an arrow.

(A)



(B)

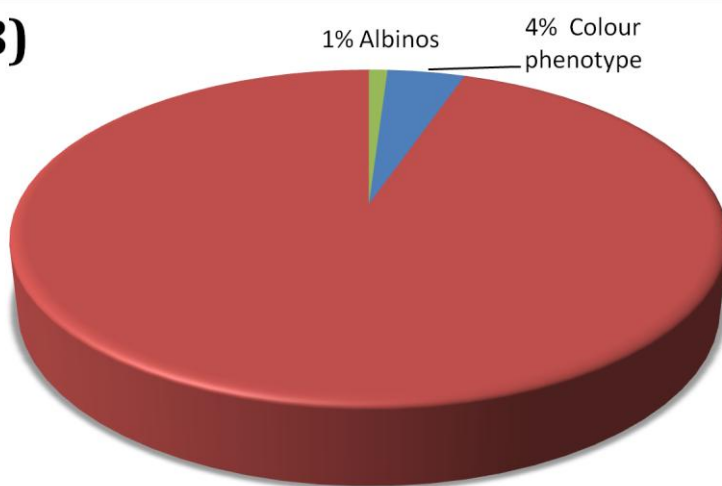


Figure 5.5 Effectiveness of EMS treatment. (A) Percentage of non-germinating M2 seeds. (B) Percentage of M2 plants with pigment phenotypes (albinos and other colour phenotypes).

5.2. Mutagenised seeds were grown over the summer of 2009 and those plants which produced seeds (+/*pi*-1 and wild-type plants) were bagged individually (see Figure 5.3). In broad terms, two strategies can be adopted for M1 plant handling: pedigrees can be kept separated (as in this screening) or, alternatively, pools of M1 plants can be bagged together (Lightner and Caspar, 1998). Pooling of M1 lines greatly reduces the cost, time and effort needed for M1 handling (Lightner and Caspar, 1998). However, in the present screening it was impossible to phenotypically differentiate between +/*pi*-1 and wild-type plants and, consequently, it was decided to bag plants individually to allow the later identification of wild-type lines in the M2 generation.

During growth of the M1 population, the first signs of the effectiveness of the EMS mutagenesis were observed as several somatic mutations were commonly recorded (see Figure 5.4). These somatic mutations included pigment sector mutants (see Figure 5.4A) and mutants with fused leaves (see Figure 5.4B).

5.3.2 Forward screening and putative mutant isolation

Due to time constraints, seeds from only 600 M1 lines were grown. From each M1 progeny, only those M2 plants carrying the *pi/pi* mutation were screened, so that plants with petals and/or stamens were pulled out during the screening process. Putative mutants identified in the *pistillata* background would have to carry both the *pi/pi* mutation and the parthenocarpy conferring mutation, that is, a segregation of two loci within each M1 progeny was expected (1:16 segregation rate). If 40 plants were grown from each M1 line, this will ensure a 92% probability of finding at least one homozygous mutant plant ($1-(1-1/16)^{40}$). However, *Arabidopsis* germline is formed by two cells and, thus, it is possible that mutagenesis of seeds could result in chimeric M1 plants. In this case, growing 40 M2 plants will provide a 72% chance of finding at least one homozygous mutant ($1-(1-1/32)^{40}$) whilst by growing 60 M2 plants the probability will increase to 85% ($1-(1-1/32)^{60}$). Taking these calculations into consideration, it was decided that screening 60 M2 plants per M1 progeny would provide the most effective strategy.

Mutant	Parthenocarpic siliques length	Additional phenotypes	Phenotype confirmation
35.1	4.2 mm	Terminal flowers Reduced plant size	Confirmed
35.2	4.2 mm	None recorded	Not shown in F2
117.1	4.3 mm	Reduced plant size	Confirmed
156.1	5 mm	None recorded	Not shown in F2
306.1	5 mm	None recorded	To be confirmed
280.1	5.1 mm (max 8 mm)	Increased number of curved carpels	To be confirmed
291.1	5 mm	Split styles	To be confirmed
258.1	4.5 mm	None recorded	To be confirmed
288.1	5.1 mm	None recorded	To be confirmed
307.1	>4 mm	None recorded	To be confirmed
299.1	>4 mm	None recorded	To be confirmed
285.1	>4 mm	None recorded	To be confirmed
301.1	>4 mm	None recorded	To be confirmed
241.1	>4 mm	None recorded	To be confirmed
390.1	>4 mm	None recorded	To be confirmed
403.1	>4 mm	None recorded	To be confirmed
425.1	>4 mm	None recorded	To be confirmed
379.1	>4 mm	None recorded	To be confirmed
368.1	>4 mm	None recorded	To be confirmed
354.1	>4 mm	None recorded	To be confirmed
503.1	>4 mm	None recorded	To be confirmed
503.2	>4 mm	None recorded	To be confirmed
487.1	>4 mm	None recorded	To be confirmed
447.1	>4 mm	None recorded	To be confirmed
447.2	>4 mm	None recorded	To be confirmed
430.1	>4 mm	None recorded	To be confirmed
445.1	>4 mm	None recorded	To be confirmed
456.1	>4 mm	None recorded	To be confirmed
456.2	>4 mm	None recorded	To be confirmed

Figure 5.6 Putative parthenocarpic mutants. Mutants were named according to their M1 progeny line and 600 M1 lines were screened. Due to time constraints, the average parthenocarpic siliques length was not quantified in the last 300 lines. Few M1 lines more than one putative mutant was isolated.

During the forward screening process, frequencies of pigment phenotypes and of non-germinating mutagenised seeds were recorded to determine whether the EMS treatment had been effective (see Figure 5.5). The validity of the survival or germination percentage of the mutagenised seeds as a good criterion to determine the effectiveness of the mutagenesis treatment has been questioned because even high mutagen doses in *Arabidopsis* only result in delayed germination mutagenised material, germination is only delayed in *Arabidopsis* (Koornneef, 2002). Consequently, percentage of pigment phenotype was chosen as a better criterion. According to previous mutagenesis protocols, in populations that have been mutagenised effectively 2-15% frequencies of pigment phenotypes are observed in the M2 population at the seedling level (Lightner and Caspar, 1998). In our M2 population 5% of the M2 population showed a pigment phenotype (see Figure 5.5), suggesting that the EMS mutagenesis had been effective.

In addition to recording the percentage of non-germinating seeds and pigment phenotypes, the lines for which no homozygous *pi-1* plants were observed was also recorded (data not shown). The mutagenesis was carried out in a heterozygous *pi-1* background and, thus, during the bagging of the M1 population both *+/pi-1* and wild-type plants were bagged (see Figure 5.2) as these plants were phenotypically identical. Nevertheless, during the screening of the M2 plants, it was possible to determine whether the M1 progeny line carried the *pi-1* mutation by segregation of such mutation. Although wild-type M1 progenies were not used in this study, these lines were marked and separated for possible future studies.

Preliminary measurements of *pi-1* pistils showed that, on average, these pistils reached a maximum length of 3.2mm in our growing conditions (data not shown). Thus, during putative mutant isolation those plants that consistently produced pistils longer than 4mm were selected. Figure 5.6 shows the 29 putative parthenocarpic mutants isolated during the screening of 600 M1 lines. Mutants were named according to the number of the M1 progeny line and, in four cases, two putative parthenocarpic mutant siblings were isolated from the same M1 progeny line (see Figure 5.6) in support of the parthenocarpy-conferring nature of these mutations. Once identified, putative mutants were backcrossed

(A)



(B)



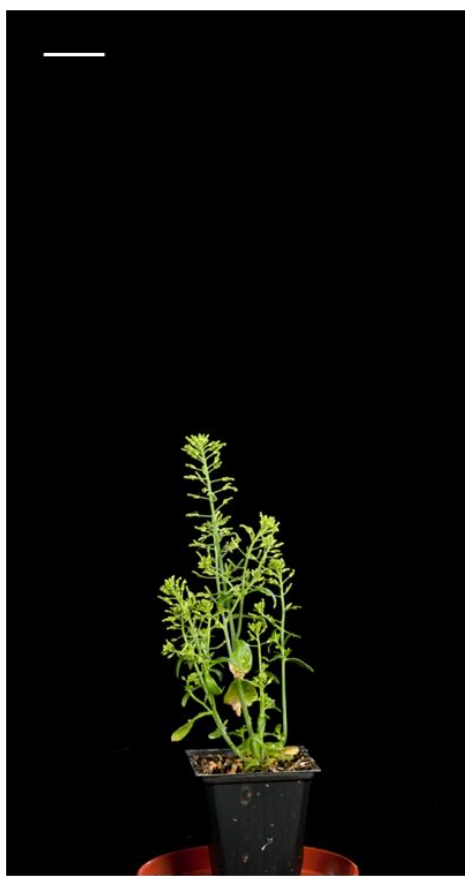
Figure 5.7 Mutant 35.1. (A) Mutant 35.1 in the mutagenised *pi-1* background. Close up of the occasional patterning defects observed in 35.1 mutants including split pistils and stigmatic outgrowths, both indicated by an arrow, (B) Wild type in the same mutagenised background. Scale bars, 1cm

both to *Ler* (in order to start the cleaning up of the background mutations) and to *Col-0* (in order to generate the mapping population).

5.3.3 Putative mutant confirmation

After putative mutant isolation, confirmation of the mutant phenotype in subsequent generations is required in order to establish the monogenic nature of the mutation and/or to discard the possible false positives. Due to time constraints, only the F2 from the M2 x *Ler* backcross of four putative parthenocarpic mutants was analysed. None of the F1 of the M2 x *Ler* backcross showed a fertilisation-independent fruit elongation when emasculated, suggesting that the putative mutations may be of a recessive nature (data not shown). For the F2 analysis, those plants homozygous for the *pistillata-1* mutation were assessed, as this avoided the necessity of emasculation. If the pistil growth-conferring mutation is of a monogenic nature, 1:16 segregation rate for *pi-1* and the parthenocarpy-conferring mutation would be expected in the F2 population. 120 F2 plants for each putative mutant to be analysed were grown to ensure a very high probability of finding at least one homozygous mutant ($1 - (1 - 1/16)^{120} = 99.96\%$). Although two of the putative mutants analysed, 35.2 and 156.1, did not show a fertilisation-independent pistil elongation in the F2 population (data not shown), two others did (35.1 and 117.1). It is interesting to note that while the F2 of the 35.1 *pi-1* x *Ler* backcross *pi-1* mutation followed the expected 1:3 segregation ratio, this was not the case in the F2 of the 117.1 *pi-1* x *Ler* backcross (data not shown). Out of the 120 F2 seeds from the 117.1 *pi-1* x *Ler* backcross sown, only 3 plants showed a *pi-1* phenotype (approximately 1:39 segregation ratio) and, out of these plants, 2 plants a 117.1 *pi-1* phenotype (approximately 1:59 segregation ratio). Many factors could explain the skewed segregation ratio observed for the 117.1 *pi-1* mutations including a complete penetrance of the mutations and the influence of environmental factors amongst others. Alternatively, the skewed segregation ratio might indicate that *pi-1* and 117.1 mutations are linked.

(A)



(B)

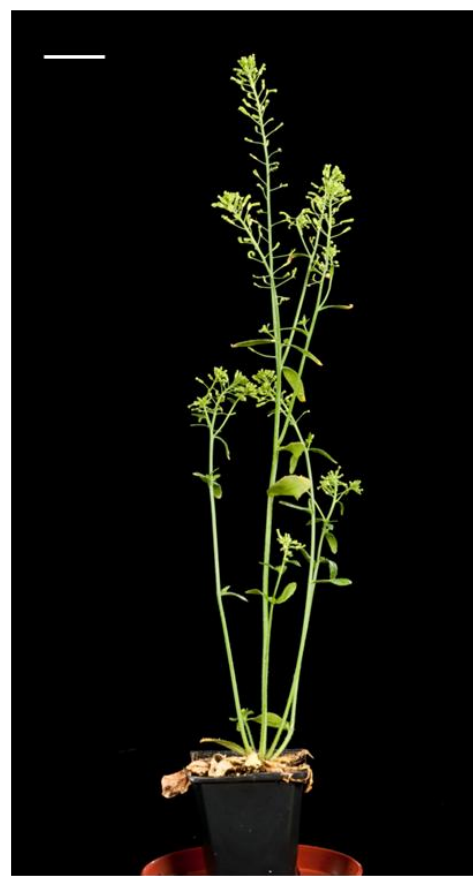


Figure 5.8 Mutant 117.1. (A) Mutant 117.1 in the mutagenised *pi-1* background.
(B) *pi-1* mutant of the same M1 progeny. Scale bar, 2cm

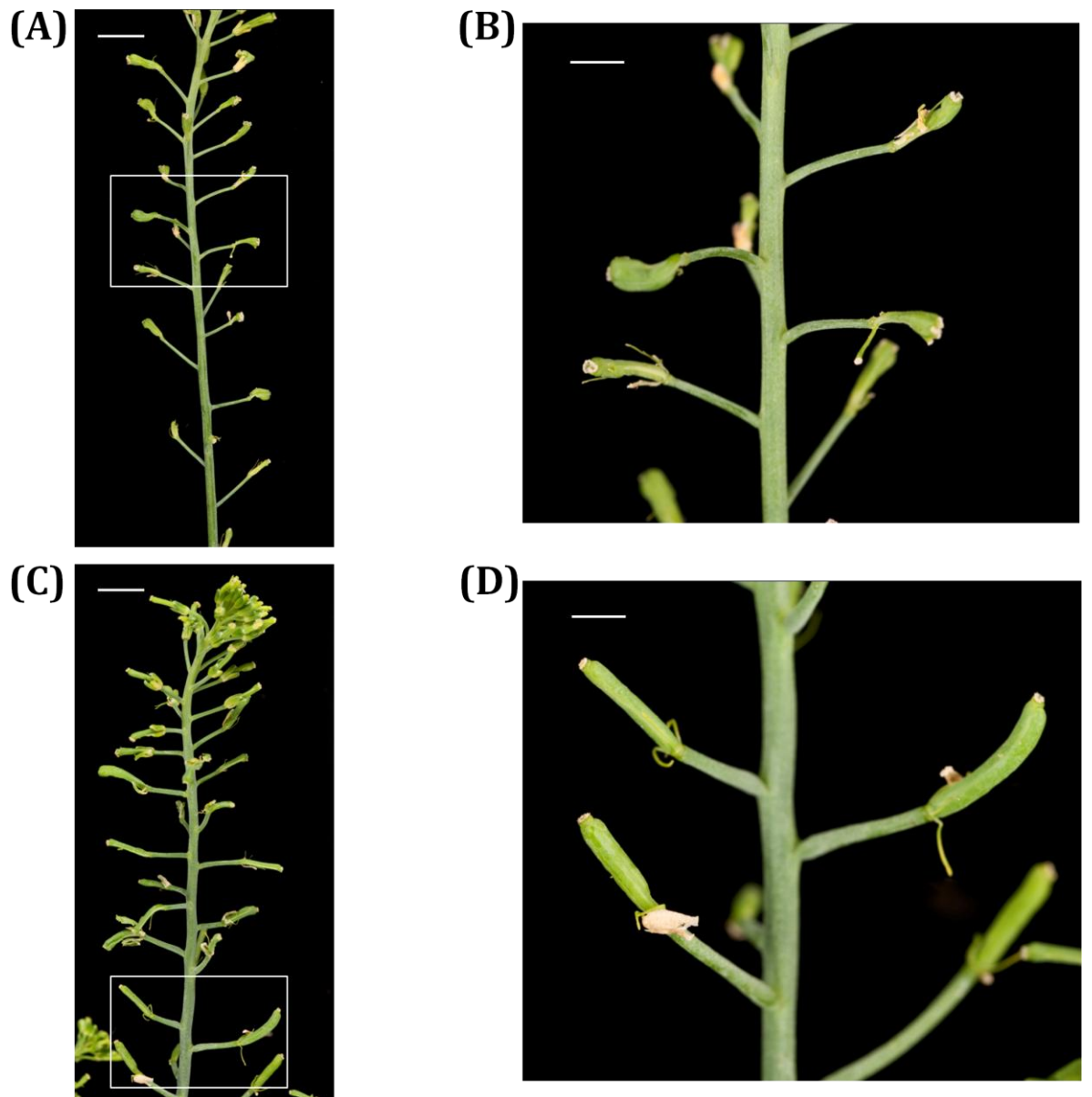


Figure 5.9 Pistil close-ups of mutant 117.1 showing consistent fertilisation-independent pistil elongation. (A,B) *pi-1* mutant pistil close-ups of the same M1 progeny. (C,D) 117.1 *pi-1* mutant pistil close-ups. Scale bars (A, C), 1cm. Scale bars (B,D), 2mm

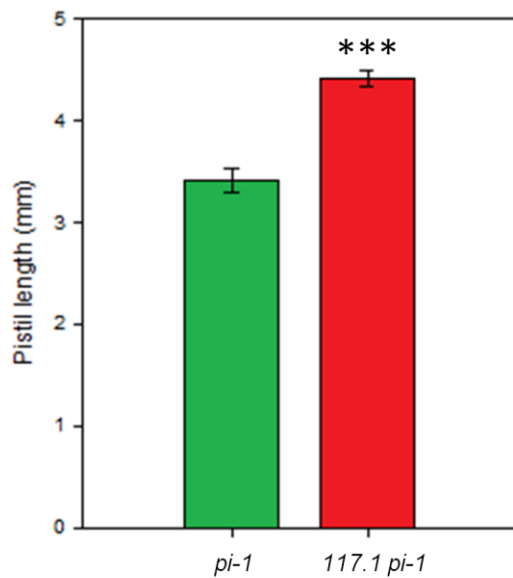


Figure 5.10 *117.1 pi-1* pistils are significantly longer than *pi-1* pistils.

Asterisks indicate statistically significant differences compared to *pi-1* pistils (*** for $P < 0.001$). Error bars: 95% CI, $n \geq 24$

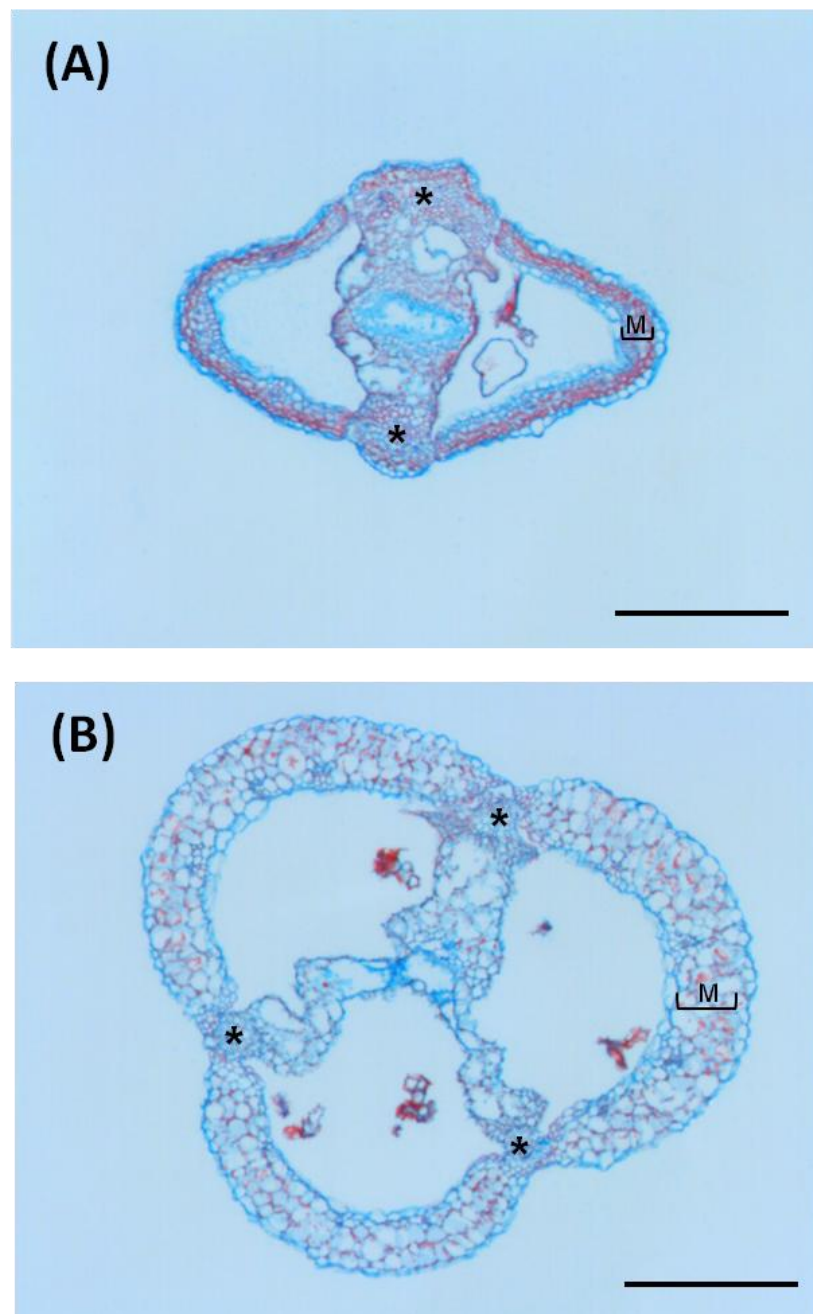


Figure 5.11 117.1 carries a parthenocarpy-conferring mutation and results in enlarged mesocarp cells. Cross sections of (A) *pi-1* showing enlarged repla and (B) 117.1 *pi-1* pistils showing a *replumless* phenotype. Both Mesocarp cells (M) and repla (*) in 117.1 *pi-1* are distinct from those of *pi-1* mutants. Sections were stained with Alcian blue 8Gx (which dyes unlignified tissue in blue) and Safranin-O (which dyes lignified tissue, nuclei and chloroplasts in red) (see Chapter 2). Scale bars, 0.2mm

5.3.3.1 Mutant 35.1

The 35.1 *pi-1* pistils are longer than *pi-1* pistils but, occasionally, they show other patterning defects such as split pistils, stigmatic outgrows (see Figure 5.7A) as well as reduced fertility (data not shown). Furthermore, the fertilisation-independent pistil elongation was only observed in association with a mutant background characterised by several pleiotropic traits such as terminal flowers and reduced size (see Figure 5.6). Taking into account the time limitations and the complex nature of the 35.1, it was decided to focus on those mutants where fertilisation-independent pistil elongation was not linked to patterning defects.

5.3.3.2 Mutant 117.1

The 117.1 *pi-1* pistils are also longer than *pi-1* pistils (see Figures 5.8, 5.9). Quantitative analysis of pistil length showed that 117.1 *pi-1* pistils are approximately 30% longer than *pi-1* pistils (see Figure 5.10). No additional patterning defects were observed during close analysis of 117.1 *pi-1* pistils (see Figure 5.9), indicating that 117.1 mutation may only result in fertilisation-independent fruit growth promotion. The only other pleiotropic trait observed in 117.1 *pi-1* compared to *pi-1* was a reduced plant stature (see Figure 5.8).

5.3.4 Characterisation of mutant 117.1

5.3.4.1 117.1 is a parthenocarpic mutant

In order to determine whether the 117.1 is an apomixis or a parthenocarpy-conferring mutation, cross sections of 117.1 *pi-1* and *pi-1* pistils were carried out (see Figure 5.11). No seed development was observed in 117.1 *pi-1* pistils (see Figure 5.10B), thus, 117.1 carries a parthenocarpy-conferring mutation.

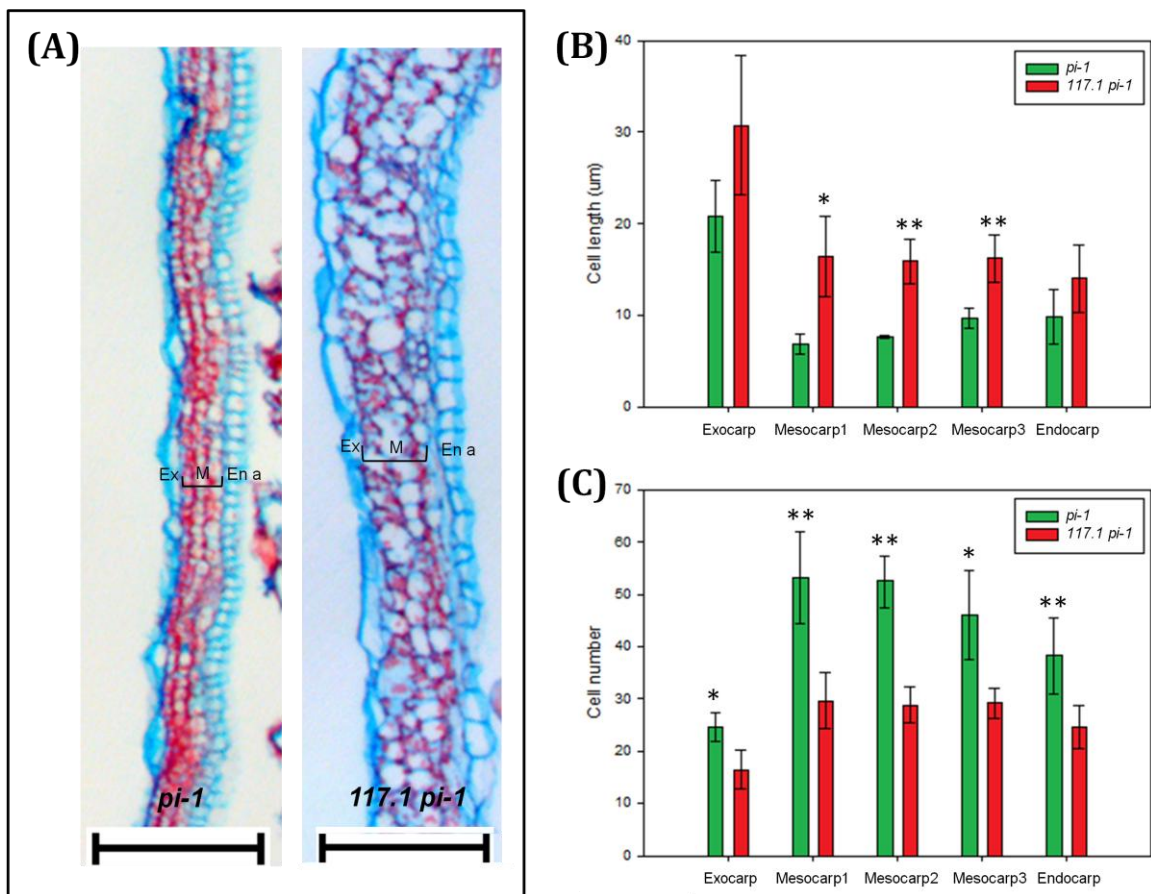


Figure 5.12 Tissue analysis of longitudinal sections of fully elongated 117.1 *pi-1* mutant pistils. (A) Longitudinal sections of *pi-1* and 117.1 *pi-1* valves. Sections were stained with Alcian blue 8Gx (which dyes un lignified tissue in blue) and Safranin-O (which dyes lignified tissue, nuclei and chloroplast in red) (see Chapter 2). Scale bar, 0.12mm. (B) Comparison of cell length normal to the pistil elongation axis in *pi-1* and 117.1 *pi-1* exocarp, mesocarp (1, 2, 3) and endocarp a (En a) tissue layers. (C) Comparison of cell number normal to the pistil elongation axis in *pi-1* and 117.1 *pi-1* exocarp, mesocarp (1, 2, 3) and endocarp a (En a) tissue layers (distance considered for cell count= 0.4mm). Asterisks indicate statistically significant differences compared to *pi-1* pistils (* for P < 0.05 and ** for P < 0.01). Error bars: 95% CI, n≥4

Cross sections of *117.1 pi-1* also allowed the closer examination of the different tissue layers. Three different tissue layers can be differentiated in *Arabidopsis* pistil walls or valves: an outer epidermal layer formed by a single cell-layer (exocarp), a medial tissue-layer formed by three or four cell layers containing chloroplasts (mesocarp) inside of which runs the vascular bundle and an inner tissue layer formed by two cell layers (endocarp a, inner cell layer and endocarp b, lignified cell layer formed by narrow elongated cells in between endocarp a and mesocarp layer). Close examination of *117.1 pi-1* cross sections showed that in addition to the lack of seeds, *117.1 pi-1* valves have larger mesocarp cells than *pi-1* valves (see Figure 5.11). The visualisation of the different tissue layers was made possible by staining the cross sections with Alcian blue 8Gx and Safranin-O dyes (see Chapter 2). Alcian blue stains un lignified tissue in blue while Safranin-O stains lignified tissue, nuclei and chloroplasts in red. It is worth noting that in addition to larger mesocarp cells, *117.1 pi-1* cross sections also showed greater intracellular Safranin-O uptake while in *pi-1* cross sections the red staining was more evenly distributed around the cells (see Figure 5.11). Chloroplast development in *Arabidopsis* pistils occurs mainly at stage 14 of fruit development, that is, at fertilisation (Roeder and Yanofsky, 2006). Thus, the greater organelle staining in *117.1 pi-1* cross sections compared to *pi-1* cross sections may be a further indication of the failure to arrest fruit development in *117.1 pi-1* mutants.

In *Arabidopsis* as well as in many Brassicaceae, the valves are separated by a replum, the outer portion of the septum which divides the fruit (see Figure 5.11). Most *pi-1* mutant cross sections showed enlarged repla (see Figure 5.11A) while in *117.1 pi-1* pistils reduced repla were observed. Furthermore, in most cases, the replum appeared to be completely absence and *117.1 pi-1* resembled the strong *replumless* mutant alleles where the valves encompass the replum area (Roeder et al, 2003; see Figure 5.11B). During plant grow and tissue sectioning, it was also noticed that multiple carpel development is a frequent trait in both *117.1 pi-1* (see Figure 5.11B) and *pi-1* pistils (data not shown). Multiple carpel development has previously been described in *pi-1* mutants (Bowman et al, 1989) and, thus, examination of the *117.1* phenotype in a wild-type background would be required in order to determine whether this mutation alone results in multiple carpel development.

5.3.4.2 117.1 *pi-1* show longer mesocarp cells than *pi-1* mutants

To further characterise the cellular basis of the parthenocarpic phenotype observed in 117.1 *pi-1* pistils, longitudinal sections of fully elongated pistils were also analysed. Histological analysis of longitudinal valve sections revealed that the 117.1 mutant contains larger cells across all tissue layers (see Figure 5.12A). However, quantitative analysis of cell length showed that only mesocarp cells of 117.1 *pi-1* valves were significantly longer (see Figure 5.12B). Cell numbers were also quantified in a 0.4mm stretch and it was concluded that the mutation in 117.1 results in a significantly reduced number of cells across all tissue layers (see Figure 5.11C).

As with the pistil cross sections, visualisation of the different tissue layers in longitudinal valve sections was made possible by staining with Alcian blue 8Gx and Safranin-O dyes (see Chapter 2). It was similarly noticed that in addition to significantly longer mesocarp cells, 117.1 *pi-1* longitudinal sections also showed greater intracellular Safranin-O uptake while in *pi-1* longitudinal sections the red staining was more evenly distributed around the cell walls (see Figure 5.12A). This greater organelle staining in 117.1 *pi-1* longitudinal sections compared to *pi-1* sections may be a further indication of the failure to arrest the fruit developmental programme in 117.1 *pi-1* mutants.

5.3.5 Mapping the 117.1 locus

The final aim of any forward screen is the identification of the mutated gene conferring the mutant phenotype as this will enable a more thorough genetic and molecular characterisation. To do so, a map-based cloning approach was adopted to initially map the mutation in 117.1 to a concrete chromosome arm. An F2 population was generated by self-pollination of the 117.1 *pi-1* (Ler background) x Col-0 cross. To facilitate the phenotyping of F2 plants, only plants homozygous for the *pistillata-1* mutation in the F2 population were screened for parthenocarpic fruit development. 3600 F2 seeds from the 117.1 *pi-1* x Col-0 backcross were sown but

	chr1				chr2		chr3		
Primer numbers	33-34	9-10	1-2	5-6	11-12	13-14	15-16	17-18	19-20
Col	9	10	14	20	9	23	13	9	14
Ler	20	20	10	7	16	9	8	18	19
Heterozygote	36	35	41	35	33	28	43	36	30
Recombination frequency	42	42	53	60	44	62	54	43	46

	chr4			chr5			
Primer numbers	21-22	23-24	25-26	99-100	27-28	29-30	31-32
Col	24	15	21	0	0	12	25
Ler	19	23	20	55	57	20	3
Heterozygote	20	27	24	10	4	31	36
Recombination frequency	54	44	51	8	3	44	67

Figure 5.13 Recombination frequency of markers used in 117.1 mapping.

Significantly reduced frequencies are highlighted in red.

(A)		(B)		(C)							
Line	99-100	Mut	27-28	Line	99-100	Mut	27-28	Line	99-100	27-28	Mut
5	Het	X	Ler	5	Ler	X	Het	5	Het	Het	X
6	Ler		Ler	6	Ler		Ler	6	Ler	Ler	
7	Ler		Ler	7	Ler		Ler	7	Ler	X	Het
8	Ler		Ler	8	Ler		Ler	8	Ler	X	Het
17	Het	X	Ler	17	Ler	X	Het	17	Het	X	Ler
23	Het	X	Ler	23	Ler	X	Het	23	Het	X	Ler
24	Ler		Ler	24	Ler		Ler	24	Ler	X	Het
35	Het	X	Ler	35	Ler	X	Het	35	Het	X	Ler
40	Het	X	Ler	40	Ler	X	Het	40	Het	X	Ler
43	Het	X	Ler	43	Ler	X	Het	43	Het	X	Ler
51	Het	X	Ler	51	Ler	X	Het	51	Het	X	Ler
58	Het	X	Ler	58	Ler	X	Het	58	Het	X	Ler

12 CROSSOVERS

18 CROSSOVERS

14 CROSSOVERS

Figure 5.14 Three-point cross-analysis to determine the correct order of the three loci. (A) Possible order: marker 99-100, mutation 117.1, marker 27-28. (B) Possible order: mutation 117.1, marker 27-28, marker 99-100. (C) Possible order: marker 99-100, marker 27-28, mutation 117.1. Mut= mutation 117.1

only 65 plants showed parthenocarpic fruit development (segregation ratio 1:54). It has previously been indicated that 117.1 *pi-1* phenotype showed a skewed segregation ratio in the wild-type backcrosses (see Section 5.2.3). In addition to the previously mentioned explanations, during the phenotyping of the F2 from the 117.1 *pi-1* x Col-0 backcross only material from those plants for which fertilisation-independent pistil elongation was absolutely clear was collected. It is therefore likely that due to the quantitative nature of the phenotype, these plants represent an underestimation of the plants showing fertilisation-independent pistil elongation. Nevertheless, more than 50 plants with parthenocarpic fruit development were successfully isolated which allowed a first-pass mapping (Jander, 2006). The 65 plants showing parthenocarpic fruit development were genotyped with the 16 markers listed in Table 5.1. Given the small size differences of the Ler and Col-0 alleles in most of the markers, both parental lines as well as the F1 progeny plant (to ensure that it was truly heterozygous) were also genotyped (see Appendix figures 5.1-5.16).

The scoring of the gels showed that two markers in particular, 99-100 and 27-28, had an overabundance of the Ler allele (see Appendix figures 5.6, 5.12). Indeed, calculation of the recombination frequency indicated that these markers had a significantly reduced recombination frequency (see Figure 5.13). Three-point cross-analysis was carried out in to determine the most likely order of these three loci (see Figure 5.14). Thanks to the *Arabidopsis* sequence, the relative location of the different markers used in this study is known and, thus, we know that marker 99-100 is further upstream on chromosome 5 than marker 27-28. However, the 117.1 locus could be located either in between marker 99-100 and marker 27-28 (see Figure 5.14A), upstream of marker 99-100 (see Figure 5.14B) or downstream of marker 27-28 (see Figure 5.14C). Three-point analysis is based on the fact that double meiotic recombination events in a short DNA region are less common than single recombination events, that is, the order requiring fewest recombination events is assumed to be the correct one (Jander, 2006). Taking into account the number of recombination events that each of the above mentioned possibilities requires, the order with fewest recombination events was assumed to be the correct one, that is, marker 99-100 followed by locus 117.1 followed by marker 27-28 (see Figure 5.14).

5.4 Discussion

5.4.1 EMS mutagenesis as a discovery tool in parthenocarpy studies

Forward screening is a powerful approach for the identification of new molecular players involved in the biological function being investigated. Thus, in order to uncover new genetic players involved in fertilisation-independent fruit development, a forward-genetic approach was adopted. Fast neutron radiation and EMS are the most commonly used mutagens in forward-genetic studies. Fast neutron radiation usually gives rise to large deletions which result almost exclusively in knockout alleles (Koornneeff, 2002). Large deletions facilitate the identification of the mutated gene for example by microarray analysis (Gong et al, 2004; Hazen et al, 2005). However in this study, EMS was chosen for the mutagenesis treatment in order to ensure a wider array of mutations. EMS mutagenesis results in base pair substitutions (GC→ AT) which may alter the function of proteins but not necessarily result in a knockout allele (Koornneeff, 2002; Henikoff and Comai, 2003). Based on the nature of the genetic code, it is predicted that only approximately 5% of the recovered mutations within coding regions are knockout mutations resulting from premature stop codons (Stephenson et al., 2010). Thus, in order to ensure a wide allelic series which will provide a more comprehensive resource to understand the role of the mutated genes, an EMS mutagenesis strategy was adopted.

Initially the *pop-1 ats-1* mutant background was chosen for the genetic screen. *pop-1* is a conditional pollen-fertility mutant which pollen is unable to germinate at humidity levels below 90% (Preuss et al, 1993). It was decided that by using this mutation, both the time and effort required for mutant isolation would be significantly reduced. Unfortunately, although preliminary small-scale tests were carried out to ensure that the optimal pollen-germinating conditions were achievable, no seeds were recovered from the M1 population. This resulted in a substantial time loss which significantly affected the advancement of this project. After the failure of the *pop-1 ats-1* EMS mutagenesis, heterozygous *pistillata-1* (+/*pi-1*) seeds were mutagenised and subjected to a forward-genetic screen.

Screening in this mutant background had already proven to be successful in the isolation of fertilisation-independent fruit development mutants (Chaudhury et al, 1997; Vivian-Smith et al, 2001). However to date, relatively few parthenocarpy-conferring mutations have been isolated in *Arabidopsis* and, consequently, a modified approach of the heterozygous *pistillata* EMS mutagenesis used by Chaudhury et al (1997) was adopted as the base for the identification of novel fertilisation-independent fruit growth promotion conferring mutations. Furthermore, screening of only those M2 plants homozygous for *pi-1* mutations also reduced the time and effort devoted to mutant isolation as no emasculations were required.

Several putative parthenocarpic mutants have already been isolated in the forward screen performed in this study. Although, confirmation and further characterisation of these putative mutants is still required, preliminary results suggest that EMS mutagenesis is a powerful tool for the discovery of new genetic players involved in fertilisation-independent fruit development.

5.4.2 117.1 is a parthenocarpy-conferring mutation and acts at the mesocarp tissue level

2,400 M2 plants corresponding to 400 +/*pi-1* M1 lines were screened, as screening of 60 M2 plants per M1 line provided a 85% chance of finding at least one homozygous mutant (see Section 5.3.2). In addition, previous studies have concluded that growing large numbers of M1 plants and screening between 2000 and 125,000 M2 plants is the most cost effective strategy in *Arabidopsis* (Lightner and Caspar, 1998).

29 putative fertilisation-independent fruit growth conferring mutations were isolated during the screening of 400 +/*pi-1* M1 lines (see Figure 5.6). Four of the 29 putative parthenocarpic mutants identified in this screen were analysed in subsequent generations to confirm their mutant phenotype. Only two of the four putative mutants showed fertilisation-independent fruit elongation in the F2 analysis, 35.1 and 117.1 mutants. Due to the complex nature of the 35.1 mutation and time constraints, only the characterisation of 117.1 was further pursued.

117.1 pi-1 mutants are approximately 30% longer than *pi-1* mutants (see Figure 5.10). Cross sections of *117.1 pi-1* mutants showed that *117.1* contains a parthenocarpy-conferring mutation, as no seed development was observed (see Figure 5.11). To further characterise the cellular basis of the parthenocarpy observed in *117.1 pi-1* pistils, longitudinal sections of fully elongated pistils were also performed. Histological analysis of the pod walls (valves) of these revealed that *117.1 pi-1* mutants have significantly longer mesocarp cells than *pi-1* mutants (see Figure 5.12). Larger mesocarp cells were also observed in *117.1 pi-1* cross sections when compared to *pi-1* cross sections (see Figure 5.11). Close examination of both longitudinal and cross sections of *117.1 pi-1* pistils also showed that the enlarged mesocarp cells present a distinct staining pattern compared to that of the *pi-1* mesocarp cells (see Figures 5.11, 5.12A). A greater intracellular Safranin-O uptake was observed in *117.1 pi-1* mesocarp cells compared to *pi-1* mesocarp cells (see Figures 5.11, 5.12A). Safranin-O is known to stain lignified materials as well as cell nuclei and chloroplasts, consequently, the uneven staining pattern observed in *117.1 pi-1* mesocarp cells can likely be attributed to a greater organelle presence in *117.1 pi-1* sections. Chloroplast development in *Arabidopsis* pistils occurs mainly at stage 14 of fruit development, that is, at fertilisation (Roeder and Yanofsky, 2006). Thus, the greater organelle staining in *117.1 pi-1* sections compared to *pi-1* sections may be a further indication of the failure to arrest fruit development in *117.1 pi-1* mutants.

It is worth mentioning that all histological analyses and measurements of *117.1* were carried out in the *pi-1* background due to time constraints. Under our growing conditions, *pi-1* mutant pistils were shorter than wild-type pistils (data not shown), hence, it is likely that single *117.1* mutants may result in longer parthenocarpic pistils than *117.1 pi-1* mutants. Consequently, analysis and confirmation of the *117.1* phenotype in a wild-type background is required.

After confirmation of the mutant phenotype in subsequent generations, rough mapping of *117.1* was undertaken. To facilitate the isolation of those plants that showed parthenocarpic fruit development, only plants homozygous for the *pi-1* mutation were screened. Thus, during the rough mapping approach both *117.1*

and *pi-1* mutations were mapped. However, the map position of *PISTILLATA* has previously been described and, therefore, it was concluded that the differentiation between both mapped regions should be possible.

Only the region between markers 99-100 and 27-28 showed an overabundance of the Ler allele (see Appendix figures 5.1-5.16, 5.12) which corresponds to the region between AT5G14320 and AT5G20240. *PISTILLATA* (AT5G20240) is located at the distal border of that region and, thus, it is impossible to dismiss the possibility that during the mapping of 117.1 *pi-1* only the *pi-1* mutation has been mapped successfully. Although only plants which showed consistent fertilisation-independent fruit elongation were collected from the mapping population, due to the quantitative nature of this trait, human-origin mistakes cannot be completely ruled out. It is therefore possible that some of the plants collected may only carry *pi-1* mutation, in which case the mapping results may only reflect the successful mapping of *pi-1* mutation. In order to be able to conclude with complete certainty that 117.1 is located between markers 99-100 and 27-28, confirmation of the mapping position in a 117.1xCol-0 population would be necessary.

5.4.3 Future work

600 M2 lines were screened in this forward screen giving rise to 29 putative mutants with fertilisation-independent fruit growth. This suggests that the EMS population is a valuable resource for the future identification of genetic players involved in the process of regulating fruit initiation.

In this study, only the initial characterisation of one of the mutants (117.1) was pursued. Both the phenotypic characterisation and rough mapping were carried out in a *pistillata-1* mutant background. Future experiments will be required to confirm the above presented results in a single 117.1 background. Particularly in the case of 117.1 mapping, the predicted mapping position of 117.1 would need to be confirmed in a 117.1 x Col-0 F2 population by testing the two flanking markers (99-100 and 27-28) of the predicted mapping region on chromosome 5.

To further narrow the mapping position of 117.1, new markers in the predicted mapping region need to be designed. The phenotyping process of the mapping population could be a laborious process as emasculation of the 117.1 x Col-0 F2 population will be required to isolate the plants that show parthenocarpic fruit development. As an alternative to this as well as to facilitate the confirmation of the predicted rough mapping position, once the single 117.1 mutant is obtained (by backcross to Ler) a 117.1 *pop-1* double mutant could be created which could then be used to create a new mapping population by crossing it to Col-0 (117.1 *pop-1* x Col-0). The introduction of the conditional pollen-fertility mutant *pop-1* should ease the phenotyping process as no emasculations will be required. *pop-1* mutants (also known as *cer6-2*) are deficient in wax production which results not only in pollen grains unable to hydrate and germinate at low-humidity levels but in a lack of epicuticular wax which gives rise to bright green and glossy stems compared to wild-type plants (Preuss et al, 1993). Thus, in the F2 117.1 *pop-1* x Col-0 population only those plants with the *pop-1* phenotype will need to be screened for the parthenocarpic phenotype. *POP1/CER6* (AT1G68530) is not located in the predicted rough mapping region of 117.1 (region between AT5G14320-AT5G20240) which would also allow the confirmation of this rough mapping position. Alternatively and, in order to avoid the problem of mapping a segregating mutation that it is not the parthenocarpy conferring mutation, a *pi-1* mutant in Col-0 background could be used to create the mapping population. By crossing *pi-1* in Col-0 background with the parthenocarpy conferring mutation (in *pi-1* Ler background) *pi-1* mutation will be fixed and, thus, only the parthenocarpy conferring mutation to be mapped will segregate. This mapping strategy is probably the most desirable approach as it is the simplest strategy.

Allelism tests with other available parthenocarpic mutants could also be carried out whilst the mapping process is in progress. To date in Arabidopsis, only the loss of the individual action of three Auxin Response Factors (ARF2, ARF6 and ARF8) has shown to result in parthenocarpic fruit development (Vivian-Smith et al, 2001; Okushima et al, 2005; Goetz et al, 2006; Schruff et al, 2006; Wu et al, 2006). If the predicted rough map position of 117.1 is confirmed, it is unlikely that 117.1 will represent a new allele of any of these ARFs as they all map outside this region. However, it is interesting to notice that histological analysis of emasculated *arf8-4*

mutants demonstrated that the observed facultative parthenocarpy is mainly caused by cell expansion in the mesocarp (Vivian-Smith et al, 2001). Similar conclusions were reached by examination of *117.1 pi-1* longitudinal sections (see Figure 5.12) and, thus, it would be interesting to investigate the possible link between *117.1* and *ARF8* and/or auxin-dependent fruit development. Other hormones, particularly gibberellins are also involved in parthenocarpic fruit development (Chapter 5; Vivian-Smith et al, 2001; Marti et al, 2007; Dorcey et al, 2009), and the integration of *117.1* within the different molecular and hormonal pathways known to play a role in fruit development will be of great interest.

CHAPTER 6

Unexpected consequences of
investigating seed-pod
communication

CHAPTER 6

Unexpected consequences of investigating seed-pod communication

6.1 Introduction

6.1.1 Seed-pod communication during fruit development

Fruit development is a key step in the dispersal and/or survival strategy of flowering plants and, consequently, successful fruit set relies on the coordinated development of seed and ovary structures. Based on the complex nature and biological relevance of this developmental programme, it is likely that its coordination may require a dynamic seed-pod communication throughout the different stages of fruit development. However to date, relatively little is known about seed-pod communication.

At anthesis or stage 13 of *Arabidopsis* flower development, flowers are fully opened, the petals are visible and anthers dehisce (Smyth et al, 1990) (see Figure 6.1). In the mature ovules the egg cell and the synergids are located at the micropylar end, while the antipodal cells are located in the opposite end (chalazal end) (see Figure 6.1). Ovules are connected to the ovary wall through the funiculus. During pollination, pollen tubes extend through pistil tissues carrying two sperm cells. Successful double-fertilisation requires the delivery of the two sperm cells, one of which fuses to the nucleus of the egg cell to form the embryo whilst the other combines with the central cell to form the endosperm (see Figure 6.1). Pollen tube guidance to the receptive ovule relies on a tightly regulated signalling cascade which involves female gametophyte-, male gametophyte- and sporophyte- specific signals (Highashiyama et al, 2001; Marton et al, 2005; von Besser et al, 2006; Chen et al, 2007; Alandete-Saez et al, 2008; Shimizu et al, 2008; Wang et al, 2008; Chae et al, 2009; Okuda et al, 2009). Upon fertilisation, which marks the beginning of fruit development, an auxin signal is generated in the seeds (Dorcey et al, 2009). This auxin signal constitutes the first seed-pod

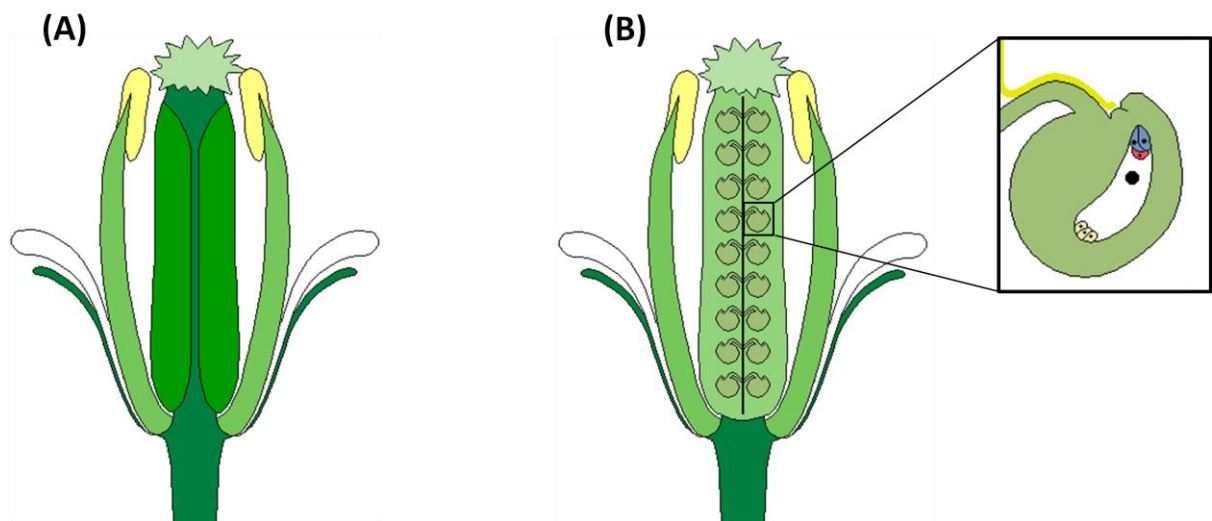


Figure 6.1 Representation of stage 13 *Arabidopsis* pistil. (A) At stage 13 of flower development, the flower is fully opened, the petals are visible and anthers dehisce. (B) Pollination occurs at stage 13, pollen tubes grow through the transmitting tract of the pistil to encounter the receptive ovules. Mature ovules contain the synergid cells (in blue) which will degenerate upon pollen tube entrance, the egg cell (in red) which fertilization will give rise to the embryo, the central cell (in the centre) which fertilization will result in the endosperm and three antipodal cells.

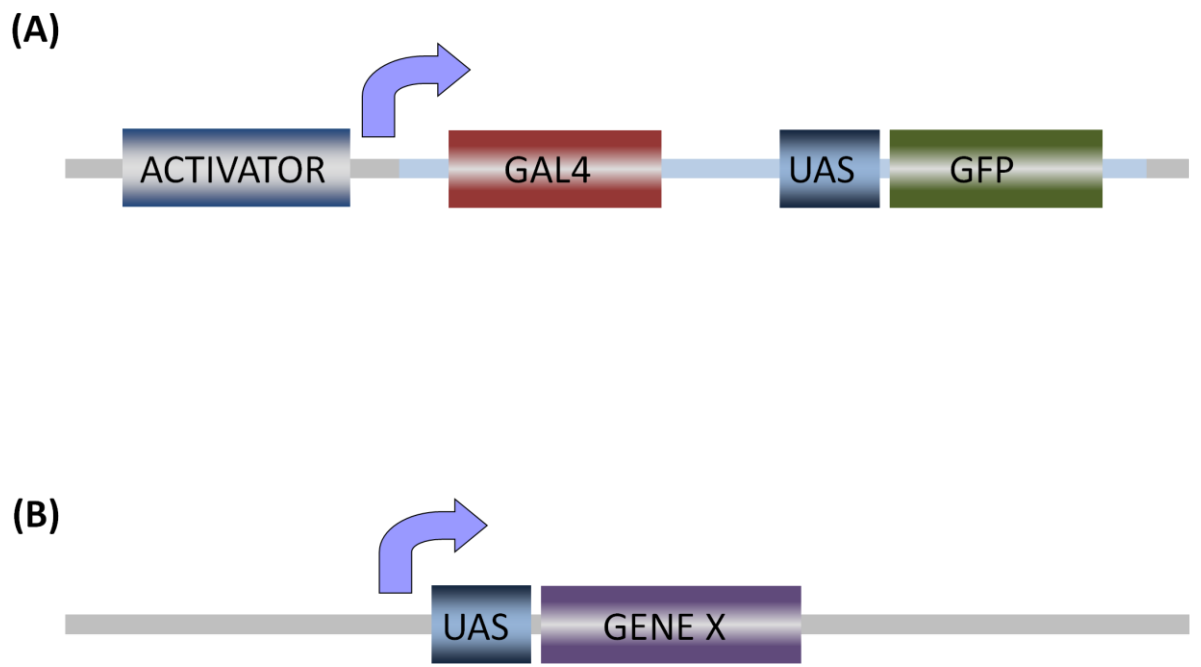


Figure 6.2 *GAL4-GFP* enhancer-trap system. (A) An enhancer-trap vector bearing a modified *GAL4-VP16* gene was inserted randomly into the *Arabidopsis* genome and proximity to a cellular enhancer results in activation of a linked GFP gene, allowing simple characterisation of expression patterns. (B) Targeted expression of another gene (X) can be induced by crossing with lines expressing genes under the control of promoters containing *GAL4*-binding sites (UAS).

communication event and it is believed to be responsible for the upregulation of GA biosynthesis observed in ovules and fruit valves (Dorcey et al, 2009). It has recently been shown that some of the developmental processes observed in seeded Arabidopsis fruits such as differentiation of the dehiscence zone and valve dehiscence are also observed in unfertilised pistils (Carbonell-Bejerano et al, 2010), suggesting that certain post-anthesis events do not rely on seed-pod communication. However, other post-anthesis processes such as the capacity to respond to GA-mediated fruit elongation relies on the presence of viable ovules and/or seeds (Carbonell-Bejerano et al, 2010). Furthermore, it is interesting to note that the post-anthesis developmental programme including ovary wall differentiation and dehiscence is delayed in the absence of developing seeds (Carbonell-Bejerano et al, 2010). Taken together, these results suggest that seed-pod communication is a dynamic process and that the dynamic nature of this communication may be the key factor controlling successful fruit development.

6.1.2 *GAL4-GFP* enhancer-trap system

The *GAL4-GFP* enhancer-trap system in *Arabidopsis* (Haseloff, 1999) is based on the *GAL4/UAS* two-component system (Brand and Perrimon, 1993). In the *GAL4-GFP* enhancer-trap system, enhancer-trap vectors bearing the *GAL4-VP16* gene and the *GFP* gene under the control of *GAL4* upstream activator sequences (UAS) are randomly inserted in the *Arabidopsis* genome via Agrobacterium mediated transformation (see Figure 6.2A). Proximity to cellular enhancers results in GFP expression and transformant plants can directly be screened for different GFP expression patterns (available at <http://www.plantsci.cam.ac.uk/Haseloff/>). Cross of the *GAL4-VP16* bearing line with lines expressing target genes under the control of a *GAL4*-activated promoter (see Figure 6.2B) allows the expression of target genes in the *GAL4*-expressing cells or tissues.

6.1.3 Targeting seed-pod communication

The objective of this study was to create an experimental setup to enable interruption of seed-pod communication during different stages of fruit

development. Such a system would allow us to study the effect this may have on the otherwise synchronous development of fruit and seeds. To this end it was hypothesised that a communication block would be most effectively achieved by production of a toxin leading to cell death in the seed attachment site (funiculus). As a first step towards this, GAL4-GFP enhancer lines with funiculus-specific expression were identified and characterised.

6.2 Materials and methods

6.2.1 TAIL-PCR

Three consecutive nested PCR reactions with arbitrary degenerate (AD) primers were carried out as part of the TAIL-PCR process. The primers used in this study are shown in Table 6.1. The primary TAIL-PCR reaction (20 μ l) contained 1xPCR buffer, 1.75mM MgCl₂, 150 μ M of each dNTP, 150nM specific primer, 0.3 μ l taq DNA polymerase, 0.4 μ l DMSO, 1 μ l DNA (1-2 μ M) and 2 μ M of the given AD primer. The primary TAIL-PCR reactions were carried out in a Mjresearch-ptc-200PCR Thermal cycler with the following cycle:

92°C (3'), 95°C (1')	x1
94°C (30s), 65°C (1'), 72°C (2')	x5
94°C (30s), 25°C (2'), ramping to 72°C over 2', 72°C (2')	x1
94°C (30s), 60°C (1'), 72°C (2')	
94°C (30s), 60°C (1'), 72°C (2')	
94°C (30s), 44°C (1'), 72°C (2')	x15
72°C (5')	x1
4°C (for ever)	

1 μ l aliquots from 40-fold dilution of the primary reaction was used in the secondary TAIL-PCR reaction (25 μ l) containing 1xPCR buffer, 1.8mM MgCl₂, 160 μ M of each dNTP, 200nM specific primer, 0.3 μ l taq DNA polymerase, 0.5 μ l DMSO and 2 μ M of the given AD primer. The secondary TAIL-PCR reactions were carried out in a Mjresearch-ptc-200PCR Thermal cycler with the following cycle:

94°C (30s), 60°C (1'), 72°C (2')	
94°C (30s), 60°C (1'), 72°C (2')	
94°C (30s), 45°C (1'), 72°C (2')	x12
72°C (5')	x1
4°C (for ever)	

After amplification, two tertiary TAIL-PCR reactions (25µl) were carried out containing 1xPCR buffer, 1.8mM MgCl₂, 160µM of each dNTP, 200nM specific primer, 0.3µl taq DNA polymerase, 0.5µl DMSO, 2µM of the given AD primer and 4µl aliquot from 40-fold dilutions from the primary or secondary reaction. The tertiary TAIL-PCR reactions were carried out in a Mjresearch-ptc-200PCR Thermal cycler with the following cycle:

94°C (30s), 45°C (1'), 72°C (2')	x35-40
72°C (5')	x1
4°C (for ever)	

Amplified products from the reactions were analysed by agarose gel electrophoresis and the difference in product size consistent with the specific primer position was used as the criterion to identify the insertion-specific amplification. Potential insertion-specific bands were later sequenced.

6.2.2 *PAP10*:GUS transgenic line construction

To generate the *PAP10*:GUS fusion construct, 3584bp of the *PAP10* promoter was amplified by using SF00115 as forward primer containing the *Hind**III* restriction site and SF00116 as reverse primer containing the *Bam**H**I* restriction site (see Table 6.1). The amplified fragment was digested with *Hind**III* and *Bam**H**I* and cloned into pBI101 which contains the reporter gene GUS. After *Arabidopsis* floral-dip transformation (see Chapter 2), transgenic plants were selected in MS medium supplemented with 50µg/ml Kanamycin. The presence of the *PAP10*:GUS in the transgenic seedlings was checked by genomic PCR with primers SF0192 (promoter-specific primer) and SF0171 (GUS-specific primer).

6.2.3 PCR genotyping of T-DNA insertion mutants

T-DNA insertion lines were obtained from The Nottingham Arabidopsis Stock Centre (NASC) (see Table 6.2) and homozygous mutants were isolated by PCR using gene-specific primers and primers anchored in the T-DNA borders (see Table 6.1). Two sets of PCR reactions were performed: a gene-specific reaction and an insert-specific reaction. Homozygous mutant plants showed no amplification in the gene-specific reaction but showed amplification in the insert-specific reaction. Heterozygous mutant plants showed amplification in both gene-specific and insert-specific reactions. Wild-type plants showed only amplification of the gene-specific reaction. Col-0 and H₂O were used as controls during PCR genotyping of insertion lines.

6.2.4 Analysis of *PAP10::GUS* expression in response to various stimuli

Transgenic *PAP10::GUS* lines 4, 6 and 10 (T2) were used as plant materials. Seedlings were germinated and grown in MS medium supplemented with 50µg/ml Kanamycin for 10 days and resistant plants were transferred to MS plates containing: gibberellic acid (100µM), mannitol (300mM), indole-3-acetic acid (10µM), abscisic acid (100µM), methyl jasmonate (50µM) or NaCl (250µM). Seedlings were grown for another 36 hours after which GUS expression was analysed in at least 5 seedlings after 40 minutes of incubation with the GUS reaction buffer. Seedlings grown in MS medium were used as controls.

6.2.5 Pollen grain analysis

In order to assess pollen viability, dehisced anthers from stage 13-14 flowers were dissected and pollen grains were spread in a microscopic slide and stained with one drop of 1% acetocarmine. The shape and staining of the pollen grains was recorded by light microscopy.

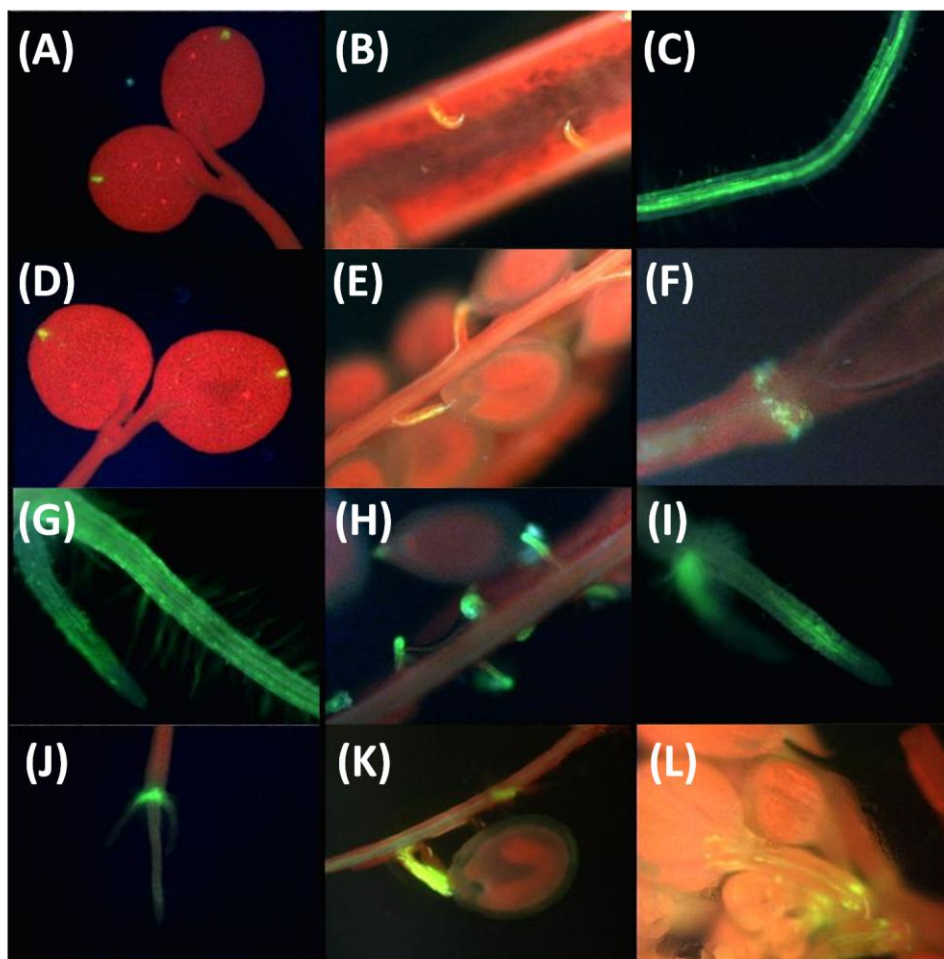


Figure 6.3 GFP expression in the *GAL4-GFP* enhancer-trap lines used in this study. GFP expression in line M0064 in (A) cotyledon tips and (B) funiculus. GFP expression in line M0070 in (C) root vasculature, (D) cotyledon tips, (E) funiculus and (F) siliques abscission zone. GFP expression in line M0090 in (G) root epidermis and (H) funiculus. GFP expression in line M0192 in (I) root vasculature, (J) hypocotyl/root transition zone, (K) funiculus and (L) in the vasculature of young flower buds. (Modified from <http://www.plantsci.cam.ac.uk/Haseloff/>)

6.3 Results

6.3.1 Funiculus-specific gene expression of *GAL4-GFP* enhancer-trap lines

Fertilisation marks the beginning of fruit development and, consequently, successful fruit set relies on the coordinated development of both seed and ovary structures. In order to investigate the importance of seed-pod communication throughout fruit development, it was decided to interrupt and/or alter this communication at different developmental stages by funiculus-specific expression of barnase or diphtheria toxin in an inducible manner. Both toxins have previously been used successfully in toxin-mediated cell ablation experiments (Day et al, 1995; Beals and Goldberg, 1997; Baroux et al, 2001; Frank and Johnson, 2009; Gardner et al, 2009). To identify those genes where expression in floral and fruit tissues is restricted to the funiculus, Dr. Jim Haseloff's *GAL4-GFP* enhancer-trap line catalogue was scrutinized (available at <http://www.plantsci.cam.ac.uk/Haseloff/>). Four *GAL4-GFP* enhancer-trap lines with funiculus-specific GFP expression were obtained from The Nottingham Arabidopsis Stock Centre (NASC) (M0064, M0070, M0090 and M0192, Donor: Dr. Jim Haseloff) (see Figure 6.3). In these enhancer-trap lines in pistils from stage 13 onwards (Smyth et al, 1990) GFP expression was restricted to the funiculus. However, GFP expression was also observed in other non-floral tissues such as cotyledons and roots (see Figure 6.3).

6.3.2 Isolation of GFP-expression drivers: *PAP10*

In order to determine the upstream elements driving the expression of GFP, the insertion sites of *GAL4-VP16* construct were investigated by TAIL-PCR (see Section 6.2.1). TAIL-PCR is a useful tool for the recovery of DNA fragments adjacent to known sequences. It relies on three nested-PCR reactions each of which is conducted with a sequence-specific primer and an arbitrary degenerate

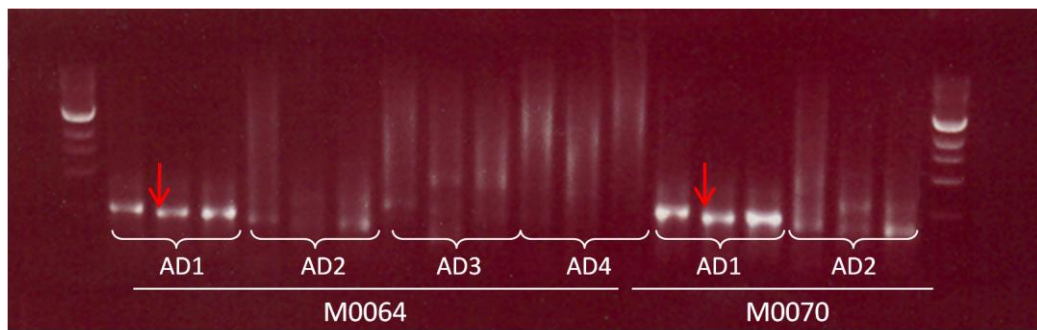


Figure 6.4 Characterisation of *GAL4-VP16* insertion site in M0064 and M0070 by TAIL-PCR. Gel photograph showing the specific amplification of sequence upstream to *GAL4-VP16* in the AD1 reaction in M0064 and M0070 lines. Gel shift between the primary and the two tertiary reactions is indicated by red arrows. Note that a 1 Kb ladder was used and, therefore, the approximately 150 bp band shift appears to be small.Ladder, 1Kb.

(A)

PAP10	-CCCTTTGTTATCGGAAAAAATCTCTCTTCA	59
M0060/M0070	TCCCCTTGTGGGATCGGAAAAAATCTCTCTTC	60
PAP10	AATGGGTGCGTCCGAAATCAGATTGCGGTCATT	119
M0060/M0070	AATGGGTGCGGTCGAAATCAAATTGCGGTCATT	120
PAP10	AAATAGCTACTCTGAATGGAGGCATCACCAGT	179
M0060/M0070	AAATAGCTACTCTGAATGGAGGCATCACCAGT	180
PAP10	CGTTGATATGCCTCTTGATAGCGATGTTTCGT	239
M0060/M0070	CGTTGATATGCCTCTTGATAGCGATGTTTCGT	240
PAP10	ACAGGTACACAAATCTTTCTTTATGAGTTTG	299
M0060/M0070	AAAGGTAC-CAA-----	251

(B)

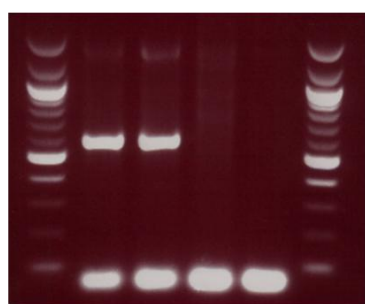


Figure 6.5 Confirmation of the GAL4-VP16 insertion site in M0064 and M0070. (A) Sequence alignment of AD1 tertiary reactions from TAIL-PCR (see Figure 6.4) and *PAP10* DNA sequence. (B) PCR reaction using GAL4-VP16 T-DNA and *PAP10* specific primers. Loaded samples from left to right, M0064, M0070, Col-0 (negative control) and H₂O (negative control). Ladder, 100 bp.

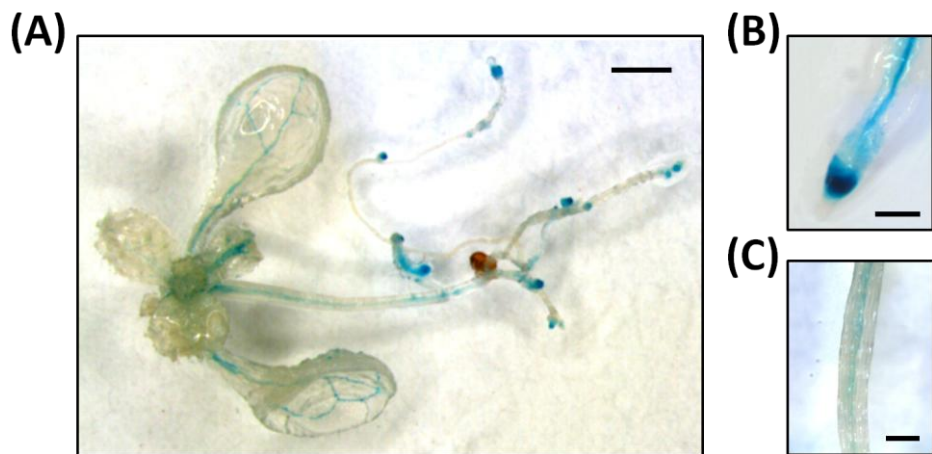


Figure 6.6 GUS staining of *PAP10::GUS* in three weeks-old seedlings of transgenic line 4. (A) GUS expression in three weeks-old seedling. (B) Root close up. (C) Stem close up. Scale bar (A), 0.15cm. Scale bar (B,C), 0.015cm

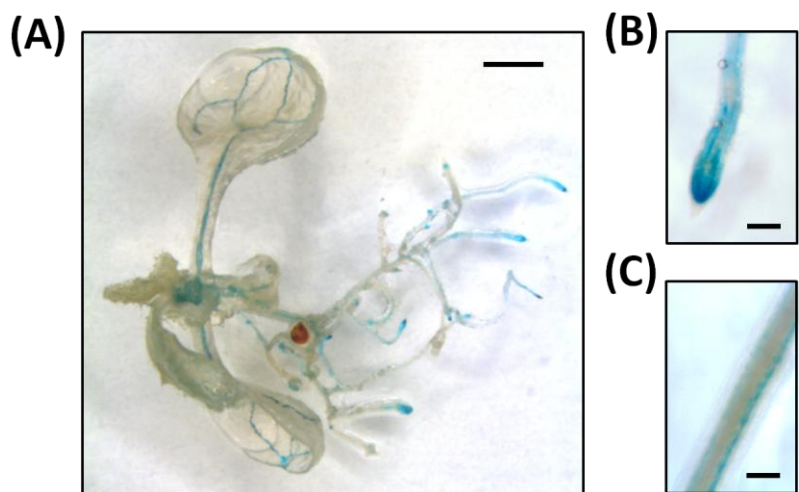


Figure 6.7 GUS staining of *PAP10::GUS* in three weeks-old seedlings of transgenic line 6. (A) GUS expression in three weeks-old seedling. (B) Root close up. (C) Stem close up. Scale bar (A), 0.15cm. Scale bar (B,C), 0.015cm

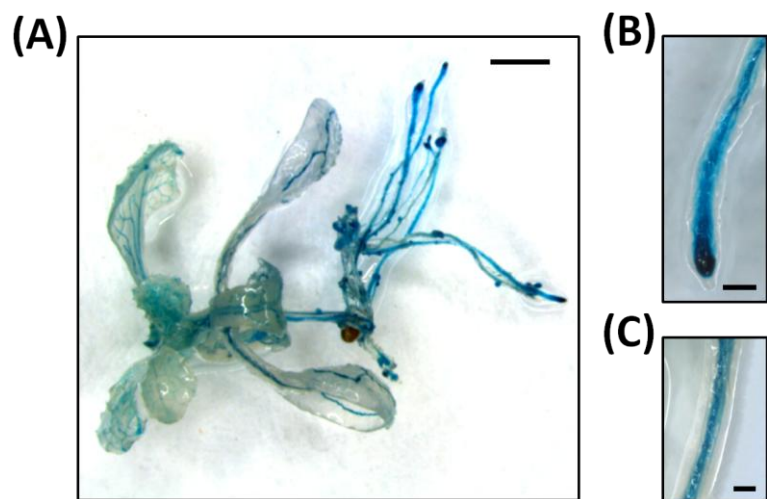


Figure 6.8 GUS staining of *PAP10::GUS* in three weeks-old seedlings of transgenic line 10. (A) GUS expression in three weeks-old seedling. (B) Root close up. (C) Stem close up. Scale bar (A), 0.15cm. Scale bar (B,C), 0.015cm

(AD) primer. As the distance between the sequence-specific primers used in the secondary and tertiary reactions is known, specific-product amplification can be determined based on this distance. Several attempts were carried out to determine the upstream elements driving the expression of GFP in the four enhancer-trap lines being investigated (data not shown) and, specific-product amplification was obtained in both M0064 and M0070 lines (see Figure 6.4). Sequencing of the bands amplified by TAIL-PCR showed that the *GAL4-VP16* construct is inserted downstream of *PURPLE ACID PHOSPHATASE 10* (*PAP10*, AT2G16430) in M0064 and M0070, suggesting that both enhancer-trap lines derived from the same transformant line. *GAL4-VP16* insertion in M0064 and M0070 was also confirmed by PCR with one primer specifically designed in *PAP10* sequence and another primer in the 5'end of the *GAL4-VP16* construct (see Figure 6.5).

Purple acid phosphatase (PAPs) are part of the metallo-phosphoesterase family of proteins and they are characterised by seven conserved amino acid residues involved in the coordination of the dimetal nuclear centre (Li et al, 2002). PAPs are present in mammals, fungi, bacteria and plants and, *in vitro*, PAPs have been shown to catalyze the hydrolysis of activated phosphoric acid ester and anhydrides (Klabunde et al, 1996). In plants, PAPs have been the focus of several studies regarding mainly their role in phosphorus nutrition (Veijanovski et al, 2006; Kuang et al, 2009; Hur et al, 2010; Hurley et al, 2010; Tran et al, 2010).

6.3.3 Expression analysis of *PAP10*

To further investigate the expression pattern of *PAP10*, transgenic *Arabidopsis* plants expressing GUS fusion protein under the control of 3584bp of the *PAP10* promoter were produced (see Section 6.2.2). After segregation analysis of T2 lines, three lines with a single transgene copy were selected namely line 4, 6 and 10. These lines show different levels of GUS activity with line 4 being the weakest line and line 10 the strongest (see Figures 6.6, 6.7, 6.8).

In three week-old seedlings, intense GUS staining was observed in the root-tips of the three independent transgenic lines assessed (see Figures 6.6, 6.7, 6.8).

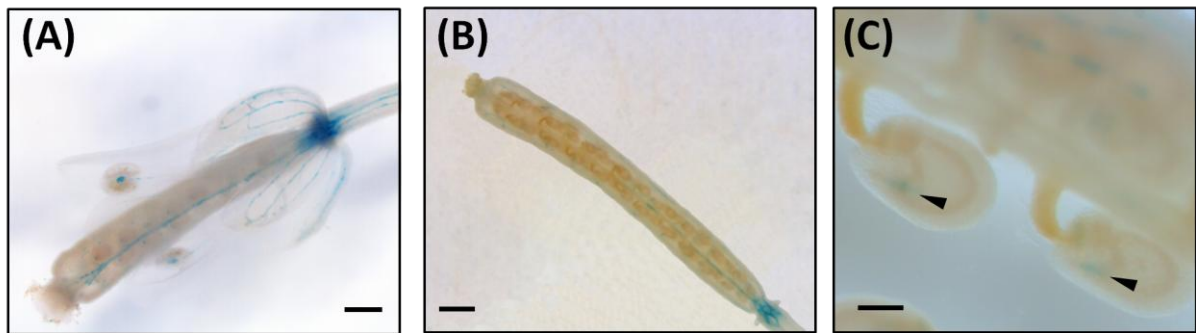


Figure 6.9 GUS staining of *PAP10::GUS* in floral and fruit tissue of transgenic line 4. (A) GUS expression in stage 15 flowers. (B) GUS expression in stage 17a siliques. (C) GUS expression in seeds from stage 17a siliques. Arrowheads indicate the micropylar-endosperm region. Scale bar (A), 0.352mm. Scale bar (B), 0.5mm. Scale bar (C), 0.08mm

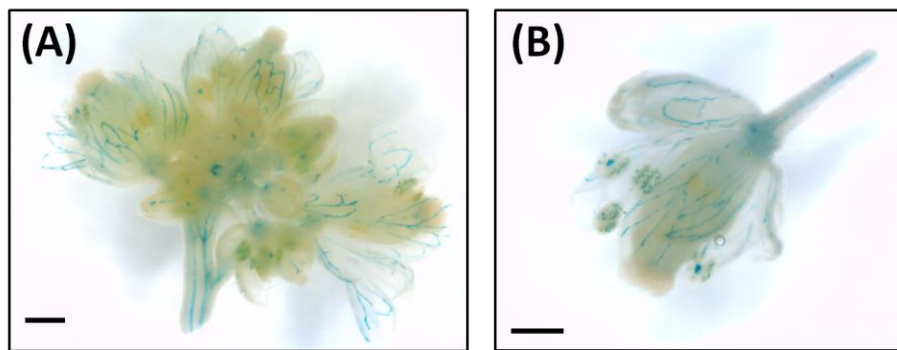


Figure 6.10 GUS staining of *PAP10::GUS* in floral and fruit tissue of transgenic line 6. (A) GUS expression in inflorescences. (B) GUS expression in stage 14 flower. Scale bar (A), 0.55mm. Scale bar (B), 0.5mm

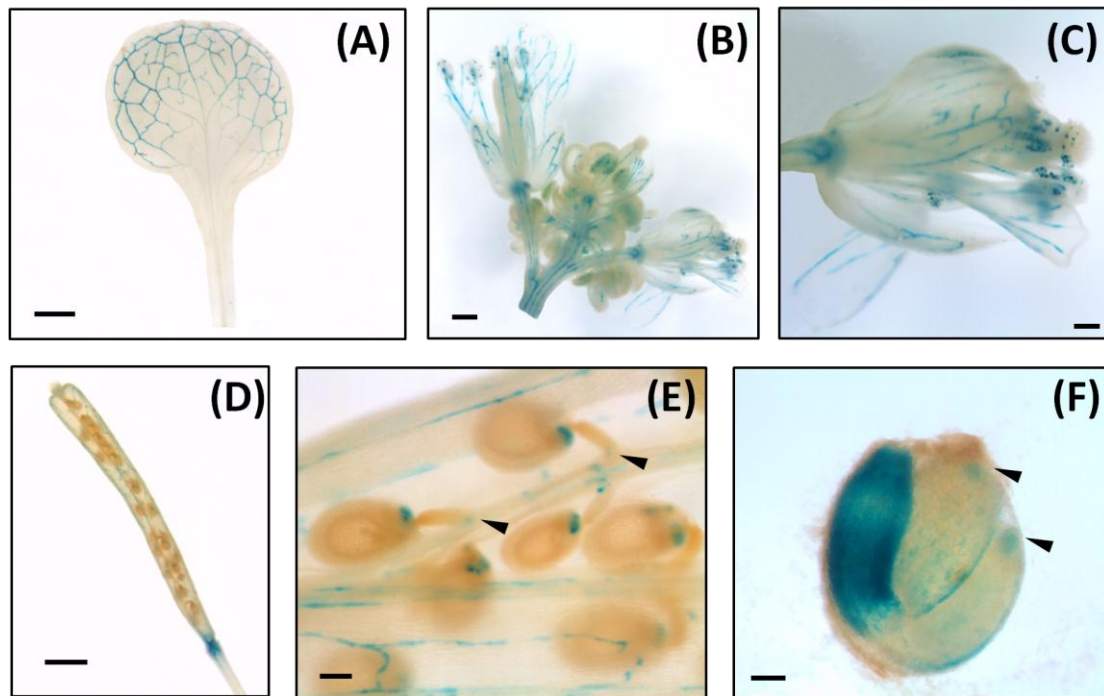


Figure 6.11 GUS staining of *PAP10::GUS* in floral and fruit tissue of transgenic line 10. (A) GUS expression in rosette leaf. (B) GUS expression in inflorescences. (C) GUS expression in stage 14 flower. (D) GUS expression in stage 17a siliques. (E) GUS expression in seeds from stage 17a siliques. Arrowheads indicate the funiculus vasculature. (F) GUS expression in fully-developed embryo. Arrowheads indicate the cotyledon tips. Scale bar (A), 1.25mm. Scale bar (B), 0.41mm. Scale bar (C), 0.17mm. Scale bar (D,E), 0.1mm. Scale bar (F), 0.07mm

GUS staining was also recorded in the vasculature of leaves, stems and roots (see Figures 6.6, 6.7, 6.8). A weak signal was also detected in the newly emerged leaves (see Figures 6.6A, 6.7A) and this signal became more diffuse in the strongest GUS-transgenic line (see Figure 6.8A).

GUS expression was also analysed in floral and fruit tissue, in order to determine whether *PAP10* promoter could be used to drive funiculus-specific gene expression. In the weakest GUS-transgenic line (line 4) at stage 15 of flower development GUS staining was observed in the junction region between anthers and filaments (see Figure 6.9A). GUS expression was also recorded in the vasculature of petals, sepals and pistils (see Figure 6.9A). At stage 17a of siliques development, GUS staining was observed in the vasculature of siliques as well as in the micropylar-endosperm region of developing seeds (see Figure 6.9B, C). In the GUS-transgenic line 6, which shows a medium GUS intensity level, a stronger GUS signal was recorded in inflorescence vasculature (see Figure 6.10). And, in addition to the GUS-expression pattern described for line 4, GUS staining was also observed in pollen grains in flowers from stage 12 onwards (see Figure 6.10). Finally, in the strongest GUS-expressing line (line 10) additional tissues such as leaf vasculature also showed GUS expression (see Figure 6.11). In this transgenic line, a more intense pollen grain GUS staining was also observed (see Figure 6.11B, C) and, in agreement with the GFP-expression patterns observed in lines M0064 and M0070, GUS staining of the funiculus vasculature and cotyledon tips was recorded (see Figure 6.3, 6.11E, F). GUS staining in fully-developed embryos was clearly restricted to the root and cotyledon tips (see Figure 6.11F).

Due to the complex GUS expression pattern observed in *PAP10* promoter::GUS inflorescences, it was concluded that *PAP10* promoter would be unsuitable to drive funiculus-specific gene expression.

6.3.4 GUS expression in *PAP10* ::GUS lines varies in response to different stimuli

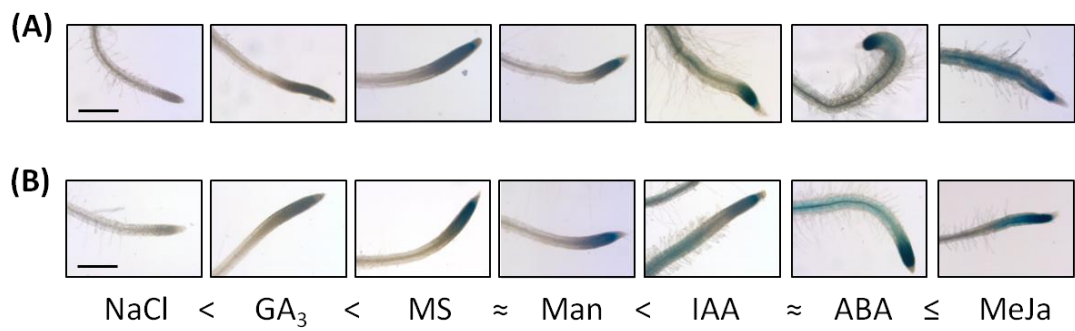


Figure 6.12 GUS expression pattern in root tips in two independent transgenic lines in response to a variety of stimuli. (A) GUS expression pattern in root tips of transgenic line 6 in response to different stimuli. (B) GUS expression pattern in root tips of transgenic line 10 in response to different stimuli. GA₃, gibberellic acid; MS, Murashige and Skoog medium (control medium); Man, mannitol; IAA, indole-3-acetic acid; ABA, abscisic acid; MeJa, methyl jasmonate. Scale bar, 0.4mm

During the expression-pattern characterisation of *PAP10::GUS* lines, the molecular and biochemical characterisation of another *Arabidopsis* purple acid phosphatase (*PAP15*) was published (Kuang et al, 2009). *PAP15* is also strongly expressed in the vasculature of many plant organs including the roots and, particularly, strong *PAP15::GUS* expression has been reported in root tips (Kuang et al, 2009). Analysis of *PAP15::GUS* expression in root tips also concluded that root-tip expression pattern is affected in response to a variety of stimuli (Kuang et al, 2009). Many of the patterns observed in *PAP15::GUS*, including the strong expression in root tips, coincide with the *PAP10::GUS* expression patterns reported in this study (see Figures 6.6-6.11). Thus, it was decided to investigate whether the *PAP10::GUS* expression in root tips also responded to a variety of stimuli. Three independent transgenic lines (line 4, 6 and 10) were analysed and a short period of incubation time (40 minutes) was used in order to detect the possible differences in GUS expression in response to a variety of stimuli. Previous expression-pattern studies have shown that GUS expression is relatively low in the transgenic line 4 (see Figures 6.6, 6.7, 6.8) and after 40 minutes of GUS staining, the observed signal was judged to be too weak to evaluate the response to different stimuli (data not shown). In the transgenic lines 6 and 10, no effects in GUS staining were observed in leaf, shoot or root vasculature in response to different stimuli (data not shown); however, a marked variation in root-tip GUS expression was recorded in response to different stimuli (see Figure 6.12). No GUS staining was observed in NaCl-treated root tips (see Figure 6.12). This effect can almost certainly be attributed to the chemical effects of NaCl as GUS staining was detected in the osmotic control treatment with mannitol (see Figure 6.12). The effects of different hormone treatments were also assessed. A weaker GUS signal was observed in the root-tips of GA₃-treated seedlings when compared to control seedlings (see Figure 6.12). An opposite result was recorded in the root-tips of IAA-, ABA- and MeJa-treated seedlings where a stronger GUS signal than in control seedlings was observed (see Figure 6.12).

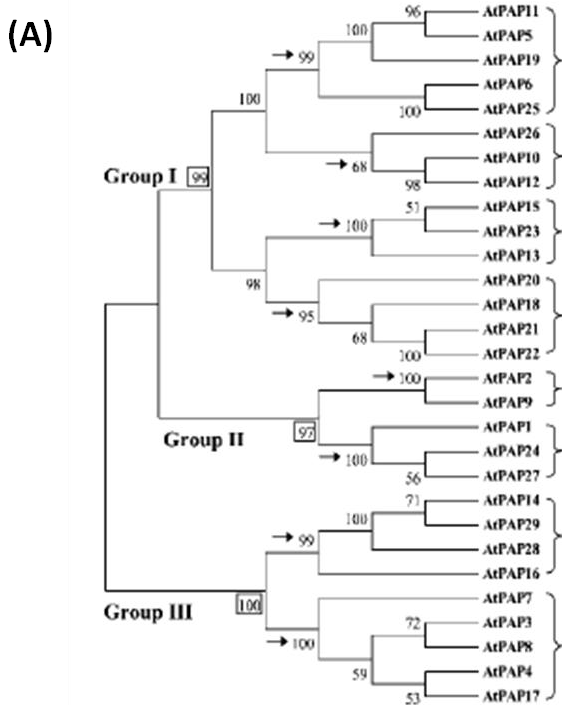


Figure 6.13 Cluster analysis of amino acid sequences of PAPs in *Arabidopsis*. (A) Cluster analysis of amino acid sequences of AtPAP. The bootstrap values are percentages of 500 replicates and the main three groups are further divided in eight subgroups. Adapted from Li et al, 2002. (B) Amino acid sequence alignment of PAP10 and PAP12. The five conserved motifs of PAPs are underlined and the seven conserved amino acid residues within these motifs coordinating the dimetal nuclear center are shown in boldface.

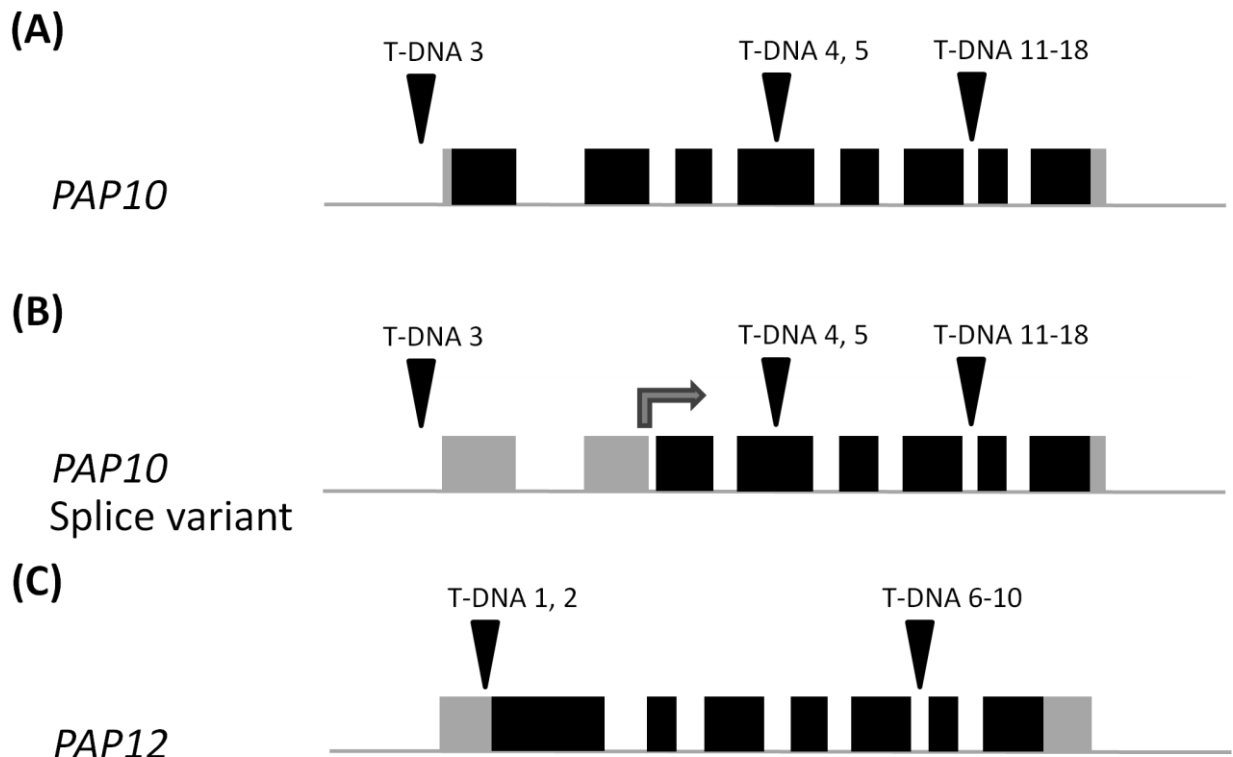


Figure 6.14 Representation of the mutant T-DNA insertion lines of *pap10* and *pap12* used in this study. (A) T-DNA insertion sites in the wild-type *PAP10*. (B) T-DNA insertion sites in the splice-variant of *PAP10*. Transcription of the *PAP10* splice-variant results in a transcript retaining the second intron. (C) T-DNA insertion sites in *PAP12*. Exons are shown as boxes and introns as lines. The 5' and 3'untranslated regions are shown in grey.

NASC ID	Mutant line	Gene	Named	Allele	Background
N307993	GK-662B07	<i>PAP12</i>	Line 1	<i>pap12-1</i>	Col-0
N307989	GK-662B07	<i>PAP12</i>	Line 2	<i>pap12-1</i>	Col-0
N622362	SALK-122362	<i>PAP10</i>	Line 3	<i>pap10-1</i>	Col-8
N845235	SAIL-12234-D05	<i>PAP10</i>	Line 4	<i>pap10-2</i>	<i>quartet</i> (Col-0)
N819843	SAIL-430-D05	<i>PAP10</i>	Line 5	<i>pap10-2</i>	<i>quartet</i> (Col-0)
N379355	GK-151C09	<i>PAP12</i>	Line 6	<i>pap12-2</i>	Col-0
N379364	GK-151C09	<i>PAP12</i>	Line 7	<i>pap12-2</i>	Col-0
N379349	GK-151C09	<i>PAP12</i>	Line 8	<i>pap12-2</i>	Col-0
N379354	GK-151C09	<i>PAP12</i>	Line 9	<i>pap12-2</i>	Col-0
N379356	GK-151C09	<i>PAP12</i>	Line 10	<i>pap12-2</i>	Col-0
N730673	GK-850G03.06	<i>PAP10</i>	Line 11	<i>pap10-3</i>	Col-0
N730674	GK-850G03.06	<i>PAP10</i>	Line 12	<i>pap10-3</i>	Col-0
N730675	GK-850G03.06	<i>PAP10</i>	Line 13	<i>pap10-3</i>	Col-0
N730668	GK-850G03.06	<i>PAP10</i>	Line 14	<i>pap10-3</i>	Col-0
N730669	GK-850G03.06	<i>PAP10</i>	Line 15	<i>pap10-3</i>	Col-0
N730671	GK-850G03.06	<i>PAP10</i>	Line 16	<i>pap10-3</i>	Col-0
N730672	GK-850G03.06	<i>PAP10</i>	Line 17	<i>pap10-3</i>	Col-0
N730670	GK-850G03.06	<i>PAP10</i>	Line 18	<i>pap10-3</i>	Col-0

Figure 6.15 List of *pap10* and *pap12* mutant lines used in this study. Note that SAIL lines are in a *quartet* mutant background.

6.3.5 *pap10*, *pap12* and *pap10pap12* mutant isolation

Based on GUS-expression analysis of *PAP10::GUS* lines, it was concluded that *PAP10* promoter could not be used to drive funiculus-specific gene expression. Nevertheless, the GUS expression observed in pollen grains, funiculus vasculature and during seed development (see Figure 6.11), suggests that *PAP10* may play a role in seed and/or fruit development. The purple acid phosphatase family consists of 29 members in Arabidopsis (Li et al, 2002) and clustering analysis of amino acid sequences have shown that *PAP12* is the closest member to *PAP10* (Li et al, 2002; see Figure 6.12). Thus, in order to determine whether *PAP10* is involved in reproductive development, a series of *pap10* and *pap12* mutant alleles and double *pap10pap12* mutants were isolated and analysed.

Three T-DNA insertion lines at the *PAP10* locus and two T-DNA insertion lines at the *PAP12* locus were obtained from The Nottingham Arabidopsis Stock Centre (NASC). A schematic representation of the T-DNA insertion sites are shown in Figure 6.14 and a summary of the NASC ID, mutant lines and nomenclature used in this study are shown in Figure 6.15.. It is worth noticing that *PAP10* translation results in two gene products: a wild-type protein of 468 amino acids and a splice-variant protein of 348 amino acids (Li et al, 2002). Although this protein is completely homologous to the wild-type *PAP10* protein, it lacks the N-terminus 120 amino residues of the wild type (Li et al, 2002; see Figure 6.13).

PCR-genotyping of the T-DNA insertion lines was carried out in order to isolate homozygous mutant plants. Two sets of PCR reactions were performed: a gene-specific reaction and an insert-specific reaction (see Section 6.2.3). Homozygous mutant plants showed no amplification in the gene-specific reaction but showed amplification in the insert-specific reaction. Two different homozygous mutant alleles were successfully isolated for *PAP12*: *pap12-1* (corresponding to the T-DNA insertion lines 1 and 2) and *pap12-2* (corresponding to the T-DNA insertion lines 6-10). Three different homozygous mutant alleles for *PAP10* were also isolated: *pap10-1* (corresponding to the T-DNA insertion line 3), *pap10-2* (corresponding to the T-DNA insertion lines 4 and 5) and *pap10-3* (corresponding to the T-DNA insertion lines 11-18 (see Figure 6.15 and Appendix figures 6.1-6.6).

A series of *pap10**pap12* double mutants were also constructed by crossing the different single homozygous mutant alleles of *pap10* and *pap12*. The following double mutant combinations were crossed and isolated by PCR-genotyping: *pap10-1pap12-2*, *pap10-2pap12-1*, *pap10-2pap12-2*, *pap10-3pap12-1* and *pap10-3pap12-2* double mutants (see Appendix figure 6.7-6.11).

6.3.6 *pap10* and *pap12* single mutants and *pap10pap12* double mutants do not show any floral or fruit phenotypes

Initial characterisation of *pap10* and *pap12* mutants did not reveal any evident phenotypes. Special attention was paid to floral and fruit tissues but, detailed microscopic analysis did not reveal any floral or fruit phenotype. Only a tetrad pollen phenotype was observed in those mutants containing the *pap10-2* allele (data not shown) due to the *quartet* mutant background (see Figure 6.15).

6.4 Discussion

6.4.1 Interruption of seed-pod communication by funiculus-specific gene expression

Successful fruit development relies on the coordinated development of both seed and ovary structures. Upon ovule fertilisation, a seed origin auxin signal is generated which marks the beginning of fruit development (Dorcey et al, 2009). Nevertheless, the importance of seed-pod communication throughout fruit and/or seed development remains to be clarified. In order to investigate the relevance of

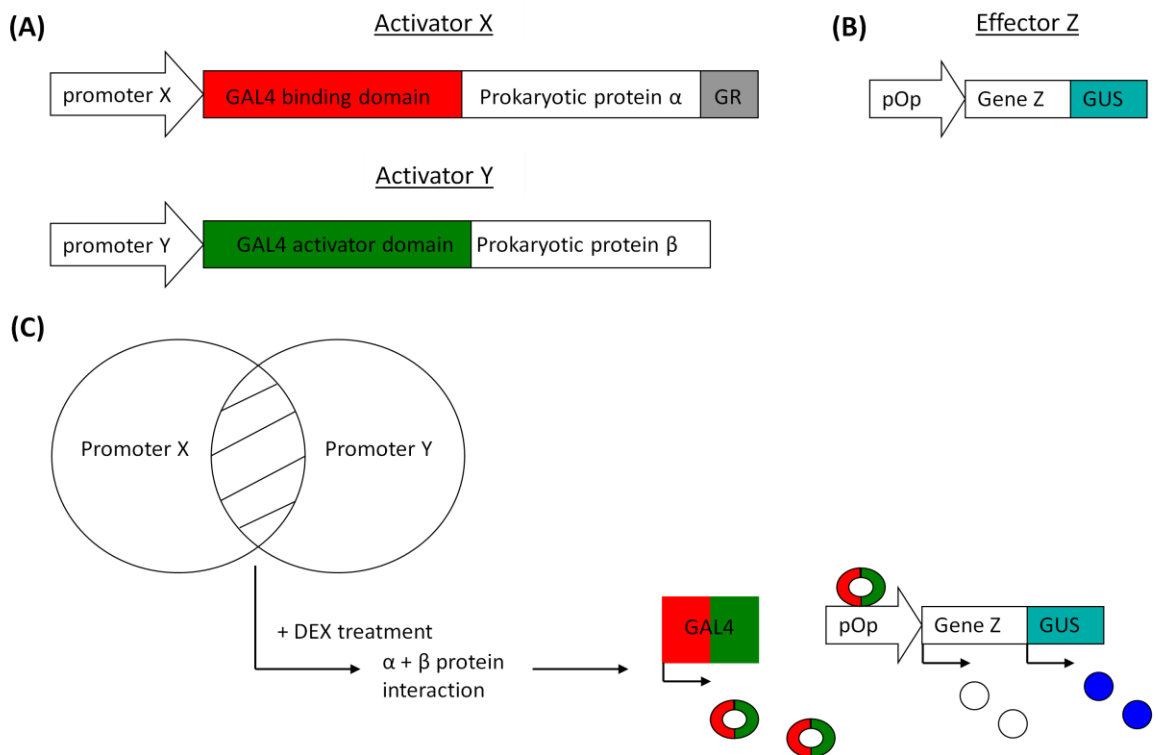


Figure 6.16 General diagram of a novel three-component gene expression system. The three-component gene expression system uses two plant lines: (A) one that expresses a chemically inducible activator construct and a non-chemically inducible construct and (B) another that contains the effector construct, that is, the gene of interest under the control of a silent promoter that is only activated by an heterologous transcription factor. One of the activator constructs consist of a tissue-specific promoter (X) which drives the expression of GAL4 binding domain, of the prokaryotic protein α and of the receptor domain of the rat glucocorticoid receptor (GR). The other activator construct consists on a tissue-specific promoter (Y) which drives the expression of GAL4 activator domain and of the prokaryotic protein β . (C) In the F1 population after dexamethasone (DEX) treatment, the interaction of the two activator constructs will be possible. These two promoters (X and Y) present an overlapping expression pattern and only in those areas/tissues where both promoters are simultaneously expressed will protein α and β interact leading to the expression of the yeast transcription factor GAL4. The expression of the genes under the control of the pOp promoter (promoter containing GAL4-binding sites) will only be possible in the presence of GAL4 and, therefore, the expression of these genes will be limited to those areas/tissues where both tissue-specific promoters (X and Y) are simultaneously expressed

seed-pod communication, it was decided to interrupt and/or alter this communication at different developmental stages by funiculus-specific expression of cell-ablation causing toxins. Four enhancer-trap lines with funiculus-specific GFP expression were studied (see Figure 6.3) and, in two of these lines, the upstream element driving GFP expression was isolated and identified as *PAP10* (see Figure 6.4). Further characterisation of *PAP10* promoter by analysis of *PAP10*:GUS transgenic lines was carried out to confirm the funiculus-specific pattern. Unfortunately, a complex GUS-expression pattern, not only limited to the funiculus, was observed in *PAP10*:GUS inflorescences and fruits (see Figures 6.9, 6.10, 6.11). Due to this extended expression pattern, the construction of funiculus-specific expression systems based on *PAP10* promoter was abandoned.

The role that seed-pod communication plays throughout fruit and/or seed development remains an interesting biological question. And, thus, the isolation of funiculus-specific promoters could further be pursued by isolation of the GFP-expression driving elements in the two remaining enhancer-trap lines (M0090 and M0192, see Figure 6.3). Alternatively, a novel three-component gene expression system could be developed. This system could allow tissue-specific gene expression in the overlapping expression areas of two tissue-specific promoters and, thus, it would provide a further degree of specificity particularly in those cases where a promoter with the desired expression pattern (such as a funiculus-specific pattern) has not yet been identified. A detailed schematic representation of this novel system is shown in Figure 6.16. To achieve funiculus-specific gene expression, for example, the *SEEDSTICK* promoter (MADS box gene involved in ovule identity and seed abscission; Pinyopich et al, 2003) and the *FUSSI* 2 (GUS marker line; Stangeland et al, 2003) could be combined.

6.4.2 Purple acid phosphatases and *PAP10*

Purple acid phosphatases (PAPs) are part of the metallo-phosphoesterase family of proteins and they are present in mammals, fungi, bacteria and plants (Li et al, 2002; Olczak et al, 2003). Plant PAPs have mainly been studied in the context of phosphate acquisition (Veijanovski et al, 2006; Kuang et al, 2009; Hur et al, 2010;

Hurley et al, 2010; Tran et al, 2010); although the enzymatic activity of only a few PAPs has been analysed to date. Investigation of four enhancer-trap lines with funiculus-specific GFP expression concluded that the *GAL4-VP16* construct responsible for the observed GFP expression was inserted downstream of *PAP10* in two of the lines studied (see Figures 6.4, 6.5). *PAP10* is a high molecular weight PAP (Li et al, 2002) whose biological role has not yet been described.

In order to characterise in detail *PAP10* expression pattern, three *PAP10::GUS* transgenic lines with a single transgene copy were selected. The intensity of the GUS staining varied among the three transgenic lines, which could be due to the different insertion sites of the transgene within the genome. Nevertheless, in all GUS transgenic lines a strong GUS signal was observed in: vasculature, root tips, seed endosperm and in the junction between anthers and filaments (see Figures 6.6-6.11). In addition, in a medium GUS-intensity line (line 6) and in a strong GUS line (line 10) pollen grain staining was also recorded from flower stage 12 onwards (see Figures 6.10, 6.11). Finally, in the strongest GUS transgenic line (line 10) funiculus and cotyledon tip specific expression was also recorded in agreement with the GFP-expression pattern observed in the enhancer-trap lines M0060 and M0070 (see Figure 6.3, 6.11).

In addition, GUS expression in *PAP10::GUS* root tips in response to a variety of stimuli was also investigated. Clustering analysis of amino acid sequences of the 29 putative PAP in *Arabidopsis* indicated that *PAP10*, *PAP12* and *PAP26* are clustered in the subgroup 1a-2 (Li et al, 2002). Several studies of *PAP12* and *PAP26* have concluded that these phosphatases may play a role in inorganic phosphate (Pi) mobilisation during nutritional phosphate deprivation (Veijanovski et al, 2006; Hue et al, 2010; Hurley et al, 2010). Thus, in order to investigate the possible relevance of *PAP10::GUS* expression in root tips, the expression pattern in response to various stimuli was recorded. Furthermore, it has previously been shown that the expression of another closely related purple acid phosphatase, *PAP15*, varies in response to stimuli such as different hormones; in contrast, no variation was observed under different nutrient stresses (Kuang et al, 2009). A different response to that observed in *PAP15::GUS* root tips was recorded in *PAP10::GUS* root tips. Treatment with NaCl induced *PAP15::GUS* expression

whilst an opposite effect was observed in *PAP10::GUS* (Kuang et al, 2009; see Figure 6.12). Treatment with MeJa had no effect in *PAP15::GUS* expression in root tips whilst in *PAP10::GUS*, a strong GUS induction was recorded (Kuang et al, 2009; see Figure 6.12). However, in addition to confirming the observed GUS expression changes by quantitative measurements of GUS activity that monitor cleavage of the β -glucuronidase substrate 4-methylumbelliferyl β -D-glucuronide (MUG) (Jefferson et al, 1987; Gallagher, 1992), the potential biological relevance of this changes would also need to be assessed. Although no nutrient starvation experiments were carried out in *PAP10::GUS* lines, it is interesting to notice that *PAP10* has previously been shown not to be transcriptionally induced during Pi deprivation (Li et al, 2002; Tran et al, 2010). This is also the case for *PAP26*, which enhanced synthesis during Pi deprivation is under post-transcriptional control (Hurley et al, 2010). Thus, given that no transcriptional regulation of *PAP10* was observed in previous studies (Li et al, 2002; Tran et al, 2010), the study of its possible post-transcriptional regulation in root tips during nutrient starvation may be more relevant.

Based on the complex expression pattern of *PAP10*, the construction of funiculus-specific gene expression systems was abandoned. However, the characterisation of *PAP10* expression pattern opened other possible lines of investigation. For example, *PAP10* is expressed in the funiculus, developing endosperm and pollen grains which suggests that *PAP10* may play a role in reproductive development.

6.4.3 Lack of phenotypes related to reproductive development in *pap10* or *pap10pap12* mutants

In order to study the possible role of *PAP10* in reproductive development, a series of *pap10*, *pap12* and *pap10pap12* mutants were isolated and characterised. Three different T-DNA insertion alleles were obtained for *PAP10* whilst two different T-DNA insertion alleles were isolated for *PAP12* (see Figure 6.15 and Appendix figures 6.1-6.6). However, none of the *pap10* mutant alleles investigated showed any developmental phenotypes. Similarly, analysis of *pap10pap12* double mutants did not reveal any phenotypes.

PAP10 transcription results in fully-processed wild-type transcript as well as in splice-variant transcripts (Li et al, 2002). The hypothetical protein resulting from the splice-variant processing is completely homologous to that of the catalytic domain of the wild-type protein but lacks the N-terminus 120 amino residues of the wild type (Li et al, 2002; see Figure 6.14). It is possible that the three *pap10* mutants alleles isolated in this study may have a different effect in the transcription of the wild-type and splice-variant transcript. PCR primers for selective amplification of either wild-type transcripts or splice variants have already been used (Li et al, 2002) and, thus, Q-PCR in the different T-DNA insertion mutants could be performed to investigate whether the expression of the wild-type and splice-variant transcripts is differently affected.

6.4.4 Future work

The initial aim of this study, the construction of a funiculus-specific gene expression system which could allow to interrupt and/or alter seed-pod communication, was soon abandoned after the discovery that *PAP10* promoted expression is not limited to the funiculus during flower and fruit development (see Figures 6.9, 6.10, 6.11). Nevertheless, the detailed characterisation of *PAP10* expression pattern opened other avenues of study. Although initial phenotypic characterisation of *pap10* mutants was unsuccessful, it is possible that *PAPs* may be highly redundant in *Arabidopsis* and, thus, multiple mutant combinations may be required in order to fully understand the possible biological function of *PAP10*. According to the cluster analysis, *PAP12* is the most closely related purple acid phosphatase to *PAP10*. Nevertheless, no developmental phenotypes were observed in *pap10pap12* double mutants. It is likely that Pi deprivation experiments may be required to uncover the biological function of *PAP10*. Alternatively, if no phenotypes were observed in Pi deprivation experiments when comparing *pap10* single or *pap10pap12* double mutants with wild type plants, triple mutant combinations with *PAP26* (the next closely related member, see Figure 6.13) may be required.

CHAPTER 7

General discussion

CHAPTER 7

General discussion

7.1 Aim and approaches

Fruit initiation and development are key steps of the life cycle of most angiosperms, as fruit development is not only responsible for nurturing the next generation but it is also often part of the dispersal and colonisation strategy. The overall aim of this project was to contribute to the understanding of the hormonal and genetic mechanisms that induce fruit development following fertilisation. In order to achieve this aim, a particular interest has been paid to the study of parthenocarpy, that is, the growth of the ovary into a seedless fruit in the absence of pollination and/or fertilisation (Lukyanenko, 1991).

Three main approaches have been adopted to investigate the hormonal and genetic mechanisms involved in fruit initiation and development. Firstly, a forward genetic screen approach was undertaken for the discovery of novel mutations resulting in parthenocarpic fruit development. Secondly, targeting of seed-pod communication was pursued to investigate its relative importance throughout the different stages of fruit development. Finally, the in-depth characterisation of GA-signalling during fruit initiation and development was also carried out.

7.2 Conclusions

Several main conclusions can be drawn from the research work carried out as part of this thesis:

- DELLA proteins play an additive role in fruit growth repression and lack of DELLA proteins results in facultative parthenocarpy.
- The facultative parthenocarpy observed in *global-DELLA* and *ga1-3 global-DELLA* pistils is not due to increased auxin levels.

- DELLA proteins are involved in several aspects of fruit development including style and stigma development.
- There is a DELLA-independent GA-response during fruit development.
- GID1, 26s proteasome and SPT are part of the newly discovered DELLA-independent GA pathway.
- DELLA-independent GA pathway plays a minor role in GA signalling during fruit development.
- DELLA proteins interact with several members of the bHLH transcription factors involved in fruit development including ALC and SPT.
- DELLA proteins are also able to interact with non-bHLH transcription factors in yeast such as ETT.
- Forward genetic screens are useful tools for the discovery of parthenocarpy conferring mutations.

7.2.1 DELLA-independent GA-signalling during fruit development

DELLA proteins are negative regulators of GA responses and central to the GA-signalling pathway. The role of DELLA proteins as fruit growth repressors has previously been characterised and, thus, lack of DELLA proteins results in facultative parthenocarpic fruit development (Marti et al, 2007; Ross et al, 2008; Dorcey et al, 2009; see Chapter 3). Lack of all functional *DELLA* genes in emasculated *Arabidopsis* *global-DELLA* mutant results in parthenocarpic pistil development; however, these pistils are significantly shorter than pollinated *global-DELLA* and wild-type pistils (see Chapter 3), suggesting that additional hormonal cues are required to promote fruit development. This hypothesis was tested by application of different hormones to emasculated *global-DELLA* and *ga1-3 global-*

DELLA and, surprisingly, application of GA₃ resulted in further pistil growth promotion (see Chapter 3). These results uncovered the existence of a DELLA-independent GA-signalling pathway during fruit development. Based on the disparity between the growth promotion caused by lack of DELLA proteins compared to the growth promotion observed in GA₃-treated *global-DELLA* and *ga1-3 global-DELLA* pistils (see Chapter 3), it is clear that the core of GA-signalling during fruit development relies on DELLA proteins with DELLA-independent GA-signalling playing a more fine-tuning role.

The existence of a DELLA-independent GA-signalling pathway during fruit development may imply that DELLA-independent GA signalling may also be relevant during additional aspects of plant development. On the other hand, the possibility that DELLA-independent GA-signalling may only be observed during fruit development cannot be excluded either. While this study was in progress, the possible existence of a DELLA-independent GA-response pathway during stem elongation was published (Maymon et al, 2009). This hypothesis is based in the following observations: unlike *spy-4* mutants, *quadruple-DELLA* mutants are sensitive to cytokinin-mediated stem-length reduction, suggesting that SPY does not act via DELLAs to promote cytokinin responses and, in addition, treatment of *quadruple-DELLA* with both GA and cytokinin results in GA-mediated suppression of cytokinin effects in stem elongation (Maymon et al, 2009). However, the GA treatment alone of *quadruple-DELLA* mutants did not promote stem elongation, suggesting that the reported GA response does not represent a direct response (Maymon et al, 2009). Furthermore, the use of *quadruple-DELLA* mutant plants in which the fifth DELLA protein RGL3 is still functional, makes it impossible to rule out a possible role of RGL3 in the observed response. Thus, further and extensive research in a *global-DELLA* or *ga1-3 global-DELLA* mutant background would undoubtedly be required to determine, beyond doubt, whether or not DELLA-independent GA-signalling is limited to fruit development.

Initial characterisation of the DELLA-independent GA-signalling pathway has shown that like DELLA-dependent GA responses, DELLA-independent GA responses also rely on GID1-mediated GA perception (see Chapter 5). These results together with previous studies (Griffiths et al, 2006; Luchi et al, 2007)

suggest that GID1A, GID1B and GID1C may be the only GA-receptors in Arabidopsis. It has long been hypothesised, based on experiments carried out in the aleurone layer of cereal seeds (Hooley et al, 1991; Gilroy and Jones, 1994), that plants have both membrane-bound and soluble GA-receptors. Nevertheless to date, only soluble GA-receptors have been identified (Ueguchi-Tanaka et al, 2005; Griffiths et al, 2006; Nakajima et al, 2006; Luchi et al, 2007; Chandler et al, 2008) and further experimental research would be required to solve this conundrum.

Two further components of the DELLA-independent GA-signalling pathway have also been identified during the course of this investigation, SPT and the 26S proteasome. 26S proteasome-mediated DELLA protein degradation was also shown to be central to most DELLA-dependent GA responses (McGinnis et al., 2003; Sasaki et al., 2003; Dill et al., 2004; Fu et al., 2004; Feng et al., 2008). However, the protein/s targeted for 26s proteasome-mediated degradation during DELLA-independent responses remain to be identified. Although SPT plays a growth repression function during DELLA-independent GA responses in fruit development, unlike DELLA proteins, it is not likely to be degraded through the 26s proteasome in the presence of GA as no SPT degradation was observed upon GA application (see Chapter 3). Moreover, SPT was found not to interact with GID1a in yeast even in the presence of GA.

7.2.2 DELLA protein interaction with transcription factors involved in fruit development

Several studies have shown that DELLA proteins' transcriptional regulating capacity relies on their ability to impair other transcription factors action by binding to their DNA-binding domain (de Lucas et al, 2008; Feng et al, 2008). DELLA proteins are able to interact with key bHLH regulators of fruit development such as ALC and SPT (see Chapter 4). Furthermore, the biological relevance of DELLA-ALC interaction has recently been confirmed in another study (Arnaud et al, *in press*).

The bHLH transcription-factor family is formed by approximately 162 members in *Arabidopsis* (Bailey et al, 2003; Toledo-Ortiz et al, 2003). Even if DELLA proteins' interaction capacity was limited to this extensive family of transcription factors, this would allow a considerable number of possible combinations and, thus, could explain the great variety of GA responses. However, as shown in this study, DELLA proteins are not able to interact with all bHLH transcription factors (see Chapter 4). Furthermore, DELLAs' interaction capacity is not only limited to certain members of the bHLH transcription-factors family but can interact with non-bHLH transcription factors such as ETT/ARF3 (see Chapter 4).

7.2.3 Forward genetic screens as discovery tools in parthenocarpy studies

Forward genetic screens have commonly been used for the identification of new molecular players responsible for the phenotype being investigated. In this thesis, an EMS forward screen in heterozygous *pistillata-1* (*pi-1*) background was successfully used for the isolation of parthenocarpy-conferring mutations (see Chapter 5). These results together with previous forward genetic screens in *pi-1* mutant background confirmed that forward screens can successfully be used for the isolation of fertilisation-independent fruit development mutants (Chaudhury et al, 1997; Vivian-Smith et al, 2001). During the course of this study, 29 putative fertilisation-independent mutants were isolated, two of which were confirmed and partially characterised (see Chapter 5). Furthermore, preliminary mapping results of 117.1 mutation suggest that this might be a novel parthenocarpy conferring mutation (see Chapter 5).

7.3 Questions and future work

7.3.1. DELLA-independent GA pathway

Initial characterisation of the DELLA-independent GA-signalling pathway during fruit development has shown that additional molecular players are likely to play a

role in this newly discovered pathway (see Chapter 3). Based on the previously described GID1-mediated GA perception mechanism, DELLA-independent GA-perception is likely to depend on a GID1-binding protein. A yeast two-hybrid screen in the presence of GA with GID1A receptor as bait could be used for the identification of such protein/s. In addition, although SPT has been identified as a growth repressing factor in this pathway (see Chapter 3) which genes are affected by SPT transcriptional repression remain unknown. Transcriptome analysis of emasculated *global-DELLA* pistils and emasculated and GA-treated *global-DELLA* pistils could be used to identify downstream components of the DELLA-independent GA-signalling pathway during fruit development.

Another key question regarding DELLA-independent GA-signalling pathway concerns its possible role in additional developmental programmes. Compared to DELLA-dependent GA signalling, DELLA-independent GA signalling plays a minor role in fruit development; consequently, the possible role of DELLA-independent GA signalling in additional aspects of plant development is also likely to be of a fine-tuning nature. Thus, careful quantitative growth assays of GA-treated *global-DELLA* and/or *ga1-3 global-DELLA* plants would be required to test whether DELLA-independent GA signalling is limited to pistil development.

7.3.2 Tissue-specific GA signal attenuation

Previous studies have shown that DELLA-dependent GA signalling in the endodermis is the rate-limiting factor during GA-mediated root elongation (Ubeda-Tomas et al, 2008). On the other hand, preliminary histological analyses in *global-DELLA* and *ga1-3 global-DELLA* pistils have suggested that the exocarp might be the primary GA-responsive tissue during fruit development (see Chapter 3). In order to test this hypothesis, exocarp-specific attenuation of GA signalling would be necessary. Characterisation of *ML1* expression pattern has shown that expression of *GAI-1* (resistant to GA-mediated degradation) under the control of *ML1* promoter could be used to this end. In addition, the use of an inducible system such as the glucocorticoid receptor-mediated induction system (Aoyama and Chua, 1997) would ensure a temporal control of *GAI-1* action and provide

additional information regarding the timing of GA-signalling response during fruit development.

7.3.3 Forward genetic screens and parthenocarpic mutant characterisation

Three phytohormones, gibberellins, auxins and cytokinins, are believed to be the main fruit growth regulators upon ovule fertilisation (King, 1947; Srinivasan et al, 1996; Vivian-Smith and Koltunow, 1999; Ozga et al, 2002; Ozga et al, 2003). However to date, only molecular players involved in gibberellins- or auxin-related fruit growth regulation have been isolated (Vivian-Smith et al, 2001; Okushima et al, 2005; Goetz et al, 2006; Schruff et al, 2006; Wu et al, 2006; Goetz et al, 2007; Marti et al, 2007; Dorcey et al, 2009;) and, therefore, the role of cytokinins remains very poorly understood. The EMS population created during this thesis could provide a useful resource for the isolation of molecular players that could improve our understanding of the hormonal control of fruit initiation and/or development.

Characterisation of newly isolated mutants will require allelism tests with other available parthenocarpic mutants, detailed histological analysis and hormone-treatment experiments. Later cloning of the identified mutations would allow the integration of the newly discovered molecular players in the different hormonal pathways involved in fruit initiation and/or development as well as in-depth characterisation of their expression pattern throughout the different stages of fruit development. It is possible that *in situ* analysis would shed light on their possible role during ovule and seed morphogenesis.

7.3.4 Seed-pod communication

Successful fruit development requires the coordinated development of both ovary and seed structures. Nevertheless, many questions remain regarding the coordination of these two distinct developmental programmes. Is seed-pod communication necessary during all stages of fruit development? Seeds have

shown to be the origin of auxin and gibberellins signals required for fruit development (Dorcey et al, 2009) but is this seed-pod communication unidirectional or does hormone synthesis in the fruit also impact in seed development? In order to answer these and other questions, funiculus-specific cell ablation could be pursued. Although initial attempts to identify funiculus-specific promoters was unsuccessful during this study, a novel three component gene-expression system could be developed which would allow the tissue-specific gene expression in the overlapping expression areas of two promoters (see Chapter 6).

7.3.5 *PAP10*

Isolation of targeted sequences with funiculus-specific expression resulted in the isolation of *PAP10* (see Chapter 6). Initial characterisation of this gene coding a PURPLE ACID PHOSPHATASE has shown that the *PAP10* gene has a complex expression pattern throughout plant development (see Chapter 6). However, further characterisation of the biological function of *PAP10* is required.

Three *pap10* mutant alleles were isolated during the course of this investigation but none of the mutant alleles showed any developmental phenotypes. Similarly, double mutants with a closely related purple acid phosphatase, *PAP12*, did not show any developmental phenotypes (see Chapter 6). PAPs have traditionally been associated with phosphate acquisition and/or mobilisation (Veijanovski et al, 2006; Kuang et al, 2009; Hur et al, 2010, Hurley et al, 2010) and *PAP10* may also be involved in phosphate acquisition and/or mobilisation. In accordance with this, *PAP12* and *PAP26*, two closely related PAPs, have been proposed to play a role in inorganic phosphate mobilisation during nutritional phosphate deprivation (Veijanovski et al, 2006; Hue et al, 2010; Hurley et al, 2010). Thus, it is possible that a role of *PAP10* in phosphate acquisition and/or mobilisation may be uncovered by assessing the growth and development of *pap10* mutant plants grown under deficient Pi conditions. Alternatively, it is also possible that due to functional redundancy, construction of multiple *pap* mutants may be required to uncover the biological function of *PAP10*.

Finally, whether the changes in GUS expression in roots in response to various stimuli are of any biological relevance would also need to be determined (see Chapter 6). After confirming the observed GUS expression changes by quantitative measurements of GUS activity that monitor cleavage of the β -glucuronidase substrate 4-methylumbelliferyl β -D-glucuronide (MUG) (Jefferson et al, 1987; Gallagher, 1992), preliminary assessment of the possible altered growth of *pap10* mutants in response to various stimuli could be carried out.

7.4 Concluding remarks: Parthenocarpy in the context of crop improvement

Parthenocarpic fruit development is a desirable trait in many crop plants. Seedless fruit provide an attractive alternative not only to consumers but often also to breeders, particularly when pollination and/or fertilisation are limiting factors. Several approaches have been taken for the development of parthenocarpic fruits which include amongst others breeding for genetic parthenocarpy (Robinson et al, 1999; Varoquaux et al, 2000), exogenous application of plant growth regulators (Rotino et al, 1997) and transgenic parthenocarpy (Rotino et al, 1997; Ficcadenti et al, 1999; Mezzetti et al, 2004). At present, the widespread use of transgenic parthenocarpy is limited due to the low public acceptance of transgenic plants and, thus, different genetic approaches are required if the interest for parthenocarpic fruit development is to be satisfied.

The study of fruit initiation and development in the model species *Arabidopsis* provides an excellent stepping stone towards future parthenocarpic crop improvement. Most horticulturally relevant fruits are fleshy fruits and, thus, the study of other model species such as tomato may also be necessary. Nevertheless, it is interesting to note that dry and fleshy fruit developmental programmes are likely to share certain common steps. This is for example true in the case of *ARF8* which has been shown to control both *Arabidopsis* and tomato fruit set (Goetz et al, 2007).

Undoubtedly, the better understanding of the hormonal and genetic mechanisms involved in fruit initiation and growth upon ovule fertilisation could greatly contribute to the discovery and commercial use of genes involved in parthenocarpy.

APPENDIX 1

Tables and Statistics

APPENDIX 1

Tables and Statistics

In this appendix a compilation of the tables and statistics carried out as part of this thesis are presented.

Chapter 3: Fruit development and DELLAs

Table 3.1 PCR primers used during Chapter 3.

Name	Type	Primer sequence (5'-3')
GAI	F qRT-PCR	CACACGACCGCTCATAG
GAI	R qRT-PCR	TGCCTATCCAATTTACCCCTC
RGA	F qRT-PCR	AGAAGCAATCCAGCAGA
RGA	R qRT-PCR	GTGTACTCTCTTACCTTC
RGL1	F qRT-PCR	CATCAATGACGACGGT
RGL1	R qRT-PCR	GTACTCTGAGTCAGGCTT
RGL2	F qRT-PCR	GGATAACGGAGAAACATGGGATCC
RGL2	R qRT-PCR	CCTCTTCTATCCACACAACCTCGG
RGL3	F qRT-PCR	CAATGATATTGCCTCTTAG
RGL3	R qRT-PCR	CTGAGTCACACCAAGGA
UBC9	F qRT-PCR	CTTCTCTCCGTTTACCAACC
UBC9	R qRT-PCR	CCAAATTCCAATTGAAGACTCTGC
UBC10	F qRT-PCR	GGGCTAAATGGAAAATCCCACC
UBC10	R qRT-PCR	CGTAGCAACTCATCACACAAACG
TUB8	F qRT-PCR	CGTGGATCACAGCAATACAGAGCC
TUB8	R qRT-PCR	CCTCCTGCACTTCACTTCGCTTTC
GAI	F Yeast two-hybrid	AAAACCCGGGCATGAAGAGAGATCATCATCATC
GAI	R Yeast two-hybrid	ATTGCTGCAGCATCTAATTGGTGG
RGA	F Yeast two-hybrid	ATAGCCCCGGAATGAAGAGAGATCATCACC
RGA	R Yeast two-hybrid	TCGACTGCACCTCAGTACGCCGCCGTG
SPT	F Yeast two-hybrid	TTGTCGGGAATGATATCACAGAGAGAAGAAAG
SPT	R Yeast two-hybrid	GGGACTGCAGTCAGTAATTGATCTTAGGTC
SF00156	F ML1 promoter cloning	GCATAAGCTGCATATGCAAATGCAGGGTCG
SF00157	R ML1 promoter cloning	GATGGGATCCGATGATGGATGCCTATC
SF00189	ML1 specific primer to check ML1::GUS presence	CGACCCTGCATTGCATATGC
SF00164	F ACI1 promoter cloning	AGAAAAGCTTAGTGGCAAATCTGGTAAT
SF00165	R ACI1 promoter cloning	GTTGGGATCCGGTATGGCTGATAATGA
SF00191	ACI1 specific primer to check ACI1::GUS presence	ATTACCAGATTGCCACT
SF00171	GUS specific primer to check promoter::GUS presence	GGAAACAGCTATGACCATGATTACG

Appendix figure 3.1 Statistical analysis of the parthenocarpy conferring capacity of the different *della* mutant combinations. (A) Emasculated *della* mutants in Ler background. (B) Hand pollinated *della* mutants in Ler background. Probability values are indicated and values significantly different are represented by asterisks (* for P<0.05, ** for P<0.01 and *** for P < 0.001). S= Selfed, P= Hand pollinated.

(A)

	Ler E	rga E	rgl1 E	rgl2 E	rgl3 E	gairga E	gairgl1 E	gairgl2 E	quad-DELLA E	global E	ga1-3 global E
Ler E											
rga E	0.988										
rgl1 E	<0.001 (***)	<0.001 (****)									
rgl2 E	0.174	0.131	<0.001 (***)								
rgl3 E	0.260	0.218	<0.001 (***)	0.904							
gairga E	0.002 (**)	0.002 (**)	0.127	0.001 (**)	0.001 (**)						
gairgl1 E	<0.001 (***)	<0.001 (***)	0.573	<0.001 (***)	<0.001 (***)	0.204					
gairgl2 E	<0.001 (***)	0.001 (**)	0.424	<0.001 (***)	<0.001 (***)	0.359	0.728				
quad-DELLA E	<0.001 (***)	<0.001 (***)	<0.001 (***)	<0.001 (***)	<0.001 (***)	<0.001 (***)	<0.001 (***)	<0.001 (***)	<0.001 (***)		
global E	<0.001 (***)	<0.001 (***)	<0.001 (***)	<0.001 (***)	<0.001 (***)	<0.001 (***)	<0.001 (***)	<0.001 (***)	0.394		
ga1-3 global E	<0.001 (***)	<0.001 (***)	<0.001 (***)	<0.001 (***)	<0.001 (***)	<0.001 (***)	<0.001 (***)	<0.001 (***)	0.003 (**)	0.006 (**)	

(B)

	Ler P	rga P	rgl1 P	rgl2 P	rgl3 P	gairga P	gairgl1 P	gairgl2 P	quad-DELLA P	global P	ga1-3 global P
Ler P											
rga P	<0.001 (***)										
rgl1 P	0.075	<0.001 (***)									
rgl2 P	<0.001 (***)	0.023 (*)	<0.001 (***)								
rgl3 P	<0.001 (***)	0.092	<0.001 (***)	0.817							
gairga P	0.023 (*)	0.275	0.001 (**)	0.006 (**)	0.015						
gairgl1 P	0.105	<0.001 (***)	0.711	<0.001 (***)	<0.001 (***)	0.001 (**)					
gairgl2 P	0.002 (**)	0.200	<0.001 (***)	<0.001 (***)	0.004 (**)	0.993	<0.001 (***)				
quad-DELLA P	<0.001 (***)	0.106	<0.001 (***)	0.839	0.749	0.031 (*)	<0.001 (***)	0.008 (**)			
global P	<0.001 (***)	0.064	<0.001 (***)	0.86	0.951	0.007 (**)	<0.001 (***)	0.001 (**)	0.774		
ga1-3 global P	<0.001 (***)	0.010 (*)	<0.001 (***)	0.274	0.341	0.002 (**)	<0.001 (***)	<0.001 (***)	0.665	0.313	

Appendix figure 3.2 Continuation of the statistical analysis of the parthenocarpy conferring capacity of the different *della* mutant combinations. (A) Emasculated *della* mutants in Col-0 background. (B) Hand pollinated *della* mutants in Col-0 background. (C) Emasculated *della* mutants in *tt1* mutant background. (D) Hand pollinated *della* mutants in *tt1* mutant background. Probability values are indicated and values significantly different are represented by asterisks (* for P<0.05, ** for P<0.01 and *** for P < 0.001). S= Selfed, P= Hand pollinated.

(A)

	Col E	<i>rgl1/2</i> E	<i>rgl1/3</i> E	<i>rgl2/3</i> E
Col E				
<i>rgl1/2</i> E	0.010 (*)			
<i>rgl1/3</i> E	0.001 (**) <0.001 (***)			
<i>rgl2/3</i> E	<0.001 (***)	<0.001 (***)	0.166	

(B)

	Col P	<i>rgl1/2</i> P	<i>rgl1/3</i> P	<i>rgl2/3</i> P
Col P				
<i>rgl1/2</i> P	<0.001 (***)			
<i>rgl1/3</i> P	<0.001 (***)	0.996		
<i>rgl2/3</i> P	<0.001 (***)	0.095	0.002 (**) <0.001 (***)	

(C)

	<i>tt1</i> E	<i>gai</i> E	<i>gairga</i> E	<i>gairgl1</i> E	<i>gairgl2</i> E	<i>quad-DELLA</i> E	<i>global</i> E	<i>ga1-3 global</i> E
<i>tt1</i> E								
<i>gai</i> E	0.724							
<i>gairga</i> E	0.768	0.592						
<i>gairgl1</i> E	0.133	0.192	0.204					
<i>gairgl2</i> E	0.368	0.550	0.359	0.728				
<i>quad-DELLA</i> E	<0.001 (***)	<0.001 (***)	<0.001 (***)	<0.001 (***)	<0.001 (***)			
<i>global</i> E	<0.001 (***)	<0.001 (***)	<0.001 (***)	<0.001 (***)	<0.001 (***)	0.394		
<i>ga1-3 global</i> E	<0.001 (***)	<0.001 (***)	<0.001 (***)	<0.001 (***)	<0.001 (***)	0.003 (**) <0.001 (***)	0.006 (**) <0.001 (***)	

(D)

	<i>tt1</i> P	<i>gai</i> P	<i>gairga</i> P	<i>gairgl1</i> P	<i>gairgl2</i> P	<i>quad-DELLA</i> P	<i>global</i> P	<i>ga1-3 global</i> P
<i>tt1</i> P								
<i>gai</i> P	0.151							
<i>gairga</i> P	0.001 (**) <0.001 (***)							
<i>gairgl1</i> P	0.853	0.226	0.001 (**) <0.001 (***)					
<i>gairgl2</i> P	<0.001 (***)	<0.001 (***)	0.993	<0.001 (***)				
<i>quad-DELLA</i> P	<0.001 (***)	<0.001 (***)	0.031 (*) <0.001 (***)	<0.001 (***)	0.008 (**) <0.001 (***)			
<i>global</i> P	<0.001 (***)	<0.001 (***)	0.007 (**) <0.001 (***)	<0.001 (***)	0.001 (**) <0.001 (***)	0.774 <0.001 (***)		
<i>ga1-3 global</i> P	<0.001 (***)	<0.001 (***)	0.002 (**) <0.001 (***)	<0.001 (***)	<0.001 (***)	0.665 <0.001 (***)	0.313 <0.001 (***)	

		WILD TYPE									
		EXOCARP			MESOCARP1			MESOCARP2			
		C	10GA	P	C	10GA	P	C	10GA	P	
WILD TYPE	EXOCARP	C									
		10GA	0.040								
		P	<0.001	0.064							
	MESOCARP1	C	0.008	0.002	<0.001						
		10GA	0.016	0.007	<0.001	0.002					
		P	0.021	<0.001	<0.001	<0.001	0.957				
	MESOCARP2	C	0.011	0.002	<0.001	0.177	0.052	0.019			
		10GA	0.023	0.007	<0.001	0.003	0.519	0.394	0.035		
		P	0.027	0.028	<0.001	0.002	0.446	0.267	0.019	0.872	
	MESOCARP3	C	0.004	0.025	<0.001	0.072	0.163	0.089	0.563	0.091	0.053
		10GA	0.408	0.036	<0.001	<0.001	0.008	<0.001	0.001	0.017	0.002
		P	0.191	0.034	<0.001	<0.001	<0.001	<0.001	<0.001	0.002	<0.001
ga1-3 global	ENDOCARP	C	0.006	0.026	<0.001	0.015	0.582	0.520	0.169	0.301	0.211
		10GA	0.372	0.036	<0.001	<0.001	0.001	<0.001	<0.001	0.004	0.001
		P	0.086	0.035	<0.001	<0.001	<0.001	<0.001	<0.001	0.001	<0.001
	EXOCARP	C	<0.001	0.202	0.694	<0.001	<0.001	<0.001	<0.001	<0.001	<0.001
		10GA	<0.001	0.505	0.106	<0.001	<0.001	<0.001	<0.001	<0.001	<0.001
		P	<0.001	0.303	0.579	0.002	<0.001	0.002	0.001	<0.001	<0.001
	MESOCARP1	C	0.014	0.026	<0.001	0.007	0.055	0.051	0.375	0.094	0.042
		10GA	0.018	0.026	<0.001	0.001	0.423	0.361	0.062	0.142	0.086
		P	0.025	0.026	<0.001	0.076	0.336	0.253	0.474	0.225	0.167
	MESOCARP2	C	0.017	0.026	<0.001	0.001	0.223	0.266	0.011	0.198	0.123
		10GA	0.019	0.027	<0.001	0.005	0.780	0.749	0.077	0.364	0.215
		P	0.031	0.026	<0.001	0.032	0.690	0.651	0.233	0.430	0.344
	MESOCARP3	C	0.021	0.028	<0.001	0.014	0.290	0.265	0.035	0.622	0.661
		10GA	0.047	0.030	<0.001	<0.001	0.047	0.007	0.001	0.177	0.157
		P	0.098	0.030	<0.001	<0.001	0.074	0.019	0.008	0.229	0.245
	ENDOCARP	C	0.092	0.033	<0.001	<0.001	0.006	<0.001	<0.001	0.024	0.011
		10GA	0.292	0.036	<0.001	<0.001	<0.001	<0.001	<0.001	<0.001	<0.001
		P	0.175	0.033	<0.001	<0.001	0.004	<0.001	<0.001	0.024	0.022

Appendix figure 3.3 Statistical analysis of cell length in Ler, global-DELLA and ga1-3 global-DELLA pistil sections.

Probability values are indicated and those values mentioned throughout the text are shown in red. Values <0.05 are statistically significant.

			WILD TYPE					
			MESOCARP3			ENDOCARP		
			C	10GA	P	C	10GA	P
WILD TYPE	EXOCARP	C						
		10GA						
		P						
	MESOCARP1	C						
		10GA						
		P						
	MESOCARP2	C						
		10GA						
		P						
	MESOCARP3	C						
		10GA	0.002					
		P	<0.001	0.399				
<i>ga1-3 global</i>	ENDOCARP	C	0.405	0.003	<0.001			
		10GA	<0.001	0.975	0.339	0.001		
		P	<0.001	0.506	0.715	<0.001	0.445	
	EXOCARP	C	<0.001	<0.001	<0.001	<0.001	<0.001	<0.001
		10GA	<0.001	<0.001	<0.001	<0.001	<0.001	<0.001
		P	<0.001	<0.001	<0.001	<0.001	<0.001	<0.001
	MESOCARP1	C	0.916	0.001	<0.001	0.338	<0.001	<0.001
		10GA	0.259	<0.001	<0.001	0.977	<0.001	<0.001
		P	0.815	0.014	0.001	0.645	0.003	<0.001
	MESOCARP2	C	0.375	0.001	<0.001	0.829	<0.001	<0.001
		10GA	0.228	<0.001	<0.001	0.767	<0.001	<0.001
		P	0.461	0.020	0.001	0.953	0.005	<0.001
	MESOCARP3	C	0.050	0.028	0.006	0.172	0.012	0.002
		10GA	0.003	0.009	0.003	0.015	0.003	0.001
		P	0.017	0.112	0.055	0.048	0.045	0.024
	ENDOCARP	C	0.001	0.213	0.327	0.003	0.127	0.179
		10GA	<0.001	0.872	0.190	<0.001	0.773	0.335
		P	0.001	0.254	0.329	0.002	0.102	0.030

			global								
			EXOCARP			MESOCARP1			MESOCARP2		
			C	10GA	P	C	10GA	P	C	10GA	P
WILD TYPE	EXOCARP	C	0.001	0.002	<0.001	0.017	0.017	0.017	0.024	0.026	0.025
		10GA	0.295	0.564	0.502	0.026	0.026	0.026	0.027	0.028	0.028
		P	0.615	0.151	0.086	<0.001	<0.001	<0.001	<0.001	<0.001	<0.001
	MESOCARP1	C	0.001	0.001	<0.001	0.002	<0.001	<0.001	<0.001	<0.001	<0.001
		10GA	0.001	0.001	<0.001	0.242	0.285	0.259	0.529	0.395	0.452
		P	0.001	0.001	<0.001	0.248	0.302	0.209	0.508	0.371	0.347
	MESOCARP2	C	0.001	0.001	<0.001	0.125	0.100	0.072	0.016	0.006	0.002
		10GA	0.001	0.001	<0.001	0.123	0.140	0.081	0.725	0.846	0.748
		P	0.001	0.001	<0.001	0.116	0.133	0.053	0.591	0.700	0.578
	MESOCARP3	C	0.001	0.001	<0.001	0.426	0.363	0.322	0.058	0.045	0.014
		10GA	<0.001	0.002	<0.001	0.002	0.002	0.018	0.029	0.004	0.029
		P	0.001	0.002	<0.001	<0.001	<0.001	<0.001	<0.001	<0.001	<0.001
<i>ga1-3 global</i>	ENDOCARP	C	0.001	0.001	<0.001	0.775	0.857	0.795	0.265	0.206	0.160
		10GA	0.001	0.002	<0.001	<0.001	<0.001	<0.001	<0.001	<0.001	<0.001
		P	0.001	0.002	<0.001	<0.001	<0.001	<0.001	<0.001	<0.001	<0.001
	EXOCARP	C	0.381	0.098	0.081	<0.001	<0.001	<0.001	<0.001	<0.001	<0.001
		10GA	0.349	0.867	0.998	<0.001	<0.001	<0.001	<0.001	<0.001	<0.001
		P	0.928	0.277	0.425	0.002	0.002	0.002	0.003	0.003	0.003
	MESOCARP1	C	0.001	0.001	<0.001	0.246	0.173	0.246	0.002	0.001	0.003
		10GA	0.001	0.001	<0.001	0.718	0.831	0.754	0.117	0.077	0.054
		P	0.001	0.001	<0.001	0.698	0.624	0.620	0.277	0.091	0.064
	MESOCARP2	C	0.001	0.001	<0.001	0.878	0.949	0.978	0.008	0.007	0.009
		10GA	0.001	0.001	<0.001	0.532	0.602	0.486	0.324	0.344	0.275
		P	0.001	0.001	<0.001	0.742	0.811	0.756	0.364	0.299	0.266
	MESOCARP3	C	0.001	0.001	<0.001	0.118	0.129	0.124	0.387	0.453	0.433
		10GA	0.001	0.002	<0.001	0.005	0.006	0.001	0.047	0.066	0.019
		P	0.001	0.002	<0.001	0.012	0.013	0.003	0.185	0.205	0.025
	ENDOCARP	C	0.001	0.002	<0.001	0.001	0.004	<0.001	0.010	0.011	0.010
		10GA	0.002	0.002	<0.001	<0.001	<0.001	<0.001	<0.001	<0.001	<0.001
		P	0.001	0.002	<0.001	<0.001	<0.001	<0.001	<0.001	<0.001	<0.001

		global						
		MESOCARP3			ENDOCARP			
		C	10GA	P	C	10GA	P	
WILD TYPE	EXOCARP	C	0.108	0.114	0.095	0.627	0.252	0.026
		10GA	0.032	0.033	0.032	0.039	0.036	0.033
		P	<0.001	<0.001	<0.001	<0.001	<0.001	<0.001
	MESOCARP1	C	0.001	<0.001	<0.001	<0.001	<0.001	<0.001
		10GA	0.034	0.003	<0.001	<0.001	<0.001	<0.001
		P	0.003	<0.001	<0.001	<0.001	<0.001	<0.001
	MESOCARP2	C	0.003	<0.001	<0.001	<0.001	<0.001	<0.001
		10GA	0.076	0.013	0.001	0.002	0.002	0.001
		P	0.029	0.005	0.001	<0.001	<0.001	<0.001
	MESOCARP3	C	0.006	<0.001	<0.001	<0.001	<0.001	<0.001
		10GA	0.281	0.287	0.182	0.482	0.784	0.114
		P	0.391	0.523	0.061	0.049	0.476	0.291
<i>ga1-3 global</i>	ENDOCARP	C	0.014	0.001	<0.001	<0.001	<0.001	<0.001
		10GA	0.222	0.187	0.007	0.378	0.750	0.054
		P	0.254	0.319	0.014	0.063	0.649	0.126
	EXOCARP	C	<0.001	<0.001	<0.001	<0.001	<0.001	<0.001
		10GA	<0.001	<0.001	<0.001	<0.001	<0.001	<0.001
		P	<0.001	<0.001	0.003	<0.001	<0.001	0.003
	MESOCARP1	C	0.004	<0.001	<0.001	<0.001	<0.001	<0.001
		10GA	0.001	<0.001	<0.001	<0.001	<0.001	<0.001
		P	0.034	0.005	<0.001	0.002	0.001	<0.001
	MESOCARP2	C	0.021	<0.001	<0.001	0.001	<0.001	<0.001
		10GA	0.003	<0.001	<0.001	<0.001	<0.001	<0.001
		P	0.055	0.009	<0.001	0.003	0.002	0.001
	MESOCARP3	C	0.147	0.046	0.089	0.003	0.008	0.044
		10GA	0.149	0.036	0.035	<0.001	0.002	0.010
		P	0.431	0.174	0.151	<0.001	0.033	0.084
	ENDOCARP	C	0.977	0.742	0.616	0.031	0.144	0.792
		10GA	0.188	0.034	<0.001	0.216	0.779	0.003
		P	0.986	0.672	0.607	0.046	0.104	0.707

		global								
		EXOCARP			MESOCARP1			MESOCARP2		
		C	10GA	P	C	10GA	P	C	10GA	P
global	EXOCARP	C								
		10GA	0.294							
		P	0.312	0.857						
	MESOCARP1	C	0.001	0.001	<0.001					
		10GA	0.001	0.001	<0.001	0.853				
		P	0.001	0.001	<0.001	0.921	0.944			
	MESOCARP2	C	0.001	0.002	<0.001	0.022	0.026	0.018		
		10GA	0.001	0.002	<0.001	0.016	0.019	0.026	0.667	
		P	0.001	0.002	<0.001	0.026	0.034	0.019	0.795	0.915
	MESOCARP3	C	0.001	0.002	<0.001	0.007	0.008	0.020	0.045	0.027
		10GA	0.001	0.002	<0.001	<0.001	<0.001	0.002	0.001	0.001
		P	0.001	0.002	<0.001	<0.001	<0.001	<0.001	<0.001	<0.001
	ENDOCARP	C	0.002	0.002	<0.001	<0.001	<0.001	<0.001	0.002	0.002
		10GA	0.001	0.002	<0.001	<0.001	<0.001	<0.001	<0.001	0.001
		P	0.001	0.002	<0.001	<0.001	<0.001	<0.001	<0.001	<0.001
		MESOCARP3			ENDOCARP					
global	EXOCARP	C								
		10GA								
		P								
	MESOCARP1	C								
		10GA								
		P								
	MESOCARP2	C								
		10GA								
		P								
	MESOCARP3	C								
		10GA	0.777							
		P	0.745	0.302						
	ENDOCARP	C	0.061	0.045	0.020					
		10GA	0.244	0.228	0.008	0.209				
		P	0.805	0.849	0.279	0.005	0.075			

			<i>ga1-3 glohal</i>									
			EXOCARP			MESOCARP1			MESOCARP2			
			C	10GA	P	C	10GA	P	C	10GA	P	
<i>ga1-3 glohal</i>	EXOCARP	C										
		10GA	0.107									
		P	0.218	0.468								
	MESOCARP1	C	<0.001	<0.001	0.002							
		10GA	<0.001	<0.001	0.002	0.198						
		P	<0.001	<0.001	<0.001	0.815	0.527					
	MESOCARP2	C	<0.001	<0.001	0.003	0.126	0.788	0.725				
		10GA	<0.001	<0.001	<0.001	0.201	0.662	0.460	0.467			
		P	<0.001	<0.001	<0.001	0.362	0.914	0.677	0.777	0.862		
	MESOCARP3	C	<0.001	<0.001	<0.001	0.043	0.149	0.172	0.125	0.147	0.298	
		10GA	<0.001	<0.001	<0.001	0.001	0.001	0.020	0.005	0.008	0.053	
		P	<0.001	<0.001	<0.001	0.067	0.006	0.071	0.097	0.033	0.123	
	ENDOCARP	C	<0.001	<0.001	<0.001	0.002	<0.001	0.008	0.004	0.001	0.016	
		10GA	<0.001	<0.001	0.004	<0.001	<0.001	<0.001	<0.001	<0.001	<0.001	
		P	<0.001	0.001	0.004	<0.001	<0.001	0.006	<0.001	<0.001	0.012	
			MESOCARP3			ENDOCARP						
<i>ga1-3 glohal</i>	EXOCARP	C										
		10GA										
		P										
	MESOCARP1	C										
		10GA										
		P										
	MESOCARP2	C										
		10GA										
		P										
	MESOCARP3	C										
		10GA	0.493									
		P	0.528	0.809								
	ENDOCARP	C	0.079	0.078	0.278							
		10GA	0.009	<0.001	<0.001	0.076						
		P	0.065	0.106	0.280	0.931	0.051					

			WILD TYPE								
			EXOCARP			MESOCARP1			MESOCARP2		
			C	10GA	P	C	10GA	P	C	10GA	P
WILD TYPE	EXOCARP	C									
		10GA	0.4567								
		P	0.0604	0.0211							
	MESOCARP1	C	0.001	0.0007	0.0046						
		10GA	<0.0001	<0.0001	<0.0001	0.0016					
		P	<0.0001	<0.0001	<0.0001	0.0004	0.0351				
	MESOCARP2	C	0.004	0.0024	0.0234	0.3269	0.0007	0.0002			
		10GA	0.0002	0.0008	<0.0001	0.007	0.5582	0.023	0.0031		
		P	0.0003	<0.0001	<0.0001	0.003	0.2121	0.4705	0.0017	0.1312	
	MESOCARP3	C	0.0056	0.0036	0.0496	0.1721	0.0005	0.0002	0.6733	0.0021	0.0013
		10GA	0.0011	0.0001	0.004	0.5605	0.004	0.0007	0.1653	0.0156	0.0049
		P	0.0001	<0.0001	<0.0001	0.0088	0.1035	0.0047	0.003	0.3463	0.0297
ga1-3 global	ENDOCARP	C	0.0072	0.0036	0.074	0.0597	0.0003	0.0001	0.3094	0.0011	0.0009
		10GA	0.0002	0.0001	0.0009	0.4684	0.0021	0.0004	0.1011	0.0105	0.0039
		P	<0.0001	<0.0001	<0.0001	0.0083	0.0672	0.0034	0.0027	0.2599	0.0297
	EXOCARP	C	0.6648	0.1912	0.048	0.0008	<0.0001	<0.0001	0.0034	0.0002	<0.0001
		10GA	0.8327	0.3188	0.0621	0.001	<0.0001	<0.0001	0.0039	0.0002	<0.0001
		P	0.4088	0.1371	0.0683	0.0009	<0.0001	<0.0001	0.0039	0.0002	<0.0001
	MESOCARP1	C	<0.0001	<0.0001	<0.0001	0.0004	0.6579	0.0428	0.0002	0.3193	0.2903
		10GA	<0.0001	<0.0001	<0.0001	0.0008	0.2065	0.2483	0.0005	0.1133	0.7886
		P	<0.0001	<0.0001	<0.0001	0.0047	0.2837	0.4339	0.0028	0.1749	0.9263
	MESOCARP2	C	<0.0001	<0.0001	<0.0001	0.0008	0.6611	0.0153	0.0003	0.7608	0.1298
		10GA	<0.0001	<0.0001	<0.0001	0.0043	0.5114	0.1734	0.0023	0.301	0.5525
		P	<0.0001	<0.0001	<0.0001	0.0062	0.5461	0.094	0.0034	0.3325	0.5617
	MESOCARP3	C	0.001	<0.0001	0.0024	0.0674	0.0906	0.006	0.0257	0.2388	0.0338
		10GA	0.0002	<0.0001	0.0004	0.0114	0.258	0.0109	0.0045	0.6078	0.0697
		P	0.0002	<0.0001	0.0005	0.0203	0.106	0.0055	0.0073	0.3113	0.0379
	ENDOCARP	C	0.0003	0.0002	0.001	0.3317	0.0035	0.0006	0.0758	0.016	0.005
		10GA	<0.0001	<0.0001	0.0001	0.1178	0.0032	0.0004	0.021	0.0182	0.0055
		P	<0.0001	<0.0001	<0.0001	0.0188	0.0076	0.0009	0.004	0.0467	0.0097

Appendix figure 3.4 Statistical analysis of cell number in Ler, global-DELLA and ga1-3 global-DELLA pistil sections.

Probability values are indicated and those values mentioned throughout the text are shown in red. Values <0.05 are statistically significant.

			WILD TYPE					
			MESOCARP3			ENDOCARP		
			C	10GA	P	C	10GA	P
WILD TYPE	EXOCARP	C						
		10GA						
		P						
	MESOCARP1	C						
		10GA						
		P						
	MESOCARP2	C						
		10GA						
		P						
	MESOCARP3	C						
		10GA	0.0893					
		P	0.0018	0.0266				
<i>ga1-3 global</i>	ENDOCARP	C	0.535	0.0345	0.0007			
		10GA	0.046	0.9527	0.0143	0.0131		
		P	0.0015	0.028	0.8234	0.0006	0.0135	
	EXOCARP	C	0.0047	0.001	<0.0001	0.0054	0.0001	<0.0001
		10GA	0.0055	0.0011	<0.0001	0.0069	0.0002	<0.0001
		P	0.0056	0.0011	<0.0001	0.0067	0.0001	<0.0001
	MESOCARP1	C	0.0001	0.0012	0.0338	0.0001	0.0005	0.0189
		10GA	0.0003	0.0017	0.0196	0.0002	0.001	0.0135
		P	0.0022	0.0076	0.0564	0.0015	0.0063	0.0452
	MESOCARP2	C	0.0002	0.0025	0.1171	0.0001	0.0009	0.0657
		10GA	0.0017	0.0076	0.0831	0.0011	0.0059	0.0635
		P	0.0026	0.0107	0.1035	0.0017	0.0086	0.0813
	MESOCARP3	C	0.0166	0.1433	0.608	0.0089	0.1187	0.6098
		10GA	0.0029	0.0274	0.677	0.0015	0.0182	0.54
		P	0.0044	0.0525	0.8593	0.0021	0.0352	0.6026
	ENDOCARP	C	0.0365	0.7584	0.0265	0.0117	0.7285	0.0271
		10GA	0.0088	0.4198	0.0291	0.0021	0.3093	0.0284
		P	0.0017	0.0946	0.1132	0.0004	0.0369	0.1281

			global								
			EXOCARP			MESOCARP1			MESOCARP2		
			C	10GA	P	C	10GA	P	C	10GA	P
WILD TYPE	EXOCARP	C	0.8427	0.7438	0.8704	<0.0001	<0.0001	<0.0001	<0.0001	<0.0001	<0.0001
		10GA	0.4898	0.6744	0.3229	<0.0001	<0.0001	<0.0001	<0.0001	<0.0001	<0.0001
		P	0.0263	0.0227	0.0496	<0.0001	<0.0001	<0.0001	<0.0001	<0.0001	<0.0001
	MESOCARP1	C	0.0007	0.0006	0.0009	0.0021	0.0003	0.0004	0.006	0.0009	0.0007
		10GA	<0.0001	<0.0001	<0.0001	0.6326	0.4879	0.1574	0.1156	0.4337	0.8299
		P	<0.0001	<0.0001	<0.0001	0.0108	0.0564	0.2309	0.0048	0.0103	0.0366
	MESOCARP2	C	0.0026	0.0024	0.0035	0.0009	0.0002	0.0002	0.0021	0.0004	0.0003
		10GA	0.0001	0.0001	0.0002	0.8518	0.2334	0.0854	0.3909	0.1043	0.4241
		P	<0.0001	<0.0001	0.0003	0.1336	0.3593	0.8019	0.0408	0.0937	0.2464
	MESOCARP3	C	0.0045	0.0033	0.0048	0.0004	0.0001	0.0002	0.0012	0.0002	0.0002
		10GA	0.0008	0.0008	0.001	0.0036	0.0009	0.0009	0.0092	0.0031	0.002
		P	<0.0001	<0.0001	<0.0001	0.1929	0.0224	0.0114	0.8812	0.1901	0.0561
ga1-3 global	ENDOCARP	C	0.0039	0.0036	0.0058	0.0003	<0.0001	0.0001	0.0005	0.0001	0.0001
		10GA	0.0001	0.0001	0.0002	0.0028	0.0004	0.0005	0.0092	0.001	0.0009
		P	<0.0001	<0.0001	<0.0001	0.1262	0.0123	0.0073	0.6953	0.1083	0.0332
	EXOCARP	C	0.3883	0.3069	0.7497	<0.0001	<0.0001	<0.0001	<0.0001	<0.0001	<0.0001
		10GA	0.6309	0.5362	0.948	<0.0001	<0.0001	<0.0001	<0.0001	<0.0001	<0.0001
		P	0.2541	0.1995	0.5429	<0.0001	<0.0001	<0.0001	<0.0001	<0.0001	<0.0001
	MESOCARP1	C	<0.0001	<0.0001	<0.0001	0.3272	0.761	0.2231	0.036	0.1572	0.8051
		10GA	<0.0001	<0.0001	<0.0001	0.1061	0.3904	0.9661	0.0208	0.0587	0.2374
		P	0.0004	0.0004	0.0005	0.1031	0.4528	0.9005	0.0609	0.1354	0.3219
	MESOCARP2	C	<0.0001	<0.0001	<0.0001	0.912	0.19	0.0508	0.1308	0.6499	0.4584
		10GA	0.0002	0.0002	0.0003	0.3238	0.8225	0.6273	0.091	0.234	0.5896
		P	0.0004	0.0004	0.0004	0.3608	0.8445	0.6398	0.1139	0.2726	0.6242
	MESOCARP3	C	0.0009	0.0008	0.001	0.1495	0.031	0.0152	0.529	0.1554	0.0594
		10GA	0.0002	0.0001	0.0002	0.44	0.0834	0.0338	0.7599	0.506	0.1723
		P	0.0002	0.0002	0.0002	0.1874	0.0207	0.0139	0.7546	0.1924	0.0633
	ENDOCARP	C	0.0002	0.0002	0.0002	0.0049	0.0006	0.0007	0.0178	0.0022	0.0015
		10GA	<0.0001	<0.0001	<0.0001	0.0044	0.0004	0.0006	0.0178	0.0013	0.0012
		P	<0.0001	<0.0001	<0.0001	0.0119	0.0008	0.0011	0.0707	0.0037	0.0026

		global						
		MESOCARP3			ENDOCARP			
		C	10GA	P	C	10GA	P	
WILD TYPE	EXOCARP	C	0.0021	<0.0001	<0.0001	0.0014	0.0001	<0.0001
		10GA	0.0014	<0.0001	<0.0001	0.0008	0.0001	<0.0001
		P	0.0066	0.0005	<0.0001	0.0091	0.0005	<0.0001
	MESOCARP1	C	0.4962	0.1373	0.0136	0.3545	0.3975	0.0317
		10GA	0.007	0.0059	0.0214	0.0006	0.002	0.0132
		P	0.001	0.0008	0.0017	0.0002	0.0004	0.0013
	MESOCARP2	C	0.1642	0.6969	0.0036	0.8677	0.0779	0.0078
		10GA	0.0244	0.0307	0.1061	0.0027	0.0104	0.0648
		P	0.0065	0.007	0.016	0.0017	0.0039	0.0118
	MESOCARP3	C	0.0456	0.0148	0.0018	0.5257	0.0339	0.0038
		10GA	0.7757	0.4007	0.0546	0.171	0.9116	0.1176
		P	0.0484	0.056	0.3357	0.0023	0.0136	0.1769
	ENDOCARP	C	0.0424	0.0047	0.0006	0.0545	0.0088	0.0012
		10GA	0.8762	0.3214	0.0244	0.0194	0.9124	0.0654
		P	0.0536	0.061	0.4195	0.0019	0.0126	0.2118
ga1-3 global	EXOCARP	C	0.0029	<0.0001	<0.0001	0.0001	<0.0001	<0.0001
		10GA	0.0021	<0.0001	<0.0001	0.0013	<0.0001	<0.0001
		P	0.0021	<0.0001	<0.0001	0.0011	<0.0001	<0.0001
	MESOCARP1	C	0.0026	0.0014	0.0047	0.0001	0.0004	0.003
		10GA	0.0026	0.0022	0.0311	0.0004	0.001	0.004
		P	0.0099	0.0113	0.0423	0.0027	0.0064	0.0288
	MESOCARP2	C	0.0054	0.0031	0.0136	0.0002	0.0007	0.0018
		10GA	0.0107	0.0118	0.0311	0.0022	0.0059	0.0218
		P	0.0144	0.0166	0.0423	0.0033	0.0087	0.0301
	MESOCARP3	C	0.1967	0.3017	0.8919	0.0251	0.1238	0.6339
		10GA	0.0438	0.0539	0.2348	0.004	0.0181	0.1382
		P	0.0838	0.1151	0.5216	0.0063	0.0354	0.3115
	ENDOCARP	C	0.9171	0.5324	0.0551	0.0702	0.7914	0.1358
		10GA	0.6026	0.8556	0.0616	0.0146	0.3284	0.1918
		P	0.1875	0.2956	0.3837	0.0021	0.0323	0.9033

		global									
		EXOCARP			MESOCARP1			MESOCARP2			
		C	10GA	P	C	10GA	P	C	10GA	P	
global	EXOCARP	C									
		10GA	0.866								
		P	0.6573	0.5536							
	MESOCARP1	C	<0.0001	<0.0001	<0.0001						
		10GA	<0.0001	<0.0001	<0.0001	0.2233					
		P	<0.0001	<0.0001	<0.0001	0.0831	0.3125				
	MESOCARP2	C	<0.0001	<0.0001	<0.0001	0.2198	0.0233	0.0118			
		10GA	<0.0001	<0.0001	<0.0001	0.7955	0.095	0.0339	0.2108		
		P	<0.0001	<0.0001	<0.0001	0.4616	0.5952	0.1779	0.0613	0.2637	
	MESOCARP3	C	0.0016	0.0025	0.0029	0.0103	0.0019	0.0015	0.0365	0.0071	0.0039
		10GA	0.0001	0.0001	0.0001	0.0087	0.001	0.0011	0.038	0.0041	0.0026
		P	<0.0001	<0.0001	<0.0001	0.0471	0.0031	0.0027	0.2448	0.0206	0.0089
	ENDOCARP	C	0.0008	0.0007	0.0011	0.0007	0.0001	0.0002	0.0015	0.0002	0.0002
		10GA	0.0001	0.0001	0.0001	0.0026	0.0003	0.0004	0.0086	0.0008	0.0008
		P	<0.0001	<0.0001	<0.0001	0.0315	0.0021	0.0019	0.1237	0.0111	0.0056
global		MESOCARP3			ENDOCARP						
		C	10GA	P	C	10GA	P				
EXOCARP	C										
	10GA										
	P										
MESOCARP1	C										
	10GA										
	P										
MESOCARP2	C										
	10GA										
	P										
MESOCARP3	C										
	10GA	0.5565									
	P	0.1066	0.1423								
ENDOCARP	C	0.1722	0.0257	0.0024							
	10GA	0.9319	0.3434	0.0224	0.0682						
	P	0.2046	0.3356	0.5475	0.0056	0.0642					

			<i>ga1-3 glohal</i>								
			EXOCARP			MESOCARP1			MESOCARP2		
			C	10GA	P	C	10GA	P	C	10GA	P
<i>ga1-3 glohal</i>	EXOCARP	C									
		10GA	0.8275								
		P	0.7005	0.6258							
	MESOCARP1	C	<0.0001	<0.0001	<0.0001						
		10GA	<0.0001	<0.0001	<0.0001	0.2928					
		P	<0.0001	<0.0001	<0.0001	0.3746	0.8828				
	MESOCARP2	C	<0.0001	<0.0001	<0.0001	0.3013	0.094	0.182			
		10GA	<0.0001	<0.0001	<0.0001	0.6889	0.669	0.6355	0.3267		
		P	<0.0001	<0.0001	<0.0001	0.7198	0.6778	0.6411	0.3678	0.7252	
	MESOCARP3	C	0.001	0.001	0.0011	0.0421	0.0219	0.0476	0.1083	0.0687	0.0826
		10GA	0.0002	0.0002	0.002	0.1191	0.0492	0.0974	0.3478	0.1675	0.1832
		P	0.0002	0.0002	0.002	0.0414	0.0219	0.055	0.1256	0.0811	0.0992
	ENDOCARP	C	0.0002	0.0003	0.002	0.0009	0.0015	0.008	0.0017	0.0079	0.0113
		10GA	<0.0001	<0.0001	<0.0001	0.0006	0.0014	0.0091	0.0011	0.0087	0.013
		P	<0.0001	<0.0001	<0.0001	0.0012	0.0027	0.0158	0.0028	0.0171	0.0246
<i>ga1-3 glohal</i>				MESOCARP3			ENDOCARP				
	EXOCARP	C									
		10GA									
		P									
	MESOCARP1	C									
		10GA									
		P									
	MESOCARP2	C									
		10GA									
		P									
	MESOCARP3	C									
		10GA	0.4336								
		P	0.7339	0.5954							
	ENDOCARP	C	0.1725	0.29	0.0582						
		10GA	0.2376	0.0346	0.0745	0.5729					
		P	0.571	0.1011	0.242	0.0992	0.1152				

Chapter 4: Protein-protein interactions and DELLAs

Table 4.1 PCR primers used during Chapter 4.

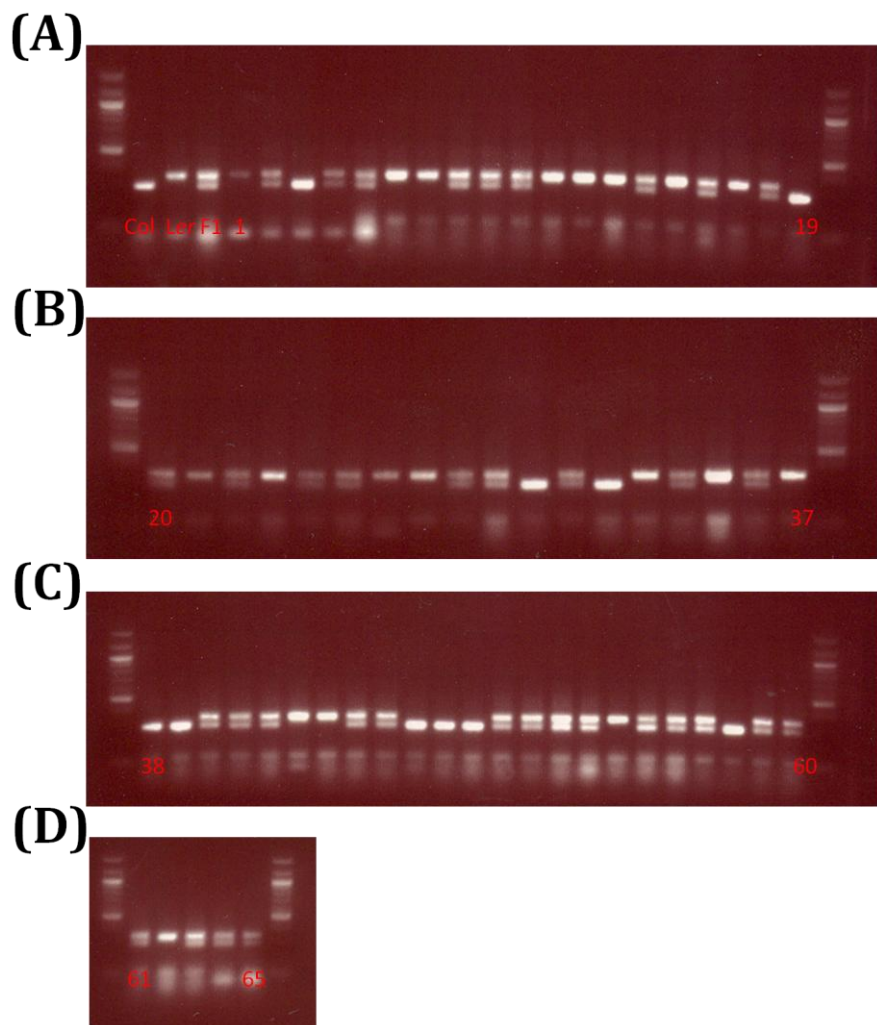
Coding sequence	Primers (5'-3')	PCR Conditions	
GAI	F AAAACCCGGGCATGAAGAGAGATCATCATCATC' R ATTGCTGCAGCATAATTGGTGG	57.5C	1min 20sec
GAI*	F CTCGCCCGGTGCTCTGGTTGACTCGCAAG R ATTGCTGCAGCATAATTGGTGG	57.5C	1min
RGA	F ATAGCCCGGAATGAAGAGAGATCATCAC R TCGACTGCACCTCAGTACGCCGCCGTCG	70C	1min 20sec
RGL2	F AACACCCGGGATGAAGAGAGGATACGG R ACCGCTGCAGCTCAGGCGAGTTCCACG	70C	1min 20sec
IND	F CCAACCCGGGCATGATGGAGCCTCAGCCTCACC R GTGTCTGCAGTCAGGGTTGGGAGTTGTGGTAATAAC	55C	30sec
IND*	F AAGACCCGGGTACGATGAAGACATGGATGC R GTGTCTGCAGTCAGGGTTGGGAGTTGTGGTAATAAC	55C	30sec
IND*1	F ACGTCCCGGAAGCGACGATCCTCAGACG R GTGTCTGCAGTCAGGGTTGGGAGTTGTGGTAATAAC	55C	30sec
IND*2	F AAGACCCGGGTACGATGAAGACATGGATGC R GGATCTGCAGTTACCTTACGTTACGGCGG	55C	30sec
ALC	F GAGACCCGGGATGGTGATTCTGACGTCGG R GAATCTGCAGTTCAAAGCAGAGTGGCTGTGG	55C	30sec
SPT	F TTGCTCCGGGAATGATATCACAGAGAGAAGAAAG R GGGACTGCAGTCAGTAATTGATCTTTAGGTC	57.5C	45sec
FUL	F GAGACCCGGGTATGGGAAGAGGTAGGGTCAGC R GTGACTGCAGTCTACTCGTTCGTAGTGGTAGG	55C	30sec
ETT	F CTCTCCGGGAATGGTGGTTAACGATCTG R AAGACTGCAGCTAGAGAGCAATGTAGAACATG	55C	2min 30sec
RPL	F ATCCGAATTATGGCTGATGCATACGAG R ACAACTGCAGTCAACCTACAAAATCATGTAGAACT	55C	2min

Chapter 5: EMS mutagenesis: Screening for parthenocarpy

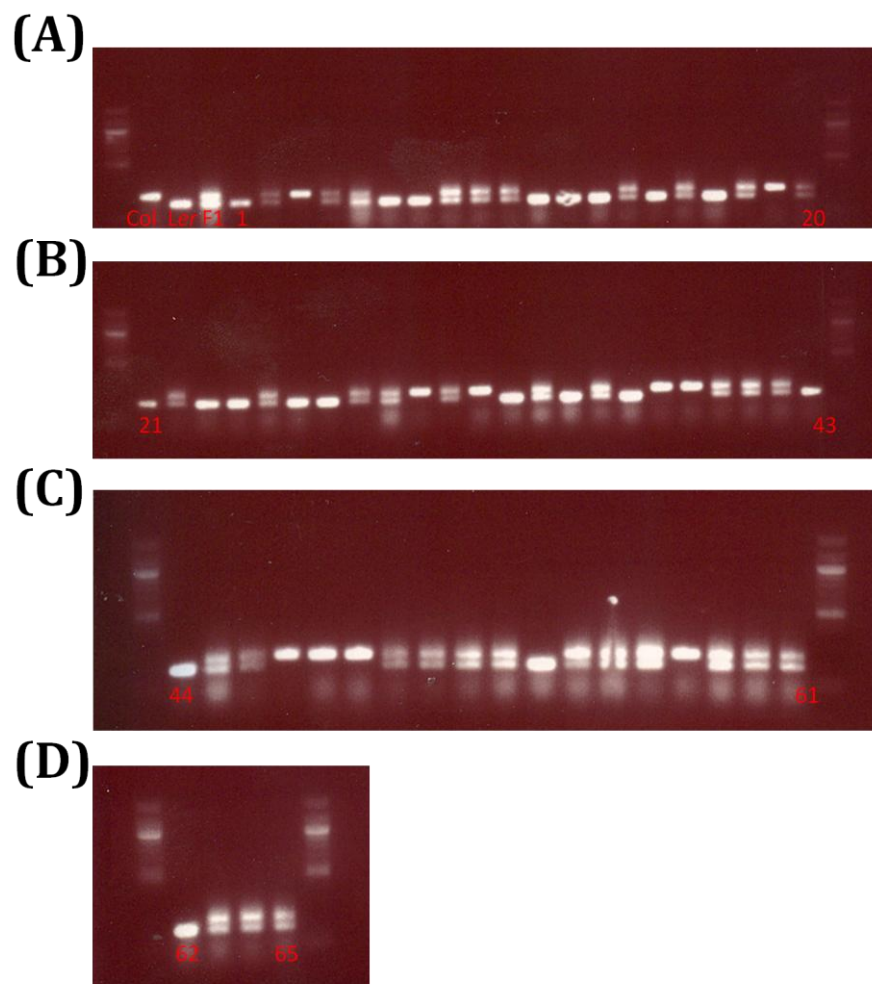
Table 5.1 PCR markers and PCR conditions used during map-based cloning.

Chr	Name	Atg	Col (bp)	Ler (bp)	Primer sequence (5'-3')	Anneling
1	33 34	At1g07810	above 300	under 300	GTTCACGGACAAAGAGCCTGAAAT	55C
					AAGCAGTCAATATTGCAGGAAGGG	
1	9 10	At1g09940	>200	<200	TCATGACGTGAAGAAGAAGAAAA	55C
					CATATCGCTGCTACTAATTAAACAA	
1	1 2	At1g30930	239	142	TCAATGGGATCGAAACTGGT	55C
					ACTGAAAAGCGAGCCAAAG	
1	5 6	At1g49610	>150	<150	ACATTTCTCAATCCTTACTC	53C
					GAGAGCTTCTTATTGTGAT	
2	11 12	At2g14890	<200	>200	GAAACTCAATGAAATCCACTT	53C
					TGAACCTGTTGTGAGCTTGAT	
2	13 14	At2g39010	150/ 151	130/ 135	TCGTCTACTGCACTGCCG	55C
					GAGGACATGTATAGGAGCCTCG	
3	15 16	At3g11220	193	174	GGATTAGATGGGGATTCTGG	55C
					TTGCTCGTATCAACACACAG	
3	17 18	At3g26605	<200	>200	CCCCGAGTTGAGGTATT	53C
					GAAGAAATTCTAAAGCATTC	
3	19 20	At3g50820	190	215	GTTCATTAAACTGCGTGTGT	55C
					TACGGTCAGATTGAGTGATTC	
4	21 22	At4g01710	>150	<150	GGTTAAAATTAGGGTACGA	53C
					AGATTACGTGGAAGCAAT	
4	23 24	At4g29860	492	404	GCCCAGAGGAAGAAGAGCAAATAGC	55C
					TGGGAATTCATGAGAGAATATGTGGGAC	
4	25 26	At4g10360	268	188	GCCAAACCCAAAATTGTAAAAC	55C
					TAGAGGGAACAAATCGGATGC	
5	99 100	At5g14320	225	271	GCGCTAACGACCAAATCAAACAA	55C
					CGTGATGAAGTCTCCAAGTACATG	
5	27 28	At5g22545	100	>130	TAGTGAAACCTTTCTCAGAT	50C
					TTATGTTTCTTCAATCAGTT	
5	29 30	At5g42600	165	145	CAGACGTATCAAATGACAAATG	55C
					GAECTACTGCTCAAATATTGG	
5	31 32	At5g63640	200	<200	GAGCATTTCACAGAGACG	50C
					ATCACTGTTGTTACCATTA	

Appendix figure 5.1 Marker primer set 33-34. (A) Col-0, Ler, F1 and 1-19 lines. (B) Lines 20-37. (C) Lines 38-60. (D) Lines 61-65. Ladder, 100bp. Run in 1.5% agarose gel.

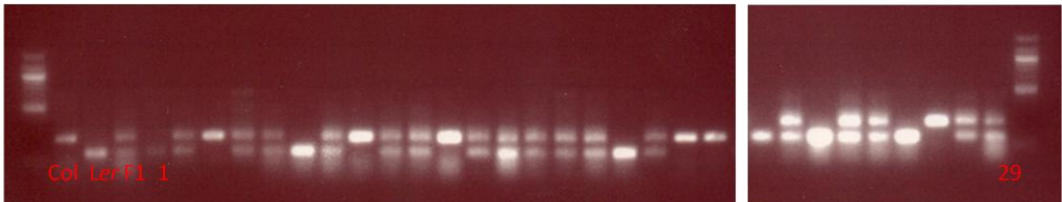


Appendix figure 5.2 Marker primer set 9-10. (A) Col-0, Ler, F1 and 1-20 lines. (B) Lines 21-43. (C) Lines 44-61. (D) Lines 62-65. Ladder, 100bp. Run in 1.5% agarose gel.

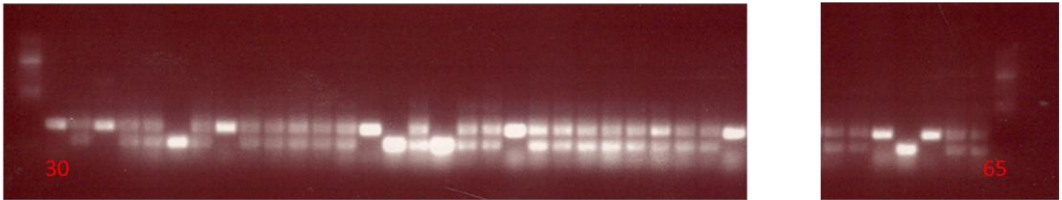


Appendix figure 5.3 Marker primer set 1-2. (A) Col-0, Ler, F1 and 1-29 lines. (B) Lines 30-65. Ladder, 100bp. Run in 1.5% agarose gel.

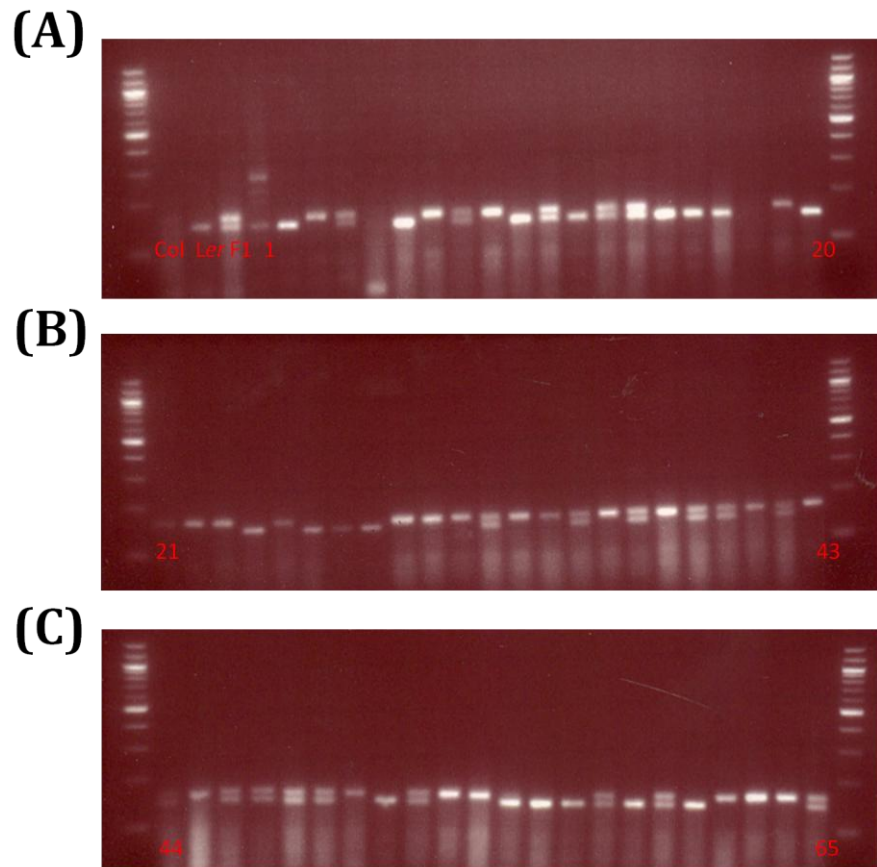
(A)



(B)

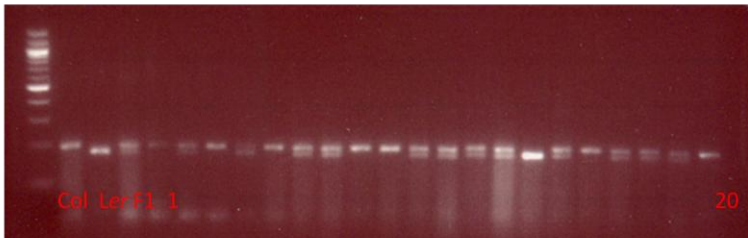


Appendix figure 5.4 Marker primer set 21-22. (A) Col-0, Ler, F1 and 1-20 lines.
(B) Lines 21-43. (C) Lines 44-65. Ladder, 100bp. Run in 3% agarose gel.

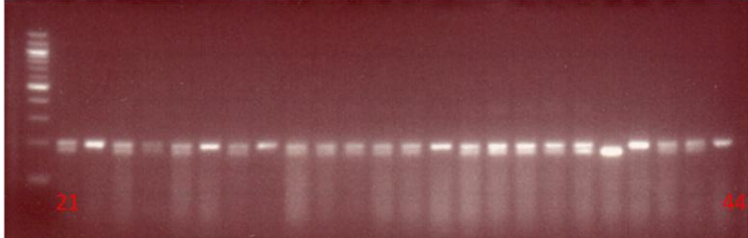


Appendix figure 5.5 Marker primer set 31-32. (A) Col-0, Ler, F1 and 1-20 lines.
(B) Lines 21-44. (C) Lines 45-65. Ladder, 100bp. Run in 3% agarose gel.

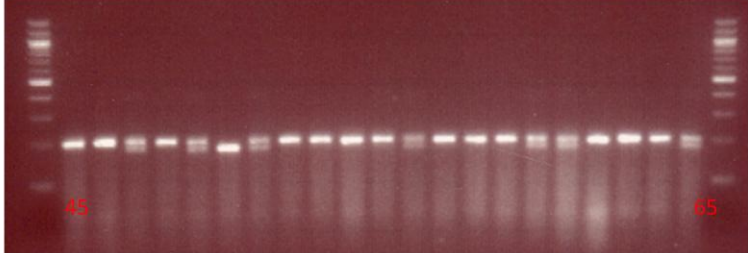
(A)



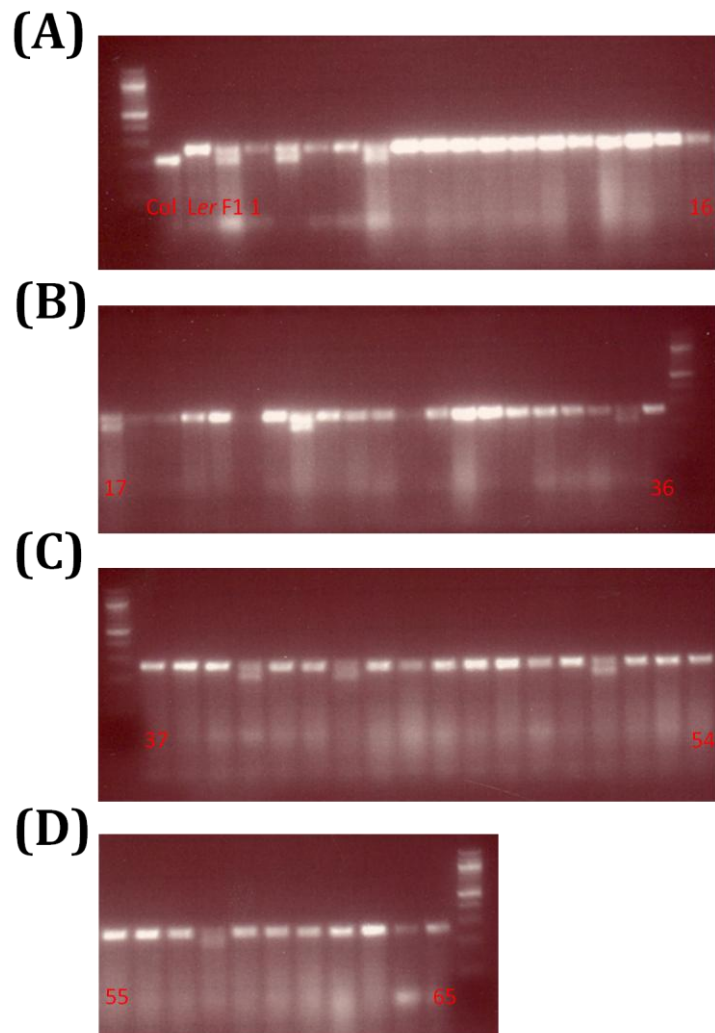
(B)



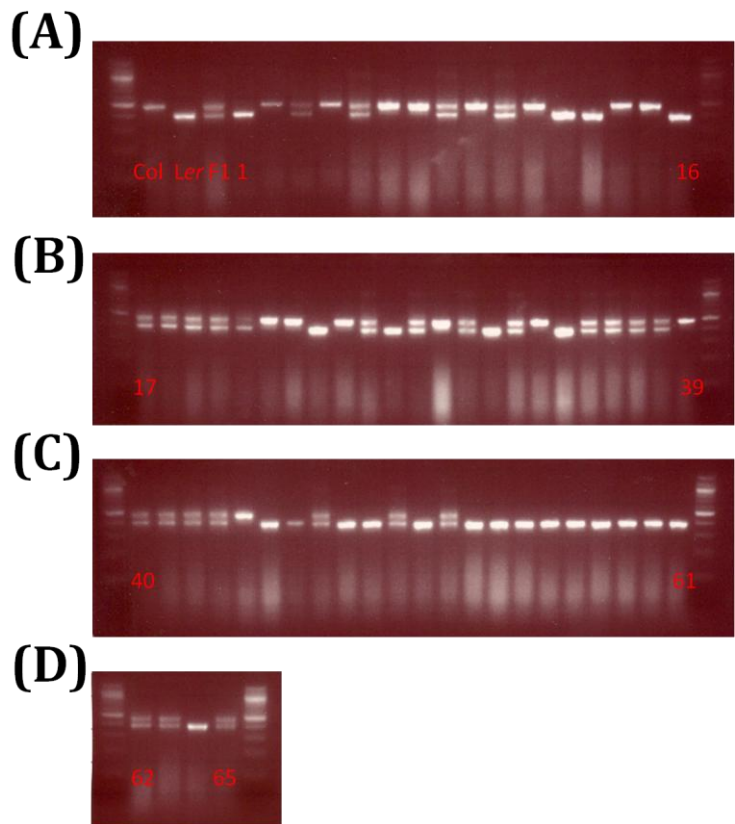
(C)



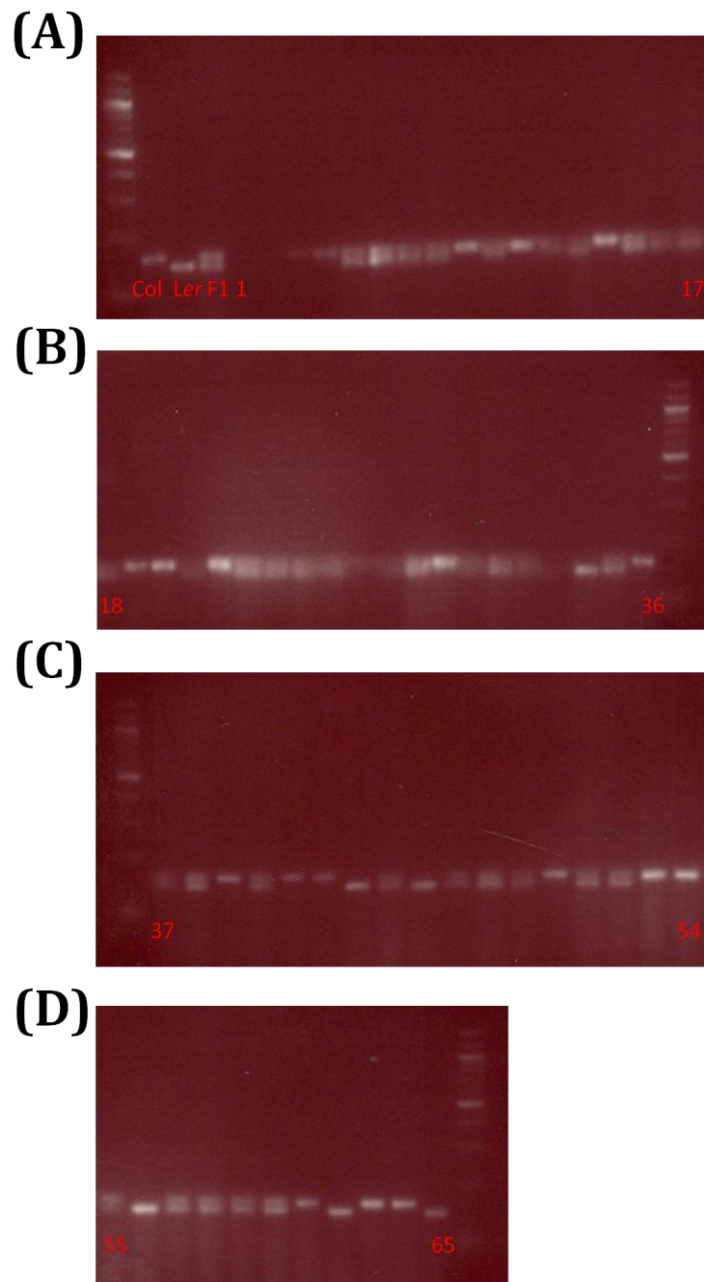
Appendix figure 5.6 Marker primer set 99-100. (A) Col-0, Ler, F1 and 1-16 lines. (B) Lines 17-36. (C) Lines 37-54. (D) Lines 55-65. Ladder, 100bp. Run in 3% agarose gel.



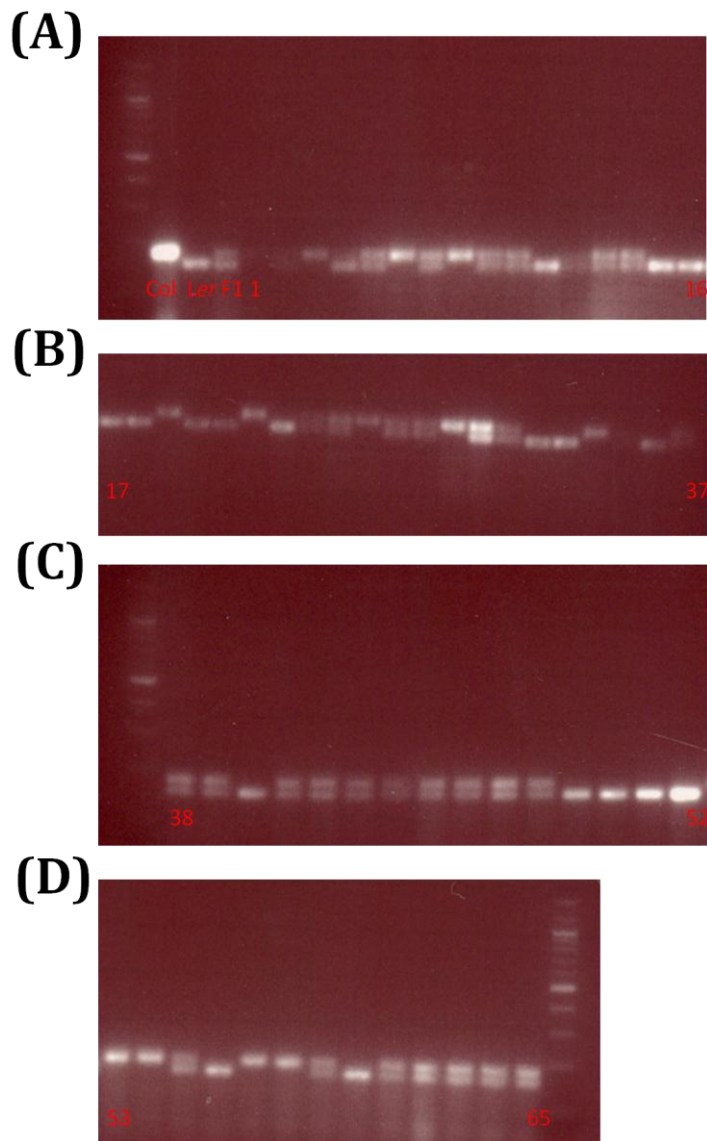
Appendix figure 5.7 Marker primer set 23-24. (A) Col-0, Ler, F1 and 1-16 lines. (B) Lines 17-39. (C) Lines 40-61. (D) Lines 62-65. Ladder, 100bp. Run in 1.5% agarose gel.



Appendix figure 5.8 Marker primer set 5-6. (A) Col-0, Ler, F1 and 1-17 lines. (B) Lines 18-36. (C) Lines 37-54. (D) Lines 55-65. Ladder, 100bp. Run in 3% agarose gel.

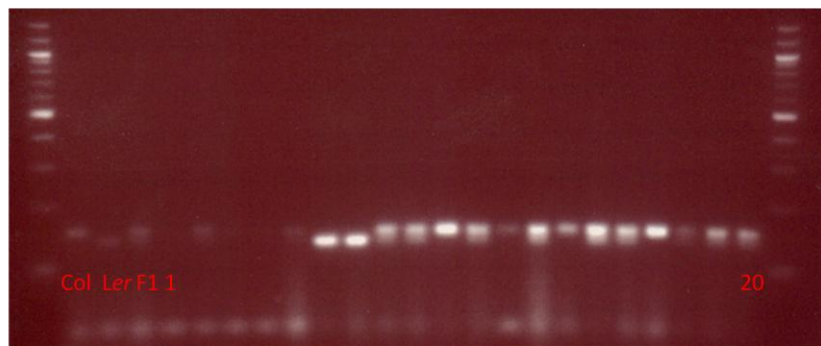


Appendix figure 5.9 Marker primer set 29-30. (A) Col-0, Ler, F1 and 1-16 lines. Lines 1 and 2 failed to amplify. (B) Lines 17-37. Line 35 failed to amplify. (C) Lines 38-52. (D) Lines 53-65. Ladder, 100bp. Run in 3% agarose gel.

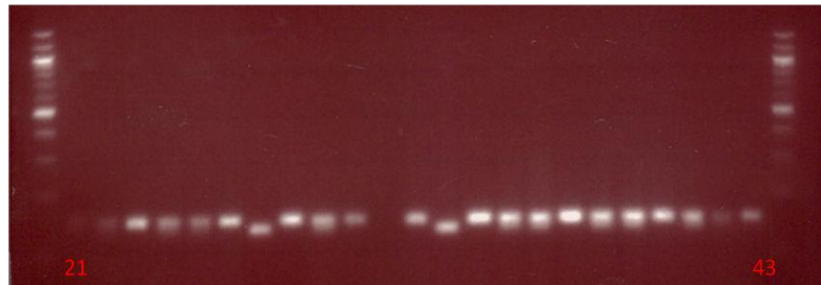


Appendix figure 5.10 Marker primer set 13-14. (A) Col-0, Ler, F1 and 1-20 lines. Lines 1, 3 and 4 failed to amplify. (B) Lines 21-43. Line 31 failed to amplify. (C) Lines 44-65. Ladder, 100bp. Run in 3% agarose gel.

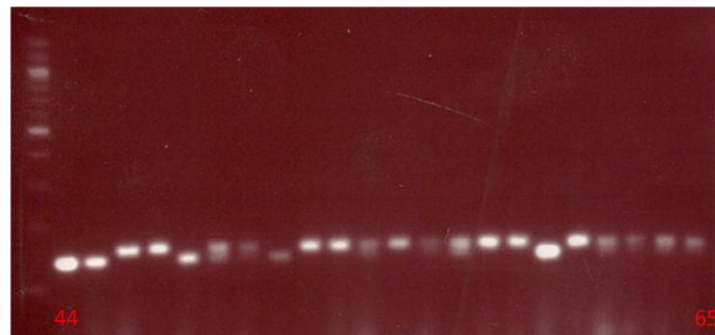
(A)



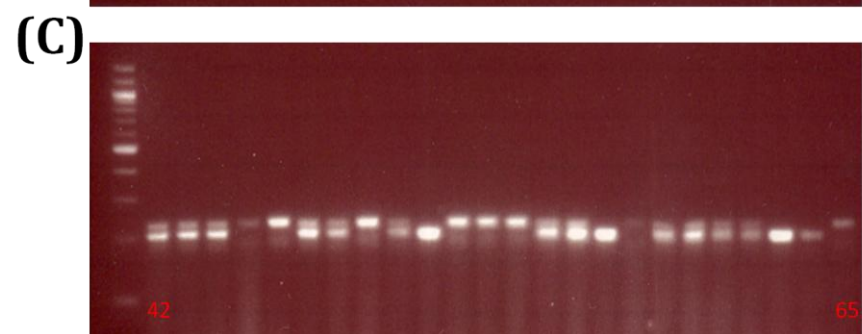
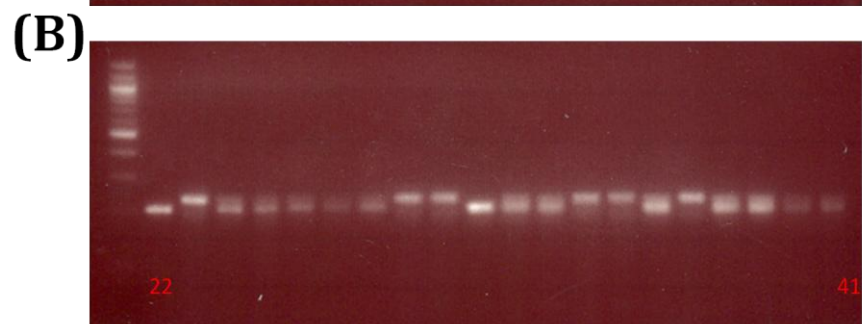
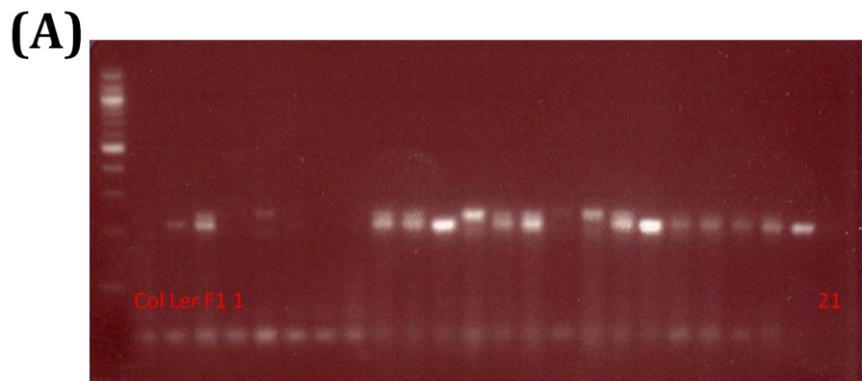
(B)



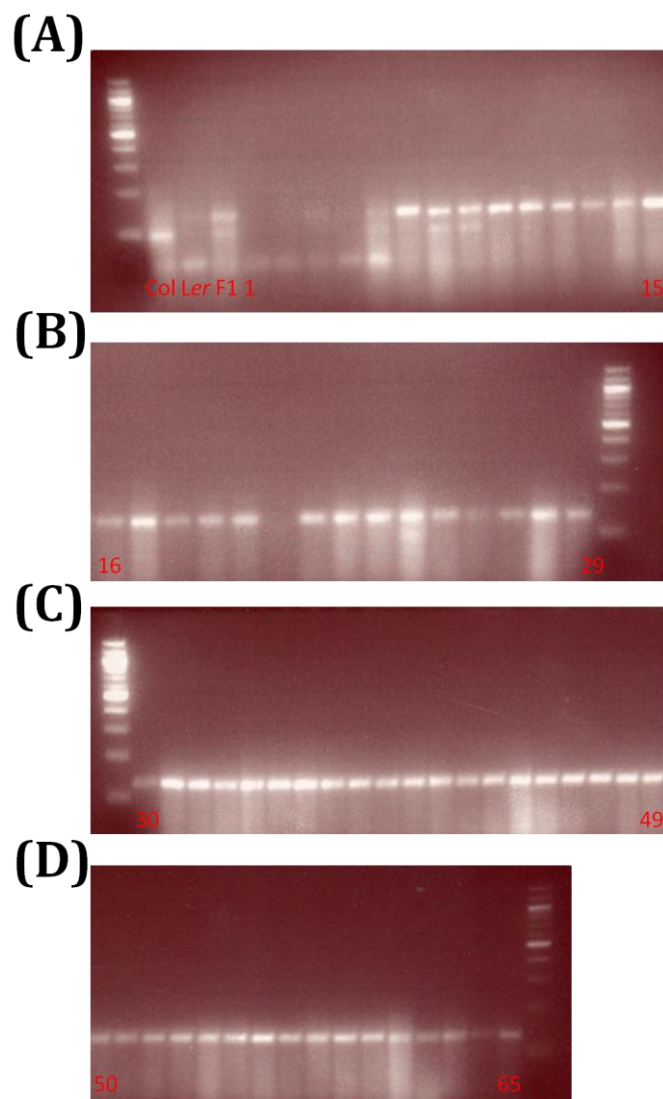
(C)



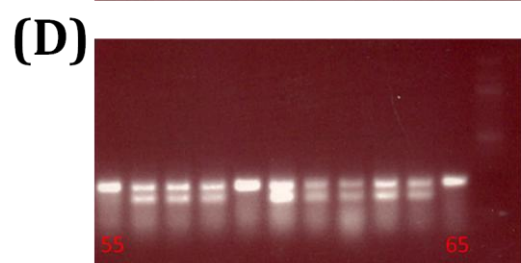
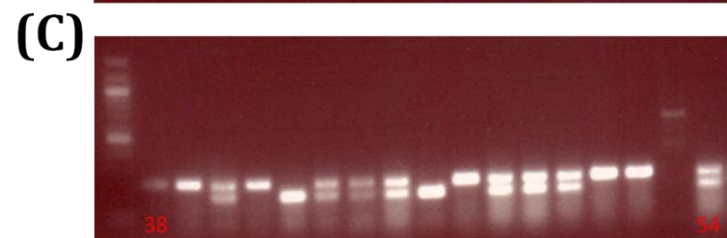
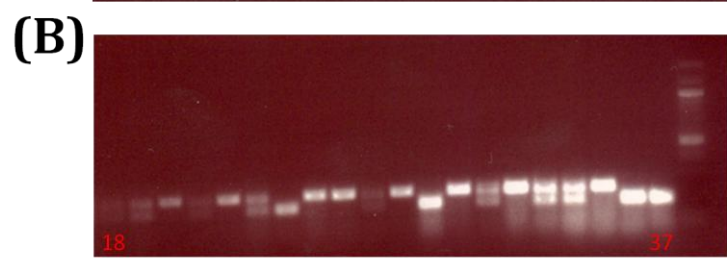
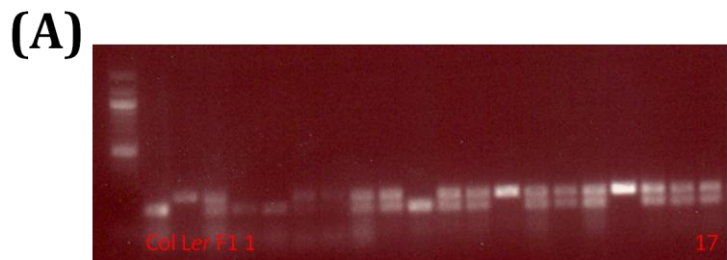
Appendix figure 5.11 Marker primer set 11-12. (A) Col-0, Ler, F1 and 1-21 lines. Lines 1, 2, 3, 4, 5, 12 and 21 failed to amplify. (B) Lines 22-41. (C) Lines 42-65. Ladder, 100bp. Run in 3% agarose gel.



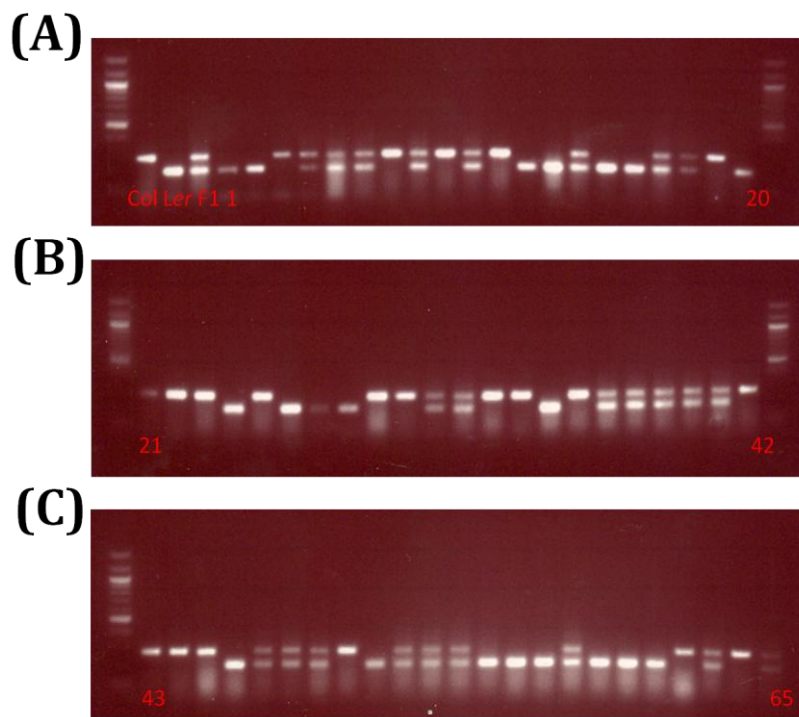
Appendix figure 5.12 Marker primer set 27-28. (A) Col-0, Ler, F1 and 1-15 lines. Lines 1, 2, 3 and 4 failed to amplify. (B) Lines 16-29. Gap at position 21. (C) Lines 30-49. (D) Lines 50-65. Ladder, 100bp. Run in 3% agarose gel.



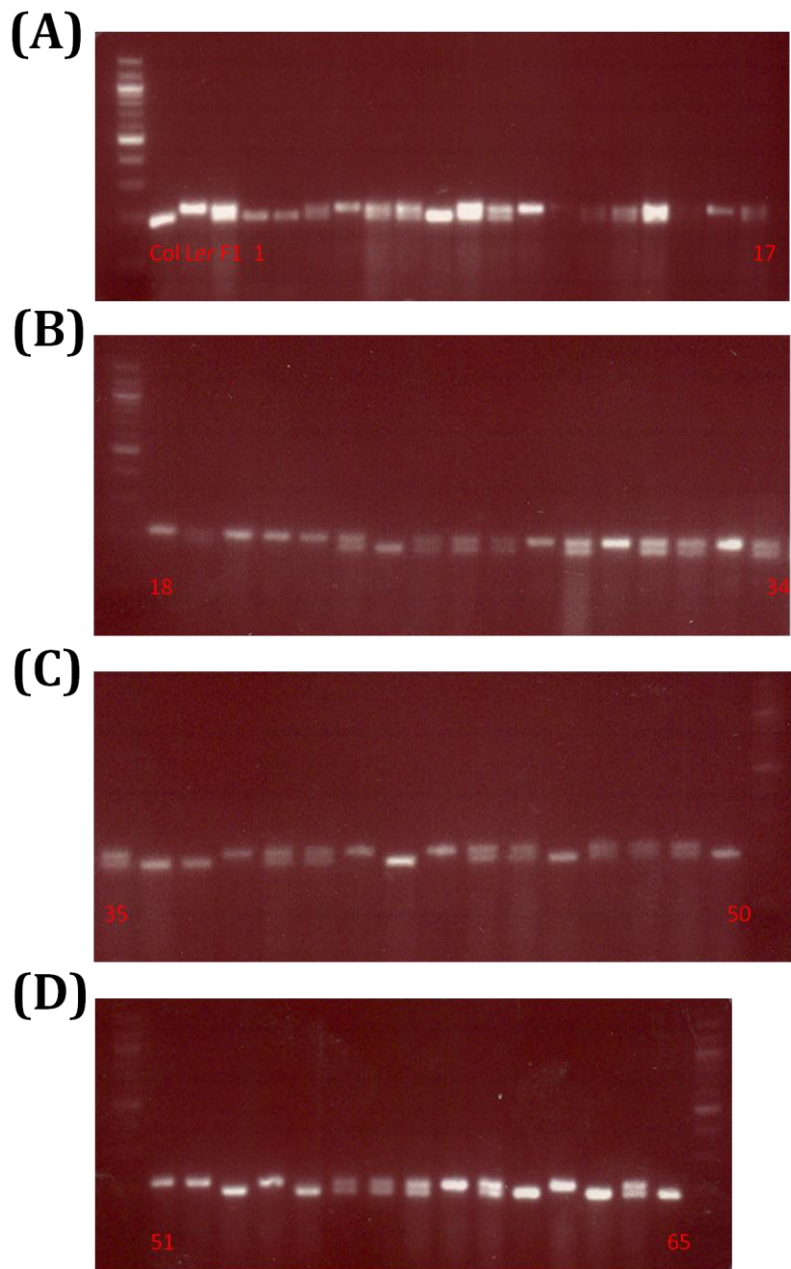
Appendix figure 5.13 Marker primer set 17-18. (A) Col-0, Ler, F1 and 1-17 lines. (B) Lines 18-37. (C) Lines 38-54. Line 53 failed to amplify. (D) Lines 55-65. Ladder, 100bp. Run in 1.5% agarose gel.



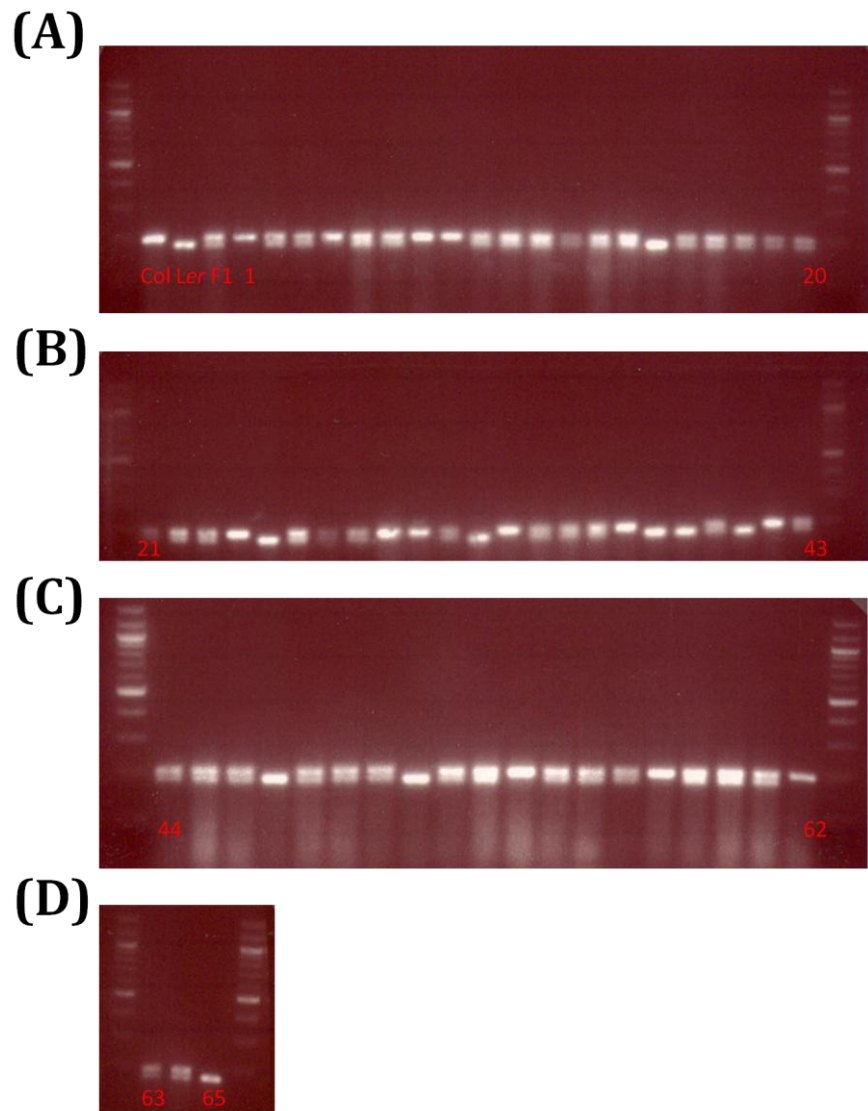
Appendix figure 5.14 Marker primer set 25-26. (A) Col-0, Ler, F1 and 1-20 lines.
(B) Lines 21-42. (C) Lines 43-65. Ladder, 100bp. Run in 1.5% agarose gel.



Appendix figure 5.15 Marker primer set 19-20. (A) Col-0, Ler, F1 and 1-17 lines. Line 15 failed to amplify. (B) Lines 18-34. (C) Lines 35-50. (D) Lines 51-65. Ladder, 100bp. Run in 3% agarose gel.



Appendix figure 5.16 Marker primer set 15-16. (A) Col-0, Ler, F1 and 1-20 lines. (B) Lines 21-43. (C) Lines 44-62. (D) Lines 63-65. Ladder, 100bp. Run in 3% agarose gel.



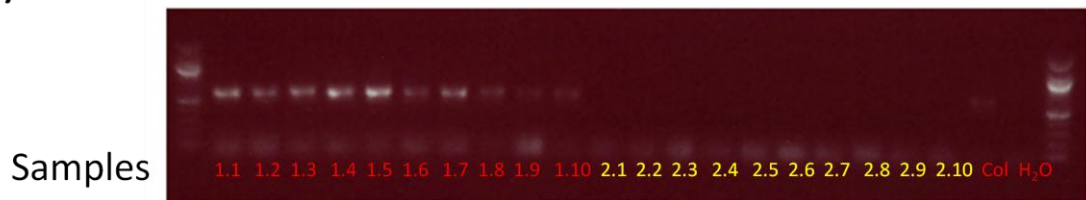
Chapter 6: Unexpected consequences of investigating seed-pod communication

Table 6.1 PCR primers used during Chapter 6.

Name	Type	Primer sequence (5'-3')
AD1	TAIL-PCR arbitrary degenerate primer	TGWGNAGWANCASAGA
AD2	TAIL-PCR arbitrary degenerate primer	AGWGNAGWANCAWAGG
AD3	TAIL-PCR arbitrary degenerate primer	CAWCAICNGAIASGAA
AD4	TAIL-PCR arbitrary degenerate primer	TCWTICGNACITWGGA
SF00115	Forward primer for <i>PAP10</i> promoter	GCGAAAGCTTGGACCAATCATACTGCACG
SF00116	Reverse primer for <i>PAP10</i> promoter	TTTGGATCCGAAAGAGAGATTTCG
SF0071	<i>PAP10</i> gene specific primer for line 3	TGTATGAGGCTTGATGTACGG
SF0072	<i>PAP10</i> gene specific primer for line 3	TCCAAGAAAATTGGTGGC
SF0073	T-DNA insertion specific primer for line 3	GCGTGGACCGCTTGCTGCAACT
SF0074	<i>PAP10</i> gene specific primer for lines 4 and 5	GCCTTTCAGAAATGGATAAT
SF0075	<i>PAP10</i> gene specific primer for lines 4 and 5	GTCCTGATGTTCCCTACACTTTGG
SF0076	T-DNA insertion specific primer for lines 4 and 5	CTGTGGTGTGTATTTCTGTCC
SF0077	T-DNA insertion specific primer for lines 1, 2 and 6-18	GACCATCATACTCATTGCTGATCC
SF0078	<i>PAP10</i> gene specific primer for lines 11-18	GGTTAACAGAACGGAAACTCCG
SF0079	<i>PAP10</i> gene specific primer for lines 11-18	GCATAACCATCATGTTCCATATGC
SF0080	<i>PAP12</i> gene specific primer for lines 6-10	GTGGTATTCCATCAAAGGGCG
SF0081	<i>PAP12</i> gene specific primer for lines 6-10	CAGAGTTAGTTACAGAGTCGG
SF0082	<i>PAP12</i> gene specific primer for lines 1 and 2	GGAGTCACCCAAGAAATGATCACTC
SF0083	<i>PAP12</i> gene specific primer for lines 1 and 2	GGAGAGTTGAGTTCTCTTCC
SF0021	GAL4 specific primer for TAIL-PCR secondary reaction	GGAGCACTTGAGCTCTTGAGGCCGC
SF0022	GAL4 specific primer for TAIL-PCR tertiary reaction	GGGAGCGCTTCCTTTGGGAGAGTCGC
SF0020	GAL4 specific primer for TAIL-PCR primary reaction	GGATCATGTCGAGGTCCTCTCGAGGG
SF00192	<i>PAP10</i> specific primer to check <i>PAP10::GUS</i> presence	GGTTAACATATGCAGCAGGACC
SF00171	GUS specific primer to check <i>PAP10::GUS</i> presence	GGAAACAGCTATGACCATGATTACG

Appendix figure 6.1 PCR-genotyping of T-DNA insertion lines 1 and 2 (GK-662B07, allele *pap12-1*). Gel photograph of (A) gene-specific reaction (B) and insert-specific reaction. Homozygous mutant samples (in yellow) show lack of amplification in the gene-specific reaction and amplification in the insert-specific reaction (expected band size \approx 400 bp). Ladder, 100 bp.

(A)

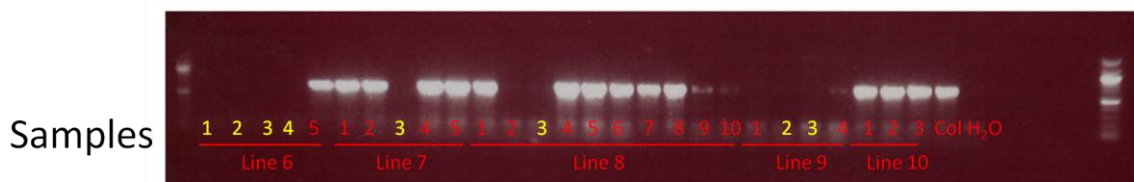


(B)

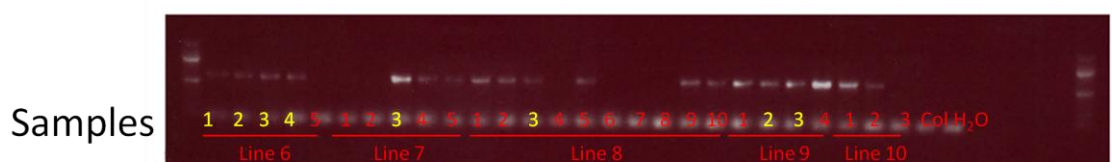


Appendix figure 6.2 PCR-genotyping of T-DNA insertion lines 6, 7, 8, 9 and 10 (GK-151C09, allele *pap12-2*). Gel photograph of (A) gene-specific reaction (B) and insert-specific reaction. Homozygous mutant samples (in yellow) show lack of amplification in the gene-specific reaction and amplification in the insert-specific reaction (expected band size \approx 650 bp). Ladder, 100 bp.

(A)

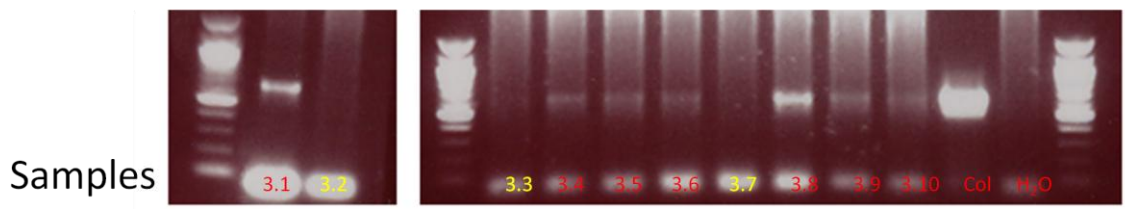


(B)

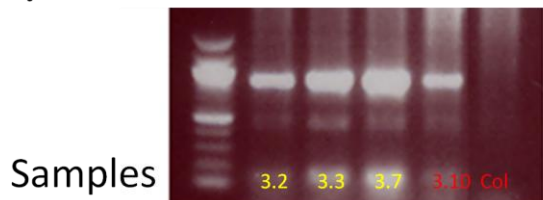


Appendix figure 6.3 PCR-genotyping of T-DNA insertion line 3 (SALK-122362, allele *pap10-1*). Gel photograph of (A) gene-specific reaction (B) and insert-specific reaction. Homozygous mutant samples (in yellow) show lack of amplification in the gene-specific reaction and amplification in the insert-specific reaction (expected band size \approx 900 bp). Ladder, 100 bp.

(A)

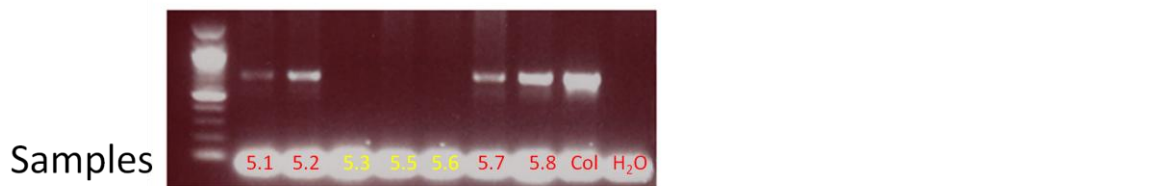


(B)

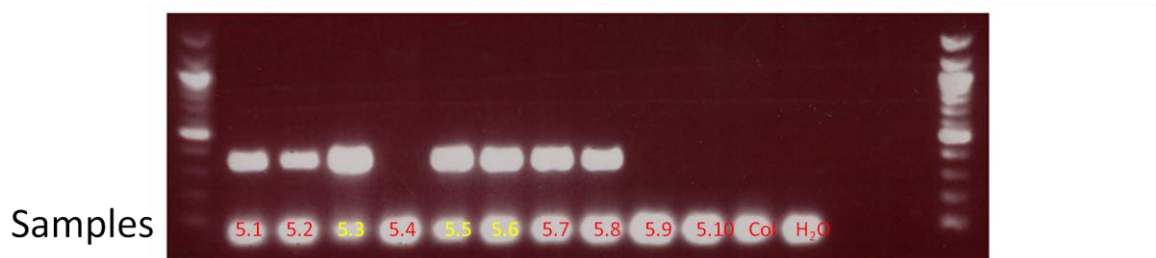


Appendix figure 6.4 PCR-genotyping of T-DNA insertion line 5 (SAIL-430-D05, allele *pap10-2*). Gel photograph of (A) gene-specific reaction (B) and insert-specific reaction. Homozygous mutant samples (in yellow) show lack of amplification in the gene-specific reaction and amplification in the insert-specific reaction (expected band size \approx 350 bp). Ladder, 100 bp.

(A)

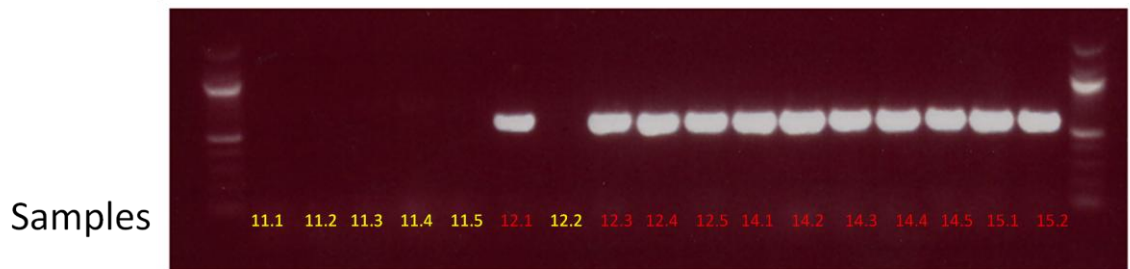


(B)

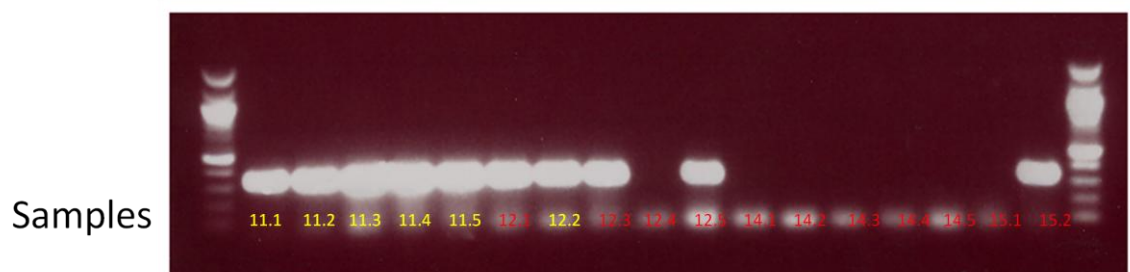


Appendix figure 6.5 PCR-genotyping of T-DNA insertion lines 11, 12, 14 and 15 (GK-850G03.06, allele *pap10-3*). Gel photograph of (A) gene-specific reaction (B) and insert-specific reaction. Homozygous mutant samples (in yellow) show lack of amplification in the gene-specific reaction and amplification in the insert-specific reaction (expected band size \approx 350 bp). Ladder, 100 bp.

(A)



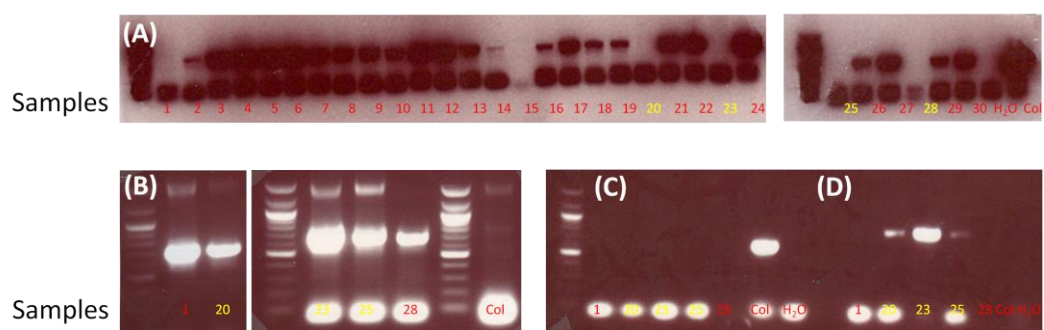
(B)



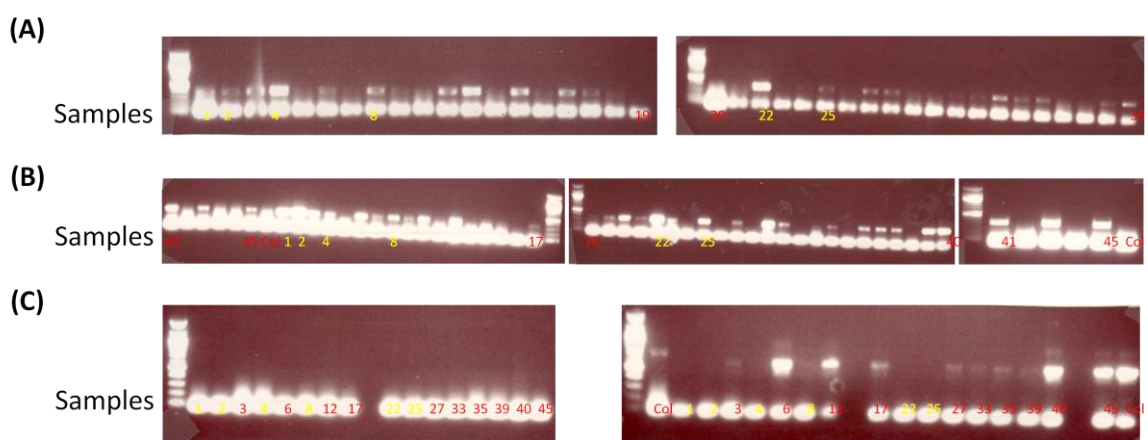
Appendix figure 6.6 PCR-genotyping of T-DNA insertion lines 17 and 18 (GK-850G03.06, allele *pap10-3*). Gel photograph of (A) gene-specific reaction (B) and insert-specific reaction. Homozygous mutant samples (in yellow) show lack of amplification in the gene-specific reaction and amplification in the insert-specific reaction (expected band size \approx 350 bp). Ladder, 100 bp.



Appendix figure 6.7 PCR-genotyping of *pap10-1pap12-2* double mutants.** (A) Gene-specific reaction of *pap12-2* allele, 30 plants. (B) Insert-specific reaction of *pap12-2* allele of plants that did not show gene-specific amplification. (C) Gene-specific reaction *pap10-1* allele. (D) Insert-specific reaction of *pap10-1* allele. Homozygous mutants, which show lack of amplification in the gene-specific reactions and amplification in the insert-specific reactions (expected band size for *pap10-1* insert-specific reaction \approx 800 bp and expected band size for *pap12-2* insert-specific reaction \approx 500 bp), are shown in yellow. Ladder, 100 bp.

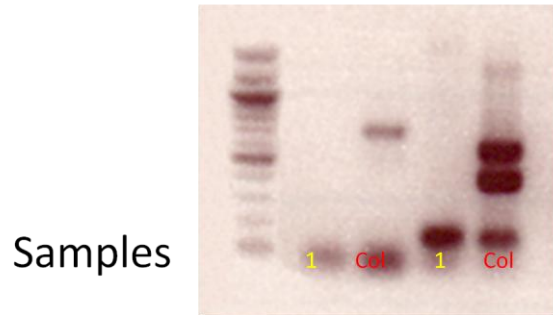


Appendix figure 6.8 PCR-genotyping of *pap10-2pap12-1* double mutants.** (A) Insert-specific reaction of *pap10-2* allele, 39 plants. (B) Insert-specific reaction of *pap10-2* allele, 5 plants and Col. Insert-specific reaction of *pap12-1* allele, 45 plants and Col. (C) Gene-specific reaction of *pap10-2* allele and of *pap12-1* allele respectively of plants that show insert-specific amplification. Homozygous mutants, which show lack of amplification in the gene-specific reactions and amplification in the insert-specific reactions (expected band size for *pap10-2* insert-specific reaction ≈ 400 bp and expected band size for *pap12-1* insert-specific reaction ≈ 400 bp), are shown in yellow. Ladder, 100 bp.

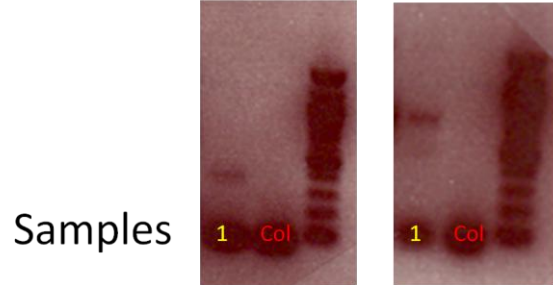


Appendix figure 6.9 PCR-genotyping of *pap10-2pap12-2* double mutants.** (A) Gene-specific reaction of *pap10-2* allele and *pap12-2* allele. (B) Insert-specific reaction of *pap10-2* allele and *pap12-2* allele respectively. Homozygous mutants, which show lack of amplification in the gene-specific reactions and amplification in the insert-specific reactions (expected band size for *pap10-2* insert-specific reaction \approx 400 bp and expected band size for *pap12-2* insert-specific reaction \approx 700 bp), are shown in yellow. Ladder, 100 bp.

(A)

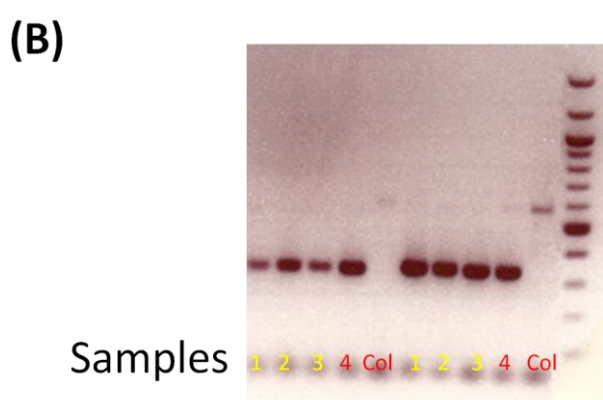
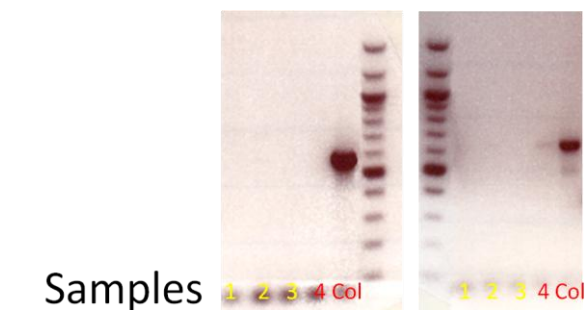


(B)



Appendix figure 6.10 PCR-genotyping of *pap10-3pap12-1* double mutants.

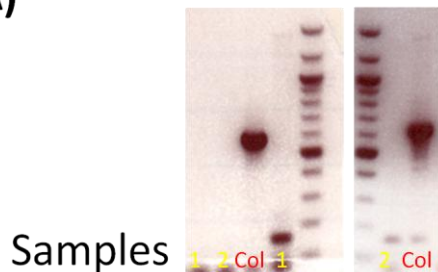
(A) Gene-specific reaction of *pap10-3* allele and *pap12-1* allele. (B) Insert-specific reaction of *pap10-3* allele and *pap12-1* allele respectively. Homozygous mutants, which show lack of amplification in the gene-specific reactions and amplification in the insert-specific reactions (expected band size for *pap10-3* insert-specific reaction \approx 325 bp and expected band size for *pap12-1* insert-specific reaction \approx 350 bp), are shown in yellow. Ladder, 100 bp.



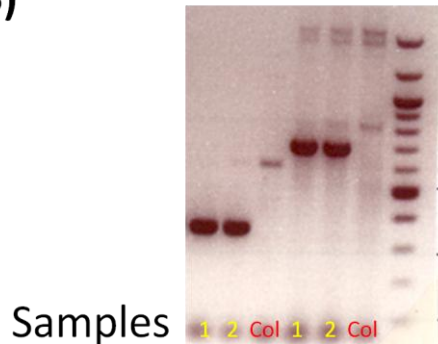
Appendix figure 6.11 PCR-genotyping of *pap10-3pap12-2* double mutants.**

(A) Gene-specific reaction of *pap10-3* allele and *pap12-2* allele respectively. (B) Insert-specific reaction of *pap10-3* allele and *pap12-2* allele respectively. Homozygous mutants, which show lack of amplification in the gene-specific reactions and amplification in the insert-specific reactions (expected band size for *pap10-3* insert-specific reaction \approx 325 bp and expected band size for *pap12-2* insert-specific reaction \approx 700 bp), are shown in yellow. Ladder, 100 bp.

(A)



(B)



APPENDIX 2

PhD rotations

APPENDIX 2

PhD Rotations

In this appendix a compilation of the reports written as part of the three laboratory rotations carried out at the start of the PhD are presented. Two of these short projects resulted in publications: first rotation (Fuentes S., Pires N., Østergaard, L., (2010) "A clade in the QUASIMODO2 family evolved with vascular plants and supports a role for cell wall composition in adaptation to environmental changes." Plant Molecular Biology **73**(6): 605-615) and second rotation (Yasumura Y., Crumpton-Taylor M., Fuentes S., Harberd N. P., (2007) "Step-by-Step Acquisition of the Gibberellin-DELLA Growth-Regulatory Mechanism during Land-Plant Evolution." Current Biology **17**(14): 1225-1230).

FIRST ROTATION REPORT

Introduction

The control of germination is an important adaptative trait with respect to plant species survival. Although seed dormancy is generally regarded as the failure of an intact viable seed to complete germination under favourable conditions (Bewley, 1997), in some cases it can be an advantageous trait. For example, dormancy impedes the germination of annual plants in autumn under optimal conditions which could lead to a poor survival of the plants during winter. Among the many factors regulating seed dormancy in *Arabidopsis*, abscisic acid (ABA) plays a vital role (Finkelstein *et al.*, 2002) (Figure 1).

Genetic screens have been a widely used tool for the identification of genes involved in ABA signalling network (Ghassemian *et al.*, 2000). However, interestingly, it was the study of the expression pattern of the *Arabidopsis* fruit margin marker YJ80 which uncovered the MEMBRANE-BOUND NOVEL METHYLTRANSFERASE (MNM) gene family (Figure 2).

Germination assays in response to exogenous ABA application indicate that at least some MNM genes may be involved in the control of germination (data not shown). *mnm1* mutants are insensitive to ABA with respect to germination and this effect is further enhanced in *mnm1 mnm2 mnm3* triple mutants.

Despite the MNM1 gene is located 3 Kb downstream YJ80 marker, MNM1 promoter rarely directs expression of β -glucuronidase in the same margin specific pattern as YJ80 (data not shown). On the contrary, β -glucuronidase expression of the MNM1 genes is localized in the developing ovules.

In the present work, we confirmed the expression pattern of the MNM1 gene by In Situ hybridisation. We have also isolated an GFP-tagged transgenic line overexpressing MNM1 which shows a similar phenotype to that of 35S::MNM1 in response to exogenous ABA application. Finally, we further characterized *mnm1mnm2mnm3* triple mutant and 35S::MNM1 phenotypes and we hypothesize that the differences in stem width observed at different growing temperatures can be explained by an abnormal organization of the stem vasculature.

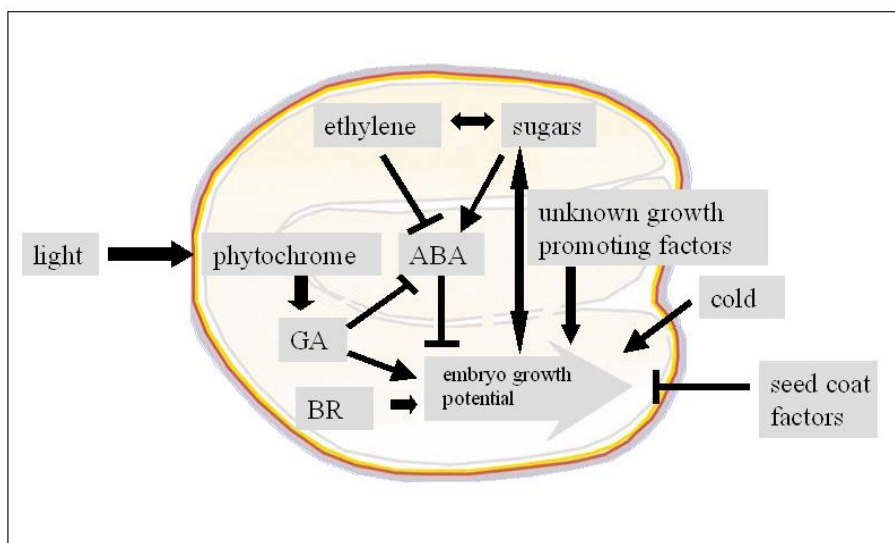


Figure 1. Main factors regulating seed germination. ABA plays a major role in the control of seed germination by repressing it. (Adapted from Bentsink *et al.*, 2002).

Objectives

Overall objective: To contribute to the characterization of the MNM gene family particularly of MNM1, MNM2 and MNM3.

Specific objectives

To assess the responsiveness of GFP-tagged 35S::MNM1 to exogenous ABA by germination assays.

To assess the changes observed in stem width in *mnm1mnm2mnm3* triple mutant, *abi4* mutant, *mnm1* mutant and 35S::MNM1 in response to different growth temperatures by tissue staining.

To confirm the expression pattern of the MNM1 gene in Col-O background observed using GUS reporter gene activity by In Situ hybridization.

To study the effect of ABA, GA and IAA on MNM1 protein localization using GFP-tagged 35S::MNM1 and confocal microscopy.

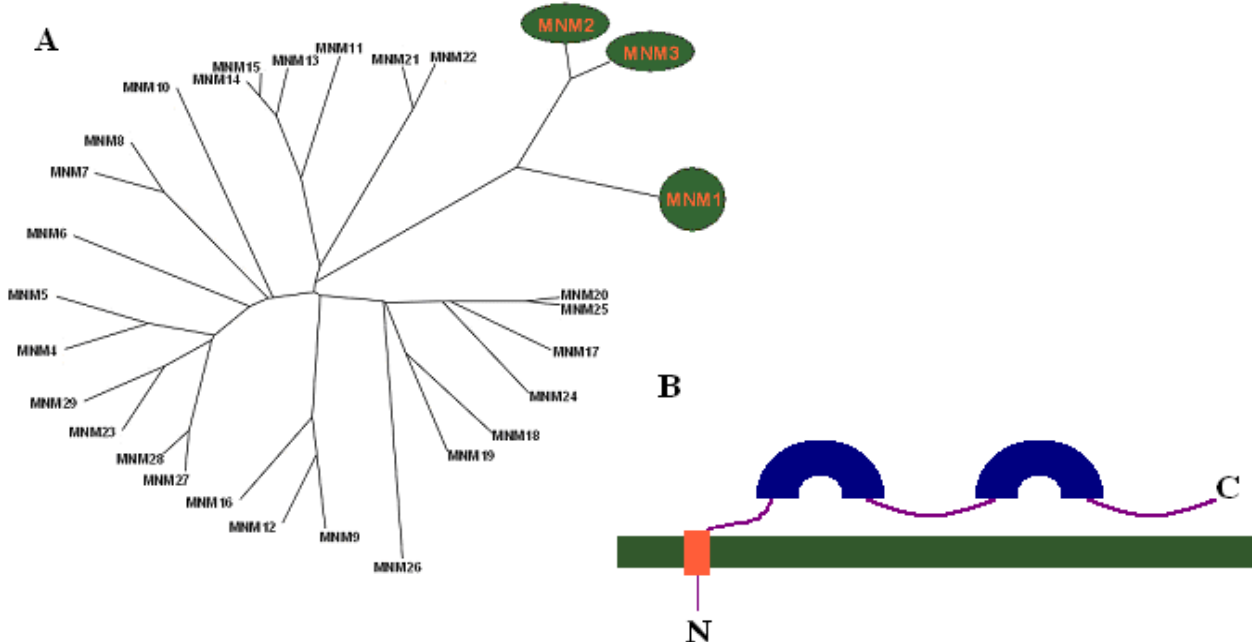


Figure 2. (A) The MNM gene family is formed by 29 genes in Arabidopsis. MNM1, MNM2 and MNM3 formed a more closely related cluster. **(B)** Predicted protein structure of MNM1. In red, the predicted transmembrane segment and, in blue, the predicted SAM-binding and methyltransferase profile.

Results

Expression of MNM1 varies during seed development

Previous work carried out with MNM1::GUS construct suggested that the MNM1 gene is expressed during seed developments (Figure 3). To verify the expression pattern of MNM1 in wt seeds, we performed antisense In Situ hybridization with an MNM1-specific probe. In early stages of fruit development (stage 15, 16a-17), MNM1 expression was localized in the funiculus (Figure 3D and 3E). After complete elongation of the fruit, MNM1 was strongly expressed in the developing embryos (Figure 3F and 3G). These results are highly consistent with those obtained with MNM1::GUS construct (Figure 3A; 3B and 3C), indicating that the expression pattern of MNM1 varies during seed development.

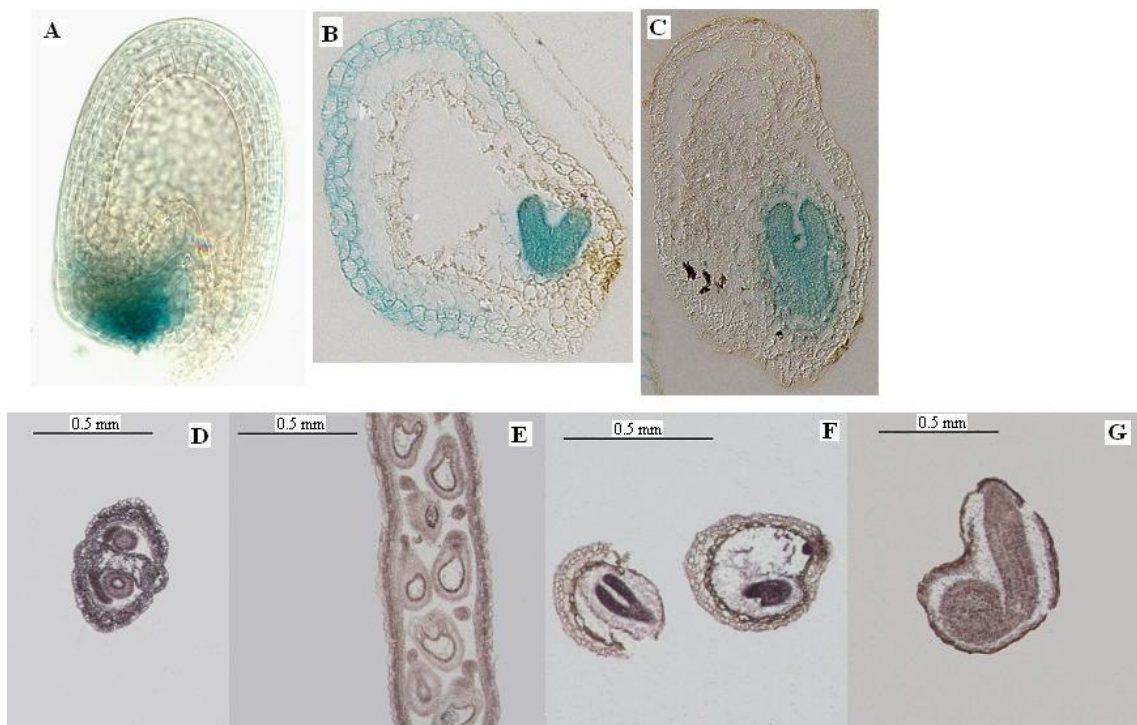


Figure 3. Expression pattern of MNM1. **(A)** MNM1::GUS expression in early fruit developments is localized in the funiculus. **(B)** MNM1::GUS expression in late heart and **(C)** torpedo embryo stages is localized in the embryo. In Situ hybridisation confirmed that MNM1 expression during fruit development **(D)** stage 15 and **(E)** stage 16-17a is localised in the funiculus, while in **(F)** stage 17b and **(G)** stage 18 is localised in the embryo.

Isolation of a GFP-tagged 35S::MNM1 line with a similar phenotype to 35S::MNM1

To determine whether transformation with GFP protein caused any effects on the 35S::MNM1 germination phenotype, a germination assay with five different lines of GFP-tagged 35S::MNM1 was carried out. Two lines (lines 3 and 4) showed a similar phenotype to that of 35S::MNM1 in response to exogenous ABA application (Figure 4). Nevertheless, none of the lines presented a completely overlapping pattern with 35S::MNM1 (Figure 4).

The *mnm1mnm2mnm3* triple mutant and 35S::MNM1 show a differential growth pattern in response to different growing temperatures

To further investigate the effects of *mnm1*, *mnm2* and *mnm3* mutations on plants development, triple mutants plants and plants constitutively overexpressing MNM1 were grown at different temperatures. A considerable difference in stem width was observed between plants grown at 15°C and 28°C (Figure 5A). *mnm1mnm2mnm3* triple mutant plants grown at 15°C showed considerably wider stems than those grown at 28°C. The opposite phenotype was observed in 35S::MNM1 plants where plants grown at 28°C presented significantly wider stems than those grown at 15°C (Figure 5A).

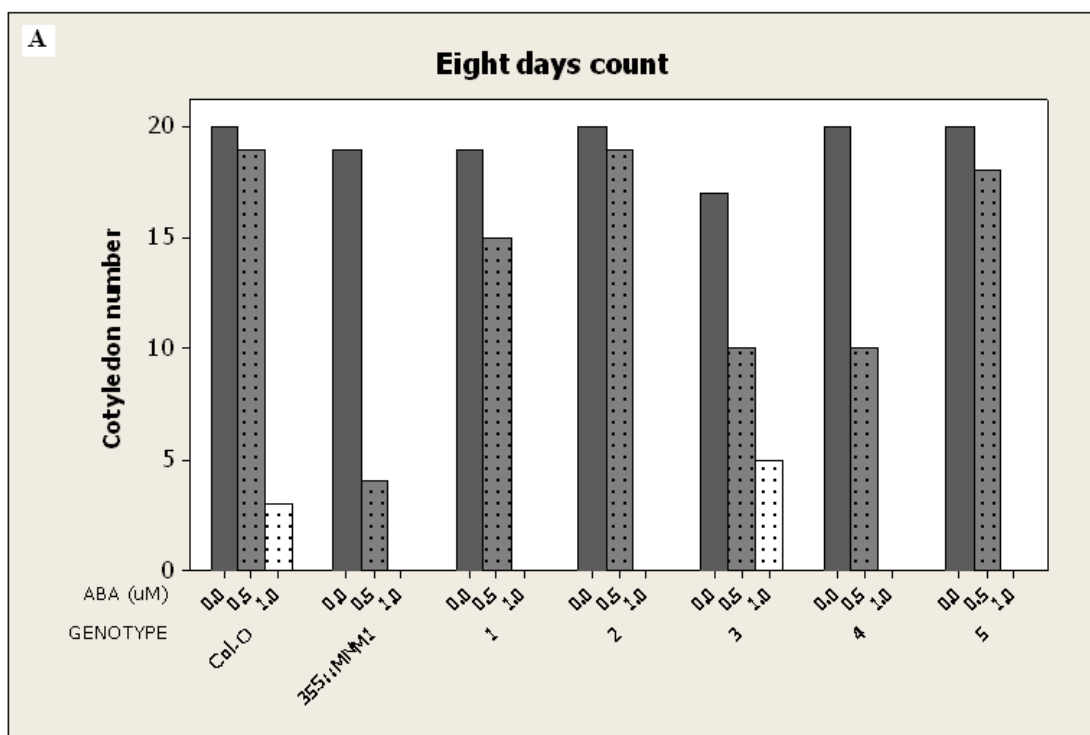


Figure 4. Final count of cotyledons. Different GFP-tagged 35S::MNM1 lines are represented by 1, 2, 3, 4 and 5. Line 4 showed the most similar phenotype to that of 35S::MNM1 in response to exogenous ABA application

To investigate the width differences of *mnm1mnm2mnm3* and 35S::MNM1 in more detail, this sections from below the first internode were observed (Figure 5B). In the wild type, the typical alternate vascular bundle/fiber organization was observed

at both temperatures (Figure 5B). In contrast, *mnm1mnm2mnm3* triple mutant plants were characterized by an abnormal organization of the stem vasculature resulting in a continuous ring of vascular tissues (Figure 5B). Conversely, overexpression of MNM1 at 28°C lead to an increase in the number of vascular bundles (Figure 5B, Table1).

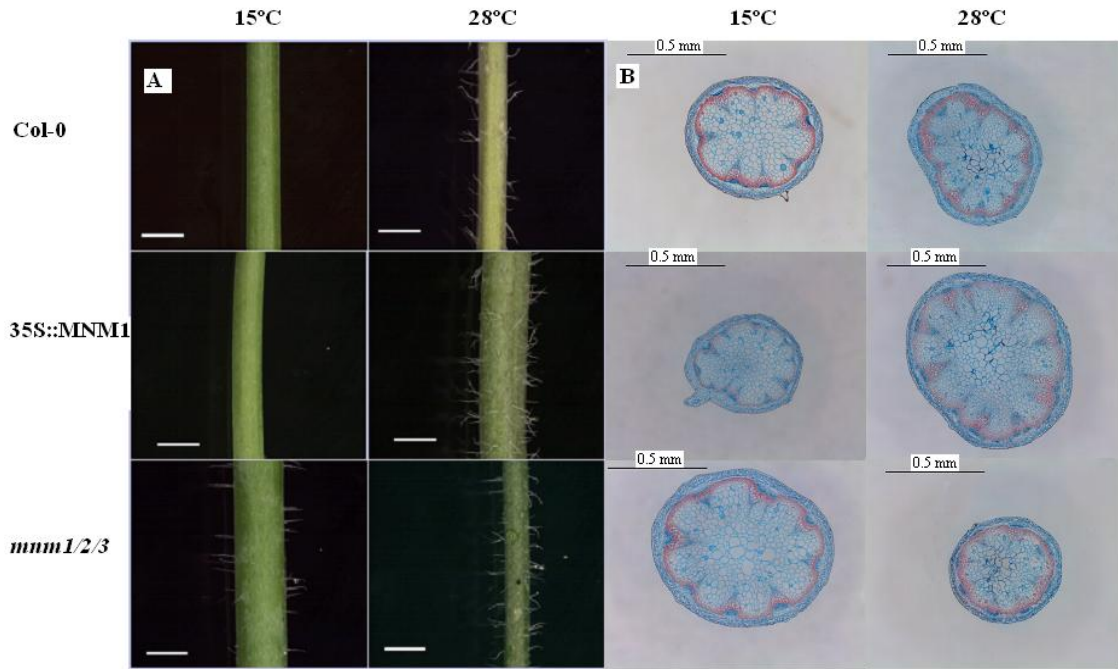


Figure 5. (A) Stems of different genotypes grown at 15°C and 28°C. **(B)** Stained stem sections.

The altered growth pattern in *mnm1mnm2mnm3* triple mutant plants and 35S::MNM1 resulted in a significant effect on the surface area of stem tissues. The total surface area of *mnm1mnm2mnm3* triple mutants grown at 28°C is less than half that of those grown at 15°C (Table 1). On the contrary, the total surface area of 35S::MNM1 plants grown at 28°C is more than twice that of those grown at 15°C (Table 1).

MNM1 may act in various hormone response and/or perception pathways

Careful phenotypic analysis have showed that several of the hormone response mutants have altered sensitivities to various hormones (Ghassemian *et al.*, 2000).

To determine whether this is the case in *mnm1* mutation, the effect of ABA, GA and IAA on MNM1 protein localization was assessed. GFP-tagged 35S::MNM1 line 4 was chosen due to its great resemblance to 35S::MNM1 (Figure 4). Nevertheless, a very low fluorescence signal was obtained by confocal microscopy and, thus, it was impossible to determine whether it constitute a truthful GFP signal (data not shown).

Table 1. Measurements carried out in stem sections of plants grown at 15°C and 28°C.

GENOTYPE	TEMPERATURE (°C)	CELL NUMBER (GREATEST DIAMETRE)	AVERAGE DIAMETRE (mm)	AREA (mm ²)	VASCULAR BUNDLE NUMBER
Col-O	15	44	1.31	1.35	8
Col-O	28	60	1.34	1.41	12
35S::MNM1	15	46	1.09	0.93	12
35S::MNM1	28	61	1.72	2.32	11
<i>mnm1/2/3</i>	15	47	1.74	2.38	9
<i>mnm1/2/3</i>	28	42	1.11	0.97	8-9*

Discussion

Although genetic screenings have successfully uncover several of the molecular genetic components of the ABA signalling pathway, ABA signalling and perception remains a poorly understood process. We have previously shown that at least some members of the MNM gene family are involved in the ABA signalling network and, therefore, in the control of germination. These results are consistent with the expression pattern of MNM1 shown in this report.

mnm1mnm2mnm3 triple mutants are insensitive to ABA application with respect to germination. We have shown that *mnm1mnm2mnm3* triple mutants are also

characterized by an altered pattern of vascular tissues when grown at 28°C. This vascular organization is very similar to that observed in *hca* (Pineau *et al.*, 2005) and *cvo* (Parker *et al.*, 2003) mutants. Although no relation with temperature has been described in *hca* and *cvo* mutants, the HCA and CVO genes are predicted to be involved in auxin and/or cytokinin perception and/or response.

In conclusion, a major aim in the future will be to continue with the study of the potential role of the MNM gene family in other phytohormone signalling pathways. More detailed histological studies of the stems of *mnm1mnm2mnm3* triple mutant and 35S::MNM1 plants will also help to verify whether, as in *hca* mutants, it is the unusually high secondary xylem production the responsible for the observed vascular patterning.

Materials and methods

Plant Materials and Growth Conditions

Arabidopsis ecotype Columbia was used as the wild type in this study. All the seeds were provided by L. Østergaard. For germination, *mnm1mnm2mnm3*, 35S::MNM1, Col-O and five lines of GFP-tagged 35S::MNM1 seeds were washed with 70% ethanol, rinsed with water and stratified on MS-sucrose plates at 4°C. Col-O, 35S::MNM1 and *mnm1mnm2mnm3* plants were grown at 15°C (16h photoperiod) and 28°C (12h photoperiod) until full development for stem tissue collection. For in Situ hybridisation, Col-O plants were grown under standard conditions and siliques samples were taken at 15, 16-17a, 17b and 18 developmental stages. T₃ seeds from GFP-tagged 35S::MNM1 line four were grown for 7 d at 22°C in MS-sucrose in order to perform confocal microscopy.

Germination assays

For germination experiments, two weeks old sterilized seeds were sown on 8% Bacto agar containing 0.25xMurashige and Skoog salts, 0.5% MES and different

concentration of ABA (0uM, 0.5uM and 1uM). After 4 d of stratification at 4^oC, the plates were placed at 22^oC under 16h photoperiod. Germination was scored every two days for cotyledon emergence. In all experiments, approximately 25 seeds were used.

Tissue staining with Alcian Blue 8Gx and Safranin-O

Stem fragments below the first internode were selected for tissue staining. Approximately 1 cm sections for each genotype grown at different temperatures were vacuum-infiltrated with FAA solution (3.7% formaldehyde, 5% acetic acid and 50% ethanol) overnight at room temperature. To continue the tissue fixation, a serial of half an hour ethanol washes were performed (50%, 60%, 70%, 80% and 90%). The tissues were stored overnight in 95% ethanol at 4^oC. A second round of half an hour washes was carried out the following day (3x100% ethanol, 75% ethanol/25% histoclear, 50% ethanol/50% histoclear, 25% ethanol/75% histoclear and 3x100% histoclear). The tissues were stored overnight in 50% histoclear/50% paraplast at 60^oC. To conclude the tissue fixation, six washes of paraplast were performed during a two day time period. Stems were finally embedded in paraffin and stored in blocks at 4^oC. To make 8um thin transversal stem sections, a RM 2255 rotary microtome (Leica) was used. After deparaffinization, sections were treated with Alcian Blue 8Gx/Safranin-O solution (0.05% Alcian Blue 8Gx and 0.01% Safranin-O in 0.1 M acetate buffer [pH 5.0]) for 20 min. Sections were examined under light microscopy using a MZ 16 stereomicroscope (Leica) and the images were captured with a DFC 280 digital camera (Leica). On captured images, measurements were performed using Leica Application Suite (LAS) software.

In Situ hybridisation

To synthesize MNM1 antisense probe in vitro, template cDNA was provided by L. Østergaard. After PCR amplification and DNA purification from gel bands (QIAquick ® Gel Extraction Kit, Qiagen), the PCR product was ligated to pGEM®-T Easy Vector (Promega) and Top 10 E. coli competent cells (Invitrogen ®) were

heat shock transformed. After plasmid purification from overnight E. coli cultures (QIAprep Spin Miniprep Kit, Qiagen), sequence orientation was checked and pSF1003 plasmid containing antisense MNM1 sequence was digested with SpeI (Roche). The resulting linear DNA was used as a template for in vitro transcription reaction (RNAMaxxx™ High Yield Transcription Kit, Stratagene ®). To synthesize digoxigenin-labeled probes, in vitro transcription reactions were carried out with digoxigenin-11-UTP using T7 RNA polymerase. The labelled RNA probe was carbonate-hydrolyzed to generate fragments between 75-150bp.

Tissue fixation, paraffin embedding and sectioning (8um) procedures were the same as described in the Alcian blue 8GX and Safranin-O staining section. After deparaffinization and rehydration, sections were treated with Proteinase K solution (100mM Tris-HCl [pH 8.0], 50mM EDTA, 1mg/ml Proteinase K) at 37 °C for 30 min, and then incubated for 2 min in PBS solution containing 2mg/ml glycine. After two further washes in PBS, slides were fixed in 3.7% formaldehyde solution for 10 min at room temperature. Sections were then subjected to two 5 min washes in PBS and to acetylation reaction with 0.5% acetic anhydride in 0.1 M triethanolamine 9pH 8.0). After dehydration, hybridization was carried out at 51 °C overnight in hybe solution (per slide: 25ul 10x in situ salts, 100ul deionized formamide, 50ul 50% Dextran sulphate, 5ul 50xDenhardt's solution, 12.5ul yeast tRNA (20ug/ml) and 7.5ul H₂O). After hybridization, the slides were washed twice in 0.2xSSC at 55 °C for 1h and then washed in PBS at room temperature for 5 min. This was followed by 45 min wash in 1% Boehringer Block (100mM Tris-HCl [pH 7.5], 150mM NaCl and 1% Boehringer Block) at room temperature and a 45 min incubation in 1% BSA at room temperature. Localisation of the digoxigenin-labelled probe was immunologically detected using anti-digoxigenin-AP (Roche) diluted in 1% BSA solution and BCIP/NBT substrate (Promega) wsa used for colour developments. Light microscopy was performed as described above.

Confocal microscopy

For confocal microscopy, 7 d old GFP-tagged 35S::MNM1 seedlings were transferred to Ms-sucrose plates containing 2 uM ABA, 1 uM GA3, 1 uM IAA or

1uM ethanol. After 24 h, the expression of MNM1 protein was monitored using a Leica DM RE confocal microscope equipped with a x20 water-immersion objective and a Leica TCS SP digital camera. The software Leica confocal software was used for image processing.

References

- Alonso, J. M., Hirayama, T., Roman, G., Nourizadeh, S. and Ecker, J. R. (1999) EIN2, a bifunctional transducer of ethylene and stress responses in *Arabidopsis*. Science 284: 2148-2152
- Altamura, M. M., Possenti, M., Matteuci, A., Baima, S., Ruberti, I. and Morelli, G. (2001) Development of the vascular system in the inflorescence stem of *Arabidopsis*. New Phytologist 151: 381-389
- Bentsink, L. and Koornneef, M. (2002) Seed dormancy and germination. The *Arabidopsis* book.
- Bewley, J. D. (1997) Seed germination and dormancy. The Plant Cell 9: 1055-1066
- Caño-Delgado, A. I., Metzlaff, K. and Bevan, M. W. (2000) The *eli1* mutation reveals a link between cell expansion and secondary cell wall formation in *Arabidopsis thaliana*. Development 127: 3395-3405
- Chen, J., Pandey, S., Huang, J., Alonso, J. M., Ecker, J. R., Assman, S. M. and Jones, A. M. (2004) GCR1 can act independently of heterotrimeric G-protein in response to brassinosteroids and gibberellins in *Arabidopsis* seed germination. Plant Physiology 135: 907-915
- Cutler, S., Ghassemian, M., Bonetta, D., Cooney, S. and McCourt, P. (1996) A protein farnesyl transferase involved in abscisic acid signal transduction in *Arabidopsis*. Science 273: 1239-1241
- Finkelstein, R. R. and Rock, C. D. (2002) Abscisic acid biosynthesis and response. The *Arabidopsis* book.
- Finkelstein, R. R., Wang, M. L., Lynch, T. J., Rao, S. and Goodman, H. M. (1998) The *Arabidopsis* abscisic acid response locus ABI4 encodes an APETALA2 domain protein. The Plant Cell 10: 1043-1054

- Ghassemian, M., Nambara, E., Cutler, S., Kawaide, H., Kamiya, Y. and McCourt, P. (2000) Regulation of abscisic acid signalling by the ethylene response pathway in *Arabidopsis*. *The Plant Cell* 12: 1117-1126
- Lopez-Molina, L., Mongrand, S. and Chua, N. (2001) A postgermination developmental arrest checkpoint is mediated by abscisic acid and requires the ABI5 transcription factor in *Arabidopsis*. *PNAS* 98 (8): 4782-4787
- Nambara, E., Kawaide, H., Kamiya, Y. and Naito, S. (1998) Characterization of an *Arabidopsis thaliana* mutant that has a defect in ABA accumulation: ABA-dependent and ABA-independent accumulation of free amino acids during dehydration. *Plant Cell Physiol.* 39(8): 853-858
- Okamoto, M., Kuwahara, A., Seo, M., Kushiro, M., Asami, R., Asami, R., Hirai, N., Kamiya, Y., Koshiba, T. and Nambara, E. (2006) CYP707A1 and CYP707A2, which encode abscisic acid 8'-hydroxylases, are indispensable for proper control of seed dormancy and germination in *Arabidopsis*. *Plant Physiology* 141: 97-107
- Parker, G., Schofield, R., Sundberg, B. and Turner, S. (2003) Isolation of COV1, a gene involved in the regulation of vascular patterning in the stem of *Arabidopsis*. *Development* 130: 2139-2148
- Penfield, S., Li, Y., Gilday, A. D., Graham, S. and Graham, I. A. (2006) *Arabidopsis* ABA INSENSITIVE4 regulates lipid mobilization in the embryo and reveals repression of seed germination by the endosperm. *The Plant Cell Preview* (on line)
- Pineau, C., Freydier, A., Ranocha, P., Jauneau, A., Turner, S., Lemonnier, G., Renou, J., Tarkowski, P., Sandberg, G., Jouanin, L., Sundberg, B., Boudet, A., Goffner, D. and Pichon, M. (2005) *hca*: an *Arabidopsis* mutant exhibiting unusual cambial activity and altered vascular patterning.
- Yamaguchi, S., Kamiya, Y. and Sun, T. (2001) Distinct cell-specific expression patterns of early and late gibberellin biosynthetic genes during *Arabidopsis* seed germination. *The Plant Journal* 28(4): 443-453

SECOND ROTATION REPORT

Introduction

The GA-DELLA mechanism plays a vital role in angiosperm growth regulation [1-13]. DELLA proteins restrain plant growth by inhibiting cell proliferation and expansion [5]. Plant growth is stimulated by GA-mediated DELLA protein destruction. In response to GA, DELLA proteins are first phosphorylated and then targeted for degradation in the 26S proteosome by polyubiquitination [3, 5, 14].

The study of GA-DELLA regulatory system in angiosperms (particularly in *Arabidopsis thaliana*) has provided deep insights into plant growth regulation. However from an evolutionary point of view, the study of GA-DELLA mediated growth regulation has been very limited as only the most recent land plant lineage has been so far considered (Figure 1).

In the present report we show that *Selaginella kraussiana* does not respond to exogenous GA₃ and that application of GA₃ does not recover PAC caused inhibited growth. Based on these findings amongst other, we hypothesize that although DELLA proteins are likely to be conserved across all land plant lineages, DELLA proteins role in growth regulation evolved subsequently, probably during lycophytes and moniliforms divergence (~420-380MYA).



Figure 1. Simplified version of the plant phylogenetic tree. Abbreviations: E, euphyllophytes; F, flowering plants (angiosperms); L, land plants; S, seed plants; V, vascular plants. Numbers represent MYA. (Adapted from Weng *et al.* [15], Pryer *et al.* [16] and Langdale *et al.* [17])

Objectives

Overall objective: To contribute to the understanding of GA-DELLA plant growth regulatory system evolution.

Specific objectives

To clone and sequence DELLA-like gene sequences from *Pinus taeda*, *Ceratopteris richardii* and *Nephrolepis exaltata variegata*.

To assess the responsiveness of *Selaginella kraussiana* and *Ceratopteris richardii* to exogenous GA₃ and/or PAC application by growth experiments.

To search for DELLA-related proteins in extracts from bryophytes, lycophytes, ferns and gymnosperms by western blot analysis.

Results

Inconclusive cloning of DELLA-like genes in *Pinus taeda*

A TAIL-PCR approach was used to clone DELLA-like genes in *Pinus taeda* based on *Pinus taeda* EST database. Two EST clones (NXRV119_F07 and NXNV012B07) with high similarity to Arabidopsis RGA protein were selected to design specific primers.

From the amplified gene candidates, three clones named Pinus1, Pinus2 and Pinus3 were partially similar to Arabidopsis DELLA proteins when compared to *Arabidopsis thaliana* genome (www.Arabidopsis.org). Pine1 and Pine2 sequences showed 43% and 51% identity respectively to AtRGL1 amino acid sequence while Pine3 sequence showed 44% identity to AtRGA amino acid sequence (Figure 2A and 2B). Pine1 and Pine2 sequences correspond with the scarecrow domain of AtRGL1 and Pine3 sequence correspond with part of the DELLA domain of AtRGA (Figure 2A and 2B).

Interestingly, several stop codons interrupted Pine1, Pine2 and Pine3 clone sequences (data not shown) and only a middle fragment flanked by two stop codons matched Arabidopsis DELLA proteins (Figure 2A and 2B). Attempts to overcome this difficulty by the design of new primers and repetition of the PCR procedure failed to produce any different results.

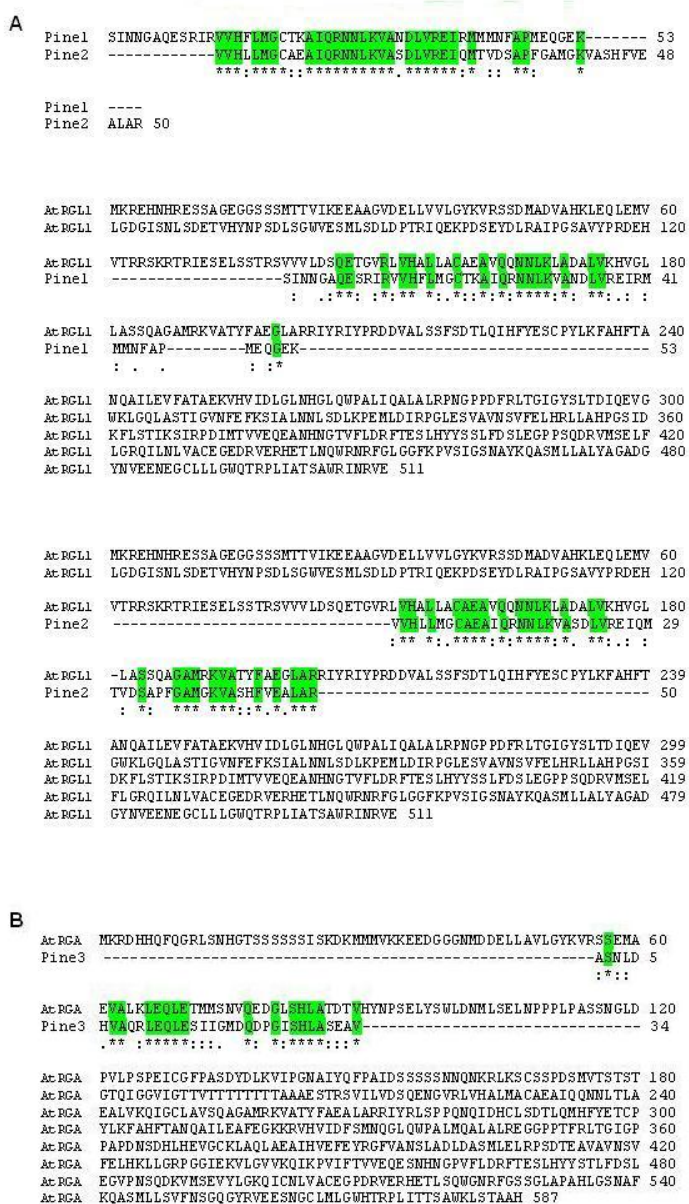


Figure 2. (A) Alignments of DELLA-like sequences from Pine1 and Pine2 clone sequences, of DELLA-like sequence from Pine1 clone with AtRGL1 and of DELLA-like sequence from Pine2 clone with AtRGL1 respectively. **(B)** Alignment of DELLA-like sequence from Pine3 clone with AtRGA.

Response of *Selaginella kraussiana* and *Ceratopteris richardii* to exogenous GA application

DELLA-like and GID1-like proteins are known to be conserved in lower plants such as *Physcomitrella patens* (Bryophyte) and *Selaginella kraussiana* (lycophytes)

(unpublished data). To test whether GA-DELLA mechanism operates in *Selaginella kraussiana*, plants were treated with GA₃ and/or PAC (GA-biosynthesis inhibitor paclobutrazol). Exogenous GA₃ did not promote the growth of *S. kraussiana* (Figure 3) and, although PAC inhibited its growth, GA₃ application did not recover this phenotype (data not shown).

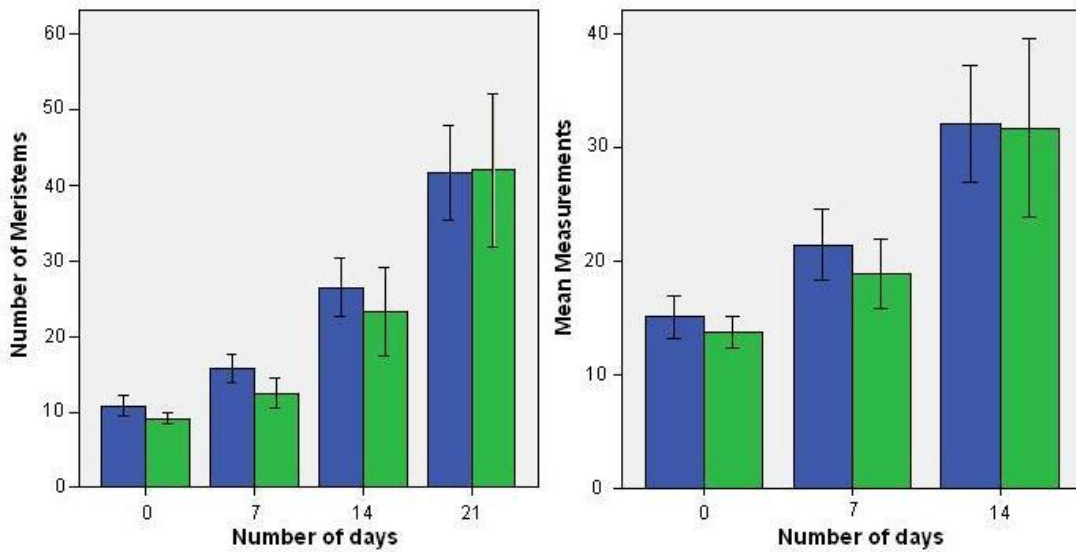


Figure 3. Representation of *S. kraussiana* growth in response to exogenous GA₃ (blue: GA₃ treatment; green: control). Growth is expressed as number of meristems (Harrison *et al.*[18]) and total length.

In order to determine whether GA-DELLA mechanism is functional in moniliforms (ferns and horsetails), fertilised hemaphrodite gametophytes were grown in GA₃ supplemented media. Although no difference was observed in the timing of sporophyte development and/or growth pattern, sporophytes grown in GA₃ supplemented media showed a paler green color pholiage (Figure 4).

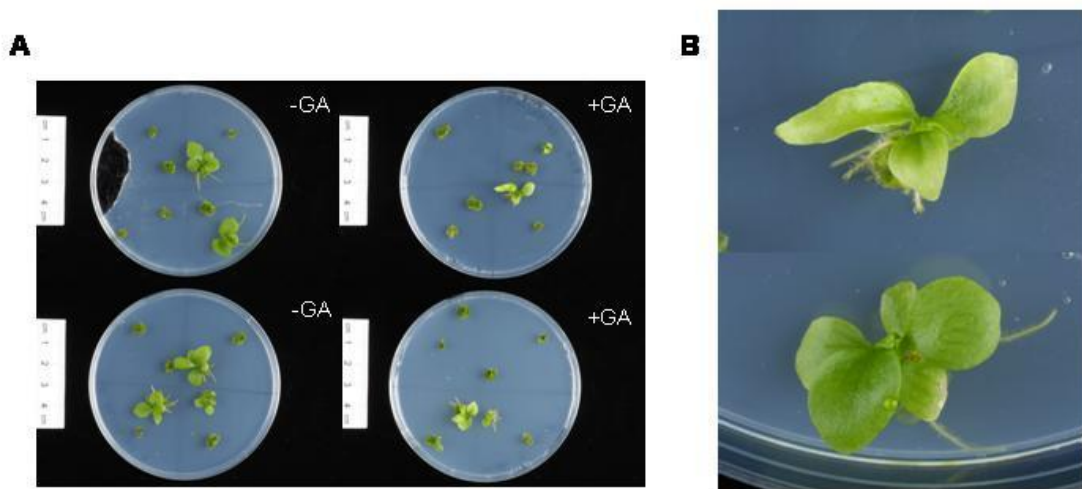


Figure 4. (A) Color difference between sporophytes grown in GA_3 supplemented plates (right) and control plates (left) **(B)** Sporophytes shown at a higher magnification (top: GA_3 treated; bottom: control).

Antibodies raised against *Arabidopsis* DELLA proteins fail to recognise *Physcomitrella patens* and *Selaginella kraussiana* DELLA-like proteins

To determine whether *Arabidopsis* DELLA specific BC9 and polyclonal antibodies could be used to search for DELLA-related proteins in lower plants, immunodetection experiments were performed in extracts from *Physcomitrella patens* and *Selaginella kraussiana* (Figure 5). BC9 antibody is raised against amino acids that form part of the DELLA domain which are partially conserved in *S. kraussiana* DELLA-like protein. Nevertheless, BC9 did not recognise *S. kraussiana* or *P. patens* DELLA-like proteins (Figure 5A).

In order to ensure that low expression levels of DELLA-like proteins were not preventing the immunodetection, crude yeast proteins extracts that contain SkDELLA (*S. kraussiana* DELLA-like protein) and PpDELLA (*P. patens* DELLA-like protein) were used. Neither BC9 antibody or polyclonal antibody recognised SkDELLA or PpDELLA proteins overexpressed in yeast (Figure 5B and 5C)

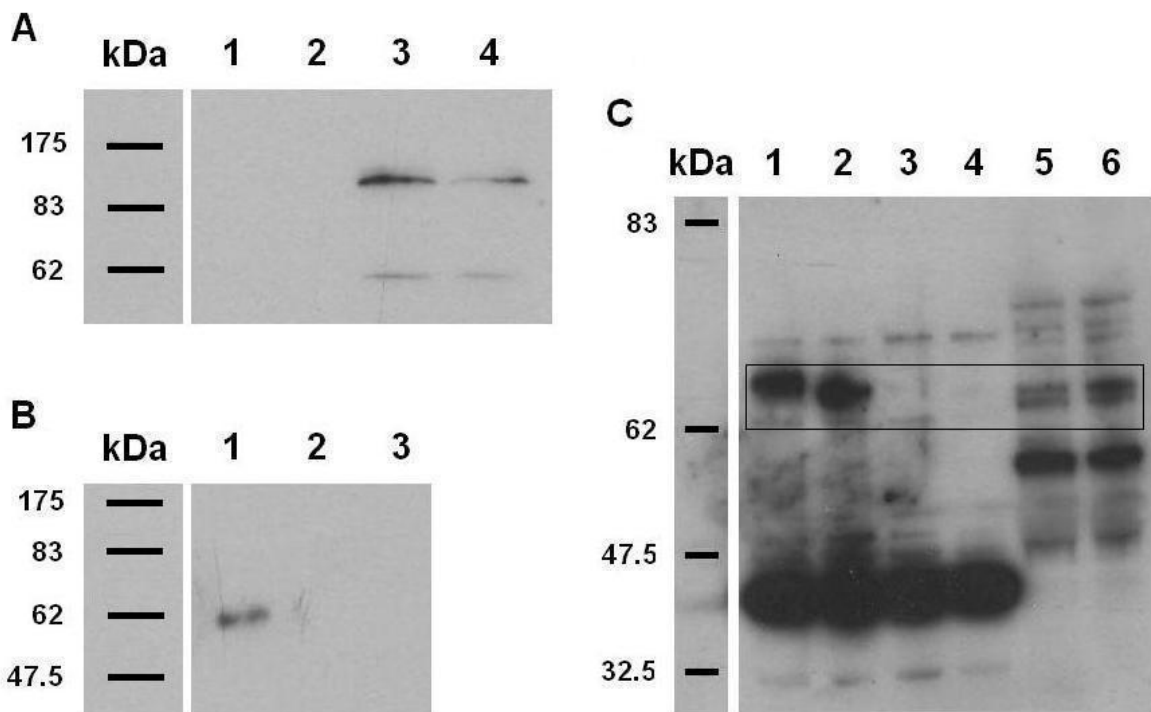


Figure 5. **(A)** Western blot analysis using BC9 antibody. Lane 1, protein extracts from *S. kraussiana* treated with GA₃; Lane 2, protein extracts from *S. kraussiana* non-treated; Lane 3, protein extracts from *P. patens* wild type; Lane 4, protein extracts from *P. patens* doble DELLA knock out. Unspecific bands shown in lane 3 and 4. **(B)** Western blot analysis using BC9. Lane 1, crude yeast protein extract containing RGA protein (positive control); Lane 2, crude yeast protein extract containing SkDELLA; Lane 3, crude yeast extract containing PpDELLA. **(C)** Western blot analysis using polyclonal antibody. In box: Lane 1, crude yeast protein extract containing RGL1 protein (positive control, single band); Lane 2, crude yeast protein extract containing RGA protein (positive control, single band), Lane 3, crude yeast extract containing PpDELLA; Lane 4, crude yeast protein extract containing SkDELLA; Lane 5, protein extracts from *A. thaliana* gai mutant (positive control, two bands showing DELLA proteins) Lane 6, protein extracts from *A. thaliana* wild type (Ler) (positive control, two bands showing DELLA proteins).

Discussion

Although GA-DELLA growth regulatory system has intensively been studied in angiosperms [1-13], to the authors knowledge, no similar studies have been carried out in lower plants. DELLA-like proteins have previously been identified in bryophytes (*P. patens*) and lycophytes (*S. kraussiana*) (Y. yasumura, unpublished data) and, thus, it is very likely that DELLA-like proteins are conserved across all land plant lineages. The failure to clone DELLA-like proteins in gymnosperms (*P. taeda*) (Figure 2) could be explained by at least 3 factors: low primer specificity, presence of pseudogenes or presence of introns (highly improbable because to date all characterised DELLA proteins lack introns).

DELLA-like and GID-like proteins are conserved in both bryophytes (*P. patens*) and lycophytes (*S. kraussiana*) (unpublished data). Nevertheless, exogenous GA₃ does not promote growth or recover PAC inhibitory effect in *P. patens* (data not shown) or *S. kraussiana* (Figure 3). Previous studies have shown that exogenous GA₃ promotes male development of sexually undetermined *Ceratopteris richardii* gametophytes [19-23]. Here we have shown that exogenous GA₃ application to already fertilised hemaphrodite gametophytes results in the development of paler green sporophytes (Figure 4), a phenotype also observed in wild type *Arabidopsis* plants repeatedly treated with GA₃ [7].

The findings in this report support our hypothesis that GA-DELLA mechanism is conserved across all land plant lineages. However, the role of GA-DELLA mechanism in plant growth regulation evolved subsequently, probably during lycophytes and moniliforms divergence (~420-380MYA).

Materials and methods

Plant material and plant growth experiments

P. taeda needles were provided by Y. Yasumura. *Ceratopteris richardii* spores were germinated on 1% Bacto agar-C-fern solidified medium [pH 6.0] (125mg/l

NH_4NO_3 , 500mg/l KH_2PO_4 , 120mg/l $\text{MgSO}_4 \cdot 7\text{H}_2\text{O}$, 26mg/l $\text{CaCl}_2 \cdot 2\text{H}_2\text{O}$, 0.25mg/l $\text{MnSO}_4 \cdot \text{H}_2\text{O}$, 0.37 mg/l $\text{CuSO}_4 \cdot 5\text{H}_2\text{O}$, 0.52mg/l $\text{ZnSO}_4 \cdot 7\text{H}_2\text{O}$, 1.86mg/l H_3BO_3 , 0.037mg/l $(\text{NH}_4)_6\text{Mo}_7\text{O}_{24} \cdot 4\text{H}_2\text{O}$, 27.8 mg/l $\text{FeSO}_4 \cdot 7\text{H}_2\text{O}$ and 37.3 mg/l Disodium EDTA $\cdot 2\text{H}_2\text{O}$). Plates were kept in a growth chamber under 16h light/8h dark regime and 25°C temperature. For *Ceratopteris richardii* GA growth experiments, fertilised *Ceratopteris* hermaphrodites gametophytes were placed on 1% Bacto agar-solidified C-fern medium plates containing 10uM GA_3 or 10uM ETOH (controls). Growth was scored every two days. In all experiments, 24 gametophytes were used. For genomic DNA extraction, mature *Nephrolepis exaltata variegata* sporophytes and *Selaginella kraussiana* cuttings were grown in a growth chamber under 16h light/8h dark regime and 23°C. For *S. kraussiana* GA growth experiments, twelve cuttings with similar number of meristems were grown in individual pots in a growth chamber under 16h light/8h dark regime and 23°C. Pots were sprayed twice a week with 100uM GA_3 or 100uM ETOH (control). For PAC and GA growth experiments, six cuttings with similar number of meristems were grown in individual pots in a growth chamber under 16h light/8h dark regime and 23°C. Pots were watered twice a week with 125uM PAC and sprayed with 100uM GA_3 or 100uM ETOH (control) [7].

DNA extraction

Genomic DNA from *P. taeda* needles, *Ceratopteris richardii* gametophytes and *Nephrolepis exaltata variegata* buds frozen at -80°C was extracted as follows: tissue was ground to fine powder using a morter and pessel in the presence of liquid N_2 . A spatula full of ground tissue was added to centrifuge tubes containing 1ml of extraction buffer (1% PEG, 100mM TrisHCl [pH 7.0], 1.4M NaCl, 2% CTAB, 20mM EDTA and 0.3% SLS) and 10ul of 10mg/ml RNase. Tubes were incubated at 65°C for 15 min. After incubation, 714ul of chloroform:isoamyl alcohol (24:1) were added to the tubes and mixed. The volume was equally distributed into EPPS and centrifugated at 13,000 r.p.m. for 5 min. The supernatant was transferred to new EPPS and 70ul of 3M ammonium acetate were added. After mixing by inversion, 726ul of isopropanol were added, mixed and centrifugated at 13,000 r.p.m. for 5 min. The supernatant was discarded and the pellet was

washed with 600ul of 70% ETOH. After resuspending the pellet, EPPS were centrifugated at 14,000 r.p.m. for 15 min. The pellet was finally dissolved in 60ul of TE buffer and DNA concentration was determined by agarose gel electrophoresis.

TAIL-PCR and Degenerative PCR

Thermal asymmetric interlaced (TAIL)-PCR was used to amplify DELLA-like proteins from *P. taeda* genomic DNA. Primary TAIL-PCR reactions (20ul) contained 1xPCR buffer (Invitrogen), 150uM dNTPs, 1-20uM genomic DNA, 0.3ul of Taq DNA polymerase (Invitrogen), 0.4ul DMSO, 1.75mM MgCl₂, 0.15uM of specific primer and 2uM AD1 primer. Aliquots (1ul) from 40-fold dilutions of the primary PCR products were used as template for the secondary TAIL-PCR reactions (25ul) containing 1xPCR buffer (Invitrogen), 160uM dNTPs, 0.3ul of Taq DNA polymerase (Invitrogen), 0.5ul DMSO, 1.8mM MgCl₂, 0.2uM of specific primer and 2uM AD2 primer. After amplification, the primary TAIL-PCR products (1ul aliquots of 10-fold dilutions) and the secondary TAIL-PCR products (1ul aliquots of 10-fold dilutions) were re-amplified in 25ul tertiary reactions. Components and their concentrations were the same as in the secondary reaction except that AD2 was replace by AD3. Amplified products from the secondary and tertiary reactions were analysed by agarose gel electrophoresis. A difference in product size consistent with primer positions was used to choose the candidates for sequencing.

Degenerative PCR was used to amplify DELLA-like proteins from *Ceratopteris richardii* and *Nephrolepis exaltata variegata* genomic DNA. Degenerative PCR reactions (25ul) contained 1xPCR buffer (Invitrogen), 200uM dNTPs, 0.25ul of Taq DNA polymerase (Invitrogen), 1.5mM MgCl₂ and 2uM of each primer. After amplification, 1ul aliquots of the primary PCR reaction were re-amplified in a 25ul nested PCR reaction. Components and their concentrations were the same as in the primary reaction. Amplified products from the degenerative PCR reactions were analysed by agarose gel electrophoresis. Expected product size was used to choose the candidates for sequencing.

Western Blot analysis

BC9 and polyclonal antibodies were provided by J. Rakonjac. Wild type *Physcomitrella patens* protein extract, double DELLA knock out *P. patens* protein extract, crude yeast protein extract that contain RGA protein, crude yeast protein extract that contain RGL1 protein, crude yeast protein extract that contain SkDELLA (*Selaginella kraussiana* DELLA-like protein) and crude yeast protein extract that contain PpDELLA (*P. patens* DELLA-like protein) were kindly provided by Y. Yasumura. Total protein extracts from *S. kraussiana* meristems (from GA₃ treated and untreated plants) and *Ceratopteris richardii* gametophytes were obtained by grinding 10mg of tissue per 20ul of grinding buffer (50mM Tris-HCl [pH 7.5], 400mM NaCl, 1mM EDTA, 20uM MG132 and complete protease inhibitor cocktail (Sigma-Aldrich)) and pelleting insoluble debris by centrifugation at 14,000 r.p.m for 10 min at 4°C. Protein concentration in the supernatant was determined by the Bradford assay. Samples were separated on SDS-PAGE gels (Invitrogen) of 12% and transferred to PVDF membranes. Western blots were done according to His-Taq Monoclonal antibody protocol (Novagen). BC9 antibody was used at 1:1000 dilution and polyclonal antibody was used at 1:100 dilution. Anti-mouse HRP conjugate IgG (SouthernBiotech) and HRP conjugated anti-rabbit (Sigma) at 1:10,000 dilution were used respectively as secondary antibodies. Membranes were developed by using the ECL Plus (Amersham Pharmacia).

References

1. C. Bolle, *Planta* 218, 683-692 (2004)
2. J. Peng, P. Carroll, D. E. Richards, K. E. King, R. J. Cowling, G. P. Murphy, N. P. Harberd, *Genes and Development* 11, 3194-3205 (2007)
3. N. P. Harberd, *Science* 299, 1853-1854 (2003)
4. P. Archard, H. Cheng, L. D. Grauwe, J. Decat, H. Schoutteten, T. Moritz, D. V. D. Straeten, J. Peng, N. P. Harberd, *Science* 311, 91-94 (2006)
5. L. Alvey, N. P. Harberd, *Physiologia Plantarum* 123, 153-160 (2005)

6. J. Peng, D. E. Richards, N. M. Hartley, G. P. Murphy, K. M. Devos, J. E. Flinham, J. Beales, L. J. Fish, A. J. Worland, F. Pelica, D. Sudhakar, P. Christou, J. W. Snape, M. D. Gale, N. P. Harberd, *Nature* 400, 256-261 (1999)
7. S. E. Jacobsen, N. E. Olszewski, *The Plant Cell* 5, 887-896 (1993)
8. H. Cheng, L. Qin, S. Lee, X. Fu, D. E. Richards, D. Cao, D. Luo, N. P. Harberd, J. Peng, *Development* 131, 1055-1064 (2004)
9. L. Tyler, S. G. Thomas, J. Hu, A. Dill, J. M. Alonso, J. R. Ecker, T. Sun, *Plant Physiology* 135, 1008-1019 (2004)
10. A.L. Silverstone, C. N. Ciampaglio, T. Sun, *The Plant Cell* 10, 155-169 (1998)
11. K. Gomi, A. Sasaki, H. Itoh, M. Ueguchi-Tanaka, M. Ashikari, H. Kitano, M. Matsuoka, *The Plant Journal* 37, 626-634 (2004)
12. M. Nakajima, A. Shimada, Y. Takashi, Y. Kim, S. Park, M. Ueguchi-Tanaka, H. Suzuki, E. Katoh, S. Luchi, M. Kobayashi, T. Maeda, M. Matsuoka, I. Yamaguchi, *The Plant Journal* 46, 880-889 (2006)
13. A. Dill, S. G. Thomas, J. Hu, C. M. Steber, T. Sun, *The Plant Cell* 16, 1392-1405 (2004)
14. H. Itoh, M. Matsuoka, S. M Steber, *TRENDS in Plant Science* 8(10), 492-496 (2003)
15. J. Weng, M. Tanurdzic, C. Chapple, *BMC Genomics* 6(85) (2005)
16. K. M. Pryer, H. Schneider, E. A. Zimmer, J. A. Banks, *TRENDS in Plant Science* 7(12), 550-554
17. J. A. Langdale, C.J. Harrison, personal communication
18. C. J. Harrison, M. Rezvani, J. A. Langdale, *Development* 134, 881-889 (2007)
19. T. R. Warne, L. g. Hickok, *Plant Physiology* 89, 535-538 (1989)
20. J. A. Banks, *Development* 120, 1949-1958 (1994)
21. J. A. Banks, *Annual Review of Plant Molecular Biology* 50, 163-186 (1999)
22. M. D. Schedlbauer, *Planta* 116, 39-43 (1974)
23. M. Tanurdzic, J. A. Banks, *The Plant Cell* 16, S61-S71 (2004)
24. A. Chatterjee, S. J. Roux, *Journal of Plant Growth Regulation* 19, 284-289 (2000)
25. S. K. Floyd, J. L Bowman, *International Journal of Plant Science* 168, 1-36 (2007)
26. A. Maizel, M. A. Busch, T. Tanahashi, J. Perkovic, M. Kato, M. Hasebe, D. Weigel, *Science* 308, 260-263 (2005)

27. T. Nishiyama, T. Fujita, T. Shin, M. Seki, H. Nishide, I. Uchiyama, A. Kamiya, P. Carninci,, Y. Hayashizaki, k. Shinozaki, Y. Kohara, M. Hasebe, *PNAS* 100(13), 8007-8012 (2003)
28. J. E. B. de la Torre, M. G. Egan, M. S. Katari, E. D. Brenner, S. W. Stevenson, G. M. Coruzzi, D. DeSalle, *BMC Evolutionary Biology* 6 (2006)
29. D. T. Dennis, C. D. Upper, C. A. West, *Plant Physiology* 113 (1965)
30. V. Busov, R. Meilan, D. W. Pearce, S. B. Rood, C. Ma, T. J. Tschaplinski, S. H. Strauss, *Planta* (2006)

THIRD ROTATION REPORT

Introduction

RNA silencing is a nucleotide sequence-specific RNA degradation in which the specificity is conferred by short RNA molecules (20-24nt) [1]. Our understanding of RNA silencing has improved significantly in recent years and it is now clear that there is a considerable diversity of RNA silencing pathways in plants (Figure 1) [2]. Roles of RNA silencing in plants include amongst others genome defence and specification of heterochromatin formation, posttranscriptional inhibition of gene expression by miRNAs and trans-acting siRNAs, and antiviral defence [3].

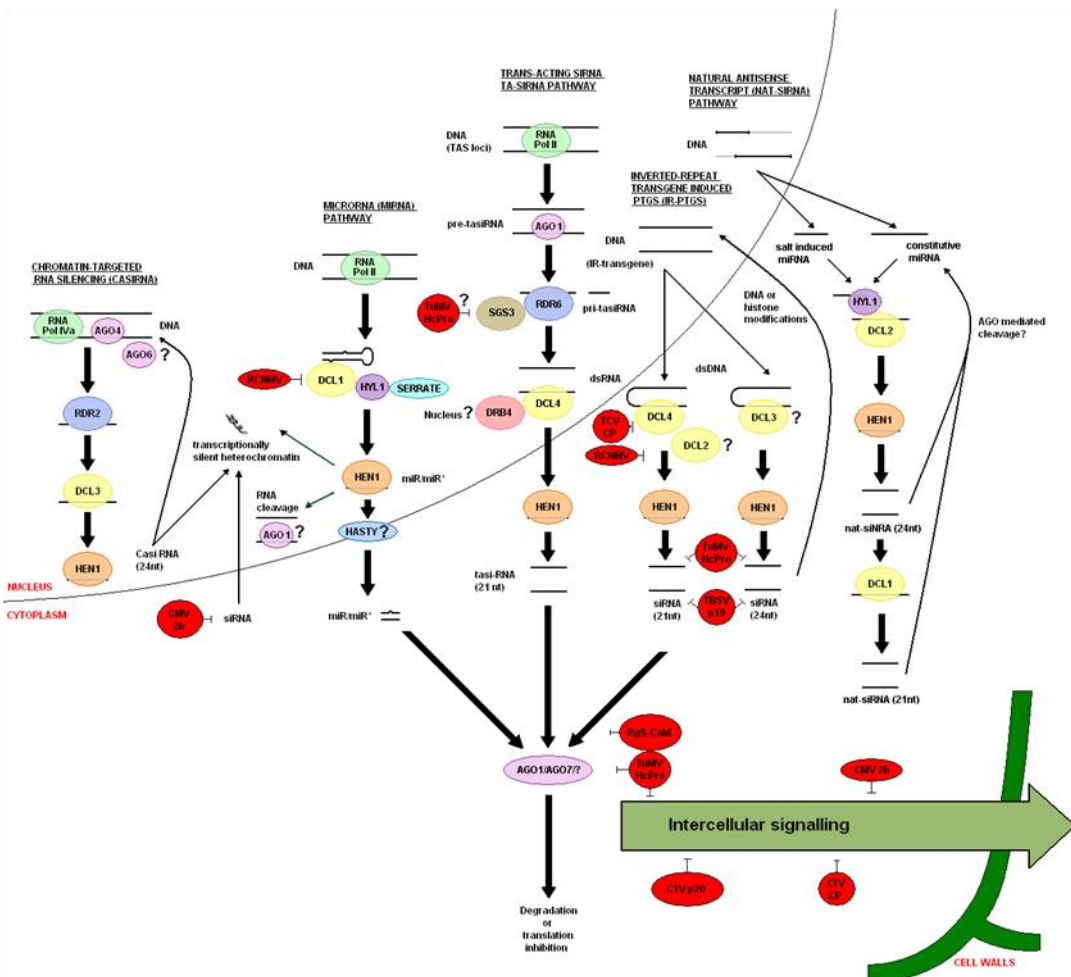


Figure 1. Summary of RNA silencing pathways. In red, some of the virus RNA silencing suppressors in their predicted acting point. (Based on 1-30)

A common strategy to counteract RNA silencing during virus infection is the use of silencing suppressors [3,4] (Figure 1). For example, the coat protein of TCV (*Turnip Crinkle Virus*) (a small carmovirus with a single-stranded positive-sense RNA genome [5-8]) is able to suppress posttranscriptional gene silencing at an early initiation step in order to survive host defence mechanisms [9]. Although this might partially explain the transient changes in host gene regulation during virus infection, the mechanism of host gene shut-off is still poorly understood.

Recently, Olivier Voinnet's lab (Strasbourg, personal communication) has identified a number of viral RNA-specific small RNAs in TCV that could mediate the degradation of host gene transcripts during infection by RNA silencing. The aim of this project was to confirm preliminary observations suggesting that these sRNAs could be responsible for the altered host gene expression observed during TCV virus infection by *in situ* hybridisation.

Objectives

Overall objective: To contribute to the understanding of host gene expression alteration through the mediation of the RNA silencing pathway during early TCV virus infection.

Specific objective: To confirm preliminary observations made by Olivier Voinnet's lab of host target gene downregulation during early TCV virus infection by *in situ* hybridisation.

Results

Previous work carried out in Olivier Voinnet's lab suggested that viral RNA-specific sRNAs derived from TCV might be responsible for the host gene downregulation observed during TCV virus infection. Five potential TCV derived sRNA (TVsRNA) (Figure 2) and their predicted host target genes were identified by a bioinformatic approach. RT-PCR experiments carried out in *Arabidopsis* wt and several *dicer-like* mutants (that is, in mutants with impaired RNA silencing, and thus, more

susceptible to TCV virus infection) suggested that TVsRNA5 (Figure 2) might be responsible for the increased downregulation of At4g19110, At4g11010, At3g07810 and At2g32960 observed in *dicer-like* mutants when compared to wt.

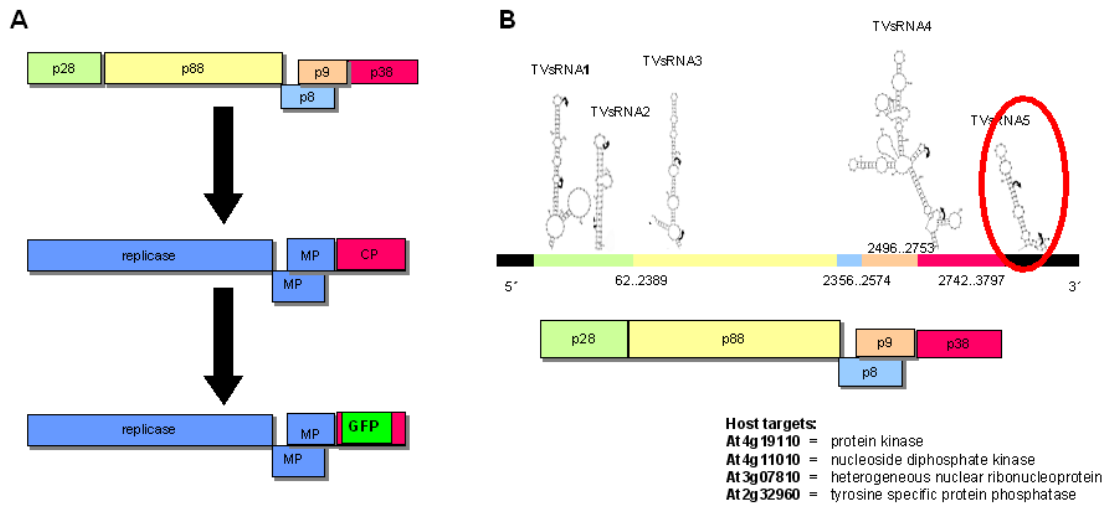


Figure 2. (A) TCV virus and TCV ΔCP – GFP construct structure. **(B)** Predicted TCV sRNA. This study focused on TVsRNA5 (in red), which host targets are predicted to be amongst other At4g19110, At4g11010, At3g07810 and At2g32960.

In the present work, a TCV ΔCP – GFP construct was used in order to verify these preliminary observations by *in situ* hybridisation. Firstly, two *Agrobacterium tumefaciens* clones carrying TCV ΔCP – GFP binary construct were made using gateway cloning and agrobacterium electrotransformation (Figure 3).

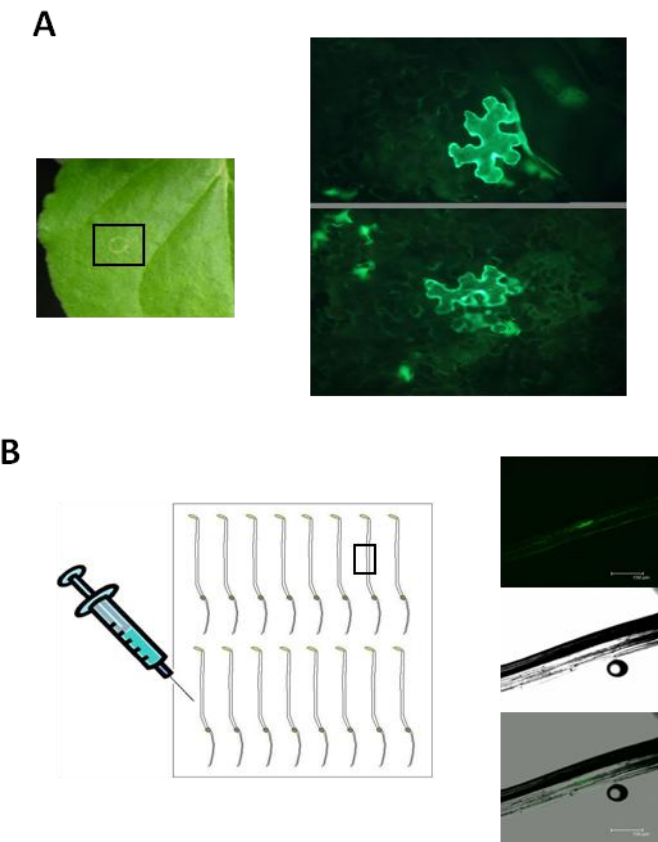


Figure 3. Infectivity of TCV ΔCP – GFP construct shown by GFP protein expression. **(A)** In *Nicotiana benthamiana* leaves. **(B)** In *Arabidopsis thaliana dcl2* hypocotyls.

After checking the infectivity of the *Agrobacterium* clones carrying TCV ΔCP – GFP binary construct (Figure 3), hypocotyls of wt, *dcl2*, *dcl3*, *dcl2/3*, *dcl2/4* and *dcl2/3/4* Arabidopsis were infected (Figure 3B). Plant material was successfully fixed and prepared for in situ hybridisation. Parallelly, At4g19110, At4g11010, At3g07810 and At2g32960 antisense and virus replicase sense and antisense probes (in order to determine the spread of the virus infection) were also synthesised for in situ hybridisation. However due to the time limitation, it was not possible to carry a round of in situ hybridisation and, thus, corroborate the data obtained in Olivier Voinnet's lab.

Discussion

Plant virus infection results in highly specific, localised and transient changes in host gene regulation [10]. However, the mechanism of host gene downregulation is still poorly understood.

Preliminary observations (Olivier Voinnet, personal communication) have suggested the involvement of viral RNA-specified sRNA, generated by RNA silencing, in the degradation of host gene transcripts during infection. The main aim in the future will be to verify this data by using the already established resources necessary for *in situ* hybridisation.

Materials and methods

Virus and Plant Materials

The TCV ΔCP – GFP construct (Figure 2) and *Arabidopsis thaliana Dicer-like* mutant line seeds (*dcl2*, *dcl3*, *dcl2/3*, *dcl2/4* and *dcl2/3/4*) were kindly provided by Olivier Voinnet. For plant infection, TCV ΔCP – GFP construct was cloned into pB7WG2.0 vector by gateway cloning (<http://genetics.biol.ttu.edu/tpcg/gatewayman.pdf>). For hypocotyl's growth, seeds were dry sterilised and grown in the dark under standard conditions in 0.8% MS plates supplemented with 1% sucrose. Col-O ecotype seeds used as the wild type in this study and *Nicotiana benthamiana* plants were kindly provided by Carole Thomas.

***Agrobacterium* infiltration/infection**

Two days old *Agrobacterium tumefaciens* cultures carrying TCV ΔCP – GFP binary construct were pelleted and resuspended in 3ml 10mM MgCl₂ containing 100uM Acetosyringone to an OD600 of 0.1. *Nicotiana benthamiana* leaves were infiltrated until saturation with a 1ml needleless syringe. Two days old

Agrobacterium colonies carrying TCV ΔCP – GFP binary construct were also grown in LB plates supplemented with the appropriate antibiotics and used to infect *Arabidopsis thaliana* hypocotyls by puncturing them with a needle.

In situ hybridisation preparation

Arabidopsis thaliana hypocotyls mock-inoculated and inoculated with Agrobacterium carrying TCV ΔCP – GFP binary construct were selected 5 days after inoculation for tissue fixation. At least ten hypocotyls from each genotype (mock-inoculated and inoculated) were vacuum-infiltrated with FAA solution (3.7% formaldehyde, 5% acetic acid and 50% ethanol) for 30 min and left in FAA for 2h at room temperature. To continue the tissue fixation, a serial of half an hour ethanol washes were performed (50%, 60% and 70%) and the hypocotyls were stored overnight in 70% ethanol at 4°C. A VIP machine was used to finish the tissue fixation and hypocotyls were finally embedded in paraffin and stored in blocks at 4°C. 10um transversal sections were made using a manual microtome and at least three slides of each genotype (mock-inoculated and inoculated) were stored for future hybridisation.

To synthesize At4g19110, At4g11010, At3g07810 and At2g32960 antisense probes in vitro, template cDNA was provided by C. Thomas. After PCR amplification and DNA purification from gel bands (QIAquick ® Gel Extraction Kit, Qiagen), the PCR product was ligated to pGEM®-T Easy Vector (Promega) and electrocompetent E. coli cells were electrotransformed. After plasmid purification from overnight E. coli cultures (QIAprep Spin Miniprep Kit, Qiagen), sequence orientation was checked and the plasmids containing antisense At4g11010, At3g07810 or At2g32960 sequences were digested with Spel (Roche). The plasmids containing antisense At4g19110 sequence were digested with PstI (Roche) with provided products. 3403 bp gel band was purified and used together with the At4g11010, At3g07810 and At2g32960 linear plasmids as a template for in vitro transcription reaction (DIG Northern Starter Kitm Roche). To synthesize digoxigenin-labeled probes, in vitro transcription reactions were carried out with digoxigenin-11-UTP using T7 RNA polymerase. The labelled RNA probe was

carbonate-hydrolyzed to generate fragments between 75-150bp. Similarly, TCV virus replicase sense and antisense probes in vitro were also designed in order to determine the spread of the virus infection.

Confocal microscopy

For confocal microscopy, *Nicotiana benthamiana* leaves and *dcl2* hypocotyls were monitored 7 days and 5 days after infection respectively. GFP-tagged TCV was monitored using a Leica DM RE confocal microscope equipped with a x20 water-immersion objective and a Leica TCS SP digital camera.

References

1. D. C. Baulcombe, *Nature* 431, 356-363 (2004)
2. P. Brodersen and O. Voinnet, *TRENDS in Genetics* 22 (5), 268-280 (2006)
3. L. Lakatos, T. Csorba, V. Pantaleo, E. J. Chapman, J. C. Carrington, Y. P. Liu, V. V. Dolja, L. Fernández-Calvino, J. J. López-Moya and J. Burgýán, *The EMBO Journal* 25, 2768-2780 (2006)
4. R. MacDiarmid, *Annu. Rev. Phytopathol.* 43, 523-544 (2005)
5. L. A. Heaton, J. C. Carrington and T. J. Morris, *Virology* 170, 214-218 (1989)
6. J. C. Carrington, L. A. Heaton, D. Zuidema, B. I. Hillman and T. J. Morris, *Virology* 170, 219-226 (1989)
7. Y. Cohen, F. Qu, A. Gisel, T. J. Morris and P. C. Zambryski, *Virology* 273, 276-285 (2000)
8. Y. Cohen, A. Gisel and P. C. Zambryski, *Virology* 273, 258-266 (2000)
9. F. Qu, T. Ren and T. J. Morris, *Journal of Virology* 77 (1), 511-522 (2003)
10. F. Wang and A. Maule, *Science* 267, 229-231 (1995)
11. Y. Tomari and P. D. Zamore, *Genes and Development* 19, 517-529 (2005)
12. S. Lu and B. R. Cullen, *Journal of Virology* 78 (23), 12868-12876 (2004)
13. O. Borsani, J. Zhu, P. E. Verslues, R. Sunkar and J. K. Zhu, *Cell* 123, 1279-1291 (2005)
14. I. Hernández-Pinzón, N. E. Yelina, F. Schwach, D. J. Studholme, D. Baulcombe and T. Dalmay, *The Plant Journal* 50, 140-148 (2007)

15. V. Vance and H. Vaucheret, *Science* 292, 2277-2280 (2001)
16. X. Zheng, J. Zhu, A. Kapoor and J. K. Zhu, *The EMBO Journal* 26, 1-11 (2007)
17. T. Blevins, R. Rajeswaran, P. V. Shivaprasad, D. Beknazarians, A. Si-Ammour, H. S. Park, F. Vázquez, D. Robertson, F. Meins Jr, T. Hohn and M. M. Pooggin, *Nucleic Acids Research* 00 (00), 1-14 (2006)
18. A. Takeda, M. Tsukuda, H. Mizumoto, K. Okamoto, m. Caído, K. Mise and T. Okuno, *The EMBO Journal* 24, 3147-3157 (2005)
19. N. Bouche, D. Lauressergues, V. Gasciolli and H. Vaucheret, *The EMBO Journal* 25, 3347-3356 (2006)
20. M. W. Jones-Rhoades, S. P. Bartel and B. Bartel, *Annu. Rev. Plant Biol.* 57, 19-53 (2006)
21. V. Gasciolli, A. C. Mallory, D. P. Bartel and H. Vaucheret, *Current Biology* 15, 1494-1500 (2005)
22. Z. Xie, L. K. Johansen, A. M. Gustafson, k. D. Kasschau, A. D. Lellis, D. Zilberman, S. E. Jacobsen and J. C. Carrington, *PLOS Biology* 2 (5), 0642-0652 (2004)
23. C. Yang, R. Guo, F. Jie, D. Nettleton, J. Peng, T. Carr, J. M. Yeakley, J. B. Fan and S. A. Whitham, *Molecular Plant-Microbe Interactions* 20 (4), 358-370 (2007)
24. A. Deleris, J. Gallego-Bartolome, J. Bao, K. D. Kasschau, J. C. Carrington and O. Voinnet, *Scienceexpress*, 1-5 (2006)
25. X. Zhang, I. E. Henderson, C. Lu, P. J. Green and S. E. Jacobsen, *PNAS* 104 (11), 4536-4541 (2007)
26. A. Itaya, X. Zhong, R. Bundschuh, Y. Qi, Y. Wang, R. Takeda, A. R. Harris, C. Molina, R. S. Nelson and B. Ding, *Journal of Virology* 81 (6), 2980-2994 (2007)
27. J. C. Carrington, K. D. Kasschau and L .K. Johansen, *Virology* 281, 1-5 (2001)
28. A. F. Fusaro, L. Matthew, N. A. Smith, S. j. Curtin, J. Dedic-hagan, G. A. Ellacott, J. M. Watson, M. B. Wang, C. Brosnan, B. J. Carroll and P. M. Waterhouse, *EMBO reports* 7 (11), 1168-1175 (2006)
29. P. Dunoyer, C. Himber and O. Voinnet, *Nature genetics* 37 (12), 1356-1360 (2005)
30. H. Vaucheret, *Genes and Development* 20, 759-771 (2006)

APPENDIX 3

Publications

APPENDIX 3

Publications

The research work presented as part of this thesis resulted in several publications which are listed below:

Arnaud, N., Girin, T., Sorefan, K., Fuentes, S., Wood, T.A., Lawrenson, T., Sablowski, R., and Ostergaard, L. (in press). Gibberellins control fruit patterning in *Arabidopsis thaliana*. *Genes and development*.

Fuentes, S., Pires, N., and Ostergaard, L. A clade in the QUASIMODO2 family evolved with vascular plants and supports a role for cell wall composition in adaptation to environmental changes. *Plant Molecular Biology* **73**, 605-615.

Yasumura, Y., Crumpton-Taylor, M., Fuentes, S., and Harberd, N.P. (2007). Step-by-step acquisition of the gibberellin-DELLA growth-regulatory mechanism during land-plant evolution. *Current Biology* **17**, 1225-1230.

REFERENCES

Achard, P., and Genschik, P. (2009). Releasing the brakes of plant growth: how GAs shutdown DELLA proteins. *Journal of Experimental Botany* **60**, 1085-1092.

Achard, P., Gusti, A., Cheminant, S., Alioua, M., Dhondt, S., Coppens, F., Beemster, G.T.S., and Genschik, P. (2009a). Gibberellin Signaling Controls Cell Proliferation Rate in *Arabidopsis*. *Current Biology* **19**, 1188-1193.

Alandete-Saez, M., Ron, M., and McCormick, S. (2008). GEX3, Expressed in the Male Gametophyte and in the Egg Cell of *Arabidopsis thaliana*, Is Essential for Micropylar Pollen Tube Guidance and Plays a Role during Early Embryogenesis. *Mol Plant* **1**, 586-598.

Allen, S., Detlef, W., and Martin, F.Y. (1999). The *Arabidopsis thaliana* MERISTEM LAYER 1 promoter specifies epidermal expression in meristems and young primordia. *The Plant Journal* **20**, 259-263.

Aloni, R., Aloni, E., Langhans, M., and Ullrich, C.I. (2006). Role of auxin in regulating *Arabidopsis* flower development. *Planta* **223**, 315-328.

Alvarez, J., and Smyth, D.R. (1999). CRABS CLAW and SPATULA, two *Arabidopsis* genes that control carpel development in parallel with AGAMOUS. *Development* **126**, 2377-2386.

Alvarez, J.P., Goldshmidt, A., Efroni, I., Bowman, J.L., and Eshed, Y. (2009). The NGATHA Distal Organ Development Genes Are Essential for Style Specification in *Arabidopsis*. *Plant Cell* **21**, 1373-1393.

Aoyama, T., and Chua, N.H. (1997). A glucocorticoid-mediated transcriptional induction system in transgenic plants. *The Plant Journal* **11**, 605-612.

Ariizumi, T., Murase, K., Sun, T.P., and Steber, C.M. (2008). Proteolysis-independent downregulation of DELLA repression in *Arabidopsis* by the gibberellin receptor GIBBERELLIN INSENSITIVE DWARF1. *Plant Cell* **20**, 2447-2459.

Arnaud, N., Girin, T., Sorefan, K., Fuentes, S., Wood, T.A., Lawrenson, T., Sablowski, R., and Ostergaard, L. (in press). Gibberellins control fruit patterning in *Arabidopsis thaliana*. *Genes and development*.

Ashburner, M., Golic, K.G., and Hawley, R.S. (2004). *Drosophila: a laboratory handbook*. Drosophila: a laboratory handbook, xxviii + 1409 pp.

Bailey, P.C., Martin, C., Toledo-Ortiz, G., Quail, P.H., Huq, E., Heim, M.A., Jakoby, M., Werber, M., and Weisshaar, B. (2003). Update on the basic helix-loop-helix transcription factor gene family in *Arabidopsis thaliana*. *Plant Cell* **15**, 2497-2501.

Baroux, C., Blanvillain, R., Moore, I.R., and Gallois, P. (2001). Transactivation of BARNASE under the AtLTP1 promoter affects the basal pole of the embryo and shoot development of the adult plant in *Arabidopsis*. *Plant Journal* **28**, 503-515.

Bassel, G.W., Mullen, R.T., and Bewley, J.D. (2008). procera is a putative DELLA mutant in tomato (*Solanum lycopersicum*): effects on the seed and vegetative plant. *J. Exp. Bot.* **59**, 585-593.

Beals, T.P., and Goldberg, R.B. (1997). A novel cell ablation strategy blocks tobacco anther dehiscence. *Plant Cell* **9**, 1527-1545.

BenCheikh, W., PerezBotella, J., Tadeo, F.R., Talon, M., and PrimoMillo, E. (1997). Pollination increases gibberellin levels in developing ovaries of seeded varieties of citrus. *Plant Physiology* **114**, 557-564.

Benkova, E., Michniewicz, M., Sauer, M., Teichmann, T., Seifertova, D., Jurgens, G., and Friml, J. (2003). Local, efflux-dependent auxin gradients as a common module for plant organ formation. *Cell* **115**, 591-602.

Bicknell, R.A., and Koltunow, A.M. (2004). Understanding Apomixis: Recent Advances and Remaining Conundrums. *Plant Cell* **16**, S228-245.

Bittencourt, N.S., Gibbs, P.E., and Semir, J. (2003). Histological study of post-pollination events in *Spathodea campanulata* Beauv. (Bignoniaceae), a species with late-acting self-incompatibility. *Annals of Botany* **91**, 827-834.

Bittencourt, N.S., and Semir, J. (2005). Late-acting self-incompatibility and other breeding systems in *Tabebuia* (Bignoniaceae). *International Journal of Plant Sciences* **166**, 493-506.

Blumenfeld, A., and Gazit, S. (1970). Cytokinin Activity in Avocado Seeds during Fruit Development. *Plant Physiol.* **46**, 331-333.

Boavida, L.C., Vieira, A.M., Becker, J.D., and Feijo, J.A. (2005). Gametophyte interaction and sexual reproduction: how plants make a zygote. *International Journal of Developmental Biology* **49**, 615-632.

Bolle, C. (2004). The role of GRAS proteins in plant signal transduction and development. *Planta* **218**, 683-692.

Bowman, J.L., Smyth, D.R., and Meyerowitz, E.M. (1989). GENES DIRECTING FLOWER DEVELOPMENT IN ARABIDOPSIS. *Plant Cell* **1**, 37-52.

Brand, A.H., and Perrimon, N. (1993). Targeted gene expression as a means of altering cell fates and generating dominant phenotypes. *Development* **118**, 401-415.

Bunger-Kibler, S., and Bangerth, F. (1982). Relationship between cell number, cell size and fruit size of seeded fruits of tomato (*Lycopersicon esculentum* Mill.), and those induced parthenocarpically by the application of plant growth regulators. *Plant Growth Regulation* **1**, 143-154.

Burrows, W.J., and Carr, D.J. (1970). Cyto Kinin Content of Pea-D Seeds During Their Growth and Development. *Physiologia Plantarum* **23**, 1064-1070.

Capron, A., Chatfield, S., Provart, N., and Berleth, T. (2008). Embryogenesis: Pattern Formation from a Single Cell. In *The Arabidopsis Book* (The American Society of Plant Biologists), pp. 1-28.

Carbonell-Bejerano, P., Urbez, C., Carbonell, J., Granell, A., and Perez-Amador, M.A. A fertilization-independent developmental program controls developmental processes and senescence in pistils of *Arabidopsis thaliana*. *Plant Physiol.*, pp.110.160044.

Chae, K., Kieslich, C.A., Morikis, D., Kim, S.C., and Lord, E.M. (2009). A Gain-of-Function Mutation of Arabidopsis Lipid Transfer Protein 5 Disturbs Pollen Tube Tip Growth and Fertilization. *Plant Cell* **21**, 3902-3914.

Chandler, P.M., Harding, C.A., Ashton, A.R., Mulcair, M.D., Dixon, N.E., and Mander, L.N. (2008). Characterization of gibberellin receptor mutants of barley (*Hordeum vulgare* L.). *Molecular Plant* **1**, 285-294.

Chareonboonsit, S., Splittstoesser, W.E., and George, W.L. (1985). THE EFFECTS OF POLLINATION METHODS AND AUXIN APPLICATIONS UPON PARTHENOCARPIC FRUIT-SET AND DEVELOPMENT IN TOMATO. *Scientia Horticulturae* **27**, 1-8.

Chaudhury, A.M., Ming, L., Miller, C., Craig, S., Dennis, E.S., and Peacock, W.J. (1997). Fertilization-independent seed development in *Arabidopsis thaliana*. *Proceedings of the National Academy of Sciences of the United States of America* **94**, 4223-4228.

Chen, W.S. (1983). CYTOKININS OF THE DEVELOPING MANGO FRUIT - ISOLATION, IDENTIFICATION, AND CHANGES IN LEVELS DURING MATURATION. *Plant Physiology* **71**, 356-361.

Chen, Y.H., Li, H.J., Shi, D.Q., Yuan, L., Liu, J., Sreenivasan, R., Baskar, R., Grossniklaus, U., and Yang, W.C. (2007). The central cell plays a critical role in pollen tube guidance in *Arabidopsis*. *Plant Cell* **19**, 3563-3577.

Chen, D., and Zhao, J. (2008). Free IAA in stigmas and styles during pollen germination and pollen tube growth of *Nicotiana tabacum*. *Physiologia Plantarum* **134**, 202-215.

Cheng, H., Qin, L.J., Lee, S.C., Fu, X.D., Richards, D.E., Cao, D.N., Luo, D., Harberd, N.P., and Peng, J.R. (2004). Gibberellin regulates *Arabidopsis* floral development via suppression of DELLA protein function. *Development* **131**, 1055-1064.

Chhun, T., Aya, K., Asano, K., Yamamoto, E., Morinaka, Y., Watanabe, M., Kitano, H., Ashikari, M., Matsuoka, M., and Ueguchi-Tanaka, M. (2007). Gibberellin Regulates Pollen Viability and Pollen Tube Growth in Rice. *Plant Cell* **19**, 3876-3888.

Chiang, H.H., Hwang, I., and Goodman, H.M. (1995). Isolation of the *Arabidopsis* GA4 locus. *Plant Cell* **7**, 195-201.

Colombo, M., Brambilla, V., Marcheselli, R., Caporali, E., Kater, M.M., and Colombo, L. A new role for the SHATTERPROOF genes during *Arabidopsis* gynoecium development. *Developmental Biology* **337**, 294-302.

Cox, C.M.a.S., S. M. (2006). Localised and non-localised promotion of fruit development by seeds in *Arabidopsis*. *Functional Plant Biology* **33**, 1-8.

Crosby, K.E., Aung, L.H., and Buss, G.R. (1981). INFLUENCE OF 6-BENZYLAMINOPURINE ON FRUIT-SET AND SEED DEVELOPMENT IN 2 SOYBEAN, GLYCINE-MAX (L) MERR GENOTYPES. *Plant Physiology* **68**, 985-988.

Davidonis, G.H. (1990). GIBBERELLIC ACID-INDUCED CELL ELONGATION IN COTTON SUSPENSION-CULTURES. *Journal of Plant Growth Regulation* **9**, 243-246.

Day, C.D., Galgoci, B.F.C., and Irish, V.F. (1995). GENETIC ABLATION OF PETAL AND STAMEN PRIMORDIA TO ELUCIDATE CELL-INTERACTIONS DURING FLORAL DEVELOPMENT. *Development* **121**, 2887-2895.

Day, R.C., Herridge, R.P., Ambrose, B.A., and Macknight, R.C. (2008). Transcriptome Analysis of Proliferating *Arabidopsis* Endosperm Reveals Biological Implications for the Control of Syncytial Division, Cytokinin Signaling, and Gene Expression Regulation. *Plant Physiol.* **148**, 1964-1984.

de Jong, M., Mariani, C., and Vriezen, W.H. (2009a). The role of auxin and gibberellin in tomato fruit set. *Journal of Experimental Botany* **60**, 1523-1532.

de Jong, M., Wolters-Arts, M., Feron, R., Mariani, C., and Vriezen, W.H. (2009b). The *Solanum lycopersicum* auxin response factor 7 (SIARF7) regulates auxin signaling during tomato fruit set and development. *Plant Journal* **57**, 160-170.

de Lucas, M., Daviere, J.M., Rodriguez-Falcon, M., Pontin, M., Iglesias-Pedraz, J.M., Lorrain, S., Fankhauser, C., Blazquez, M.A., Titarenko, E., and Prat, S. (2008). A molecular framework for light and gibberellin control of cell elongation. *Nature* **451**, 480-U411.

Dharmasiri, N., Dharmasiri, S., and Estelle, M. (2005). The F-box protein TIR1 is an auxin receptor. *Nature* **435**, 441-445.

Dill, A., Jung, H.S., and Sun, T.P. (2001). The DELLA motif is essential for gibberellin-induced degradation of RGA. *Proceedings of the National Academy of Sciences of the United States of America* **98**, 14162-14167.

Dill, A., and Sun, T. (2001). Synergistic derepression of gibberellin signaling by removing RGA and GAI function in *Arabidopsis thaliana*. *Genetics* **159**, 777-785.

Dill, A., Thomas, S.G., Hu, J., Steber, C.M., and Sun, T.P. (2004). The Arabidopsis F-box protein SLEEPY1 targets gibberellin signaling repressors for gibberellin-induced degradation. *Plant Cell* **16**, 1392-1405.

Dong, J., Kim, S.T., and Lord, E.M. (2005). Plantacyanin Plays a Role in Reproduction in Arabidopsis. *Plant Physiol.* **138**, 778-789.

Dorcey, E., Urbez, C., Blazquez, M.A., Carbonell, J., and Perez-Amador, M.A. (2009). Fertilization-dependent auxin response in ovules triggers fruit development through the modulation of gibberellin metabolism in Arabidopsis. *Plant Journal* **58**, 318-332.

Dreher, K., and Callis, J. (2007). Ubiquitin, hormones and biotic stress in plants. *Annals of Botany* **99**, 787-822.

Dresselhaus, T. (2006). Cell-cell communication during double fertilization. *Current Opinion in Plant Biology* **9**, 41-47.

Dubrovsky, J.G., Sauer, M., Napsucialy-Mendivil, S., Ivanchenko, M.G., Friml, J., Shishkova, S., Celenza, J., and Benkova, E. (2008). Auxin acts as a local morphogenetic trigger to specify lateral root founder cells. *Proceedings of the National Academy of Sciences of the United States of America* **105**, 8790-8794.

Duncan, R.E., and Curtis, J.T. (1942). Intermittent growth of fruits of Phalaenopsis. A correlation of the growth phases of an orchid fruit with internal development. *Bulletin of the Torrey botanical club* **69**, 167-183.

Ebel, C., Mariconti, L., and Gruisse, W. (2004). Plant retinoblastoma homologues control nuclear proliferation in the female gametophyte. *Nature* **429**, 776-780.

Eeuwens, C.J., and Schwabe, W.W. (1975). SEED AND POD WALL DEVELOPMENT IN PISUM-SATIVUM, L IN RELATION TO EXTRACTED AND APPLIED HORMONES. *Journal of Experimental Botany* **26**, 1-14.

Emery, R.J.N., Leport, L., Barton, J.E., Turner, N.C., and Atkins, C.A. (1998). cis-Isomers of Cytokinins Predominate in Chickpea Seeds throughout Their Development. *Plant Physiol.* **117**, 1515-1523.

Escobar-Restrepo, J.M., Huck, N., Kessler, S., Gagliardini, V., Gheyselinck, J., Yang, W.C., and Grossniklaus, U. (2007). The FERONIA receptor-like kinase mediates male-female interactions during pollen tube reception. *Science* **317**, 656-660.

Fagoaga, C., Tadeo, F.R., Iglesias, D.J., Huerta, L., Lliso, I., Vidal, A.M., Talon, M., Navarro, L., Garcia-Martinez, J.L., and Pena, L. (2007). Engineering of gibberellin levels in citrus by sense and antisense overexpression of a GA 20-oxidase gene modifies plant architecture. *Journal of Experimental Botany* **58**, 1407-1420.

Fan, Y.F., Jiang, L., Gong, H.Q., and Liu, C.M. (2008). Sexual reproduction in higher plants I: Fertilization and the initiation of zygotic program. *Journal of Integrative Plant Biology* **50**, 860-867.

Fang, W., Dong-Qiao, S., Jie, L., and Wei-Cai, Y. (2008). Novel Nuclear Protein ALC-INTERACTING PROTEIN1 is Expressed in Vascular and Mesocarp Cells in *< i>Arabidopsis</i>*. *Journal of Integrative Plant Biology* **50**, 918-927.

Faure, J.E., Rotman, N., Fortune, P., and Dumas, C. (2002). Fertilization in *Arabidopsis thaliana* wild type: Developmental stages and time course. *Plant J* **30**, 481-488.

Feng, S.H., Martinez, C., Gusmaroli, G., Wang, Y., Zhou, J.L., Wang, F., Chen, L.Y., Yu, L., Iglesias-Pedraz, J.M., Kircher, S., Schafer, E., Fu, X.D., Fan, L.M., and Deng, X.W. (2008). Coordinated regulation of *Arabidopsis thaliana* development by light and gibberellins. *Nature* **451**, 475-U479.

Ficcadenti, N., Sestili, S., Pandolfini, T., Cirillo, C., Rotino, G.L., and Spena, A. (1999). Genetic engineering of parthenocarpic fruit development in tomato. Molecular Breeding **5**, 463- 470.

FitzGerald, J., Luo, M., Chaudhury, A., and Berger, F. (2008). DNA Methylation Causes Predominant Maternal Controls of Plant Embryo Growth. Plos One **3**.

Fleck, B., and Harberd, N.P. (2002). Evidence that the Arabidopsis nuclear gibberellin signalling protein GAI is not destabilised by gibberellin. Plant Journal **32**, 935-947.

Fos, M., Nuez, F., and Garcia-Martinez, J.L. (2000). The gene *pat-2*, which induces natural parthenocarpy, alters the gibberellin content in unpollinated tomato ovaries. Plant Physiol. **122**, 471-480.

Fos, M., Proano, K., Nuez, F., and Garcia-Martinez, J.L. (2001). Role of gibberellins in parthenocarpic fruit development induced by the genetic system *pat-3/pat-4* in tomato. Physiol. Plant **111**, 545-550.

Francis, K.E., Lam, S.Y., and Copenhaver, G.P. (2006). Separation of Arabidopsis pollen tetrads is regulated by QUARTET1, a pectin methylesterase gene. Plant Physiology **142**, 1004-1013.

Frank, A.C., and Johnson, M.A. (2009). Expressing the Diphtheria Toxin A Subunit from the HAP2(GCS1) Promoter Blocks Sperm Maturation and Produces Single Sperm-Like Cells Capable of Fertilization. Plant Physiology **151**, 1390-1400.

Franklin-Tong, V.E. (2008). Self-Incompatibility in Flowering Plants: Evolution, Diversity, and Mechanisms. Self-Incompatibility in Flowering Plants: Evolution, Diversity, and Mechanisms.

Friml, J., Benkova, E., Blilou, I., Wisniewska, J., Hamann, T., Ljung, K., Woody, S., Sandberg, G., Scheres, B., Jurgens, G., and Palme, K. (2002).

AtPIN4 mediates sink-driven auxin gradients and root patterning in Arabidopsis. Cell **108**, 661-673.

Friml, J., Vieten, A., Sauer, M., Weijers, D., Schwarz, H., Hamann, T., Offringa, R., and Jurgens, G. (2003). Efflux-dependent auxin gradients establish the apical-basal axis of Arabidopsis. Nature **426**, 147-153.

Fu, X., Richards, D.E., Ait-ali, T., Hynes, L.W., Ougham, H., Peng, J., and Harberd, N.P. (2002). Gibberellin-Mediated Proteasome-Dependent Degradation of the Barley DELLA Protein SLN1 Repressor. Plant Cell **14**, 3191-3200.

Gallagher, S.R. (1992). Quantitation of GUS activity by fluorometry. In GUS Protocols: Using the GUS Gene as a Reporter of Gene Expression, S.R. Gallagher, ed (San Diego: Academic Press), pp. 47-59.

Gallego-Bartolome, J., Minguet, E.G., Marin, J.A., Prat, S., Blazquez, M.A., and Alabadi, D. Transcriptional Diversification and Functional Conservation between DELLA Proteins in Arabidopsis. Molecular Biology and Evolution **27**, 1247-1256.

Garcia-Martinez, J.L., Lopez-Diaz, I., Sanchez-Beltran, M.J., Phillips, A.L., Ward, D.A., Gaskin, P., and Hedden, P. (1997). Isolation and transcript analysis of gibberellin 20-oxidase genes in pea and bean in relation to fruit development. Plant Molecular Biology **33**, 1073-1084.

García-Martínez, J.L., and Carbonell, J. (1980). Fruit-set of unpollinated ovaries of *Pisum sativum* L. Influence of plant growth regulators. Planta **147**, 451-456.

Gardner, N., Felsheim, R., and Smith, A.G. (2009). Production of male- and female-sterile plants through reproductive tissue ablation. Journal of Plant Physiology **166**, 871-881.

Gibbs, P., Bianchi, M.B., and Ranga, N.T. (2004). Effects of self-, chase and mixed self/cross-pollinations on pistil longevity and fruit set in *Ceiba* species (Bombacaceae) with late-acting self-incompatibility. *Annals of Botany* **94**, 305-310.

Gillaspy, G., Ben-David, H., and Grussem, W. (1993). Fruits: A Developmental Perspective. *Plant Cell* **5**, 1439-1451.

Gilroy, S., and Jones, R.L. (1994). PERCEPTION OF GIBBERELLIN AND ABSCISIC-ACID AT THE EXTERNAL FACE OF THE PLASMA-MEMBRANE OF BARLEY (*HORDEUM-VULGARE* L) ALEURONE PROTOPLASTS. *Plant Physiology* **104**, 1185-1192.

Goetz, M., Vivian-Smith, A., Johnson, S.D., and Koltunow, A.M. (2006). AUXIN RESPONSE FACTOR8 is a negative regulator of fruit initiation in *Arabidopsis*. *Plant Cell* **18**, 1873-1886.

Goetz, M., Hooper, L.C., Johnson, S.D., Rodrigues, J.C.M., Vivian-Smith, A., and Koltunow, A.M. (2007). Expression of Aberrant Forms of AUXIN RESPONSE FACTOR8 Stimulates Parthenocarpy in *Arabidopsis* and Tomato. *Plant Physiol.* **145**, 351-366.

Gong, J.M., Waner, D.A., Horie, T., Li, S.L., Horie, R., Abid, K.B., and Schroeder, J.I. (2004). Microarray-based rapid cloning of an ion accumulation deletion mutant in *Arabidopsis thaliana*. *Proceedings of the National Academy of Sciences of the United States of America* **101**, 15404-15409.

Goodwillie, C., Kalisz, S., and Eckert, C.G. (2005). The evolutionary enigma of mixed mating systems in plants: Occurrence, theoretical explanations, and empirical evidence. *Annual Review of Ecology Evolution and Systematics* **36**, 47-79.

Goto, K., and Meyerowitz, E.M. (1994). FUNCTION AND REGULATION OF THE ARABIDOPSIS FLORAL HOMEOTIC GENE PISTILLATA. *Genes & Development* **8**, 1548-1560.

Gray, W.M., Kepinski, S., Rouse, D., Leyser, O., and Estelle, M. (2001). Auxin regulates SCFTIR1-dependent degradation of AUX/IAA proteins. *Nature* **414**, 271-276.

Greene, E.A., Codomo, C.A., Taylor, N.E., Henikoff, J.G., Till, B.J., Reynolds, S.H., Enns, L.C., Burtner, C., Johnson, J.E., Odden, A.R., Comai, L., and Henikoff, S. (2003). Spectrum of chemically induced mutations from a large-scale reverse-genetic screen in *Arabidopsis*. *Genetics* **164**, 731-740.

Gremski, K., Ditta, G., and Yanofsky, M.F. (2007). The HECATE genes regulate female reproductive tract development in *Arabidopsis thaliana*. *Development* **134**, 3593-3601.

Grieneisen, V.A., Xu, J., Maree, A.F.M., Hogeweg, P., and Scheres, B. (2007). Auxin transport is sufficient to generate a maximum and gradient guiding root growth. *Nature* **449**, 1008-1013.

Griffiths, J., Murase, K., Rieu, I., Zentella, R., Zhang, Z.-L., Powers, S.J., Gong, F., Phillips, A.L., Hedden, P., Sun, T.-p., and Thomas, S.G. (2006). Genetic Characterization and Functional Analysis of the GID1 Gibberellin Receptors in *Arabidopsis*. *Plant Cell* **18**, 3399-3414.

Grossniklaus, U., Vielle-Calzada, J.P., Hoeppner, M.A., and Gagliano, W.B. (1998). Maternal control of embryogenesis by medea, a Polycomb group gene in *Arabidopsis*. *Science* **280**, 446-450.

Grossniklaus, U., Spillane, C., Page, D.R., and Kohler, C. (2001). Genomic imprinting and seed development: endosperm formation with and without sex. *Current Opinion in Plant Biology* **4**, 21-27.

Groszmann, M., Bylstra, Y., Lampugnani, E.R., and Smyth, D.R. Regulation of tissue-specific expression of SPATULA, a bHLH gene involved in carpel development, seedling germination, and lateral organ growth in *Arabidopsis*. *Journal of Experimental Botany* **61**, 1495-1508.

Guitton, A.E., and Berger, F. (2005). Loss of function of MULTICOPY SUPPRESSOR OF IRA 1 produces nonviable parthenogenetic embryos in *Arabidopsis*. *Current Biology* **15**, 750-754.

Guo, D., Rajamaki, M.-L., and Valkonen, J. (2008). Protein-protein interactions: The yeast two-hybrid system. In *Methods in Molecular Biology*, G.D. Foster, I.E. Johansen, Y. Hong, and P.D. Nagy, eds, pp. 421-439.

Gustafson, F.G. (1936). Inducement of fruit development by growth promoting chemicals. *Proc. Natl. Acad. Sci. USA* **22**, 629-636.

Gustafson, F.G. (1939). Auxin distribution in fruits and its significance in fruit development. *American Journal of Botany* **26**, 189-194.

Harberd, N.P. (2003). Botany. Relieving DELLA restraint. *Science* **299**, 1853-1854.

Harberd, N.P., Belfield, E., and Yasumura, Y. (2009). The Angiosperm Gibberellin-GID1-DELLA Growth Regulatory Mechanism: How an "Inhibitor of an Inhibitor" Enables Flexible Response to Fluctuating Environments. *Plant Cell* **21**, 1328-1339.

Hartweck, L.M., and Olszewski, N.E. (2006). Rice GIBBERELLIN INSENSITIVE DWARF1 is a gibberellin receptor that illuminates and raises questions about GA signaling. *Plant Cell* **18**, 278-282.

Haseloff, J. (1999). GFP variants for multispectral imaging of living cells. *Methods in Cell Biology*, Vol 58 **58**, 139-+.

Hazen, S.P., Borevitz, J.O., Harmon, F.G., Pruneda-Paz, J.L., Schultz, T.F., Yanovsky, M.J., Liljegren, S.J., Ecker, J.R., and Kay, S.A. (2005). Rapid array mapping of circadian clock and developmental mutations in *Arabidopsis*. *Plant Physiology* **138**, 990-997.

Hedden, P., and Phillips, A.L. (2000). Gibberellin metabolism: new insights revealed by the genes. *Trends Plant Sci* **5**, 523-530.

Heisler, M.G.B., Atkinson, A., Bylstra, Y.H., Walsh, R., and Smyth, D.R. (2001). SPATULA, a gene that controls development of carpel margin tissues in *Arabidopsis*, encodes a bHLH protein. *Development* **128**, 1089-1098.

Henikoff, S., and Comai, L. (2003). Single-nucleotide mutations for plant functional genomics. *Annual Review of Plant Biology* **54**, 375-401.

Higashiyama, T., Kuroiwa, H., Kawano, S., and Kuroiwa, T. (1998). Guidance in vitro of the pollen tube to the naked embryo sac of *Torenia fournieri*. *Plant Cell* **10**, 2019-2031.

Higashiyama, T., Yabe, S., Sasaki, N., Nishimura, Y., Miyagishima, S., Kuroiwa, H., and Kuroiwa, T. (2001). Pollen tube attraction by the synergid cell. *Science* **293**, 1480-1483.

Hildebrand, F. (1865). Bastardierungsversuche on Orchideen. *Botanische Zeitung* **23**, 245-249.

Hooley, R., Beale, M.H., and Smith, S.J. (1991). GIBBERELLIN PERCEPTION AT THE PLASMA-MEMBRANE OF AVENA-FATUA ALEURONE PROTOPLASTS. *Planta* **183**, 274-280.

Hou, X.L., Hu, W.W., Shen, L.S., Lee, L.Y.C., Tao, Z., Han, J.H., and Yu, H. (2008). Global identification of DELLA target genes during *Arabidopsis* flower development. *Plant Physiology* **147**, 1126-1142.

Hu, J.H., Mitchum, M.G., Barnaby, N., Ayele, B.T., Ogawa, M., Nam, E., Lai, W.C., Hanada, A., Alonso, J.M., Ecker, J.R., Swain, S.M., Yamaguchi, S., Kamiya, Y., and Sun, T.P. (2008). Potential sites of bioactive gibberellin production during reproductive growth in *Arabidopsis*. *Plant Cell* **20**, 320-336.

Huang, S.S., Raman, A.S., Ream, J.E., Fujiwara, H., Cerny, R.E., and Brown, S.M. (1998). Overexpression of 20-oxidase confers a gibberellin-overproduction phenotype in *Arabidopsis*. *Plant Physiology* **118**, 773-781.

Huck, N., Moore, J.M., Federer, M., and Grossniklaus, U. (2003). The *Arabidopsis* mutant feronia disrupts the female gametophytic control of pollen tube reception. *Development* **130**, 2149-2159.

Hue T, T., Weiqiang, Q., Brenden A, H., Yi-Min, S.H.E., Daowen, W., and William C, P. Biochemical and molecular characterization of AtPAP12 and AtPAP26: the predominant purple acid phosphatase isozymes secreted by phosphate-starved *Arabidopsis thaliana*. *Plant, Cell & Environment* **9999**.

Hulskamp, M., Schneitz, K., and Pruitt, R.E. (1995). GENETIC-EVIDENCE FOR A LONG-RANGE ACTIVITY THAT DIRECTS POLLEN-TUBE GUIDANCE IN ARABIDOPSIS. *Plant Cell* **7**, 57-64.

Hur, Y.J., Jin, B.R., Nam, J., Chung, Y.S., Lee, J.H., Choi, H.K., Yun, D.J., Yi, G., Kim, Y.H., and Kim, D.H. Molecular characterization of OsPAP2: transgenic expression of a purple acid phosphatase up-regulated in phosphate-deprived rice suspension cells. *Biotechnology Letters* **32**, 163-170.

Hurley, B.A., Tran, H.T., Marty, N.J., Park, J., Snedden, W.A., Mullen, R.T., and Plaxton, W.C. The Dual-Targeted Purple Acid Phosphatase Isozyme AtPAP26 Is Essential for Efficient Acclimation of *Arabidopsis* to Nutritional Phosphate Deprivation. *Plant Physiology* **153**, 1112-1122.

Ichihashi, Y., Horiguchi, G., Gleissberg, S., and Tsukaya, H. The bHLH Transcription Factor SPATULA Controls Final Leaf Size in *Arabidopsis thaliana*. *Plant and Cell Physiology* **51**, 252-261.

Inada, S., and Shimmen, T. (2000). Regulation of elongation growth by gibberellin in root segments of *Lemna minor*. *Plant and Cell Physiology* **41**, 932-939.

Ingouff, M., Jullien, P.E., and Berger, F. (2006). The Female Gametophyte and the Endosperm Control Cell Proliferation and Differentiation of the Seed Coat in Arabidopsis. *Plant Cell* **18**, 3491-3501.

Israelsson, M., Mellerowicz, E., Chono, M., Gullberg, J., and Moritz, T. (2004). Cloning and overproduction of gibberellin 3-oxidase in hybrid aspen trees. Effects of gibberellin homeostasis and development. *Plant Physiology* **135**, 221-230.

Iuchi, S., Suzuki, H., Kim, Y.C., Iuchi, A., Kuromori, T., Ueguchi-Tanaka, M., Asami, T., Yamaguchi, I., Matsuoka, M., Kobayashi, M., and Nakajima, M. (2007). Multiple loss-of-function of Arabidopsis gibberellin receptor AtGID1s completely shuts down a gibberellin signal. *Plant Journal* **50**, 958-966.

Jacobsen, S.E., and Oleszewski, N.E. (1993). Mutations at the *SPINDLY* locus of Arabidopsis alter signal transduction. *Plant Cell* **5**, 887-896.

Jacobsen, S.E., Binkowski, K.A., and Olszewski, N.E. (1996). SPINDLY, a tetratricopeptide repeat protein involved in gibberellin signal transduction in Arabidopsis. *Proceedings of the National Academy of Sciences of the United States of America* **93**, 9292-9296.

Jander, G. (2006). Gene identification and cloning by molecular marker mapping. *Methods in Molecular Biology*, 115-126.

Jansen, J.G., Vrieling, H., Vanteijlingen, C.M.M., Mohn, G.R., Tates, A.D., and Vanzeeland, A.A. (1995). MARKED DIFFERENCES IN THE ROLE OF O-6-ALKYLGUANINE IN HPRT MUTAGENESIS IN T-LYMPHOCYTES OF RATS EXPOSED IN-VIVO TO ETHYLMETHANESULFONATE, N-(2-HYDROXYETHYL)-N-NITROSOUREA, OR N-ETHYL-N-NITROSOUREA. *Cancer Research* **55**, 1875-1882.

Jefferson, R.A., Kavanagh, T.A., and Bevan, M.W. (1987). GUS FUSIONS - BETA-GLUCURONIDASE AS A SENSITIVE AND VERSATILE GENE FUSION MARKER IN HIGHER-PLANTS. *Embo Journal* **6**, 3901-3907.

Jullien, P.E., Mosquna, A., Ingouff, M., Sakata, T., Ohad, N., and Berger, F. (2008). Retinoblastoma and its binding partner MSI1 control imprinting in *Arabidopsis*. *Plos Biology* **6**, 1693-1705.

Kaida, R., Serada, S., Norioka, N., Norioka, S., Neumetzler, L., Pauly, M., Sampedro, J., Zarra, I., Hayashi, T., and Kaneko, T.S. Potential Role for Purple Acid Phosphatase in the Dephosphorylation of Wall Proteins in Tobacco Cells. *Plant Physiol.* **153**, 603-610.

Kaida, R., Satoh, Y., Bulone, V., Yamada, Y., Kaku, T., Hayashi, T., and Kaneko, T.S. (2009). Activation of β -Glucan Synthases by Wall-Bound Purple Acid Phosphatase in Tobacco Cells. *Plant Physiol.* **150**, 1822-1830.

Kasahara, R.D., Portereiko, M.F., Sandaklie-Nikolova, L., Rabiger, D.S., and Drews, G.N. (2005). MYB98 is required for pollen tube guidance and synergid cell differentiation in *Arabidopsis*. *Plant Cell* **17**, 2981-2992.

Kepinski, S., and Leyser, O. (2005). The *Arabidopsis* F-box protein TIR1 is an auxin receptor. *Nature* **435**, 446-451.

Kim, Y., Schumaker, K.S., and Zhu, J.-K. (2006). EMS mutagenesis of *Arabidopsis*. *Methods in Molecular Biology*, 101-103.

King, G.N. (1947). Artificial Parthenocarpy in *Lycopersicum esculentum*; Tissue Development. *Plant Physiol* **22**, 572-581.

King, K.E., Moritz, T., and Harberd, N.P. (2001). Gibberellins Are Not Required for Normal Stem Growth in *Arabidopsis thaliana* in the Absence of GAI and RGA. *Genetics* **159**, 767-776.

Kislev, M.E., Hartmann, A., and Bar-Yosef, O. (2006). Early Domesticated Fig in the Jordan Valley. *Science* **312**, 1372-1374.

Klabunde, T., Strater, N., Frohlich, R., Witzel, H., and Krebs, B. (1996). Mechanism of Fe(III)-Zn(II) purple acid phosphatase based on crystal structures. *Journal of Molecular Biology* **259**, 737-748.

Kohler, C., Hennig, L., Bouvieret, R., Gheyselinck, J., Grossniklaus, U., and Gruissem, W. (2003). *Arabidopsis* MSI1 is a component of the MEA/FIE Polycomb group complex and required for seed development. *EMBO J* **22**, 4804-4814.

Koini, M.A., Alvey, L., Alien, T., Tilley, C.A., Harberd, N.P., Whitelam, G.C., and Franklin, K.A. (2009). High temperature-mediated adaptations in plant architecture require the bHLH transcription factor PIF4. *Current Biology* **19**, 408-413.

Koltunow, A.M. (1993). Apomixis: Embryo Sacs and Embryos Formed without Meiosis or Fertilization in Ovules. *Plant Cell* **5**, 1425-1437.

Koornneef, M., van Eden, J., Hanhart, C.J., Stam, P., Braaksma, F.J., and Feenstra, W.J. (1983). Linkage map of *Arabidopsis thaliana*. *J Hered* **74**, 265-272.

Koornneef, M., and Gilmartin, P.M. (2002). Classical mutagenesis in higher plants. *Molecular plant biology: A practical approach*. Volume One, 1-11.

Kreppel, L.K., Blomberg, M.A., and Hart, G.W. (1997). Dynamic glycosylation of nuclear and cytosolic proteins - Cloning and characterization of a unique O-GlcNAc transferase with multiple tetratricopeptide repeats. *Journal of Biological Chemistry* **272**, 9308-9315.

Krieg, D.R. (1963). ETHYL METHANESULFONATE-INDUCED REVERSION OF BACTERIOPHAGE T4RII MUTANTS. *Genetics* **48**, 561-&.

Kuang, R.B., Chan, K.H., Yeung, E., and Lim, B.L. (2009). Molecular and Biochemical Characterization of AtPAP15, a Purple Acid Phosphatase with Phytase Activity, in *Arabidopsis*. *Plant Physiology* **151**, 199-209.

Kuusk, S., Sohlberg, J.J., Long, J.A., Fridborg, I., and Sundberg, E. (2002). STY1 and STY2 promote the formation of apical tissues during *Arabidopsis* gynoecium development. *Development* **129**, 4707-4717.

Lee, S., Cheng, H., King, K.E., Wang, W., He, Y., Hussain, A., Lo, J., Harberd, N.P., and Peng, J. (2002). Gibberellin regulates *Arabidopsis* seed germination via RGL2, a GAI/RGA-like gene whose expression is up-regulated following imbibition. *Genes Dev* **16**, 646-658.

Léon-Kloosterziel, K.M., Keijzer, C.J., and Koornneef, M. (1994). A seed shape mutant of *Arabidopsis* that is affected in integument development. *Plant Cell* **6**, 385-392.

Li, D.P., Zhu, H.F., Liu, K.F., Liu, X., Leggewie, G., Udvardi, M., and Wang, D.W. (2002). Purple acid Phosphatases of *Arabidopsis thaliana* - Comparative analysis and differential regulation by phosphate deprivation. *Journal of Biological Chemistry* **277**, 27772-27781.

Lightner, J., and Caspar, T. (1998). Seed mutagenesis of *Arabidopsis*. Methods in Molecular Biology; *Arabidopsis* protocols, 91-103.

Liljegren, S.J., Roeder, A.H.K., Kempin, S.A., Gremski, K., Ostergaard, L., Guimil, S., Reyes, D.K., and Yanofsky, M.F. (2004). Control of fruit patterning in *Arabidopsis* by INDEHISCENT. *Cell* **116**, 843-853.

Lin, Z., Zhong, S., and Grierson, D. (2009). Recent advances in ethylene research. *J. Exp. Bot.* **60**, 3311-3336.

Llop-Tous, I., Barry, C.S., and Grierson, D. (2000). Regulation of Ethylene Biosynthesis in Response to Pollination in Tomato Flowers. *Plant Physiol.* **123**, 971-978.

Lubas, W.A., Frank, D.W., Krause, M., and Hanover, J.A. (1997). O-linked GlcNAc transferase is a conserved nucleocytoplasmic protein containing tetratricopeptide repeats. *Journal of Biological Chemistry* **272**, 9316-9324.

Luk'yanenko, A.N. (1991). Parthenocarpy in tomato. Genetic improvement of tomato., 167-177.

Luo, M., Bilodeau, P., Koltunow, A., Dennis, E.S., Peacock, W.J., and Chaudhury, A.M. (1999). Genes controlling fertilization-independent seed development in *Arabidopsis thaliana*. *Proceedings of the National Academy of Sciences of the United States of America* **96**, 296-301.

Makarevich, G., Leroy, O., Akinci, U., Schubert, D., Clarenz, O., Goodrich, J., Grossniklaus, U., and Kohler, C. (2006). Different Polycomb group complexes regulate common target genes in Arabidopsis. *EMBO Rep* **7**, 947-952.

Maraschin, F.D., Memelink, J., and Offringa, R. (2009). Auxin-induced, SCFTIR1-mediated poly-ubiquitination marks AUX/IAA proteins for degradation. *Plant Journal* **59**, 100-109.

Marti, C., Orzaez, D., Ellul, P., Moreno, V., Carbonell, J., and Granell, A. (2008). Silencing of DELLA induces facultative parthenocarpy in tomato fruits. *Plant J* **52**, 865-876.

Marton, M.L., Cordts, S., Broadhurst, J., and Dresselhaus, T. (2005). Micropylar pollen tube guidance by egg apparatus 1 of maize. *Science* **307**, 573-576.

Maymon, I., Greenboim-Wainberg, Y., Sagiv, S., Kieber, J.J., Moshelion, M., Olszewski, N., and Weiss, D. (2009). Cytosolic activity of SPINDLY implies the existence of a DELLA-independent gibberellin-response pathway. *Plant Journal* **58**, 979-988.

McAbee, J.M., Hill, T.A., Skinner, D.J., Izhaki, A., Hauser, B.A., Meister, R.J., Reddy, G.V., Meyerowitz, E.M., Bowman, J.L., and Gasser, C.S. (2006). ABERRANT TESTA SHAPE encodes a KANADI family member, linking polarity determination to separation and growth of *Arabidopsis* ovule integuments. *Plant Journal* **46**, 522-531.

McGinnis, K.M., Thomas, S.G., Soule, J.D., Strader, L.C., Zale, J.M., Sun, T.P., and Steber, C.M. (2003). The *Arabidopsis* SLEEPY1 gene encodes a putative F-box subunit of an SCF E3 ubiquitin ligase. *Plant Cell* **15**, 1120-1130.

Mezzetti, B., Landi, L., Pandolfini, T., and Spena, A. (2004). The *defH9-iaaM* auxin-synthesizing gene increases plant fecundity and fruit production in strawberry and raspberry. *BMC Biotechnol.* **4**, 1-4.

Miller, C.O., Skoog, F., Vonsaltza, M.H., and Strong, F.M. (1955). KINETIN, A CELL DIVISION FACTOR FROM DEOXYRIBONUCLEIC ACID. *Journal of the American Chemical Society* **77**, 1392-1392.

Mitchum, M.G., Yamaguchi, S., Hanada, A., Kuwahara, A., Yoshioka, Y., Kato, T., Tabata, S., Kamiya, Y., and Sun, T.P. (2006). Distinct and overlapping roles of two gibberellin 3-oxidases in *Arabidopsis* development. *Plant J* **45**, 804-818.

Molesini, B., Pandolfini, T., Rotino, G.L., Dani, V., and Spena, A. (2009). Aucsia Gene Silencing Causes Parthenocarpic Fruit Development in Tomato. *Plant Physiol.* **149**, 534-548.

Muir, R.M. (1942). Growth hormones as related to the setting and development of fruit in *Nicotiana tabacum*. *American Journal of Botany* **29**, 716-720.

Murase, K., Hirano, Y., Sun, T.P., and Hakoshima, T. (2008). Gibberellin-induced DELLA recognition by the gibberellin receptor GID1. *Nature* **456**, 459-463.

Murre, C., McCaw, P.S., and Baltimore, D. (1989a). A NEW DNA-BINDING AND DIMERIZATION MOTIF IN IMMUNOGLOBULIN ENHANCER BINDING, DAUGHTERLESS, MYOD, AND MYC PROTEINS. *Cell* **56**, 777-783.

Murre, C., McCaw, P.S., Vaessin, H., Caudy, M., Jan, L.Y., Jan, Y.N., Cabrera, C.V., Buskin, J.N., Hauschka, S.D., Lassar, A.B., Weintraub, H., and Baltimore, D. (1989b). INTERACTIONS BETWEEN HETEROLOGOUS HELIX-LOOP-HELIX PROTEINS GENERATE COMPLEXES THAT BIND SPECIFICALLY TO A COMMON DNA-SEQUENCE. *Cell* **58**, 537-544.

Nakajima, M., Shimada, A., Takashi, Y., Kim, Y.C., Park, S.H., Ueguchi-Tanaka, M., Suzuki, H., Katoh, E., Iuchi, S., Kobayashi, M., Maeda, T., Matsuoka, M., and Yamaguchi, I. (2006). Identification and characterization of *Arabidopsis* gibberellin receptors. *Plant Journal* **46**, 880-889.

Nemhauser, J.L., Feldman, L.J., and Zambryski, P.C. (2000). Auxin and ETTIN in *Arabidopsis* gynoecium morphogenesis. *Development* **127**, 3877-3888.

Ngo, P., Ozga, J.A., and Reinecke, D.M. (2002). Specificity of auxin regulation of gibberellin 20-oxidase gene expression in pea pericarp. *Plant Mol Biol* **49**, 439-448.

Nitsch, L.M.C., Oplaat, C., Feron, R., Ma, Q., Wolters-Arts, M., Hedden, P., Mariani, C., and Vriezen, W.H. (2009). Abscisic acid levels in tomato ovaries are regulated by LeNCED1 and SICYP707A1. *Planta* **229**, 1335-1346.

Ogawa, M., Hanada, A., Yamauchi, Y., Kuwalhara, A., Kamiya, Y., and Yamaguchi, S. (2003). Gibberellin biosynthesis and response during *Arabidopsis* seed germination. *Plant Cell* **15**, 1591-1604.

Oh, E., Yamaguchi, S., Hu, J., Yusuke, J., Jung, B., Paik, I., Lee, H.S., Sun, T.P., Kamiya, Y., and Choi, G. (2007). PIL5, a phytochrome-interacting bHLH protein, regulates gibberellin responsiveness by binding directly to the GAI and RGA promoters in *Arabidopsis* seeds. *Plant Cell* **19**, 1192-1208.

Ohad, N., Margossian, L., Hsu, Y.-C., Williams, C., Repetti, P., and Fischer, R.L. (1996). A mutation that allows endosperm development without fertilization. Proc. Natl. Acad. Sci. **93**, 5319-5324.

Ohad, N., Yadegari, R., Margossian, L., Hannon, M., Michaeli, D., Harada, J.J., Goldberg, R.B., and Fischer, R.L. (1999). Mutations in FIE, a WD polycomb group gene, allow endosperm development without fertilization. Plant Cell **11**, 407-415.

Okuda, S., Tsutsui, H., Shiina, K., Sprunck, S., Takeuchi, H., Yui, R., Kasahara, R.D., Hamamura, Y., Mizukami, A., Susaki, D., Kawano, N., Sakakibara, T., Namiki, S., Itoh, K., Otsuka, K., Matsuzaki, M., Nozaki, H., Kuroiwa, T., Nakano, A., Kanaoka, M.M., Dresselhaus, T., Sasaki, N., and Higashiyama, T. (2009). Defensin-like polypeptide LUREs are pollen tube attractants secreted from synergid cells. Nature **458**, 357-361.

Okushima, Y., Mitina, I., Quach, H.L., and Theologis, A. (2005). AUXIN RESPONSE FACTOR 2 (ARF2): a pleiotropic developmental regulator. Plant Journal **43**, 29-46.

Olczak, M., Morawiecka, B., and Watorek, W. (2003). Plant purple acid phosphatases - genes, structures and biological function. Acta Biochimica Polonica **50**, 1245-1256.

Olimpieri, I., Siligato, F., Caccia, R., Mariotti, L., Ceccarelli, N., Soressi, G.P., and Mazzucato, A. (2007). Tomato fruit set driven by pollination or by the parthenocarpic fruit allele are mediated by transcriptionally regulated gibberellin biosynthesis. Planta **226**, 877-888.

Olszewski, N., Sun, T.P., and Gubler, F. (2002). Gibberellin signaling: Biosynthesis, catabolism, and response pathways. Plant Cell **14**, S61-S80.

Ozga, J.A., van Huizen, R., and Reinecke, D.M. (2002). Hormone and seed-specific regulation of pea fruit growth. Plant Physiol **128**, 1379-1389.

Ozga, J.A., Yu, J., and Reinecke, D.M. (2003). Pollination-, development-, and auxin-specific regulation of gibberellin 3beta-hydroxylase gene expression in pea fruit and seeds. *Plant Physiol* **131**, 1137-1146.

Ozga, J.A., and Reinecke, D.M. (2003). Hormonal interactions in fruit development. *Journal of Plant Growth Regulation* **22**, 73-81.

Ozga, J.A., Reinecke, D.M., Ayele, B.T., Ngo, P., Nadeau, C., and Wickramarathna, A.D. (2009). Developmental and Hormonal Regulation of Gibberellin Biosynthesis and Catabolism in Pea Fruit. *Plant Physiology* **150**, 448-462.

Palanivelu, R., Brass, L., Edlund, A.F., and Preuss, D. (2003). Pollen tube growth and guidance is regulated by POP2, an *Arabidopsis* gene that controls GABA levels. *Cell* **114**, 47-59.

Palanivelu, R., and Preuss, D. (2006). Distinct short-range ovule signals attract or repel *Arabidopsis thaliana* pollen tubes in vitro. *Bmc Plant Biology* **6**.

Pascual, L., Blanca, J.M., Canizares, J., and Nuez, F. (2009). Transcriptomic analysis of tomato carpel development reveals alterations in ethylene and gibberellin synthesis during pat3/pat4 parthenocarpic fruit set. *Bmc Plant Biology* **9**.

Penfield, S., Josse, E.M., Kannangara, R., Gilday, A.D., Halliday, K.J., and Graham, I.A. (2005). Cold and light control seed germination through the bHLH transcription factor SPATULA. *Current Biology* **15**, 1998-2006.

Peng, J., Carol, P., Richards, D.E., King, K.E., Cowling, R.J., Murphy, G.P., and Harberd, N.P. (1997). The *Arabidopsis* GAI gene defines a signaling pathway that negatively regulates gibberellin responses. *Genes Dev* **11**, 3194-3205.

Phillips, A.L., Ward, D.A., Uknes, S., Appleford, N.E., Lange, T., Huttly, A.K., Gaskin, P., Graebe, J.E., and Hедден, P. (1995). Isolation and expression of

three gibberellin 20-oxidase cDNA clones from Arabidopsis. *Plant Physiol.* **108**, 1049-1057.

Pien, S., and Grossniklaus, U. (2007). Polycomb group and trithorax group proteins in Arabidopsis. *Biochimica Et Biophysica Acta-Gene Structure and Expression* **1769**, 375-382.

Pinyopich, A., Ditta, G.S., Savidge, B., Liljegren, S.J., Baumann, E., Wisman, E., and Yanofsky, M.F. (2003). Assessing the redundancy of MADS-box genes during carpel and ovule development. *Nature* **424**, 85-88.

Preuss, D., Lemieux, B., Yen, G., and Davis, R.W. (1993). A CONDITIONAL STERILE MUTATION ELIMINATES SURFACE COMPONENTS FROM ARABIDOPSIS POLLEN AND DISRUPTS CELL SIGNALING DURING FERTILIZATION. *Genes & Development* **7**, 974-985.

Preuss, D., Rhee, S.Y., and Davis, R.W. (1994). TETRAD ANALYSIS POSSIBLE IN ARABIDOPSIS WITH MUTATION OF THE QUARTET (QRT) GENES. *Science* **264**, 1458-1460.

Pysh, L.D., Wysocka-Diller, J.W., Camilleri, C., Bouchez, D., and Benfey, P.N. (1999). The GRAS gene family in Arabidopsis: sequence characterization and basic expression analysis of the SCARECROW-LIKE genes. *Plant Journal* **18**, 111-119.

Radi, A., Lange, T., Niki, T., Koshioka, M., and Lange, M.J.P. (2006). Ectopic expression of pumpkin gibberellin oxidases alters gibberellin biosynthesis and development of transgenic Arabidopsis plants. *Plant Physiology* **140**, 528-536.

Rajani, S., and Sundaresan, V. (2001). The Arabidopsis myc/bHLH gene ALCATRAZ enables cell separation in fruit dehiscence. *Current Biology* **11**, 1914-1922.

Ravi, M., Marimuthu, M.P.A., and Siddiqi, I. (2008). Gamete formation without meiosis in *Arabidopsis*. *Nature* **451**, 1121-U1110.

Rebers, M., Kaneta, T., Kawaide, H., Yamaguchi, S., Yang, Y.Y., Imai, R., Sekimoto, H., and Kamiya, Y. (1999). Regulation of gibberellin biosynthesis genes during flower and early fruit development of tomato. *Plant Journal* **17**, 241-250.

Rhee, S.Y., and Somerville, C.R. (1998). Tetrad pollen formation in quartet mutants of *Arabidopsis thaliana* is associated with persistence of pectic polysaccharides of the pollen mother cell wall. *Plant Journal* **15**, 79-88.

Rhee, S.Y., Osborne, E., Poindexter, P.D., and Somerville, C.R. (2003). Microspore separation in the quartet 3 mutants of *Arabidopsis* is impaired by a defect in a developmentally regulated polygalacturonase required for pollen mother cell wall degradation. *Plant Physiology* **133**, 1170-1180.

Richards, A.J. (2003). Apomixis in flowering plants: an overview. *Philosophical Transactions of the Royal Society of London Series B-Biological Sciences* **358**, 1085-1093.

Rieu, I., Ruiz-Rivero, O., Fernandez-Garcia, N., Griffiths, J., Powers, S.J., Gong, F., Linhartova, T., Eriksson, S., Nilsson, O., Thomas, S.G., Phillips, A.L., and Hedden, P. (2008a). The gibberellin biosynthetic genes AtGA20ox1 and AtGA20ox2 act, partially redundantly, to promote growth and development throughout the *Arabidopsis* life cycle. *Plant Journal* **55**, 488-504.

Rieu, I., Eriksson, S., Powers, S.J., Gong, F., Griffiths, J., Woolley, L., Benlloch, R., Nilsson, O., Thomas, S.G., Hedden, P., and Phillips, A.L. (2008b). Genetic analysis reveals that C19-GA 2-oxidation is a major gibberellin inactivation pathway in *Arabidopsis*. *Plant Cell* **20**, 2420-2436.

Robinson, R.W., and Reiners, S. (1999). Parthenocarpy in summer squash. *Hortscience* **34**, 715-717.

Roe, J.L., Nemhauser, J.L., and Zambryski, P.C. (1997). TOUSLED participates in apical tissue formation during gynoecium development in *Arabidopsis*. *Plant Cell* **9**, 335-353.

Roeder, A.H.K., Ferrández, C., and Yanofsky, M.F. (2003). The Role of the REPLUMLESS Homeodomain Protein in Patterning the *Arabidopsis* Fruit. *Current biology : CB* **13**, 1630-1635.

Roeder Adrienne, H.K., and Yanofsky Martin, F. (2006). Fruit Development in *Arabidopsis*. In *The Arabidopsis Book* (The American Society of Plant Biologists), pp. 1-50.

Ross, J.J., Murfet, I.C., and Reid, J.B. (1997). Gibberellin mutants. *Physiologia Plantarum* **100**, 550-560.

Ross, J.J., Reid, J.B., Murfet, I.C., and Weston, D.E. (2008). The slender phenotype of pea is deficient in DELLA proteins. *Plant Signalling and Behavior* **3**, 590–592.

Rotino, G.L., Perri, E., Zottini, M., Sommer, H., and Spena, A. (1997). Genetic engineering of parthenocarpic plants. *Nat. Biotechnol.* **15**, 1398-1401.

Rotman, N., Rozier, F., Boavida, L., Dumas, C., Berger, F., and Faure, J.E. (2003). Female control of male gamete delivery during fertilization in *Arabidopsis thaliana*. *Current Biology* **13**, 432-436.

Rotman, N., Gourgues, M., Guitton, A.E., Faure, J.E., and Berger, F. (2008). A dialogue between the Sirene pathway in synergids and the Fertilization Independent Seed pathway in the central cell controls male gamete release during double fertilization in *Arabidopsis*. *Molecular Plant* **1**, 659-666.

Sachs, T. (1991). CELL POLARITY AND TISSUE PATTERNING IN PLANTS. Roberts, K., Et Al. (Ed.). Development Supplement, 1. Molecular and Cellular Basis of Pattern Formation; 9th John Innes Symposium, Norwich, England, Uk,

September 1990. V+203p. The Company of Biologists Ltd.: Cambridge, England, Uk. Illus, 83-94.

Sanchez-Fernandez, R., Ardiles-Diaz, W., Van Montagu, M., Inze, D., and May, M.J. (1998). Cloning of a novel *Arabidopsis thaliana* RGA-like gene, a putative member of the VHIID-domain transcription factor family. *Journal of Experimental Botany* **49**, 1609-1610.

Sandaklie-Nikolova, L., Palanivelu, R., King, E.J., Copenhaver, G.P., and Drews, G.N. (2007). Synergid Cell Death in *Arabidopsis* Is Triggered following Direct Interaction with the Pollen Tube. *Plant Physiol.* **144**, 1753-1762.

Sasaki, A., Itoh, H., Gomi, K., Ueguchi-Tanaka, M., Ishiyama, K., Kobayashi, M., Jeong, D.H., An, G., Kitano, H., Ashikari, M., and Matsuoka, M. (2003). Accumulation of phosphorylated repressor for gibberellin signaling in an F-box mutant. *Science* **299**, 1896-1898.

Savaldi-Goldstein, S., Peto, C., and Chory, J. (2007). The epidermis both drives and restricts plant shoot growth. *Nature* **446**, 199-202.

Scarpella, E., Marcos, D., Friml, J., and Berleth, T. (2006). Control of leaf vascular patterning by polar auxin transport. *Genes & Development* **20**, 1015-1027.

Schijlen, E.G.W.M., de Vos, C.H.R., Martens, S., Jonker, H.H., Rosin, F.M., Molthoff, J.W., Tikunov, Y.M., Angenent, G.C., van Tunen, A.J., and Bovy, A.G. (2007). RNA Interference Silencing of Chalcone Synthase, the First Step in the Flavonoid Biosynthesis Pathway, Leads to Parthenocarpic Tomato Fruits. *Plant Physiology* **144**, 1520-1530.

Schneitz, K., Hulskamp, M., and Pruitt, R.E. (1995). WILD-TYPE OVULE DEVELOPMENT IN *ARABIDOPSIS-THALIANA* - A LIGHT-MICROSCOPE STUDY OF CLEARED WHOLE-MOUNT TISSUE. *Plant Journal* **7**, 731-749.

Schruff, M.C., Spielman, M., Tiwari, S., Adams, S., Fenby, N., and Scott, R.J. (2006). The AUXIN RESPONSE FACTOR 2 gene of *Arabidopsis* links auxin signalling, cell division, and the size of seeds and other organs. *Development* **133**, 251-261.

Serrani, J.C., Sanjuan, R., Ruiz-Rivero, O., Fos, M., and Garcia-Martinez, J.L. (2007). Gibberellin regulation of fruit set and growth in tomato. *Plant Physiology* **145**, 246-257.

Serrani, J.C., Ruiz-Rivero, O., Fos, M., and Garcia-Martinez, J.L. (2008). Auxin-induced fruit-set in tomato is mediated in part by gibberellins. *The Plant Journal Early view (online)*.

Sessions, R.A., and Zambryski, P.C. (1995). ARABIDOPSIS GYNOECIUM STRUCTURE IN THE WILD-TYPE AND IN EFFIN MUTANTS. *Development* **121**, 1519-1532.

Sessions, A., Nemhauser, J.L., McColl, A., Roe, J.L., Feldmann, K.A., and Zambryski, P.C. (1997). ETTIN patterns the *Arabidopsis* floral meristem and reproductive organs. *Development* **124**, 4481-4491.

Shimizu, K.K., and Okada, K. (2000). Attractive and repulsive interactions between female and male gametophytes in *Arabidopsis* pollen tube guidance. *Development* **127**, 4511-4518.

Shimizu, K.K., Ito, T., Ishiguro, S., and Okada, K. (2008). MAA3 (MAGATAMA3) Helicase Gene is Required for Female Gametophyte Development and Pollen Tube Guidance in *Arabidopsis thaliana*. *Plant and Cell Physiology* **49**, 1478-1483.

Sidaway-Lee, K., Josse, E.-M., Brown, A., Gan, Y., Halliday, K.J., Graham, I.A., and Penfield, S. SPATULA Links Daytime Temperature and Plant Growth Rate. *Current Biology* **20**, 1493-1497.

Silverstone, A.L., Ciampaglio, C.N., and Sun, T.-P. (1998). The Arabidopsis RGA gene encodes a transcriptional regulator repressing the gibberellin signal transduction pathway. *Plant Cell* **10**, 155-169.

Silverstone, A.L., Jung, H.-S., Dill, A., Kawaide, H., Kamiya, Y., and Sun, T.-p. (2001). Repressing a Repressor: Gibberellin-Induced Rapid Reduction of the RGA Protein in Arabidopsis. *Plant Cell* **13**, 1555-1566.

Silverstone, A.L., Tseng, T.-S., Swain, S.M., Dill, A., Jeong, S.Y., Olszewski, N.E., and Sun, T.-p. (2007). Functional Analysis of SPINDLY in Gibberellin Signaling in Arabidopsis. *Plant Physiol.* **143**, 987-1000.

Singh, D.P., Jermakow, A.M., and Swain, S.M. (2002). Gibberellins are required for seed development and pollen tube growth in Arabidopsis. *Plant Cell* **14**, 3133-3147.

Smyth, D.R., Bowman, J.L., and Meyerowitz, E.M. (1990). EARLY FLOWER DEVELOPMENT IN ARABIDOPSIS. *Plant Cell* **2**, 755-767.

Sorefan, K., Girin, T., Liljegren, S.J., Ljung, K., Robles, P., Galvan-Ampudia, C.S., Offringa, R., Friml, J., Yanofsky, M.F., and Ostergaard, L. (2009). A regulated auxin minimum is required for seed dispersal in Arabidopsis. *Nature* **459**, 583-U114.

Sponsel, V.M., Schmidt, F.W., Porter, S.G., Nakayama, M., Kohlstruk, S., and Estelle, M. (1997). Characterization of new gibberellin-responsive semidwarf mutants of Arabidopsis. *Plant Physiol.* **115**, 1009-1020.

Srinivasan, A., and Morgan, D.G. (1996). Growth and development of the pod wall in spring rape (*Brassica napus*) as related to the presence of seeds and exogenous phytohormones. *Journal of Agricultural Science* **127**, 487-500.

Srivastava, L.M., Sawhney, V.K., and Taylor, I.E. (1975). Gibberellic-Acid-Induced Cell Elongation in Lettuce Hypocotyls. Proc Natl Acad Sci U S A **72**, 1107-1111.

Stangeland, B., Salehian, Z., Aalen, R., Mandal, A., and Olsen, O.A. (2003). Isolation of GUS marker lines for genes expressed in *Arabidopsis* endosperm, embryo and maternal tissues. Journal of Experimental Botany **54**, 279-290.

Stephenson, P., Baker, D., Girin, T., Perez, A., Amoah, S., King, G.J., and Ostergaard, L. A rich TILLING resource for studying gene function in *Brassica rapa*. Bmc Plant Biology **10**.

Sun, T.P., and Kamiya, Y. (1994). The *Arabidopsis* Ga1 Locus Encodes the Cyclase Ent-Kaurene Synthetase-a of Gibberellin Biosynthesis. Plant Cell **6**, 1509-1518.

Suzuki, G. (2009). Recent Progress in Plant Reproduction Research: The Story of the Male Gametophyte through to Successful Fertilization. Plant Cell Physiol. **50**, 1857-1864.

Talon, M., Koornneef, M., and Zeevaart, J.A.D. (1990). Endogenous gibberellins in *Arabidopsis thaliana* and possible steps blocked in the biosynthetic pathways of the semi-dwarf ga4 and ga5 mutants. Proc. Natl. Acad. Sci. USA **87**, 7983-7987.

Talon, M., Zacarias, L., and Primo-Millo, E. (1992). Gibberellins and Parthenocarpic Ability in Developing Ovaries of Seedless Mandarins. Plant Physiol. **99**, 1575-1581.

Tang, Y. (2003). Analysis of auxin and abscisic acid signal transduction in *Arabidopsis thaliana*. In Institut für Botanik und Mikrobiologie (Munich: Technische Universität München), pp. 245.

Tarkowski, P., Tarkowska, D., Novak, O., Mihaljevic, S., Magnus, V., Strnad, M., and Salopek-Sondi, B. (2006). Cytokinins in the perianth, carpels, and developing fruit of *Helleborus niger* L. *J. Exp. Bot.* **57**, 2237-2247.

Tarutani, Y., Shiba, H., Iwano, M., Kakizaki, T., Suzuki, G., Watanabe, M., Isogai, A., and Takayama, S. Trans-acting small RNA determines dominance relationships in *Brassica* self-incompatibility. *Nature* **466**, 983-986.

Tiwari, S.B., Wang, X.J., Hagen, G., and Guilfoyle, T.J. (2001). AUX/IAA proteins are active repressors, and their stability and activity are modulated by auxin. *Plant Cell* **13**, 2809-2822.

Toledo-Ortiz, G., Huq, E., and Quail, P.H. (2003). The *Arabidopsis* Basic/Helix-Loop-Helix Transcription Factor Family. *Plant Cell* **15**, 1749-1770.

Tran, H.T., Hurley, B.A., and Plaxton, W.C. Feeding hungry plants: The role of purple acid phosphatases in phosphate nutrition. *Plant Science (Oxford)* **179**, 14-27.

Trigueros, M., Navarrete-Gomez, M., Sato, S., Christensen, S.K., Pelaz, S., Weigel, D., Yanofsky, M.F., and Ferrandiz, C. (2009). The NGATHA Genes Direct Style Development in the *Arabidopsis* Gynoecium. *Plant Cell* **21**, 1394-1409.

Tyler, L., Thomas, S.G., Hu, J.H., Dill, A., Alonso, J.M., Ecker, J.R., and Sun, T.P. (2004). DELLA proteins and gibberellin-regulated seed germination and floral development in *Arabidopsis*. *Plant Physiology* **135**, 1008-1019.

Ubeda-Tomas, S., Swarup, R., Coates, J., Swarup, K., Laplaze, L., Beemster, G.T.S., Hedden, P., Bhalerao, R., and Bennett, M.J. (2008). Root growth in *Arabidopsis* requires gibberellin/DELLA signalling in the endodermis. *Nature Cell Biology* **10**, 625-628.

Ueguchi-Tanaka, M., Ashikari, M., Nakajima, M., Itoh, H., Katoh, E., Kobayashi, M., Chow, T.Y., Hsing, Y.I.C., Kitano, H., Yamaguchi, I., and Matsuoka, M. (2005). GIBBERELLIN INSENSITIVE DWARF1 encodes a soluble receptor for gibberellin. *Nature* **437**, 693-698.

Ueguchi-Tanaka, M., Hirano, K., Hasegawa, Y., Kitano, H., and Matsuoka, M. (2008). Release of the repressive activity of rice DELLA protein SLR1 by gibberellin does not require SLR1 degradation in the gid2 mutant. *Plant Cell* **20**, 2437-2446.

Ulmasov, T., Murfett, J., Hagen, G., and Guilfoyle, T.J. (1997). Aux/IAA proteins repress expression of reporter genes containing natural and highly active synthetic auxin response elements. *Plant Cell* **9**, 1963-1971.

van Huizen, R., Ozga, J.A., Reinecke, D.M., Twitchin, B., and Mander, L.N. (1995). Seed and 4-chloroindole-3-acetic acid regulation of gibberellin metabolism in pea pericarp. *Plant Physiol* **109**, 1213-1217.

van Overbeek, J., Conklin, M.E., and Blakeslee, A.F. (1941). Factors in coconut milk are essential for growth and development of very young *Datura* embryos. *Science* **94**, 350-351.

Varga, A., and Bruinsma, J. (1976). ROLES OF SEEDS AND AUXINS IN TOMATO FRUIT GROWTH. *Zeitschrift Fur Pflanzenphysiologie* **80**, 95-104.

Varoquaux, F., Blanvillain, R., Delseny, M., and Gallois, P. (2000). Less is better: new approaches for seedless fruit production. *Trends in Biotechnology* **18**, 233-242.

Veljanovski, V., Vanderbeld, B., Knowles, V.L., Snedden, W.A., and Plaxton, W.C. (2006). Biochemical and molecular characterization of AtPAP26, a vacuolar purple acid phosphatase up-regulated in phosphate-deprived *Arabidopsis* suspension cells and seedlings. *Plant Physiology* **142**, 1282-1293.

Vivian-Smith, A., and Koltunow, A.M. (1999). Genetic analysis of growth-regulator-induced parthenocarpy in *Arabidopsis*. *Plant Physiol.* **121**, 437-452.

Vivian-Smith, A. (2001). The molecular basis for the initiation of fruit development and parthenocarpy. In *Plant Science* (Adelaide: The University of Adelaide), pp. 196.

Vivian-Smith, A., Luo, M., Chaudhury, A., and Koltunow, A. (2001). Fruit development is actively restricted in the absence of fertilization in *Arabidopsis*. *Development* **128**, 2321-2331.

von Besser, K., Frank, A.C., Johnson, M.A., and Preuss, D. (2006). *Arabidopsis HAP2 (GCS1)* is a sperm-specific gene required for pollen tube guidance and fertilization. *Development* **133**, 4761-4769.

Vriezen, W.H., Feron, R., Maretto, F., Keijman, J., and Mariani, C. (2007). Changes in tomato ovary transcriptome demonstrate complex hormonal regulation of fruit set. *New Phytologist* **177**, 60-76.

Wang, H., Jones, B., Li, Z., Frasse, P., Delalande, C., Regad, F., Chaabouni, S., Latche, A., Pech, J.-C., and Bouzayen, M. (2005). The Tomato Aux/IAA Transcription Factor IAA9 Is Involved in Fruit Development and Leaf Morphogenesis. *Plant Cell* **17**, 2676-2692.

Wang, H.Z., Boavida, L.C., Ron, M., and McCormick, S. (2008). Truncation of a Protein Disulfide Isomerase, PDIL2-1, Delays Embryo Sac Maturation and Disrupts Pollen Tube Guidance in *Arabidopsis thaliana*. *Plant Cell* **20**, 3300-3311.

Wang, H., Schauer, N., Usadel, B., Frasse, P., Zouine, M., Hernould, M., Latche, A., Pech, J.-C., Fernie, A.R., and Bouzayen, M. (2009). Regulatory Features Underlying Pollination-Dependent and -Independent Tomato Fruit Set Revealed by Transcript and Primary Metabolite Profiling. *Plant Cell* **21**, 1428-1452.

Wells, L., Vosseller, K., and Hart, G.W. (2001). Glycosylation of nucleocytoplasmic proteins: Signal transduction and O-GlcNAc. *Science* **291**, 2376-2378.

Wen, C.K., and Chang, C. (2002). Arabidopsis RGL1 encodes a negative regulator of gibberellin responses. *Plant Cell* **14**, 87-100.

Weterings, K., and Russell, S.D. (2004). Experimental analysis of the fertilization process. *Plant Cell* **16**, S107-S118.

Willige, B.C., Ghosh, S., Nill, C., Zourelidou, M., Dohmann, E.M.N., Maier, A., and Schwechheimer, C. (2007). The DELLA domain of GA INSENSITIVE mediates the interaction with the GA INSENSITIVE DWARF1A gibberellin receptor of Arabidopsis. *Plant Cell* **19**, 1209-1220.

Wu, M.F., Tian, Q., and Reed, J.W. (2006). Arabidopsis microRNA167 controls patterns of ARF6 and ARF8 expression, and regulates both female and male reproduction. *Development* **133**, 4211-4218.

Wu, J.-Z., Lin, Y., Zhang, X.-L., Pang, D.-W., and Zhao, J. (2008a). IAA stimulates pollen tube growth and mediates the modification of its wall composition and structure in *Torenia fournieri*. *J. Exp. Bot.* **59**, 2529-2543.

Wu, J.Z., Qin, Y., and Zhao, J. (2008b). Pollen tube growth is affected by exogenous hormones and correlated with hormone changes in styles in *Torenia fournieri* L. *Plant Growth Regulation* **55**, 137-148.

Xu, Y.L., Li, L., Wu, K., Peeters, A.J., Gage, D.A., and Zeevaart, J.A. (1995). The GA5 locus of *Arabidopsis thaliana* encodes a multifunctional gibberellin 20-oxidase: molecular cloning and functional expression. *Proc Natl Acad Sci U S A* **92**, 6640-6644.

Yang, J.C., Zhang, J.H., Huang, Z.L., Wang, Z.Q., Zhu, Q.S., and Liu, L.J. (2002). Correlation of cytokinin levels in the endosperms and roots with cell

number and cell division activity during endosperm development in rice. Annals of Botany **90**, 369-377.

Yasuda, S. (1936). Some contributions on parthenocarpy caused by the stimulation of pollination. A report on parthenocarpy caused by self-pollination in egg plants and cucumbers, with some additional discussions. Kyushu Teikokudaigaku Nogakubu Gakugeizasshi **7**, 34-55.

Ye, X.L., Yeung, E.C., and Zee, S.Y. (2002). Sperm movement during double fertilization of a flowering plant, *Phaius tankervilliae*. Planta **215**, 60-66.

Yin, Z.M., Malinowski, R., Ziolkowska, A., Sommer, H., Plader, W., and Malepszy, S. (2006). The DefH9-iaaM-containing construct efficiently induces parthenocarpy in cucumber. Cellular & Molecular Biology Letters **11**, 279-290.

Zentella, R., Zhang, Z.L., Park, M., Thomas, S.G., Endo, A., Murase, K., Fleet, C.M., Jikumaru, Y., Nambara, E., Kamiya, Y., and Sun, T.P. (2007). Global analysis of DELLA direct targets in early gibberellin signaling in Arabidopsis. Plant Cell **19**, 3037-3057.

Zhang, X.S., and O'Neill, S.D. (1993). Ovary and Gametophyte Development Are Coordinately Regulated by Auxin and Ethylene following Pollination. Plant Cell **5**, 403-418.

Zichao, M., Qiuju, Y., Wei, Z., Junyi, G., Yuanlei, H., Yin , G., and Zhongping, L. (2002). Expression of ipt gene driven by tomato fruit specific promoter and its effects on fruit development of tomato. Chinese Science Bulletin **47**, 928-933.